



# Numerical Simulation and Optimisation of Polymer Flooding in a Heterogenous Reservoir: Constrained Versus Unconstrained Optimisation

Emmanuel Ibiam

Submitted for the degree of Doctor of Philosophy  
School of Energy, Geoscience, Infrastructure and Society  
Institute of GeoEnergy Engineering  
Heriot-Watt University

July 2021

The copyright in this thesis is owned by the author. Any quotation from the thesis or use of any information contained in it must acknowledge this thesis as the source of the quotation or information.

## Research Thesis Submission

Please note this form should be bound into the submitted thesis.

Name:	Emmanuel Ibiam		
School:	EGIS		
Version: <i>(i.e. First, Resubmission, Final)</i>	Final	Degree Sought:	PhD.

### Declaration

In accordance with the appropriate regulations I hereby submit my thesis and I declare that:

1. The thesis embodies the results of my own work and has been composed by myself
2. Where appropriate, I have made acknowledgement of the work of others
3. The thesis is the correct version for submission and is the same version as any electronic versions submitted\*.
4. My thesis for the award referred to, deposited in the Heriot-Watt University Library, should be made available for loan or photocopying and be available via the Institutional Repository, subject to such conditions as the Librarian may require
5. I understand that as a student of the University I am required to abide by the Regulations of the University and to conform to its discipline.
6. I confirm that the thesis has been verified against plagiarism via an approved plagiarism detection application e.g. Turnitin.

### ONLY for submissions including published works


Please note you are only required to complete the Inclusion of Published Works Form (page 2) if your thesis contains published works)

7. Where the thesis contains published outputs under Regulation 6 (9.1.2) or Regulation 43 (9) these are accompanied by a critical review which accurately describes my contribution to the research and, for multi-author outputs, a signed declaration indicating the contribution of each author (complete)
8. Inclusion of published outputs under Regulation 6 (9.1.2) or Regulation 43 (9) shall not constitute plagiarism.

\* Please note that it is the responsibility of the candidate to ensure that the correct version of the thesis is submitted.

Signature of Candidate:		Date:	02-07-2021
-------------------------	---	-------	------------

### Submission

Submitted By <i>(name in capitals)</i> :	EMMANUEL IBIAM
Signature of Individual Submitting:	
Date Submitted:	02-07-2020

### For Completion in the Student Service Centre (SSC)

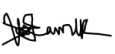
Limited Access	Requested	Yes	No	Approved	Yes	No
<i>E-thesis Submitted (mandatory for final theses)</i>						
Received in the SSC by <i>(name in capitals)</i> :				Date:		

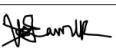
### Inclusion of Published Works

Please note you are only required to complete the Inclusion of Published Works Form if your thesis contains published works under Regulation 6 (9.1.2)

#### Declaration

This thesis contains one or more multi-author published works. In accordance with Regulation 6 (9.1.2) I hereby declare that the contributions of each author to these publications is as follows:

Citation details	E. Ibiam, S. Geiger, V. Damyanov, and D. Arnold, "Optimisation of Polymer Flooding in a Heterogeneous Reservoir Considering Geological and History Matching Uncertainties", SPE Reservoir Evaluation and Engineering, SPE-200568-PA, 2020.
Emmanuel Ibiam	Conception of ideas, carrying out the research and writing the paper
Sebastian Geiger	Supervision of the research and reviewing the paper
Signature:	
Date:	02-07-2021

Citation details	E. Ibiam, S. Geiger, A. Almaqbali, V. Damyanov, and D. Arnold, "Numerical Simulation and Optimisation of Polymer Flooding in a Heterogenous – Constrained vs Unconstrained Optimisation", - SPE Nigeria Annual International Conference and Exhibition, Lagos, Nigeria, SPE – 193400 – MS, 2018.
Emmanuel Ibiam	Conception of ideas, carrying out the research and writing the paper
Sebastian Geiger	Supervision of the research and reviewing the paper
Signature:	
Date:	02-07-2021

Please included additional citations as required.

---

# Abstract

---

Polymer flooding offers the potential to recover more oil from reservoirs but requires significant investments which necessitate a robust analysis of economic upsides and downsides. Key uncertainties in designing a polymer flood are often reservoir geology and polymer degradation. The objective of this study is to understand the impact of geological uncertainties and history matching techniques on designing the optimal strategy for, and quantifying the economic risks of, polymer flooding in a heterogeneous clastic reservoir.

We applied two different history matching techniques (adjoint-based and a stochastic algorithm) to match data from a prolonged waterflood in the Watt Field, a semi-synthetic reservoir that contains a wide range of geological and interpretational uncertainties. Next, sensitivity studies were carried out to identify first-order parameters that impact the Net Present Value (NPV). These parameters were then deployed in an experimental design study using Latin Hypercube Sampling to generate training runs from which a proxy model was created using polynomial regression. A particle swarm optimization algorithm was employed to optimize the NPV for the polymer flood. The same approach was used to optimize a standard water flood for comparison. Optimizations of the polymer flood and water flood were performed for the history matched model ensemble and the original ensemble.

The Adjoint technique yielded a better quality match compared to stochastic history matching, whereas, the stochastic history matching resulted in a more diverse set of history matched ensemble. The optimal strategy to deploy the polymer flood and maximize NPV varies based on the history matching technique. The average NPV and the variance is predicted to be higher by 4% (\$600 million) and 1.9% (\$149 million) respectively in the stochastic history matching compared to the adjoint technique. This difference is due to the ability of the stochastic algorithm to explore the parameter space more broadly, which created situations where the oil in place was shifted upwards, resulting in higher NPV. Optimizing a history matched ensemble leads to a narrower range in absolute NPV compared to optimizing the original ensemble. This difference is because the uncertainties associated with polymer flooding are not captured during history matching. The result of cross comparison, where an optimal polymer design strategy for one ensemble member is deployed to the other ensemble members, predicted a decline in NPV but surprisingly still shows that the overall NPV is higher than for an optimized water food, even for sub-optimal polymer injection strategies. This observation indicates that a polymer flood could be beneficial compared to a water flood, even if geological uncertainties are not captured properly. This thesis reported the bias of stochastic algorithm by creating reservoir models where oil in place were shifted upwards. This can be further investigated and addressed.

Dedicated to my beautiful wife, my lovely kids and my loving mother.

---

# Acknowledgement

---

The successful completion of this thesis hinges on a lot of support and help received from many individuals. I would like to first and foremost express my gratitude to Almighty God for His grace and faithfulness.

My special thanks goes to my main supervisor Prof Sebastian Geiger for your consistent support, patience, kindness and for being a mentor and inspiration throughout my studies. You have left an incredible impact in my life. I would like to thank Prof Vasily Demyanov and Dr Dan Arnold for your valuable feedbacks on my PhD and for reviewing some of my papers. Thank you also for building the reservoir model (The Watt Field) I used for my research.

I would like to thank Dr Seyed Shariatipour and Dr Karl Stephen for being my examiners. Thank you for the insightful discussions during my viva and for providing constructive feedbacks on my thesis.

Special shout out to all the members of the great Carbonates Reservoir Group. It has been an amazing experience being part of this multicultural and multinational research group. The Christmas dinners are unforgettable experiences. Thank you all for being perfect travel companions to Paris and Copenhagen. Thank you Jane for always being willing to help out with travels and conferences.

Thank you Simeon and Alexandro for helping me settle in quickly and for all your valuable advice. Thank you to all my office mates, David, Adnan, Raphael, Zhao, Tunsien, Saeeda, Jackson and Ali, it was always a delight sharing the same office together. Thank you for comic relief during coffee breaks and diverse discussion on many aspects of life, they were very educative.

My immense gratitude is extended to my sponsors, PTFD, for giving me this opportunity to study for both Master's degree and PhD in Heriot Watt University. Thank you to Energi Simulation for providing CMG suits I used for my studies and also for partly sponsoring my research. Thank you HOT Engineering for providing SENEX software I used for history matching.

My sincere gratitude goes to my beautiful wife for your endless patience, encouragement, prayers and support with running the home. Thank you for allowing me finish the PhD and I will forever remember all your sacrifices. Special thanks to my adorable daughter and amazing son for always making daddy laugh hard. I am blessed to have all of you travelling through the amazing journey of life together.

Last and not the least, I would like to express my heartfelt gratitude to my loving mother and late Dad, who were the architect, laid good foundation and instilled excellent virtues in me, such as working hard, valuing education and to believe in myself and in my creator. The sacrifices you made in raising I and my siblings will forever be in my heart. To all my siblings and in-laws, you are the best support system anyone can have and I say a big thank you.

Glasgow, July 2021

Emmanuel I. Ibiam

## Table of Contents

Chapter 1.	Introduction.....	1
1.1.	Energy Market .....	1
1.2.	Enhanced Oil Recovery .....	5
1.3.	Polymer Flooding in Field Applications.....	6
1.3.1.	Current Polymer Projects .....	9
1.4.	Research Objectives and Scientific Hypothesis.....	11
1.5.	Structure of Thesis .....	12
Chapter 2.	Literature Review.....	13
2.1.	Introduction.....	13
2.2.	Geological Uncertainty .....	16
2.3.	EOR Optimization .....	18
2.4.	Polymer Flooding.....	19
2.4.1.	Types of Polymers .....	21
2.4.2.	Mathematical Model for Polymer Flooding.....	23
2.4.3.	Properties of Polymer Solutions .....	25
2.5.	History Matching .....	31
2.5.1.	Manual History Matching .....	33
2.5.2.	Assisted History Matching.....	35
2.6.	Parameterisation of Uncertain Properties .....	39
2.7.	Probabilistic Uncertainty Quantification.....	40
2.8.	Summary.....	43
Chapter 3.	Methodology .....	45
3.1.	The Watt Field .....	45
3.1.1.	Overview of the Watt Field.....	46
3.1.2.	Geological and Interpretational Uncertainties .....	47
3.1.3.	Truth Model .....	55
3.2.	Particle Swarm Optimisation .....	58
3.2.1.	PSO History Matching.....	60
3.3.	Adjoint Technique .....	62
3.4.	Design of Experiment .....	64
3.4.1.	Latin Hypercube Sampling .....	65

3.5.	Proxy Models .....	66
3.5.1.	Polynomial Regression .....	67
3.5.2.	Proxy Model Validation.....	68
3.6.	Monte Carlo Markov Chain with Proxy-Based Rejection and Acceptance.....	68
3.7.	Polymer Data .....	70
3.8.	Summary .....	71
Chapter 4.	Comparative Analysis of the Impact of History Matching Techniques on Reservoir Uncertainty Quantification.....	73
4.1.	Introduction.....	73
4.2.	Workflow .....	73
4.2.1.	History Matching .....	74
4.3.	Results.....	78
4.3.1.	History match quality.....	78
4.3.2.	Reliability of the Forecast.....	86
4.4.	Discussion .....	89
4.5.	Summary .....	90
Chapter 5.	Optimisation of polymer flooding in a Heterogenous Reservoir Considering Geological and History Matching Uncertainties .....	91
5.1.	Introduction.....	91
5.2.	Workflow .....	92
5.2.1.	Parameter Screening .....	94
5.2.2.	Objective Function for Optimisation .....	93
5.2.3.	Optimisation and Design of Experiments .....	95
5.2.4.	Uncertainty Analysis.....	96
5.3.	Results.....	97
5.3.1.	Proxy Modelling .....	97
5.3.2.	Adjoint vs PSO-Based History Matching .....	100
5.3.3.	Proxy-Based vs Full Physics Optimisation .....	100
5.3.4.	Constrained vs Unconstrained Optimisation.....	103
5.3.5.	Uncertainty Quantification.....	108
5.4.	Discussions .....	112
5.5.	Summary .....	113
Chapter 6.	Summary, Conclusions and Future Work .....	115
6.1.	Summary and Conclusion .....	115
6.2.	Future Work.....	117



---

## List of Figures

---

*Figure 1-1. The projected demographic of the global population (billions of people) by age and countries (from ExxonMobil Corporation 2019)..... 2*

*Figure 1-2 The global energy mix shifts to lower carbon fuel (from ExxonMobil Corporation 2019)..... 2*

*Figure 1-3 The global energy mix shifts to lower carbon sources (after BP 2019) ..... 3*

*Figure 1-4 Oil and gas field discoveries in Barrels of Oil Equivalent (BOE) and downturn in conventional exploration (number of new field wildcat wells, NFWs) (IHS Markit 2020)..... 5*

*Figure 1-5 Recovery mechanisms in a conventional oil and gas reservoir (from Oil & Gas Journal 2000). ..... 6*

*Figure 1-6 Global EOR projects at different points in time (IEA 2020). ..... 8*

*Figure 1-7 Estimated contribution of different EOR methods to global oil production (IEA 2020) ..... 8*

*Figure 1-8 Estimated contribution of polymer flooding to global oil production (South et al. 2018)..... 9*

*Figure 2-1. Design and implementation steps of a comprehensive EOR program (from Abu et al. 2014).14*

*Figure 2-2. Methods of geological uncertainty quantification (from Ringrose and Bentley 2015)..... 17*

*Figure 2-3. Fingering effect with Water flooding (left) and decreased effects of fingering with polymer flooding (right) (Zerkalov 2015). ..... 21*

*Figure 2-4. The molecular structure of Xanthan (from Dominguez and Willhite 1977). ..... 22*

*Figure 2-5. The molecular structure of HPAM (from Sheng 2011)..... 23*

*Figure 2-6. Viscosity curves of the rheology measurements of investigated xanthan gum solution of different concentrations (Mrokowska and Krztoń-Maziopa 2019). ..... 27*

*Figure 2-7. Polymer bank delay factor caused by polymer retention (after Green and Willhite 1998)..... 28*

*Figure 2-8. Polymer retention in porous media (after Huh et al. 1990)..... 29*

*Figure 2-9. Basic workflow during history matching - Big loop versus small loop. .... 33*

*Figure 2-10. The manual history matching procedure (Kelkar and Perez 2002)..... 34*

*Figure 2-11. A schematic classification of optimisation algorithms according to their strength of exploitation and exploration (from Sambridge and Mosegaard 2002)..... 36*

*Figure 2-12. Bayesian framework for uncertainty quantification (after Christie et al. 2013) ..... 42*

*Figure 3-1. Seismic top structure and major identified faults modelling (a) is the plan view of the reservoir, (b) is a cross section (Line 1), (c) is a cross section (Line 2) (from Arnold et al. 2013). ..... 48*

*Figure 3-2. Example of three top structural models of the Watt Field (from Arnold et al. 2013). ..... 49*

*Figure 3-3. Uncertainty in fault network models of the Watt Field developed by three different interpreters (from Arnold et al. 2013). ..... 50*

*Figure 3-4. Permeability distribution of the Watt Field model for three different cut-offs. .... 52*

*Figure 3-5. Porosity Permeability (left) and kv/kh (right) plot for Well C (from Arnold et al. 2013)..... 53*

*Figure 3-6. Porosity distributions for well core plug data and neutron density predictions. The two distributions are very similar (from Arnold et al. 2013)..... 53*

*Figure 3-7. 3D model of the Watt Field showing porosity distribution (top) and permeability distribution (bottom) for one geological realisation. .... 54*

*Figure 3-8. Relative permeability curves from Wells A, C and F for the fine sand (left) and coarse sand (right) facies..... 55*

Figure 3-9. Historic production data (oil rate, water rate, cumulative oil production and average reservoir pressure) generated from the truth case model. ....	56
Figure 3-10. 3D view of the Watt Field model showing oil saturation as well as the location of injection and production wells. ....	57
Figure 3-11. Third layer (top) and cross section (bottom) of the Watt Field model showing oil saturation as well as the location of injection and production wells after 40 years of production. ....	57
Figure 3-12. Forecast for cumulative oil production assuming a do-nothing scenario for all realisations after 40 years of production. ....	58
Figure 3-13. Workflow used by SENEX in adjoint based history matching process (from SENEX 2013). ....	63
Figure 3-14. Full Factorial Design for a system with three parameters and three parameter settings (low, medium, high). Each dot connotes a parameter combination (after Astakhov 2012). ....	65
Figure 3-15: Latin Hypercube sampling for a system with two parameters and 6 parameter settings. Each dot represents a parameter combination (after Astakhov 2012). ....	66
Figure 3-16. The evolution of the proxy model as the number of simulations for a single in fill well optimisation problem. (after Zubarev (2009)). ....	67
Figure 3-17. Polymer viscosity model (left) and polymer adsorption model (right) used in this study. ....	71
Figure 4-1. A flowchart describing the entire workflow used in this chapter. ....	74
Figure 4-2. Permeability distribution field of 12 of the 26 geological realisations of the Watt Field model used in this chapter. ....	75
Figure 4-3. Workflow adjoint history matching employed to match the Watt Field model using SENEX (Senex 2013). ....	77
Figure 4-4. History match error minimization speed for 26 geological realisations using the Adjoint technique. ....	79
Figure 4-5. History match error minimization speed for 12 geological realisation using PSO algorithm. ....	79
Figure 4-6. Global history match error for base (blue) and the best-so-far models for Adjoint technique (orange) and PSO algorithm (yellow). ....	80
Figure 4-7. Example of field-based history matching results using the adjoint technique and the PSO method for one geological realization of the Watt Field. ....	80
Figure 4-8. Example of well-based history matching results using the adjoint technique and the PSO method for one geological realization of the Watt Field. ....	81
Figure 4-9. Porosity (bottom) and permeability (top) for the original reservoir model (left), the history matched model (middle) as well as the difference map (right) using an adjoint technique. Note how parameters are changed only in the location of the wells. ....	82
Figure 4-10. Average horizontal and vertical permeability, porosity, and transmissibility for each of the 26 geological realizations before (blue) and after history matching using the adjoint technique (green) and stochastic history matching (yellow). ....	83
Figure 4-11. Permeability distribution for 6 of the 26 realisations of the Watt Field model before (left) and after history matching using Adjoint technique (middle) and PSO (right). ....	84
Figure 4-12. Averages of horizontal permeability (left), vertical permeability (center), and porosity (right) across the 26 geological realizations before (Base) and after history matching using the adjoint method (Adjoint) and stochastic history matching (PSO). ....	85
Figure 4-13. Variance in horizontal permeability (left), vertical permeability (center), and porosity (right) across the best matched cases of 26 geological realizations before (Base) and after history matching using the adjoint method (Adjoint) and stochastic history matching (PSO). ....	85
Figure 4-14. Forecast for cumulative oil production assuming a do-nothing scenario before – unconstrained (left) and after history matching using the Adjoint technique (centre) and PSO technique (right). ....	87

<i>Figure 4-15. Recovery prediction uncertainties based on PSO ensemble (left) and PSO ensemble (right)</i>	87
<i>Figure 4-16. Boxplots of average uncertainties forecast obtained based on the base, Adjoint and PSO Ensemble.</i>	88
<i>Figure 4-17. Boxplots of uncertainties forecast obtained based on the individual 26 realizations of the Adjoint Ensemble.</i>	88
<i>Figure 4-18. Boxplots of uncertainties forecast obtained based on the individual 26 realizations of the PSO Ensemble.</i>	89
<i>Figure 5-1. Flowchart showing the workflow used in this chapter.</i>	93
<i>Figure 5-2. Results from sensitivity analysis using one-parameter-at-a-time approach (left) and response surface (right), showing the operational parameters that have the largest impact on NPV during polymer flooding in the Watt Field.</i>	94
<i>Figure 5-3. 2D plan view of a single geological realization of the Watt Field, showing the initial oil saturation, the location of the injector wells and the location of major faults.</i>	96
<i>Figure 5-4. Response surfaces for the NPV computed using polynomial regression for 16 training runs (left), 100 training runs (centre), and 160 training runs (right).</i>	98
<i>Figure 5-5. Response surfaces for the NPV computed using Artificial Neural Network for 16 training runs (left), 100 training runs (centre), and 160 training runs (right).</i>	99
<i>Figure 5-6. Comparison of NPV predictions for the full-physics simulations and for the proxy models for three different geological realizations of the Watt Field</i>	99
<i>Figure 5-7. Optimization convergence of Full Physics (left) and Proxy-Based optimization(right) for three geological realization.</i>	102
<i>Figure 5-8. Absolute NPV for waterflood optimisation for Unconstrained, Adjoint and PSO ensemble.</i>	103
<i>Figure 5-9. 3D view and cross section of the Watt Field model showing oil saturation as well as injection and production wells after 40 years of waterflood (left) and polymer flood (right).</i>	104
<i>Figure 5-10. Optimal polymer concentrations (left) and location of injector wells (centre) for the unconstrained optimization (blue) and for optimization after history matching using the adjoint method (green) and stochastic history matching (yellow), and the range in NPV based on different geological uncertainties (right). TS refers to the Top Structure of the individual models, FM to the Fault Models, CO to the Cut Off value for the net-to-gross ratio, and MM to the Modelling Methods.</i>	105
<i>Figure 5-11. Incremental NPV for the the unconstrained optimization (Base Case) and for the optimization after history matching using the adjoint method and stochastic history matching.</i>	105
<i>Figure 5-12. Absolute NPV for the the unconstrained optimization (Base Case) and for the optimization after history matching using the adjoint method and stochastic history matching.</i>	107
<i>Figure 5-13. Cumulative oil production forecast for the unconstrained optimization (left) and for the optimization after history matching using the adjoint method (centre) and PSO-based history matching (right).</i>	107
<i>Figure 5-14. Incremental oil recovery for the unconstrained optimization (left) and for the optimization after history matching using the adjoint method (centre) and stochastic history matching (right). The different colours correspond to different top structures in the reservoir model.</i>	108
<i>Figure 5-15. Cross-comparison of the optimal NPV for three different geological realizations (top to bottom) considering unconstrained and two constrained optimization techniques (left to right columns). During this cross-comparison, the optimal polymer flood design for one realization is deployed to all other 25 geological realizations to estimate the risk of using an incorrectly optimized polymer flood for a given reservoir geology by comparing the NPV for and optimized water flood (blue), NPV for the “right” optimal strategy (red) and NPV for the “wrong” optimal strategy for each realisations (light blue).</i>	109

*Figure 5-16. Boxplots of average absolute NPV uncertainties forecast for waterflood (left) and polymer flood (right)..... 111*

*Figure 5-17. Cumulative Probability distribution of average absolute NPV uncertainties forecast for waterflood (left) and polymer flood (right)..... 111*

## List of Tables

Table 1-1. Review of current, planned, and ongoing polymer flood projects across the globe (from Sheng et al, 2015). ..... 10

Table 3-1. Table of uncertainties considered in the Watt Field model. The combination of grid resolution, top structure, fault model and facies cut-off uncertainty results in 81 different realizations. .... 47

Table 3-2. Key Parameters of the Watt Field model..... 56

Table 3-3. Uncertain reservoir properties adjusted during history matching..... 61

Table 3-4. Input parameters used in PSO algorithm..... 61

Table 3-5. Metropolis-Hasting MCMC Algorithm (Liang et al.2010) ..... 69

Table 5-1. Operational parameters for polymer flood (see Figure 5 3 for well locations). ..... 96

Table 5-2. Input Parameter and ranges for uncertainty quantification..... 97

Table 5-3. The R2 Training (Train) and Verification (Ver) values of Polynomial regression and RBF Neural Network for three geological realizations of the Watt Field. .... 98

Table 5-4 Optimal injection rates for all the 7 polymer injectors in bbl/day..... 102

Table 5-5. Absolute NPV for Full Physics and Proxy-Based Polymer Flood Optimization of the three realizations of the Watt Field ..... 103

---

## List of Publications

---

1. **E. Ibiam**, S. Geiger, V. Damyanov, and D. Arnold, “Optimisation of Polymer Flooding in a Heterogeneous Reservoir Considering Geological and History Matching Uncertainties”, SPE Reservoir Evaluation and Engineering, SPE-200568-PA, 2020.
2. **E. Ibiam**, S. Geiger, A. Almaqbali, V. Damyanov, and D. Arnold, “Numerical Simulation and Optimisation of Polymer Flooding in a Heterogenous – Constrained vs Unconstrained Optimisation”, - SPE Nigeria Annual International Conference and Exhibition, Lagos, Nigeria, SPE – 193400 – MS, 2018.
3. **E. Ibiam**, S. Geiger, V. Damyanov, and D. Arnold, “Numerical Simulation and Optimisation of Polymer Flooding in a Heterogenous – Unconstrained Optimisation”, - 80th EAGE conference and Exhibition, Copenhagen, Denmark, 2018.
4. **E. Ibiam**, S. Geiger, D. Arnold, and V. Demyanov, “Optimizing Two Possible EOR Methods Considering Complex Geological Uncertainty” 79th EAGE Conference and Exhibition, Paris, France 2017.

# Chapter 1. Introduction

## 1.1. Energy Market

Population growth and the need to increase living standards and GDP impact energy consumption. The global population is expected to increase from 7.5 billion to 9.2 billion people between the years of 2019 and 2040 according to a report by ExxonMobil Corporation (Figure 1-1), with most population growth occurring in countries that are non-members of Organisation for Economic Cooperation and Development (OECD). Global GDP is expected to increase by 3.5 percent from 2016 and 2040 on a year-on-year basis with large part of the growth taking place in non-OECD developing countries as well (OPEC 2017). Therefore, oil demand is predicted to increase between 95.8 million BOPD in 2016 to 111.3 million BOPD in 2040 as a result of the massive increment in both global population and GDP (OPEC 2019). ExxonMobil and BP outlook also have similar projections, where they predict that oil and natural gas will be required to meet more than half of the global energy demand by 2040 as shown in Figure 1-2 and Figure 1-3, respectively. Economic growth and prosperity in developing countries will largely be driven by fossil fuels especially for transportation, as it is cheaper (Gibbs 2017). Consequently, oil will remain an important player in the economic growth of developing countries. From a global point of view, oil will still be the dominant part of the global energy mix between 2015 and 2040 (Figure 1-3).

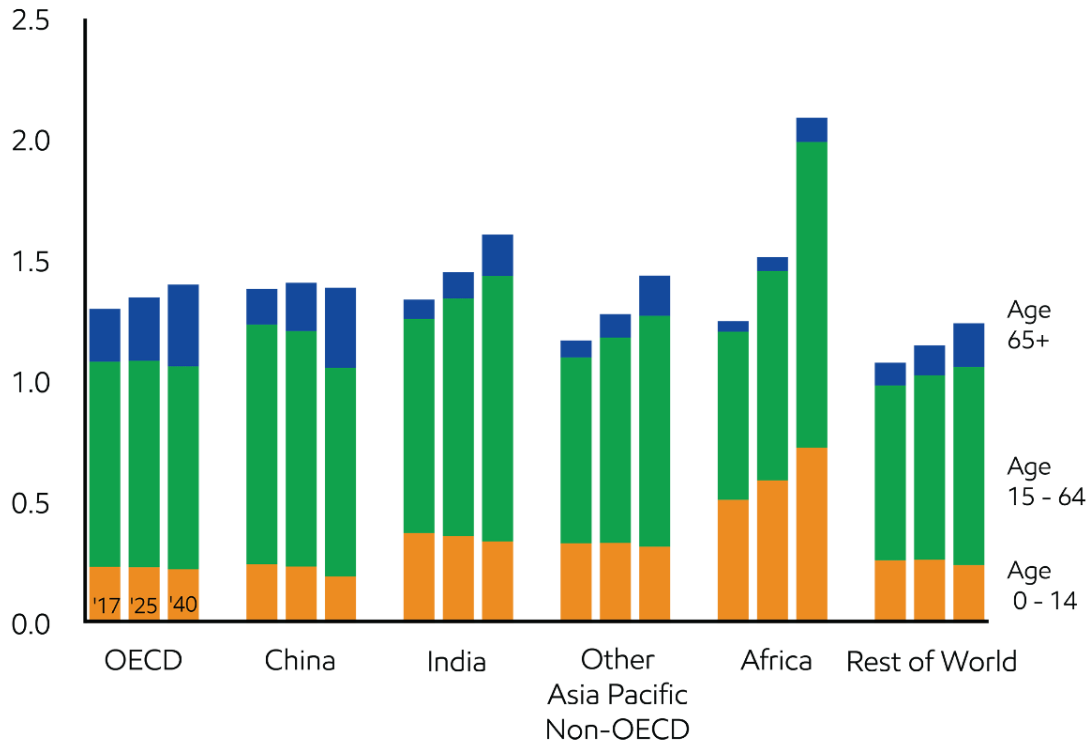


Figure 1-1. The projected demographic of the global population (billions of people) by age and countries (from ExxonMobil Corporation 2019)

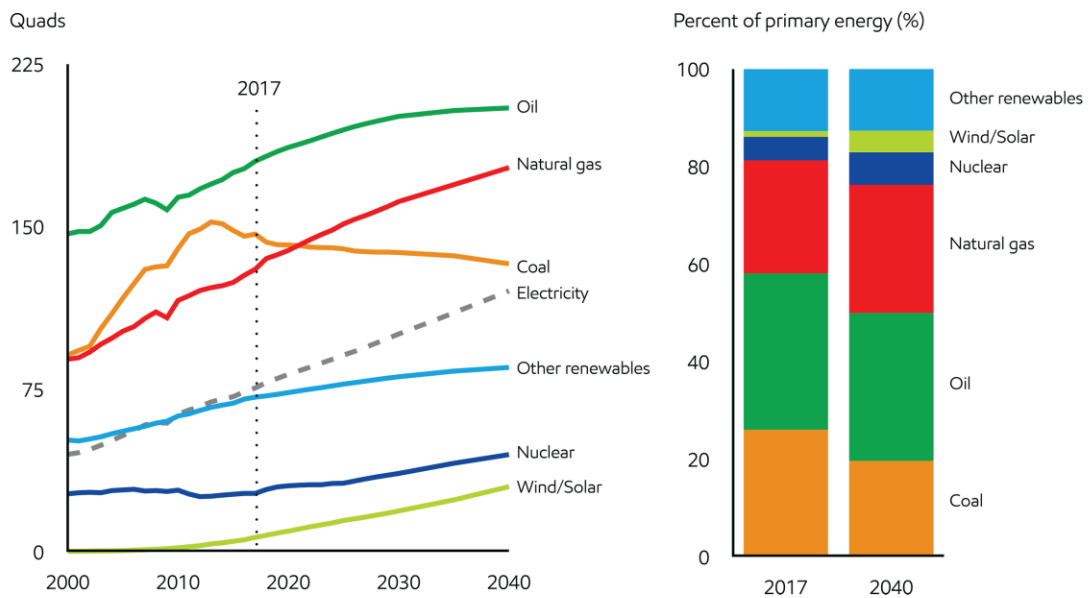
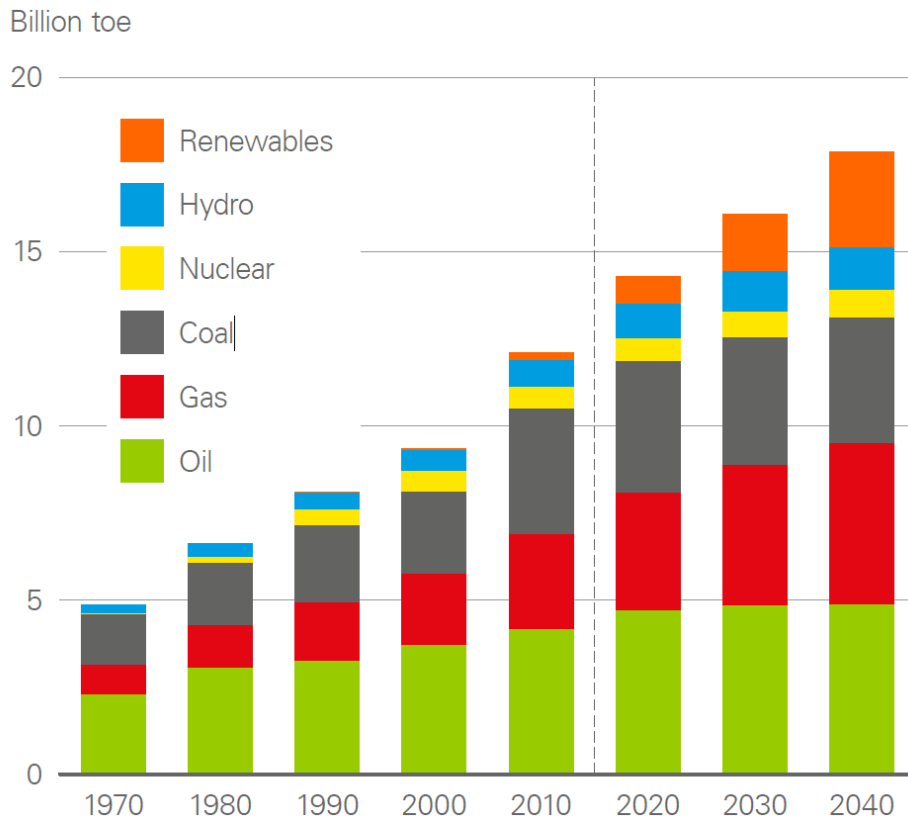


Figure 1-2 The global energy mix shifts to lower carbon fuel (from ExxonMobil Corporation 2019)



*Figure 1-3 The global energy mix shifts to lower carbon sources (after BP 2019)*

Prior to the last decade, the assumption was that oil was going to be exhausted, which led to the research of techniques to boost oil recovery from mature oil fields, including Enhanced Oil Recovery (EOR) (Total E&P 2017). Nonetheless, about ten years ago, there has been a change in discussion from the prediction of peak oil supply to the prediction of peak oil demand. A great number of economists are now convinced that global oil consumption should hit its peak demand in 10 to 30 years followed by a decline in demand (Dale and Fattouh 2018). The recent focus on oil demand trend is motivated by numerous factors, including the restructuring of energy and environmental policies on the fossil fuel industry to help mitigate global warming.

When oil prices crashed in 2015, oil companies have reduced exploration and EOR projects, focusing more on maintaining oil production capacity and developing new oil fields. Figure 1-4 shows that this behaviour has led to a downward trend of oil field discoveries that reached a 70-year low in 2018. Currently, the impact of COVID-19 outbreak which has created a short-term oversupply of approximately 16 million barrels a day and also the Vienna Alliance that is falling apart will continue to further suppress exploration activities and therefore new discoveries will continue to be on the decline (Figure 1.4). Rystad energy has predicted the discovered volume in 2020 may be lower than the historic low of 2018 (Rystad Energy 2020). The low investment to explore for and develop new oil fields might not have a short-term impact. However, in the long



term, about a decade from now, a supply crunch may occur which will push oil prices up again (Bouso 2017; Crooks and Ward 2017).

About 60% of the world oil production has been coming from mature fields and the rate of discovering new reserves has been declining steadily over the past two decades (Manrique et al. 2010). In order to meet the increasing energy global demand, it is important to apply EOR techniques to these known and existing reserves (Manrique et al. 2010).

The recovery factor of a typical oil and gas field globally is approximately 40% at after secondary recovery process such as gas flooding and water flooding (Sandrea and Sandrea 2007). This implies that about 60% of the initial oil in place is left unrecovered due to the following reasons: 1) Heterogeneity in rock permeability and by gravitational segregation of the reservoir fluids, 2) Low proportion of the reservoir volume connected to the wells i.e. the presence of sealing faults or other flow barriers which may lead to disconnected compartments of oil that are not in pressure communication with the entire reservoir, or 3) Capillary trapping in pores. Therefore, the need arises to devise advanced means to recover this residual oil in the reservoir if the oil price is right. Enhanced Oil Recovery is a tertiary recovery mechanism in which fluid (the displacing phase) is injected into the reservoir to alter the property of reservoir fluid and therefore mobilize residual oil which then leads to increased recovery of the oil initially left behind. However, it is important to note that most EOR processes are more expensive than secondary recovery processes and only become economically attractive for larger oil fields and at high oil prices (Core 2013).

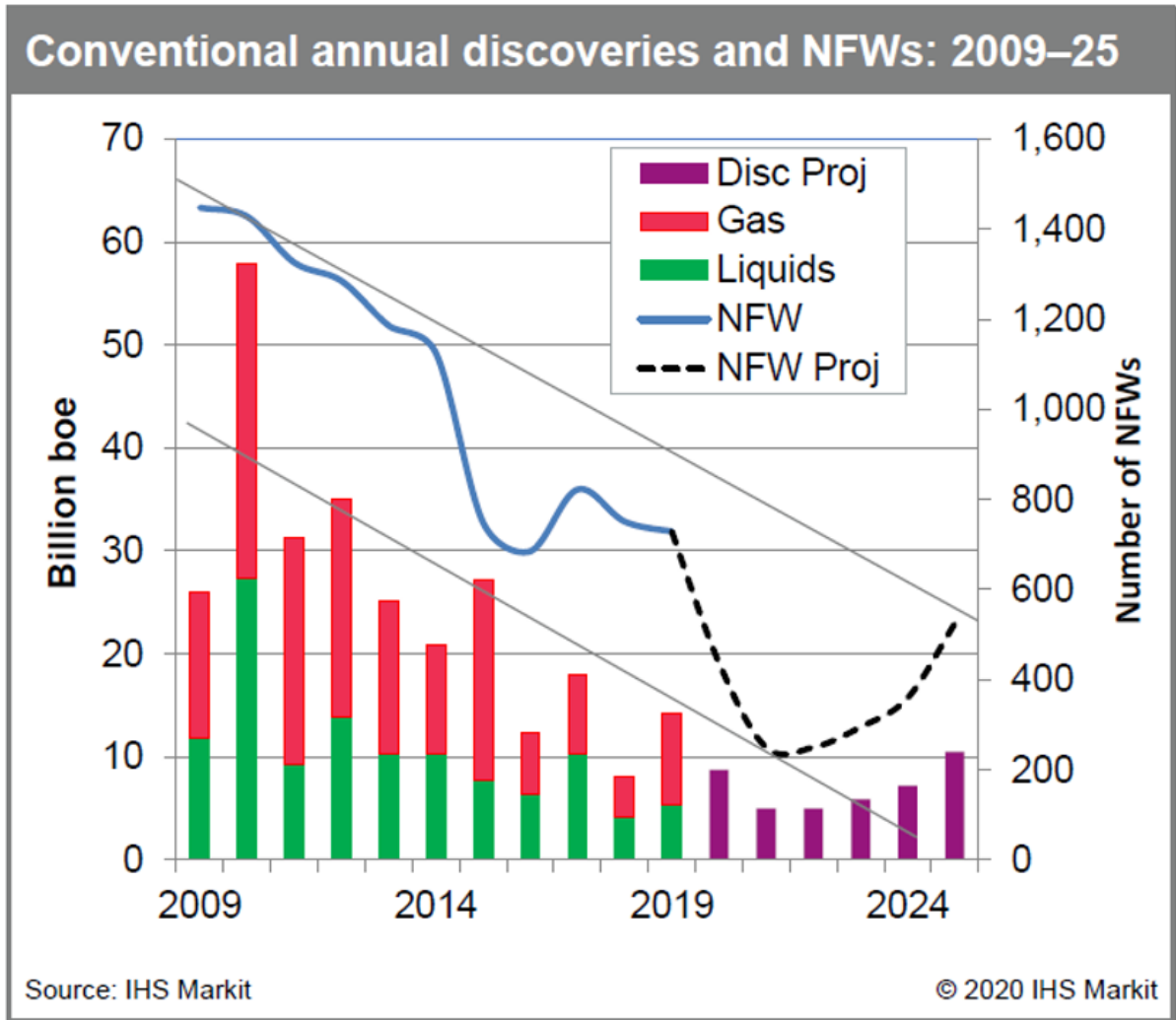


Figure 1-4 Oil and gas field discoveries in Barrels of Oil Equivalent (BOE) and downturn in conventional exploration (number of new field wildcat wells, NFWs) (IHS Markit 2020).

## 1.2. Enhanced Oil Recovery

There are three different recovery stages in a conventional oil reservoir: primary, secondary, and tertiary (Figure 1-5). Primary recovery involves the production of oil in a reservoir using its initial natural energy without any external intervention to boost production. Water influx from aquifers, rock and fluid expansion, gas cap, solution gas or the combination of these mechanisms are the sources of natural energy (Sheng 2011). At the secondary recovery stage, the reservoir no longer possesses enough energy to produce oil naturally for a long period of time and therefore supplemental energy is applied to recover more oil. Secondary recovery involves injection of water or gas into the reservoir for pressure maintenance and to displace oil to the producing wells. Lastly, tertiary recovery refers to a process where special materials and fluids are injected

in the reservoir once secondary recovery options are exhausted. Tertiary process usually involves injecting chemicals mixed with water, miscible gas, or thermal energy (Lake et al. 2014).

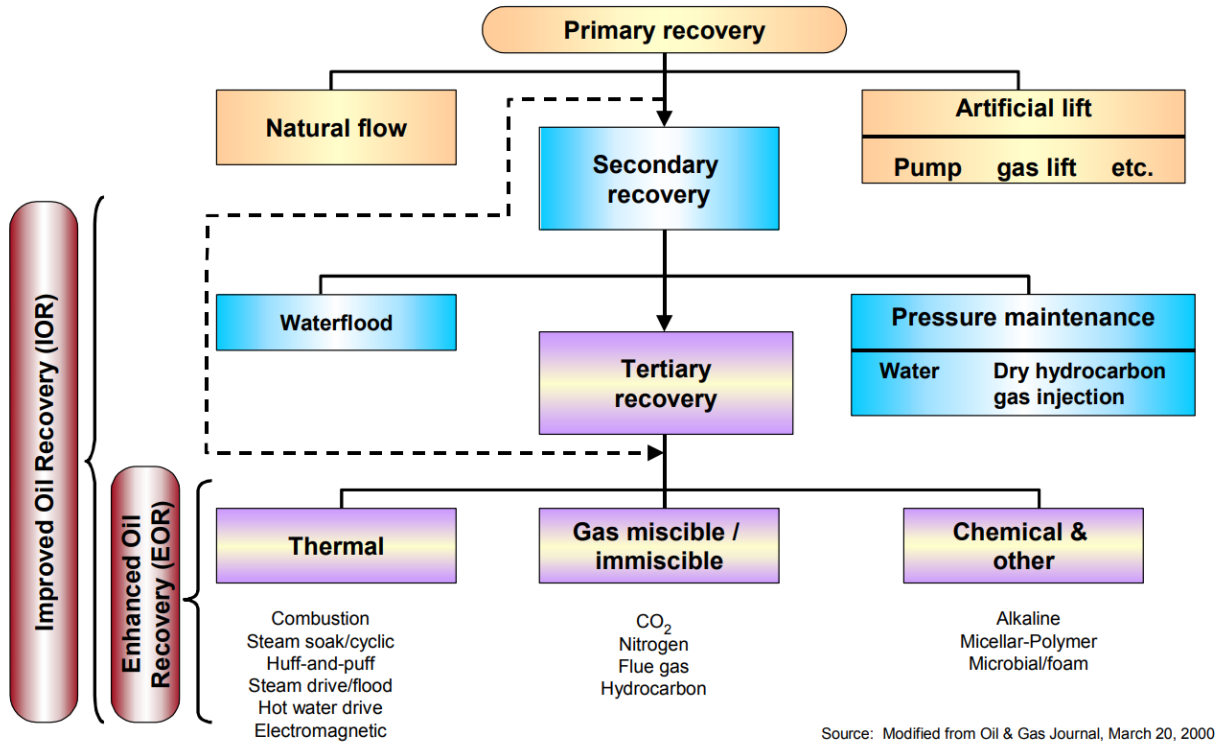


Figure 1-5 Recovery mechanisms in a conventional oil and gas reservoir (from Oil & Gas Journal 2000).

The description above shows a conventional order of developing a field. However, in practice, it can be more profitable to initiate tertiary process as soon as possible in the field development. For instance, BP started up production of Clair Ridge in 2018 with the deployment of Low Salinity EOR from the first day (BP 2018). EOR is different from Improved oil Recovery (IOR) in that EOR describes the injection of fluid into the reservoir which, in addition to pressure maintenance, also enhances displacement efficiencies. In contrast, IOR also considers infill drilling, horizontal well drilling, workovers, and EOR process. Hence, IOR is a broader term which can be applied to any depletion stage (Lake et al. 2014; Sheng 2011). A key performance indicator of an EOR project is how much incremental Net Present Value (NPV) can be realized compared to the NPV of the current field development plan (Lake et al. 2014; Sheng 2011).

### 1.3. Polymer Flooding in Field Applications

Polymer flooding is a technique of achieving a more favourable mobility ratio, and hence improve macroscopic sweep of a water flood process. Polymer flooding has the potential to recover a significant increment of the oil original in place, typically, 8% at an additional cost between US\$8 and US\$16 per incremental barrels (Muggeridge et al. 2014). However,

increasing the viscosity of the injected fluids poses injectivity challenge where it becomes difficult to inject polymer into the reservoir. More so, the resultant solutions are susceptible to shear damage at high shear rates. At high temperatures, polymer molecules become unstable and may result in degradation. Polymer flooding is usually considered to be a tertiary recovery technique. However, early studies suggested using polymer as a secondary recovery method. Studies by Pye (1964), Sandiford (1964) and Schurz (1964) all recommended to use polymers in an augmented secondary waterflood. In general, it is advisable to start any EOR process as soon as possible provided the oil price is high enough (Bondor 2011). Polymer flooding is no exception, and early injection of polymers will lead to a more effective displacement compared to a tertiary polymer flood, in addition to limiting the problems associated where additional water production. However, early polymer flooding in green fields incurs additional risks because the reservoir description is more uncertain compared to mature fields and thus future reservoir performance is more difficult to forecast. As a result, the economic benefits of an early polymer flood compared to a regular water flood are difficult to quantify. Reservoir simulation is a valuable tool to carry out comprehensive and rigorous screening to evaluate the financial risk associated with polymer flooding (Sorbie 1991). However, reservoir models do not capture all the geological uncertainties and uncertainties associated with the flow of polymer in porous medium. Therefore, to sufficiently predict the downside and upside of a polymer flooding, it is necessary to have adequate reservoir models that account for a realistic range of uncertainties relevant to the geology and modelling decision instead of perturbing a single base case (Bentley & Ringrose 2017). To increase the reliability of the forecast, reservoir simulation models are tuned such that the simulated dynamic response matches the production data, this process is known as history matching.

Standnes and Skjevrak (2014) reviewed 72 different polymer floods (66 of which were onshore) that date back to 1964; 92% of projects used Hydrolysed form of Polyacrylamide (HPAM) as a polymer. Of these 72 floods, 40 were considered a success on a technical level, 6 failed, 11 promising, 10 too early to determine and 5 not evaluated. The reasons for failure were due to a poor design process which led to underperforming floods by either injecting small slug sizes (17% Pore Volumes in comparison to 34% Pore Volumes in successful floods) or low polymer concentrations. It is worth noting that the success rate was higher in secondary flood polymer floods compared to tertiary floods.

The international Energy Agency (IEA) estimated about 375 EOR projects worldwide (Figure 1-6) produced slightly more than 2 million bbl/day in 2018. The forecast this could grow to 4.5 million bbl/day or about 4% of global production by 2040 (Figure 1-7)

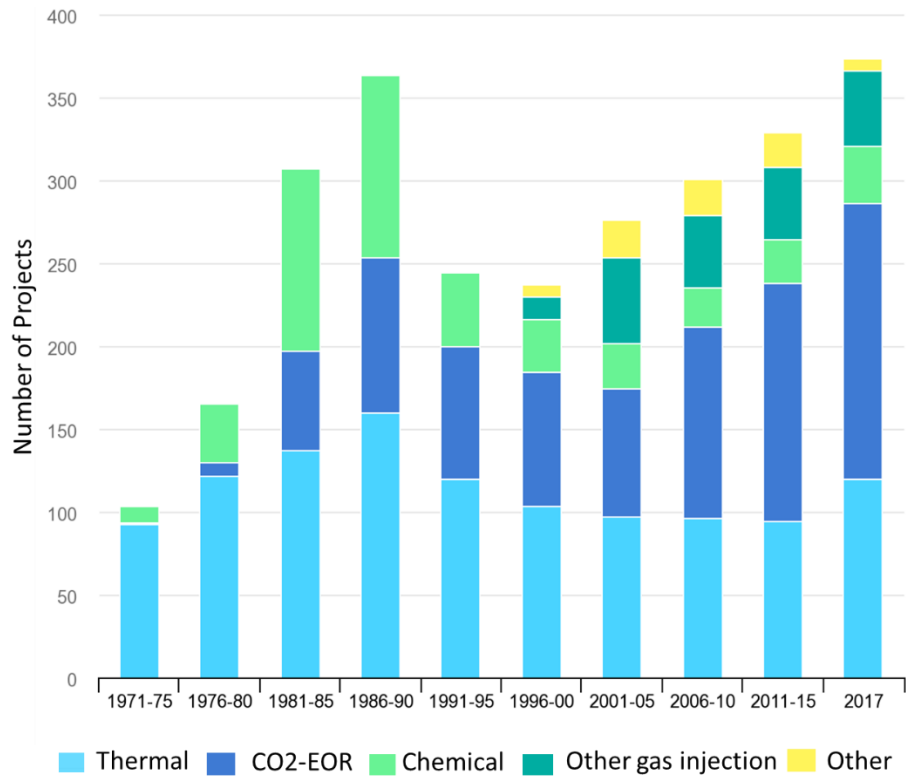


Figure 1-6 Global EOR projects at different points in time (IEA 2020).

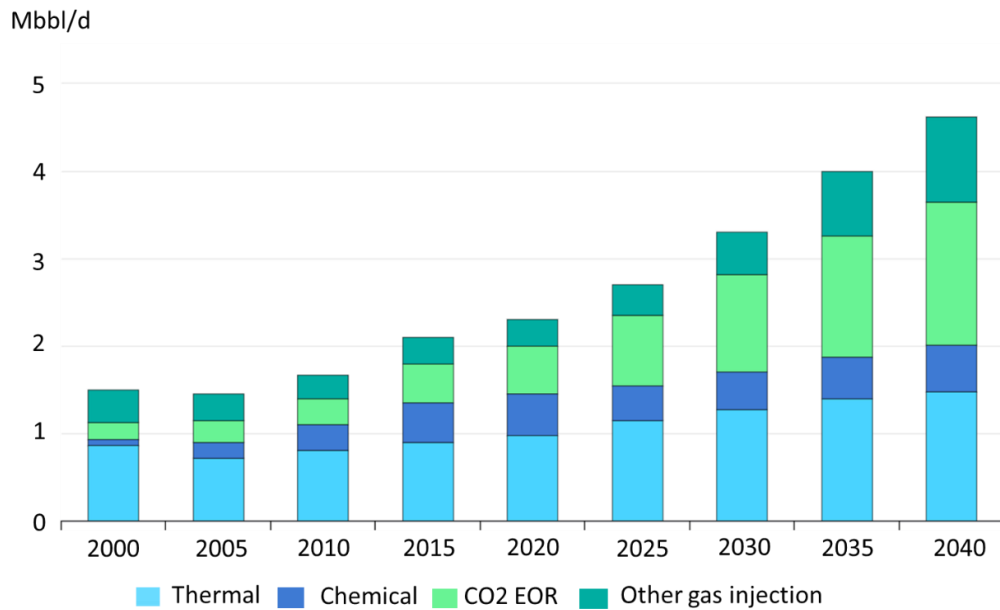


Figure 1-7 Estimated contribution of different EOR methods to global oil production (IEA 2020)

### 1.3.1. Current Polymer Projects

The contribution to the world's oil production from polymer flooding is estimated at about 80,000 bbl/day in 2020. The forecast show that the contribution from polymer flooding could grow 120,00 bbl/day by 2029 (Figure 1-8).

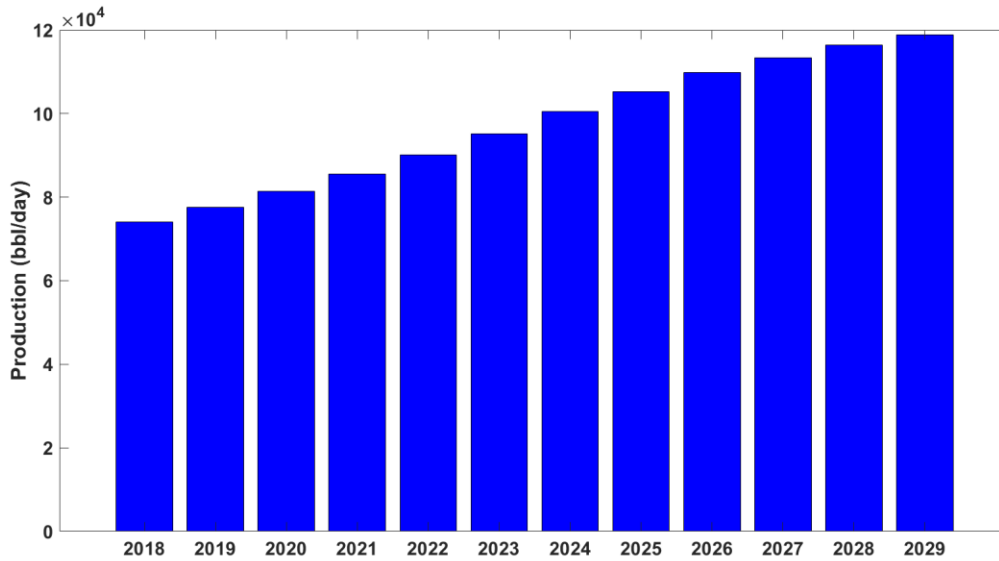


Figure 1-8 Estimated contribution of polymer flooding to global oil production (South et al. 2018)

Despite the limited contribution of chemical EOR methods to global oil production, the potential for polymer flooding is significant. It is estimated that an additional 2,100MMstb of oil could be recovered from the North Sea alone using polymer flooding (McCormack et al. 2014). Table 1-1 shows results from a global survey by Sheng et al. (2015) that indicates that over 700 pilot and large-scale polymer flood projects are either currently executed or are in the planning phase. The average incremental recovery across the projects that are currently under operation is 6.7% while the water cut could be reduced by 13%. In addition, polymer flooding can also be combined with other chemical EOR methods, including but not limited to low salinity flooding or surfactant floods, which show significant incremental recoveries in laboratory experiments but need a more stable oil price environment to move to pilot stages (Muggeridge et al. 2014).

*Table 1-1. Review of current, planned, and ongoing polymer flood projects across the globe (from Sheng et al, 2015).*

<b>Angola</b>	1	<b>Indonesia</b>	1
<b>Argentina</b>	11	<b>Kuwait</b>	1
<b>Australia</b>	1	<b>Mexico</b>	1
<b>Austria</b>	1	<b>Nigeria</b>	1
<b>Brazil</b>	2	<b>Oman</b>	2
<b>Canada</b>	50	<b>Poland</b>	1
<b>China</b>	67	<b>Romania</b>	3
<b>Colombia</b>	1	<b>Russia</b>	2
<b>France</b>	5	<b>Suriname</b>	1
<b>Germany</b>	12	<b>Trinidad</b>	1
<b>Hungary</b>	1	<b>UK</b>	1
<b>India</b>	6	<b>USA</b>	560

The most successful polymer flooding projects are located in China, and specifically the projects in the Shengli and Daqing oil fields have caused other countries to reconsider the application of chemical EOR (Kokal and Al-Kaabi 2010). The Daqing field is the world’s largest polymer flood project. Polymer flooding research in the Daqing field commenced in the early 1970s, followed by a pilot test in 1990 where an increase of 14% in recovery was observed in a single-layer test and an increase of 11.6% in a double layer-test (CNPC 2016). In 1996, a large-scale polymer flooding commenced in the northern section of the field. The polymer flooding at Daqing field has yielded an average incremental recovery of 11% compared to a water flood, and a decrease in average water cut of approximately 24.8% (Wang and Liu 2006). Another important polymer flooding project is located in Oman in the Marmul field, which at 90 cp contains the highest viscous oil in the Arabian Gulf (Delamaide 2014). The first pilot at the Marmul field commenced in 1986 but full-field polymer flooding did not start until 2010 due to low oil price. 6.3 million barrels of incremental oil were produced from the Marmul field by December 2013 (Oil & Gas News 2015). The world’s first offshore polymer flooding project is the Dalia field in Angola, which went on production in 2006 and where a feasibility study showed that polymer flooding would be economical even during the early stages of the field development (Morel et al. 2008).

Overall, polymer flooding has been tested and proven to be successful and possesses a lot of promising opportunities to recover more oil. However, it requires adequate risks and uncertainty quantifications as the economics can be very challenging, which is the reason they are not widespread. Therefore, there is a need to develop a robust workflow that will integrate the interpretation and geological uncertainties as well as uncertainties associated with the history matching process in the optimisation of the NPV of polymer flooding in a heterogenous clastic reservoir.

The novelty of this thesis is the detailed investigation of how different history matching approaches and optimization methods impact the predicted performance and optimal design of a

polymer flood. We show that an optimized polymer flood is beneficial compared to an optimized water flood even if geological uncertainties are not represented adequately in the reservoir models. Although the specific experimental design techniques (i.e. Latin Hypercube Sampling) and optimization algorithm (i.e. Particle Swarm Optimisation) are not new, the application of the experimental design and proxy modelling workflow to analyse polymer flooding to complex heterogeneous reservoirs has not been widely reported.

## 1.4. Research Objectives and Scientific Hypothesis

The objective of this thesis is a detailed analysis on the performance of a particular and well-established EOR mechanism, polymer flooding, while considering a range of uncertainties. On the one hand, uncertainties related to the reservoir geology are studied, including but not limited to the depth of top structure, presence fault networks, net-to-gross, cut-offs, and the actual reservoir modelling approach. On the other hand, a reservoir model is also calibrated to the observed data during history matching to analyse the success of possible EOR schemes. History matching introduces another source of uncertainty as history matching is an ill-posed problem, and different history matching methods can lead to different production forecasts and uncertainty estimates. This thesis therefore aims to investigate how different history matching techniques impact our ability to predict the optimal strategy of a polymer flood while considering geological uncertainties and analyses of the subsequent financial upsides and downsides.

Scientifically, the central hypothesis of this thesis is that reservoir models that have been history matched for a different displacement process may not capture the relevant geological structures needed to predict an EOR process, which changed fluid-rock interactions, adequately. Ringrose and Bentley (2015) used the so-called “Flora’s rule” to explain that the same geological heterogeneity impacts reservoir dynamics in different ways, depending on the fluids that are present in the reservoir or injected into the reservoir.

More specifically, this thesis aims to answers to the following research questions:

1. How do different history matching techniques affect our ability to forecast the performance prediction of a waterflood and polymer flooding?
2. Are the optimal polymer flooding deployment strategies obtained from fast proxy-based optimization different from optimization methods that use a full physics simulation?
3. How do geological uncertainties affect the prediction and performance of Polymer flooding?
4. How is this risk assessment affected by the history matching procedure?
5. What is the value in terms of risk assessment of history matching different realizations of geological models before carrying out polymer flooding optimization?

The answers to these research questions are obtained through the following objectives:

1. Generate an ensemble of a history matched models which account for uncertainty in reservoir geology using an adjoint technique and particle swarm method.



2. Carry out uncertainty quantification of each ensemble using Markov Chain Monte Carlo (MCMC) with proxy algorithm to assess how history matching techniques impact the prediction of uncertainty.
3. Optimise and compare a polymer injection strategy using the history matched ensembles from Step 1 (constrained optimisation) and also the original reservoir model ensemble (unconstrained optimisation).
4. Compare and contrast the results of the proxy-based method of optimization and full-physics optimisation.
5. Carry out uncertainty analysis and risk assessment of waterflood and polymer flooding using a proxy based MCMC technique.

## 1.5. Structure of Thesis

Chapter 1, this chapter, provided an overview of the world's energy market, the role oil and gas play in meeting future energy demand, and under which circumstances EOR projects can contribute to future oil production. The remainder of thesis is organised in as follows:

Chapter 2 presents the literature review on EOR, with specific emphasis on polymer flooding. This chapter discusses the types and structure of polymers used for EOR, properties of polymer solutions, and the phenomena of polymer flooding in porous media. This chapter also reviews different history matching methods, including the classification of assisted history matching techniques such as deterministic methods, stochastic sampling, and data assimilation. Chapter 2 finally ended with a review on uncertainty quantification techniques and geological parameterisation.

Chapter 3 provides a detailed description of the Watt Field, which is the semi-synthetic reservoir used in this study. Chapter 3 describes the methodology and provides the specific information about the history matching and optimisation techniques that are used throughout the thesis.

Chapter 4 explains how the ensembles of history matched models were generated using the adjoint technique and particle swarm method. The chapter further investigates how this resulting history matched models impact future reservoir performance forecasts.

Chapter 5 presents the results and detailed analysis from the optimisation of the polymer flood, using the two history matched reservoir model ensembles but also the original ensemble that was not history matched. The optimisation also includes a cross-comparison of different reservoir models and optimisation strategies to assess the financial upsides and downsides when optimising a polymer injection under geological uncertainty. Furthermore, MCMC with Proxy-based Acceptance-Rejection (PAR) were used to compute the Posterior Probability Function (PPF) of the three different ensembles.

Chapter 6 concludes the thesis, summarising the key outcomes and providing suggestions and recommendations for future research.

## Chapter 2.

## Literature Review

### 2.1. Introduction

The reasons for low oil recovery factor in reservoirs are both technical and economical. During primary recovery, there is usually insufficient energy in the system to lift all the oil. If water injection is introduced to provide pressure support and sweep oil towards the production wells, the injected water may bypass oil due to viscous fingering and/or geological heterogeneity. Economically, over the course of the lifecycle of a well, a point is always reached where the cost of producing an additional barrel of oil is higher than the price for that barrel of oil. When this point is reached, the well is abandoned with as much as 70% of the oil unrecovered in the reservoir (Lake et al. 1992). Therefore a substantial percentage of oil in place cannot be recovered by the conventional techniques and may become the target for Enhanced Oil Recovery (EOR) to increase the recovery factor (Zekri et al. 2000).

EOR techniques, such as polymer injection and Water Alternating Gas (WAG) injection, offer the potential to recover more oil and extend the life of a mature oil field that has been undergoing a water flood, which is helped by the often much-improved understanding of the reservoir geology and reservoir dynamics after many years of production and data gathering (Abu-Shiekh et al. 2012). The primary aim of all EOR methods is to increase the volumetric (i.e. macroscopic) sweep efficiency and to enhance displacement (i.e. microscopic) efficiency, which can be achieved in two ways. First, volumetric sweep can be increased by reducing the mobility ratio between the displacing and displaced fluid, which reduces the tendency of viscous fingering. Second, the effect of capillary trapping can be reduced by lowering the interfacial tension between the displacing and displaced fluids. Both mechanisms reduce the residual oil saturation and increase ultimate recovery. Therefore the final recovery factor depends upon the microscopic displacement efficiency and volumetric sweep efficiency of the displacement front (Chierici 1995).

A review by Manrique et al. (2010) indicates that thermal and chemical EOR processes dominate in sandstone reservoirs while gas and water-based recovery methods dominate in carbonate and turbidite reservoir. Applying EOR in offshore fields is more complex compared to onshore fields because of the well-spacing, limited space for new surface facilities, and environmental regulations. Lithology impact EOR both in onshore and offshore. Figure 2-1 illustrates the design and implementation steps that are needed when planning an EOR programme, from the initial data collection and management, to screening and laboratory studies, to reservoir simulation, pilot tests, and finally full field implementation.

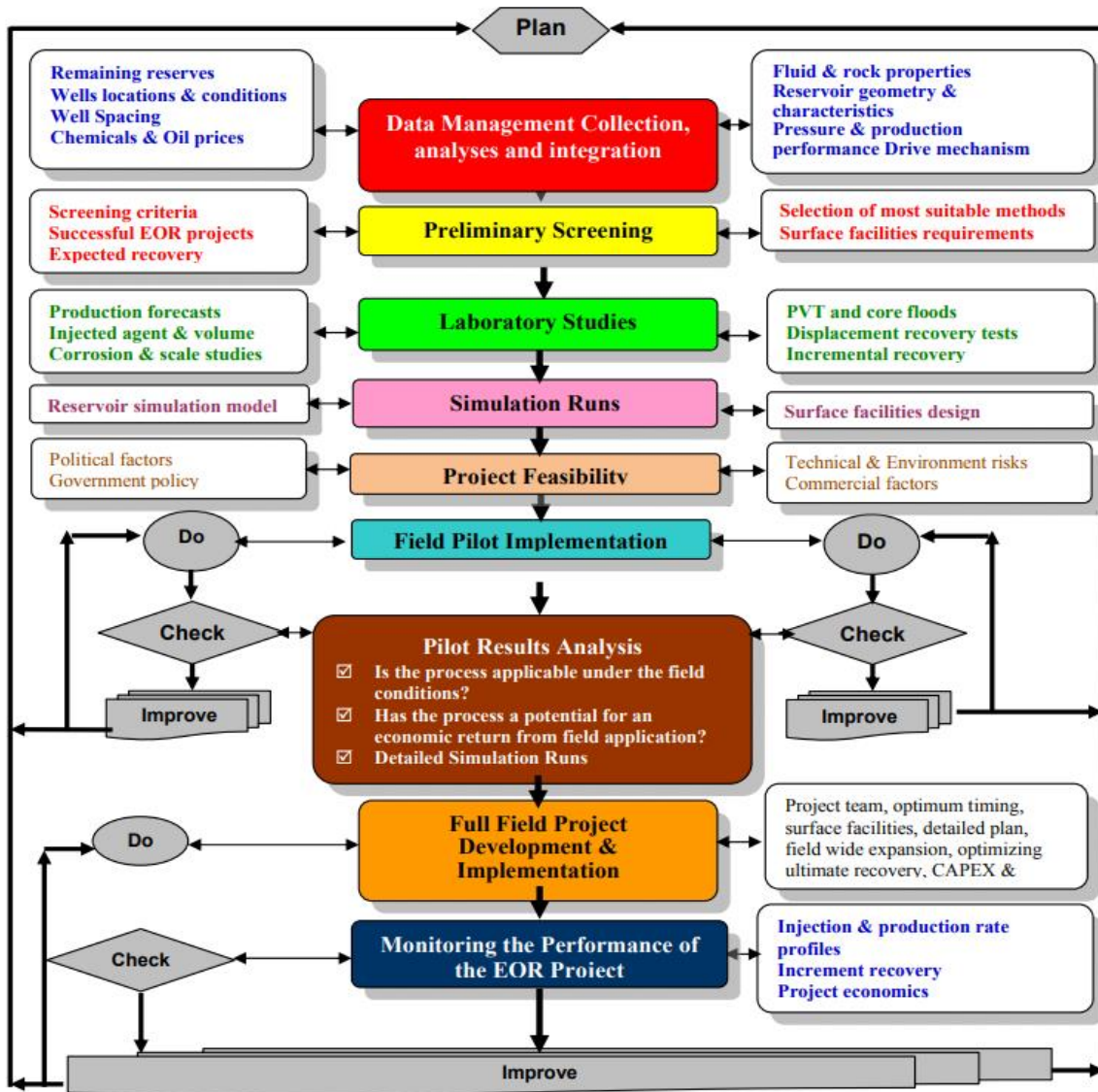


Figure 2-1. Design and implementation steps of a comprehensive EOR program (from Abu et al. 2014).

EOR methods can be separated into four generic classes, chemical methods, thermal methods, gas injection, and microbial methods, which are discussed in more detail below (Tunio et al. 2011).

- I. **Chemical methods** include polymer flooding, surfactant flooding, and alkaline flooding, or a combination, therefore. These methods aim to change the way the displacing and displaced fluids interact by altering the chemistry of the injected (displacing) fluids. More specifically, polymer flooding is the process of injecting polymers into the reservoir which lowers the mobility ratio between the injected fluid and reservoir fluid, thereby reducing viscous fingering, increasing macroscopic sweep efficiency, and delaying water breakthrough. Surfactant flooding involves the addition of surface-active chemicals (surfactant) to the injected water, which reduces the interfacial tension between the displacing and displaced fluid, i.e. decrease the capillary forces that trap oil in the pores of the reservoir rock. Alkaline flooding is a process where alkaline chemicals such as sodium hydroxide, sodium carbonate or sodium orthosilicate are added which react with in situ fluids to reduce interfacial tension between oil and water resulting in lower residual oil saturation (Broome et al. 1986). Foam flooding is another form of chemical EOR where foam is injected or generated within the reservoir to mitigate sweep inhomogeneities caused by high permeability layers or gravity override (Sheng 2011a).
- II. **Gas injection** includes the injection of CO<sub>2</sub> or N<sub>2</sub> into the reservoir, either at miscible or immiscible conditions. Gas injection improves the displacement efficiency by eliminating or lowering the interfacial tension between the oil and the displacing fluid (gas). If deployed after water flood it has the potential to re-establish a pathway to recover the remaining oil thereby reducing residual oil saturation (McGuire et al. 1995). The disadvantage of gas injection is lower macroscopic sweep efficiency because the displacing phase (gas) has a lower viscosity and density than oil, and are adversely impacted by viscous fingering, heterogeneity and gravity (Claridge 1972). Gas injection can also be combined with water injection in the form of Water Alternating Gas (WAG) injection. WAG is an efficient EOR method because it combines the benefits of gas injection to reduce oil saturation and water injection to improve mobility control and frontal stability (Lake et al. 1992).
- III. **Thermal methods** add heat to the reservoir to lower the viscosity of the reservoir fluid, and in some cases to vaporise the oil. Thermal methods are mainly applied to heavy oil reservoirs although they have been used to accelerate gravity drainage in more conventional reservoirs as well. Heat can be added to the reservoir through cyclic steam injection, steam injection or in situ combustion applied (Bera and Babadagli 2015). Thermal EOR is the most popular EOR, representing about 67% of the global EOR applications (Mokheimer et al. 2019). Steam-Assisted Gravity Drainage (SAGD) is widely used in oilfields in Canada yielding relatively high oil recovery factor between 60 to 80% (Mokheimer et al. 2019).
- IV. **Microbial methods** aim to manipulate the function or structure, or both, of the microbial environments existing in oil reservoirs in order to improve the recovery of trapped oil and extend the life of a reservoir (Bryant and Burchfield 1989). The mechanism of microbial methods includes, flow diversion, in situ upgrading, wettability modification and

generation of biosurfactants within the reservoir. Microbial methods result in reduction of the oil/water interfacial tension, promotes emulsification and leads to improvement in oil recovery from the reservoir (Bryant and Burchfield 1989). Microbial EOR has not been widely applied even though it was first proposed in 1947, this is because of the difficulty to predict its performance in the field (Muggeridge et al. 2014a).

## 2.2. Geological Uncertainty

Geological uncertainty is a major challenge that are encountered in reservoir modelling and simulation. Uncertainty is introduced due to the incomplete understanding of the geology and lack of data to populate the entire heterogenous reservoir model, as we are often provided with data from the wellbore (Ringrose and Bentley 2015). Christie et al. (2005) provided a good analogy to this challenge encountered in reservoir modelling. They likened reservoir production forecasting to “drawing a street map of London and then predicting traffic flows based on what you see from twelve street corners in a thick fog”. In reservoir simulation it therefore means that we lack knowledge on the spatial extent of our reservoir facies, and this incomplete knowledge of the geology propagates into the uncertainty in the forward prediction of the reservoir model. As already established, the real geological description of a reservoir is unknown, it is therefore imperative to devise means to account for uncertainty. Ringrose and Bentley (2015) broadly classified the methods for geological uncertainty quantification into 3: 1). Rationalist approaches (best guess): In this method, a preferred case is chosen as a base case and then run as a best guess or with the addition of a range of uncertainty to that guess. 2). Multiple stochastic approach: In this approach large realizations of geological models are probabilistically generated using geostatistical simulation. The probability of different methods is calculated based on their relative frequency. 3). Multiple deterministic approach: Unlike the best guess approach, multiple deterministic approach does not choose a preferred base-case model. In this approach, a smaller number of scenarios are modelled in such a way that each one will represent a complete reality of an explicitly defined reservoir concept. Figure 2-2 shows different methods of geological uncertainty quantifications.

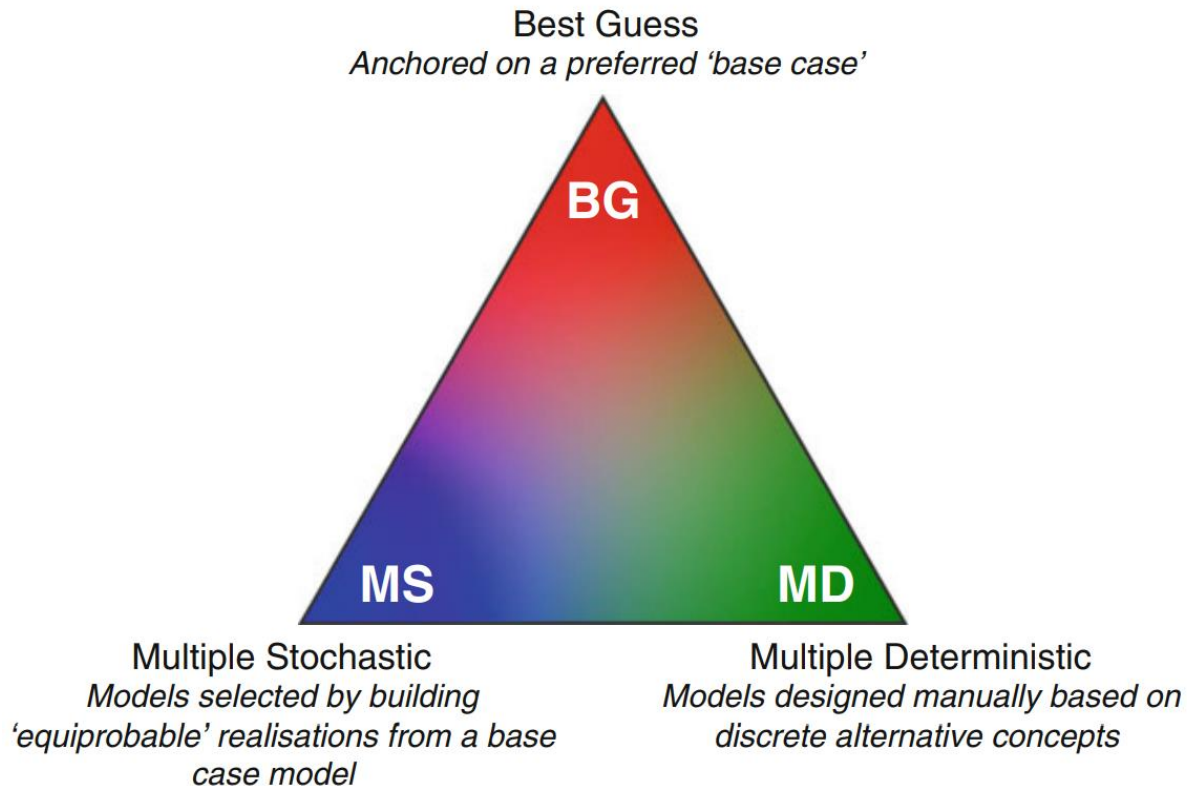


*Figure 2-2. Methods of geological uncertainty quantification (from Ringrose and Bentley 2015).*

In multiple stochastic approach, a geo-modeller will typically build hundreds of realisations of reservoir models to quantify the uncertainty of a field before production. These realisations are parameterised numerically to cover the range of uncertainty in the reservoir. However, uncertainty of interpretational elements which is impossible to account for are often neglected. Examples of such interpretational uncertainties are: uncertainties in the fault model i.e. the choice of the numbers of faults in the reservoir, uncertainties in the picking up the depth of top structure which will impact the bulk volume of the reservoir, the uncertainty of choosing a shale cut-off to define net-to-gross, the uncertainty in the permeability prediction model and the uncertainty in the depositional (Arnold et al. 2013). It is therefore essential to integrate these elements into the workflow of reservoir modelling in order to reduce risk.

Building a reservoir model should be purpose driven, which should be to provide answers to some specific questions (Bentley 2015). The first stage of reservoir modelling workflow is to observe if there are heterogeneities and other geological structures in the reservoir. The next step is to decide which of these heterogeneities to include in the reservoir model by determining which heterogeneity and geological structure is sensitive to the reservoir fluid and the production mechanism using Flora's rule. Some fluid types are more sensitive to heterogeneities than the others. For instance, gas reservoirs are less sensitive to heterogeneity in permeability than oil reservoirs under a waterflood (Bentley and Ringrose 2017). According to "Flora's Rule" (Ringrose and Bentley 2015), if an EOR process such as polymer flooding changes the fluid-rock interactions and mobility ratios, it is not guaranteed that key geological uncertainties are properly

captured in a reservoir model that was previously history matched for a different recovery mechanism. It is therefore possible that geological uncertainties are not adequately propagated into future predictions of reservoir performance, particularly when the history matched model is centred around a single base case.

### 2.3. EOR Optimization

The performance of enhanced oil recovery (EOR) processes in heterogeneous reservoirs usually suffers from low macroscopic displacement efficiency associated with early breakthrough, unstable pressure distribution, oil rate reduction, and low ultimate oil recovery (Jarrell et al. 2002). Therefore it is important to carry out production optimization to achieve maximum oil recovery within the present economic limits and geological uncertainties (Chen et al. 2012). Extensive simulation studies have been performed on how to optimize the injection profile in order to maximize the net present value (NPV) or the macroscopic displacement efficiency of EOR schemes both for synthetic reservoirs and real-field applications (Sudaryanto and Yortsos 2001). Taheri and Sajjadian (2006) carried out optimization of CO<sub>2</sub>-WAG parameters such as WAG ratio, slug sizes of gas and water and alternating time interval to maximise oil recovery at the lowest possible cost. Due to the complexity of the field-scale problem, such optimization applications have been mostly limited to small-scale problems (Davidson and Beckner 2003). Chen et al. (2010) optimised NPV in the Pubei Oil Field by identifying optimal WAG ratio, cycle time, injection rate and the bottom-hole pressure for a producing well. AlAmeri et al. (2020) developed a workflow which integrates geological uncertainties and employs multi-objective optimisation to maximize WAG injection in a complex giant carbonate reservoir.

Van Doren et al. (2011) employed adjoint-based optimization to determine the optimum values of the slug size, polymer concentration, injection and production rate in a full field of a heavy oil reservoir simulation model with viscosity of 90cp, 250 production wells and 50 injection wells. NPV increased from a base case of \$180 million to \$192 million by increasing oil recovery factor by 10% and decreasing polymer injection. Further insight from the results showed that the polymer concentration was lower in some injectors compared to other injector. The physical explanation was that the injection wells with lower polymer concentration was located in the region with smaller oil column, implying less volume of oil needed to be swept. Clemens et al. (2011) used streamline simulation to optimize the polymer utilization factor (UF) in a Romanian Field by identifying the optimal well pattern, slug size and polymer concentration. The result from their study show that the UF decreased from 3.01 kg/bbl for the base case to 2.01 kg/bbl and the incremental oil recovery over waterflood increased from  $5.01 * 10^6$  bbl to  $6.1 * 10^6$  bbl. Mantilla and Srinivasan (2011) presented a feedback control framework that quantifies uncertainties in reservoir modelling and production forecast of an ensemble. The uncertainties of the ensemble are updated by continuously monitored production data from a truth case model. The updated reservoir models representing the uncertainties are optimized using a proxy-based optimisation algorithm to maximize NPV for polymer flooding by identifying optimal injection and production rates. The NPV for polymer flooding from the presented feedback control technique showed similar NPV to the NPV of the optimized truth case model.

Additionally, most of the previous studies on production optimization have been performed using a single reservoir model, therefore, the corresponding results are deterministic, and cannot account for the uncertainties associated to the reservoir characterisation, description and history matching. Production optimisation using a single reservoir model and ignoring geological uncertainties is known as nominal optimisation. Due to the impact of reservoir heterogeneity on EOR processes, the optimal solution obtained using nominal optimisation may be suboptimal and deviate significantly from the actual optimal strategy (Yang et al. 2011). To account for geological uncertainties and reduce risks in EOR optimisation, robust optimisation has been recently employed. In robust optimisation, multiple realisations of geological models are used to determine an optimal risk weighted strategy that is most likely to yield good performance in any of the realisations (Chen et al. 2012).

Efforts have also been made to address the problem of geological uncertainty in production optimization, mostly for water flooding processes. Van Essen et al. (2009) addressed the geological uncertainty of the robust water flooding optimization process by performing the optimization over multiple models. Alhuthali et al. (2008) computed the optimal injection and production rates based on multiple geological models and then maximized the sweep efficiency during water flooding considering the geological uncertainty.

Therefore, there is a need to employ a robust approach to determine the optimal production–injection scheme of EOR processes using multiple realizations of geological models that account for uncertainties in both reservoir geology and history matching. The challenge with robust optimisation is that it is computationally expensive to use all the realisation in the optimisation workflow, to lower the computational effort, a subset of representative realisations can be selected to carry out the optimisation study (Chen et al. 2012).

## 2.4. Polymer Flooding

Polymer flooding is a chemical EOR process which involves adding relatively long chains of high molecular weight, polyelectric and soluble polymers into the injected water. The aim of adding polymers to injected water is to raise the water viscosity in order to lower its mobility and to be approximately the viscosity of oil or even higher in some scenarios. Polymer flooding therefore targets oil reservoirs that contain oil with relatively high viscosities, from 100 cp up to 5000 cp, and from 12 API° to 22.3 API° (Saleh et al. 2014). The mobility control that is induced by polymer flooding helps to overcome challenges that are encountered when injecting water into high viscosity oil reservoirs such as viscous fingering and bypassing of oil or early water breakthrough. In other words, polymer flooding can increase incremental recovery by improving the volumetric sweep efficiency (Seright 2010). Heavy oil reserves (i.e. liquid petroleum of less than 22.3 API° and more than 200 cp viscosity at reservoir conditions) represent 20-25% of the global oil resources and according to the USGS, there are estimated 355 billion barrels of viscous oil in recoverable reserves at an estimated recovery factor of 13-15% (Meyer and Attanasi 2013). From the above statistics, it is clear that recovery factors for heavy oilfields can be enhanced by using EOR techniques.



In addition to improving the sweep efficiency, polymer flooding has also been deployed in near wellbore treatments to plug off watered out high permeability zones and reduce water cut or to improve the performance of injection wells to make the injection profile even. Furthermore, cross-linked polymers can be injected to plug off high permeability zone deep in the reservoir for fluid diversion (Sorbie 1991). This thesis will focus on deploying polymer solutions for better mobility control and volumetric sweep in the entire reservoir.

The end-point mobility ratio  $M$  describes the stability of a displacement front and is given by

$$M = \frac{k_{rw}/\mu_w}{k_{ro}/\mu_o} = \frac{k_{rw}\mu_o}{k_{ro}\mu_w}, \quad 2-1$$

where  $k_{rw}$  is the relative permeability of water,  $k_{ro}$  is the relative permeability of oil,  $\mu_w$  is the viscosity of water,  $\mu_o$  is the viscosity of oil. For cases of  $M \leq 1$ , displacement piston-like, reaching 100% recovery of the displaced fluid at breakthrough (Chang 1978). In contrast, when  $M > 1$  the displacing phase is moving faster than the displaced phase, which results in early breakthrough of the displacing phase and by-passing of the displaced phase (Sorbie 1991). The inefficient displacement at unfavourable mobility conditions, i.e. for  $M > 1$ , is exacerbated if the reservoir is heterogeneous and contains, for examples, high-permeability streaks or fractures (Sorbie 1991). Since polymers alter the viscosity of the water phase, i.e. the displacing phase, the mobility ratio can become more favourable which eventually impacts the recovery factor  $RF$ , which is defined as

$$RF = E_D \times E_A \times E_V, \quad 2-2$$

where  $E_D$  is the displacement efficiency,  $E_A$  is the areal sweep efficiency, and  $E_V$  is the vertical sweep efficiency. Polymer flooding increase the volumetric sweep efficiency which is defined as the product of areal and vertical sweep efficiency. Note that polymer flooding often does not lower residual oil saturation, nor does it increase microscopic displacement efficiency (i.e. proportion of oil displaced from the pores by the injected fluid). However, polymer flooding increase the macroscopic sweep efficiency (i.e. proportion of the connected reservoir volume that is swept by the injected fluid) (*Figure 2-3*). Polymer flooding can speed up oil recovery, and therefore the estimated ultimate recovery can be reached sooner compared to water flooding, leading to higher NPV (Seright 2010). This is because polymer flooding will lower water cut and allow more oil to be produced in the earlier stage of reservoir thereby increases the cash inflow which will have a higher value compared to when the oil will be produce in the later stage of the reservoir during water flooding. However, increasing the viscosity of injectants such as polymers could substantially impact injectivity, slow down fluid throughput and delay oil production from flooded patterns (Seright et al. 2009). Injectivity is defined as the injection rate divided by downhole pressure difference between the well and the formation. The major properties of polymers that affect injectivity are debris in the polymer, polymer rheology in porous media and polymer degradation patterns (Seright et al. 2009). When preparing polymer solution, ineffective polymer hydration and debris in the polymer can lead to near wellbore plugging (Burnett 1975). Rheology in porous media can have a significant impact on injectivity for example Hydrolysed

form of Polyacrylamide (HPAM) exhibit viscoelastic (shear thickening) behaviour in porous media i.e. the effective viscosity increases with increase in shear rate (Seright 1983). Therefore the resistance factor increases with increase in flux for moderate to high viscosities which can lead to injectivity loss (Pye 1964). Mechanical degradation causes an increase in entrance pressure drop which decreases injectivity (Seright 1983).

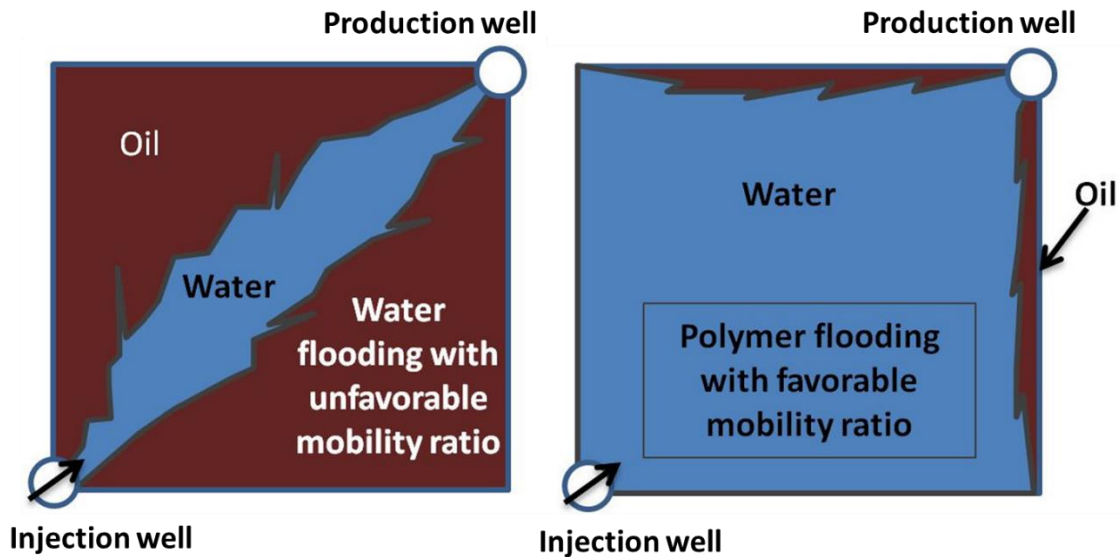


Figure 2-3. Fingering effect with Water flooding (left) and decreased effects of fingering with polymer flooding (right) (Zerkalov 2015).

## 2.4.1. Types of Polymers

Different types of polymers exist which can be used for polymer injection. These can be broadly classified into two types, synthetic and biopolymers (Sorbie 1991). The commonly used synthetic polymer is the HPAM. The commonly used biopolymer is Xanthan. HPAM is the most widely used polymer for polymer flooding. Further details on the molecular structures and different behaviour of HPAM and Xanthan are provided next.

### 2.4.1.1 Xanthan

Xanthan is produced and used by other industries, for example as a thickener in the food industry, and could therefore readily be adapted for EOR purposes. Xanthan is manufactured by bacteria fermentation and polymerization process with a micro-organism known as *Xanthomonas campestris* (Lake 1989; Sorbie 1991; Green and Willhite 1998). The Xanthan polymer base is primarily composed of cellulose-like chain of glucose monomers and glycoside links. Different variants of the *Xanthomonas* yield polymers with somewhat different properties as a result of marginal change in their molecular weight and structure of the produced polymers (Sorbie 1991).

Many authors have simplified the molecular structure of Xanthan polymer molecule to a rigid rod-like structure (Figure 2-4). A Xanthan polymer molecule consists of a straight chain with

further side groups that fold and coil helically around the backbone to form a rod-like structure that possess a certain degree of stiffness (Sorbie 1991). This presence of a rod-like structure was confirmed by rheological research and experiments, as Xanthan was seen to be relatively insensitive to brine properties, e.g. temperature, salinity, pH levels and hardness. The estimated diameter of Xanthan is approximately 2nm and its molecular weight ranges between  $1 \text{ gmol}^{-1} - 12 \times 10^6 \text{ gmol}^{-1}$  (Sorbie 1991). The choice of higher molecular weight usually causes the molecules to aggregate and gel, which may result in plugging or retention of polymer in the reservoir. This problem can be mitigated by running Xanthan polymers through filters to isolate any gel or debris prior to deployment (Sorbie 1991; Lake 1989). Xanthan polymers are also prone to bacteria attacks in the storage facilities or during injection to the reservoir. To overcome this challenge, Xanthan is often treated with biocides such as formaldehyde to suppress the growth of Xanthan gum degrading microorganisms. However, the use of biocides increases the cost of polymer flooding and also poses high environment impact (Lake 1989; Sorbie 1991).

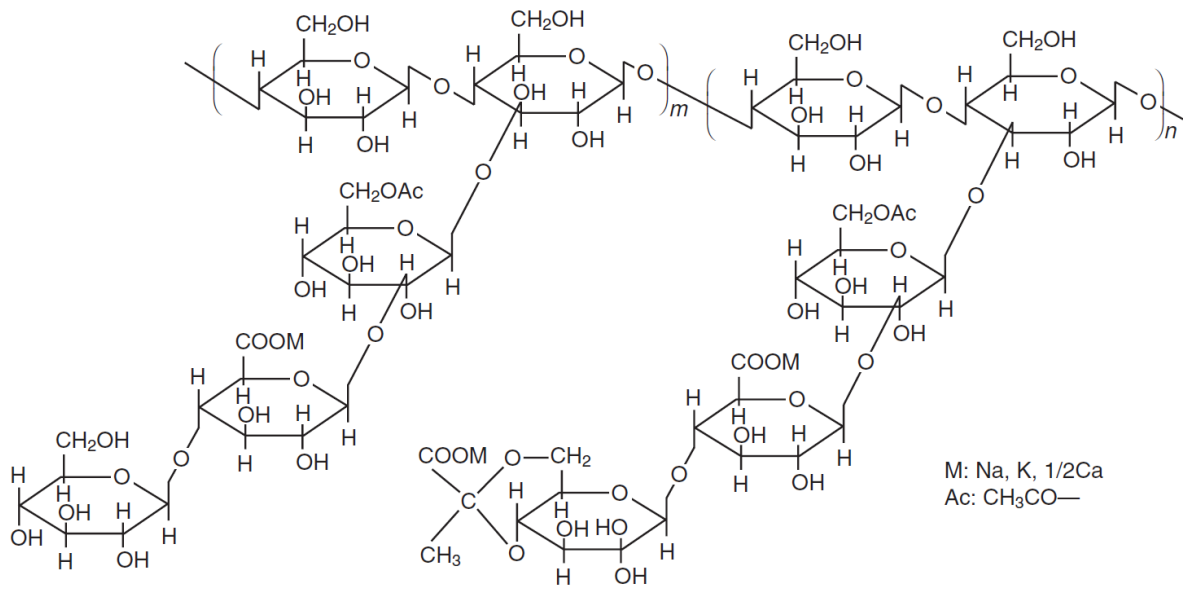


Figure 2-4. The molecular structure of Xanthan (from Dominguez and Willhite 1977).

### 2.4.1.2 Polyacrylamides

Polyacrylamides (PAM) are synthetic polymers because they are manufactured through the process of polymerisation of the acrylamide monomers (Lake 1989; Sorbie 1991; Green and Willhite 1998). PAM consist of the monomeric units of acrylamide molecules and possesses a straight chain of flexible random coil-like molecular structure. The hydrolysed version of PAM (HPAM) is widely available because it is also used by other industries. HPAM is more widely used in EOR projects than Xanthan polymers because it is resistant to bacteria attack, it has good water solubility and mobility control and it is less expensive than Xanthan. HPAM has also shown permanent permeability reduction (Lake 1989; Sorbie 1991; Green and Willhite 1998). Due to its higher photoelectric nature when hydrolysed, HPAM solutions are affected by the salinity and hardness of the formation brine (Sorbie 1991; Lake 1989; Green and Willhite 1998). In contrast to Xanthan, HPAM also does not have any supplemental structure to its backbone

(Figure 2-5) that provides stiffness to its molecules and is hence more susceptible to mechanical degradation (Sorbie 1991).

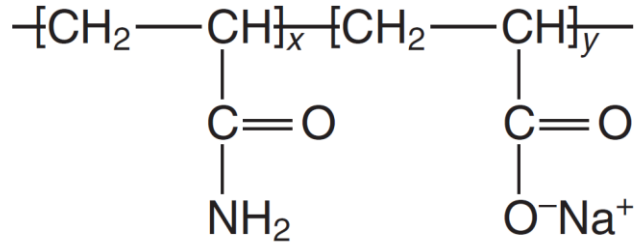


Figure 2-5. The molecular structure of HPAM (from Sheng 2011).

The molecular weight of HPAM ranges from  $2 \text{ gmol}^{-1} - 20 \times 10^6 \text{ gmol}^{-1}$ , the diameter between  $7 - 25 \text{ \AA}$ , and the approximate length  $10\mu\text{m}$ .

## 2.4.2. Mathematical Model for Polymer Flooding

### 2.4.2.1 Black-Oil Model

The Black Oil model is popularly used in reservoir simulation. It can be considered as an extension of where the mass of each phase is conserved. It models the oil, water and gas as discrete phases and can be applied to the low-compressibility fluids, and fluid systems where water and oil only contain a little fraction of dissolved gas. The Black Oil model can be used to model the primary depletion and secondary recovery as well as polymer flooding. The mass conservation equations for the Black Oil model are given by (Trangenstein and Bell 1994)

$$\frac{\partial \left( \phi \frac{\rho_{so}}{B_o} S_o \right)}{\partial t} = -\nabla \cdot \left( \frac{\rho_{so}}{B_o} v_o \right) + q_o, \quad 2-3$$

$$\frac{\partial \left( \phi \left[ \frac{\rho_{sg}}{B_g} S_g + \frac{R_{so}\rho_{so}}{B_o} S_o \right] \right)}{\partial t} = -\nabla \cdot \left( \frac{\rho_{sg}}{B_g} v_g + \frac{R_{so}\rho_{so}}{B_o} v_o \right) + q_g + q_o^g, \quad 2-4$$

and

$$\frac{\partial \left( \phi \frac{\rho_{sw}}{B_w} S_w \right)}{\partial t} = -\nabla \cdot \left( \frac{\rho_{sw}}{B_w} v_w \right) + q_w. \quad 2-5$$

$B_o, B_g, B_w$  are the formation volume factor of the oil, gas and water, respectively, and  $q_o, q_g, q_w$  are the oil, gas and water volume flow rate, respectively.  $\phi$  is the porosity,  $R_{so}$  is the gas in solution and  $v$  is the velocity which is described by Darcy's law as

$$v_\alpha = -\frac{Kk_{r\alpha}}{\mu_\alpha}(\nabla P_\alpha - \rho_\alpha g \nabla z), \text{ with } \alpha = o, g, w, \quad 2-6$$

where  $P_\alpha$  is the pressure of each fluid phase, which contains the capillary pressure as

$$P_{co} = P_o - P_w, \text{ and } P_{cg} = P_g - P_o. \quad 2-7$$

### 2.4.2.2 Two Phase Flow with a Polymer

The mathematical model of polymer flooding is an extension of the black oil two phase flow equations for oil and water presented above. In this equation, polymer is added to the water phase and the polymer concentration  $c_p$ , is expressed in mass per volume of water. The assumption is that the introduction of polymer will not alter the properties of the oil phase. The conservation equations for oil, water, and water with polymer are expressed as

$$\frac{\partial}{\partial t} \left( \frac{\phi s_o}{B_o} \right) + \nabla \cdot \left( \frac{\vec{v}_o}{B_o} \right) = \frac{q_o}{B_o}, \quad 2-8$$

$$\frac{\partial}{\partial t} \left( \frac{\phi s_w}{B_w} \right) + \nabla \cdot \left( \frac{\vec{v}_w}{B_w} \right) = \frac{q_w}{B_w}, \quad 2-9$$

$$\frac{\partial}{\partial t} \left( \frac{(1 - s_{ipv}) \phi s_w c_p}{B_w} \right) + \frac{\partial}{\partial t} ((1 - \phi_{ref}) \rho_r c_a) + \nabla \cdot \left( \frac{c_p \vec{v}_p}{B_w} \right) = \frac{q_p}{B_w}, \quad 2-10$$

and the Darcy velocities are given by

$$\vec{v}_o = -\frac{k_{ro}}{\mu_o} K(\nabla p_o - \rho_o g \nabla z) \quad 2-11$$

$$\vec{v}_w = -\frac{k_{rw}}{\mu_{w,eff} Rk} K(\nabla p_w - \rho_w g \nabla z) \quad 2-12$$

$$s_w + s_o = 1 \text{ and } p_{cow}(s_w) = p_o - p_w \quad 2-13$$

Several new parameters have been introduced that are not captured in the black oil model presented above. Each of them is explained in the following together with various physical phenomena they model.

## 2.4.3. Properties of Polymer Solutions

### 2.4.3.1 Polymer Solution Viscosity

Polymers viscosify a solution through interactions between polymer molecules with solvent molecules that lead to energy dissipation. Polymers dissipate higher energy than smaller molecules which results in higher viscosity (Sorbie 1991). Polymer solution viscosity is directly proportional to polymer concentration in the solution and molecular weight (Lake 1989; Sorbie 1991; Green and Willhite 1998). Todd-Longstaff mixing model is used to express the effective viscosity of water  $\mu_{w,eff}$  and polymer  $\mu_{p,eff}$  (Todd and Longstaff 1972). The effective viscosity of polymer is defined as

$$\mu_{p,eff} = \mu_m(c_p)^\omega \mu_p^{1-\omega}, \quad 2-14$$

where,  $\mu_m(c_p)$  is the viscosity of a completely mixed solution of water and polymer,  $c_{p,max}$  is the maximum possible polymer concentration,  $\mu_p = \mu_m(c_{p,max})$ , and  $\omega \in [0,1]$  is the Todd-Longstaff mixing parameter. The polymer solution and the water are wholly mixed when  $\omega = 1$ , and the polymer solution is completely immiscible in pure water when  $\omega = 0$ . Partial mixing occurs when the values of  $\omega$  is between 0 and 1. The viscosity of partially mixed water can be expressed as

$$\mu_{w,e} = \mu_m(c_p)^\omega \mu_w^{1-\omega}, \quad 2-15$$

The effective water viscosity  $\mu_{w,eff}$  is therefore defined as

$$\frac{1}{\mu_{w,eff}} = \frac{1 - c_p/c_{p,max}}{\mu_{w,e}} + \frac{c_p/c_{p,max}}{\mu_{p,eff}}, \quad 2-16$$

### 2.4.3.2 Rheology and Behaviour of Polymer Solution

Fluids are classified into two categories namely, Newtonian and Non-Newtonian fluids. For Newtonian fluids, the viscosity is the constant of proportionality between the shear stress and shear rate i.e. viscosity is independent of shear rate and given by

$$\tau = \mu\gamma,$$

2-17

where  $\tau$  is the shear stress, and  $\gamma$  is the shear rate. Water is an example of a Newtonian fluid. On the other hand, when polymer is added to water, the resultant polymer solution becomes non-Newtonian fluid. A non-Newtonian fluid is a fluid in which the relationship between the shear stress and shear rate is non-linear. The viscosity in this situation is termed “apparent viscosity” and it is a function of shear rate (Sorbie 1991) given by

$$\tau = \eta(\gamma)\gamma,$$

2-18

where  $\tau$  is the shear stress and  $\eta(\gamma)$  is the shear dependent apparent viscosity.

A non-Newtonian polymer solution exhibits two types of behaviour, shear thinning (pseudoplastic) or shear thickening (dilatants). Most available commercial polymers exhibit shear thinning in which the apparent polymer viscosity decreases with an increase in shear rate (Figure 2.6). This is an important feature for maintaining injectivity as high shear rates in the wells allow polymer solutions to be injected more easily. The shear rate decreases as the injected polymer solution moves away from the wells into the reservoir, which increases the flood viscosity and hence provides a better sweep efficiency.

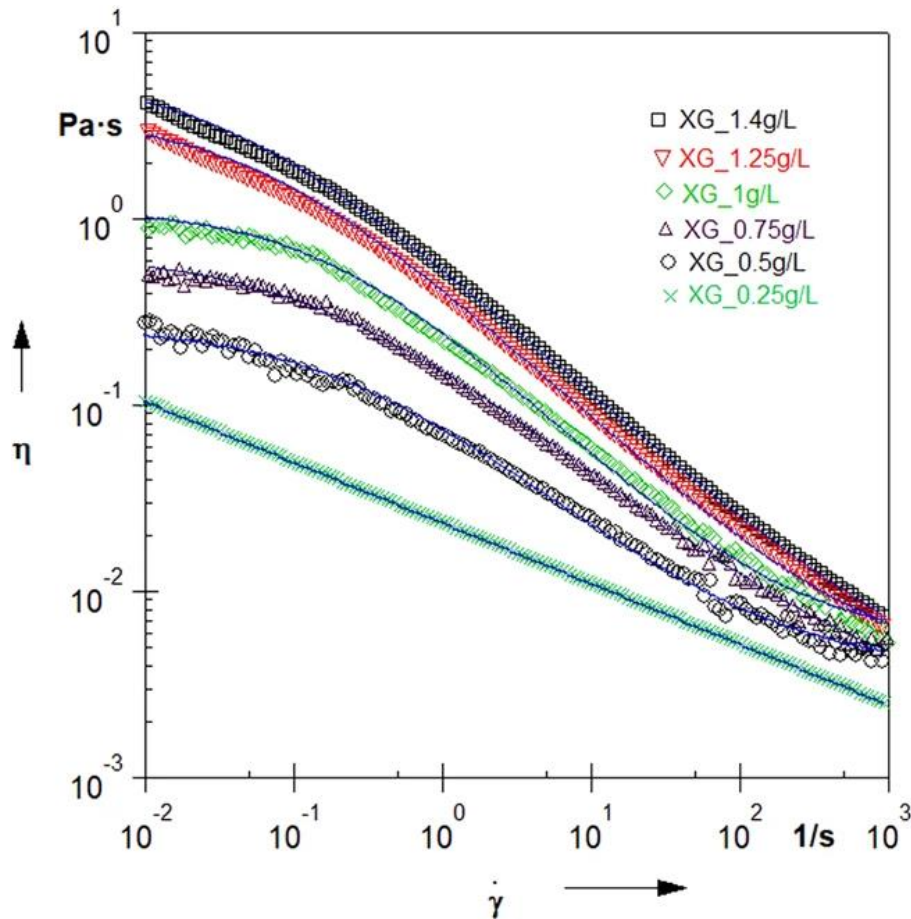


*Figure 2-6. Viscosity curves of the rheology measurements of investigated xanthan gum solution of different concentrations (Mrokowska and Krztoń-Maziopa 2019).*

### **2.4.3.3 Polymer Stability**

For a polymer flooding to be successful, it is essential to avoid degradation of the polymer as a result of mechanical, biological or chemical factors such that the original solution viscosity remains constant. Chemical degradation occurs when polymer molecules are interacting with oxygen or iron. Biological degradation occurs when polymer molecules interact with bacteria. Mechanical degradation usually occurs as a result of high polymer injection rates near the restricted flow path at the wellbore perforations, which exerts mechanical stresses on the polymer, resulting in its breakdown and loss of viscosity (Lake 1989). The stability of polymer solution can be tested in laboratory experiments. In this study, the effect of salinity, temperature, and microbial activities are not considered, and polymer degradation is not modelled.

### **2.4.3.4 Polymer Retention in Porous Media**

Polymer molecules interact with the porous media surfaces and minerals as polymer solution flows through the porous media. The interactions cause the polymer molecules to be retained by the porous media resulting in complete or partial loss of polymers. Any polymer solution flowing through a porous medium experiences retention which can adversely impact a polymer flood by delaying oil displacement and recovery (Lake 1989). To demonstrate the effect of polymer retention, Green and White 1998 presented a delaying factor ranging from a very low retention of 10 $\mu$ g to a high retention of 200 $\mu$ g (*Figure 2-7*). Given one pore volume of a polymer solution of concentration 2000 ppm at moderate retention, the delay factor is about 3%, whereas the delay factor in the case of moderate polymer retention of 100 $\mu$ g and polymer concentration of 1000ppm is approximately 51%, this implies that about 51% of more polymer is required to reach the target formation when compared a scenario where there is no polymer retention. If the rate of polymer retention is higher than 200 $\mu$ g, the rate of oil displacement and the economic feasibility of polymer flooding will be seriously affected.



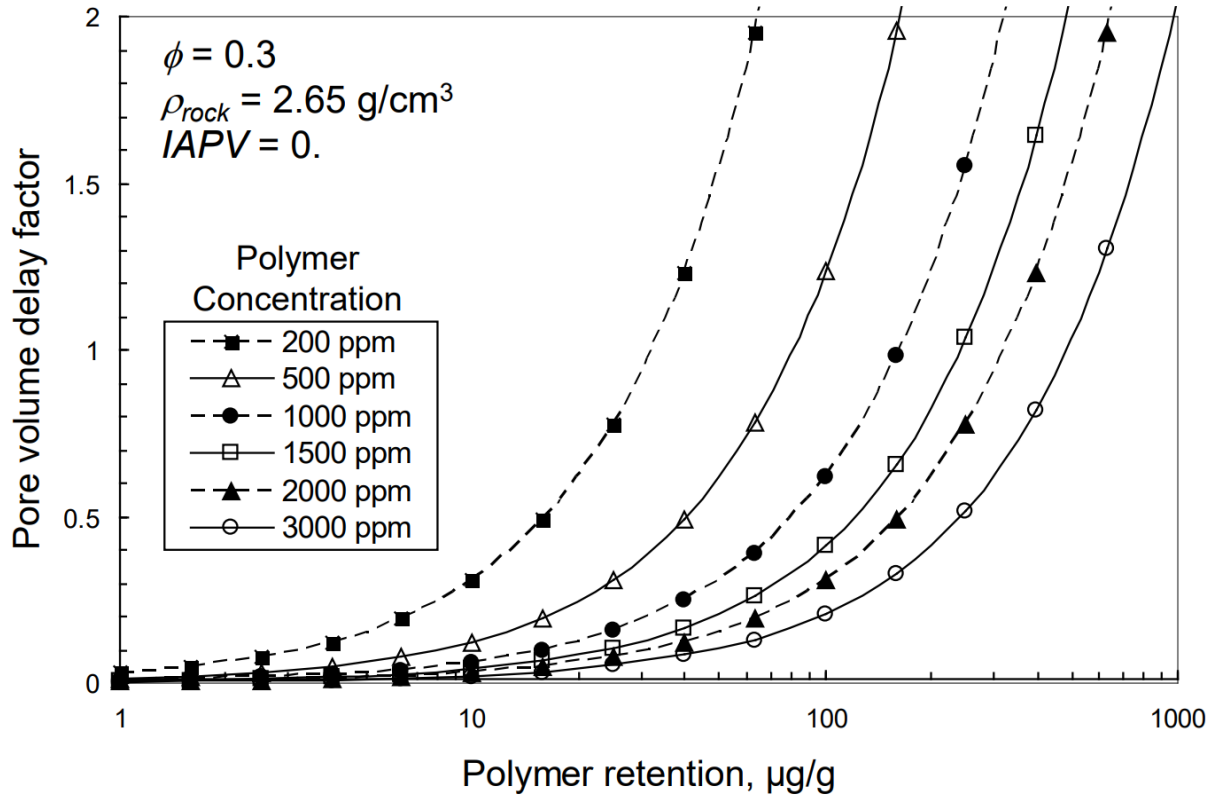


Figure 2-7. Polymer bank delay factor caused by polymer retention (after Green and Willhite 1998)

Mechanical entrapment, hydrodynamic retention and adsorption are the three mechanisms responsible for polymer retention in porous media (Figure 2-8) (Dominguez and Willhite 1977). Mechanical entrapment in the porous media occurs when polymer molecules plug small pores due to the large size of polymer molecules compared to the size of the pores. Water and salt molecules can travel through porous media because they are relatively of a smaller size, but polymer molecules are large and are trapped leading to the accumulation of polymer in small pores. Hydrodynamic retention occurs when polymers are temporarily trapped in a stagnant region of the reservoir by hydrodynamic forces called osmotic forces. Polymer Adsorption is frequently the major cause of polymer retention and is discussed next.

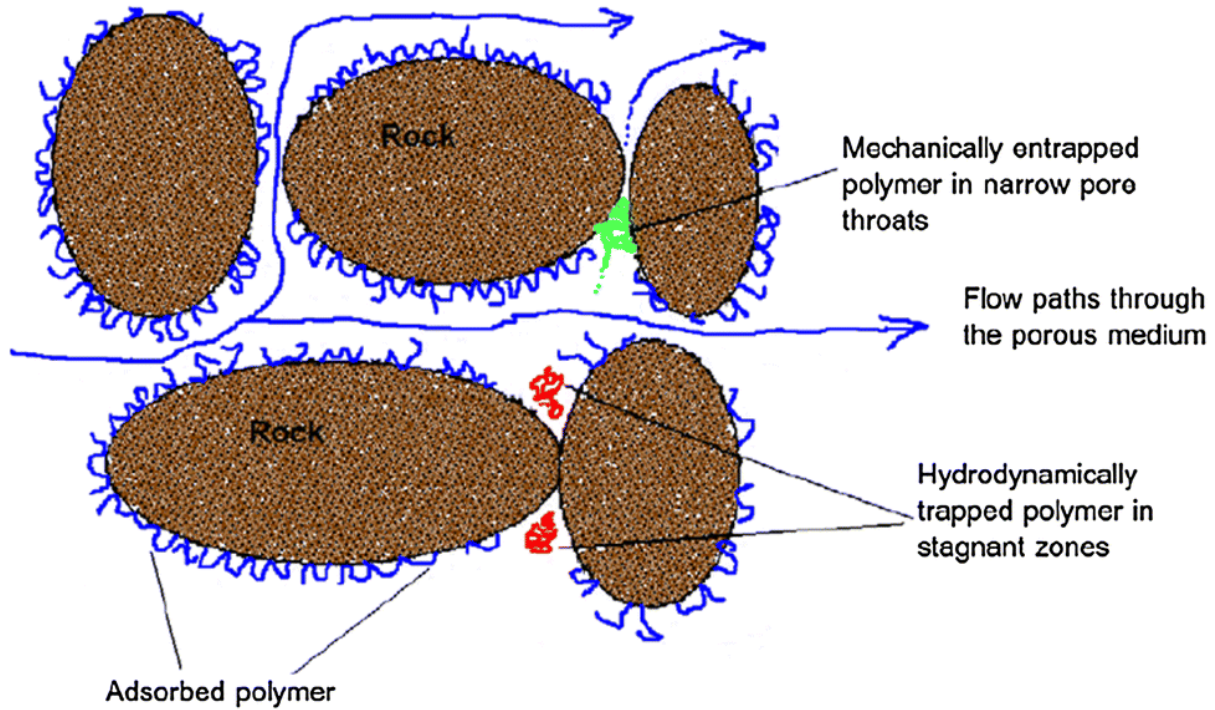


Figure 2-8. Polymer retention in porous media (after Huh et al. 1990).

#### 2.4.3.4.1 Polymer Adsorption

The mechanism where polymer molecules interact and bond with the rock surface is known as adsorption (Cohen and Christ 1986). Adsorption leads to loss of polymer from the solution which reduces its viscosity and delays polymer propagation. Adsorption has been widely reported in literature and assumed to possess an instantaneous effect (Sorbie 1991; Zhang and Seright 2014). However, this effect is only limited to physical adsorption and excludes chemisorption. Chemisorption is the chemical reaction that occurs between the polymer and the rock surface after an extended period of injecting polymer. Adsorption is assumed to be an irreversible reaction (Zhang and Seright 2014).

Adsorption can be modelled using isotherms such as the linear, Langmuir and Freundlich isotherms. The Langmuir isotherm used to model adsorption of polymer can be expressed as:

$$\hat{C}_p = \min \left( C_p \frac{ap(C_p - \hat{C}_p)}{1 + bp(C_p - \hat{C}_p)} \right), \quad 2-19$$

where,  $C_p$  is the injected polymer concentration,  $\hat{C}_p$  is the adsorbed polymer concentration.  $(C_p - \hat{C}_p)$  represents the equilibrium concentration in the rock-polymer solution system,  $ap$  and  $bp$  are empirical constants (Sheng 2010).

Note that the Langmuir model is an equilibrium relationship and assumes that adsorption is instantaneous and reversible with respect to polymer concentration. In conditions where polymer concentration is declining and polymer adsorption is considered to be irreversible, Langmuir

model cannot be applied directly. Therefore, an additional parameter must be introduced to track adsorption history (Li 2007).

#### 2.4.3.4.2 Permeability Reduction

Permeability reduction is the effect of complete or partial blockage of pore spaces as a result of polymer adsorption. Different methods can be employed to estimate permeability reduction. For instance, resistance factor, which is defined as the ratio of water mobility to polymer mobility, both during and after the flood. Resistance factor helps to uncouple the effect of adsorption and the change in viscosity, although it may not be a reliable measurement for permeability reduction, because a slight change in viscosity may counteract the change caused by adsorption. A more frequently used technique is to express permeability reduction as a function of the residual resistance factor (RRF). Permeability reduction is directly proportional to adsorption and it is estimated using the RRF in reservoir simulation. The RRF compares the water mobility prior and after the flood and therefore eliminates any impact of viscosity changes in the polymer (Jennings et al. 1971). The reduction factor  $R_k$ , expressed as

$$R_k(c_p) = 1 + (R_{RF} - 1) \frac{c_a(c_p)}{c_{a,max}}, \quad 2-20$$

where  $R_{RF} \geq 1$ ,  $c_a$  is the adsorbed polymer and  $c_{a,max}$  is the maximum adsorption.

Permeability reduction needs to be estimated during the design and planning of a polymer flood, as it can impact injectivity and lead to flow diversion. However, this assumption can only be valid in conventional reservoirs with high permeability, where retention is predominantly due to adsorption. Whereas, in tight reservoirs, entrapment is basically responsible for permeability reduction (Huh et al. 1990). Therefore, permeability reduction in a low permeability reservoir is higher compared to permeability reduction in a high permeability reservoir, even though the polymer losses as a result of adsorption is lower in low permeability reservoirs compared to high permeability reservoirs.

#### 2.4.3.4.3 Inaccessible Pore Volume

If pore throats are too narrow for a polymer molecule with a given molecular weight, this pore space is known as the inaccessible pore volume (IPV). The presence of IPV will prevent polymer solution from gaining access to some parts of the reservoir as polymer molecules will only flow through the larger pores. Polymer solution will therefore travel faster through the larger pores as compared to any accompanying tracer which will have full accessibility to the entire reservoir. The effect of IPV could therefore lead to viscous fingering and bypassing the oil (Sorbie 1991). The second explanation of the increase in travel speed of polymer solution as a result of IPV is the wall exclusion. Wall exclusion occurs when polymers molecules that are close to the wall of the porous medium are pushed to the centre of the flowing stream leading to increase in polymer concentration at the centre of the stream. Because the velocity of the streamlines at the centre of the pore is usually higher than the velocity close to the wall, the higher concentration of polymer solution at the centre of the stream will travel faster compared to any accompanying tracer that are usually more evenly distributed across the entire reservoir (Lake 1989). Note that polymer

adsorption can also restrict the flow of a polymer solution, which can have a similar effect as the IPV (Sorbie 1991).

## 2.5. History Matching

Reservoir models need to be calibrated, which is done using history matching where parameters are adjusted until model and data agree. Mathematically, this means that we seek to find plausible model variables that minimise a misfit. History matching aims to determine some plausible model variables  $\alpha$  that minimise the misfit between the observed production history and modelled response (Chen and Oliver, 2010). The objective function is a performance criterion used in assisted history matching. It estimates the misfit between the simulated response and production data. Some scientists were minimizing the sum of the absolute value of the misfits called the least-absolute-values method, whereas other scientists were minimizing the sum of the squared value of the misfits called the least-squares method

$$\mathcal{D} = \sum_{d=1}^N |obs_d - mod_d|, \quad 2-21$$

$$\mathcal{D} = \sum_{d=1}^N w_d (obs_d - mod_d)^2, \quad 2-22$$

where  $obs_d$  and  $mod_d$  are observed and modelled data at data point  $d$ , respectively,  $N$  is the number of data points, and  $w_d$  is the weight factor at data point  $d$ .

The prevalence of the least-squares method over the least-absolute-values procedure in the oil industry is due to its simplicity, even though the least-absolute-values technique is more robust to outliers than the least-square method.

A more general form of the least-squares method in misfit definition is given in Equation 2-23 below which includes a scaling factor,

$$\mathcal{D}(\alpha) = \sum_i w_i \sum_t w_{i,t} \left( \frac{obs_{i,t} - mod_{i,t}}{scale_i} \right)^2, \quad 2-23$$

where  $i$  is the data type,  $t$  is time step,  $w_i$  is the weight for the  $i$ -th data,  $w_{i,t}$  is the weight for the  $i$ -th data at the time  $t$ ,  $obs$  and  $mod$  are the observed and simulated data respectively, and the  $scale_i$  is the scale factor for the  $i$ -th data type. A scaling factor is used to consider data with different absolute ranges. A common choice is to use the standard deviation in the observed data as a scaling factor. In its simplified version, the least-squares method with scaling factor is given by

$$\mathcal{D}(\alpha) = \sum_{d=1}^N \frac{[obs_d - mod_d(\alpha)]^2}{2\sigma_d^2}, \quad 2-24$$

where  $\alpha$  is the vector of parameters that are updated during history matching,  $obs_d$  and  $mod_d$  are observed and modelled data at data point  $d$ , respectively,  $N$  is the number of data points, and  $\sigma_d^2$  is the uncertainty of the measurements with the assumption of an uncorrelated Gaussian error in the measurements (Oliver et al. 2008).

The observed (or historical) data can be production data, pressure data obtained from well tests and formation tester, tracer observations, or time-lapse seismic data (Stephen 2013). The most popular historical data for history matching are production data, i.e. time series of measurements of pressure, flow rate, ratios of flow rates such as water cut, obtained in producing or injecting wells (Hajizadeh et al. 2010). Model parameters that may be tuned include but are not limited to rock properties (porosity, horizontal and vertical permeability), fluid properties and models for rock-fluid interactions (compressibility, oil and water relative permeability, capillary pressure), fluid contacts, and geological properties (net-to-gross, fault transmissibility, fracture data, aquifer volume and strength).

History matching is a complex inverse problem with ill-posed and under-constrained characteristics when using observations such as production data to determine the model parameters. The complexity is related to the nonlinearity of the reservoir dynamics and the nonlinearity induced by the relationship between data and model parameters and there is hence no unique solution, which means that many plausible reservoir models can show similar simulation responses that match the historical data (Tavassoli et al. 2004). Figure 2.9 shows the basic workflow for history matching. History matching can be carried out either manually, where the reservoir engineer edits the reservoir model input deck and perturbs the parameters, based on experience and intuition, or automatically, using an optimization algorithm.

The method of perturbing uncertain parameters only on the dynamic model is known as Small Loop, whereas, an integrated approach where uncertain parameters are varied in the geological model is known as Big Loop. The advantage of a Small Loop approach is that it allows the Reservoir Engineer to totally investigate and understand the distributed material balance and connectivity of the reservoir. However, the disadvantage of Small Loop is that the dynamic model are often modified in such a way that it loses geological consistency. The advantage of Big Loop is that it allows greater degree of freedom in investigating all possible uncertainty while ensuring geological consistency. Figure 2-9 shows the basic workflow in history matching – Big Loop vs Small Loop.

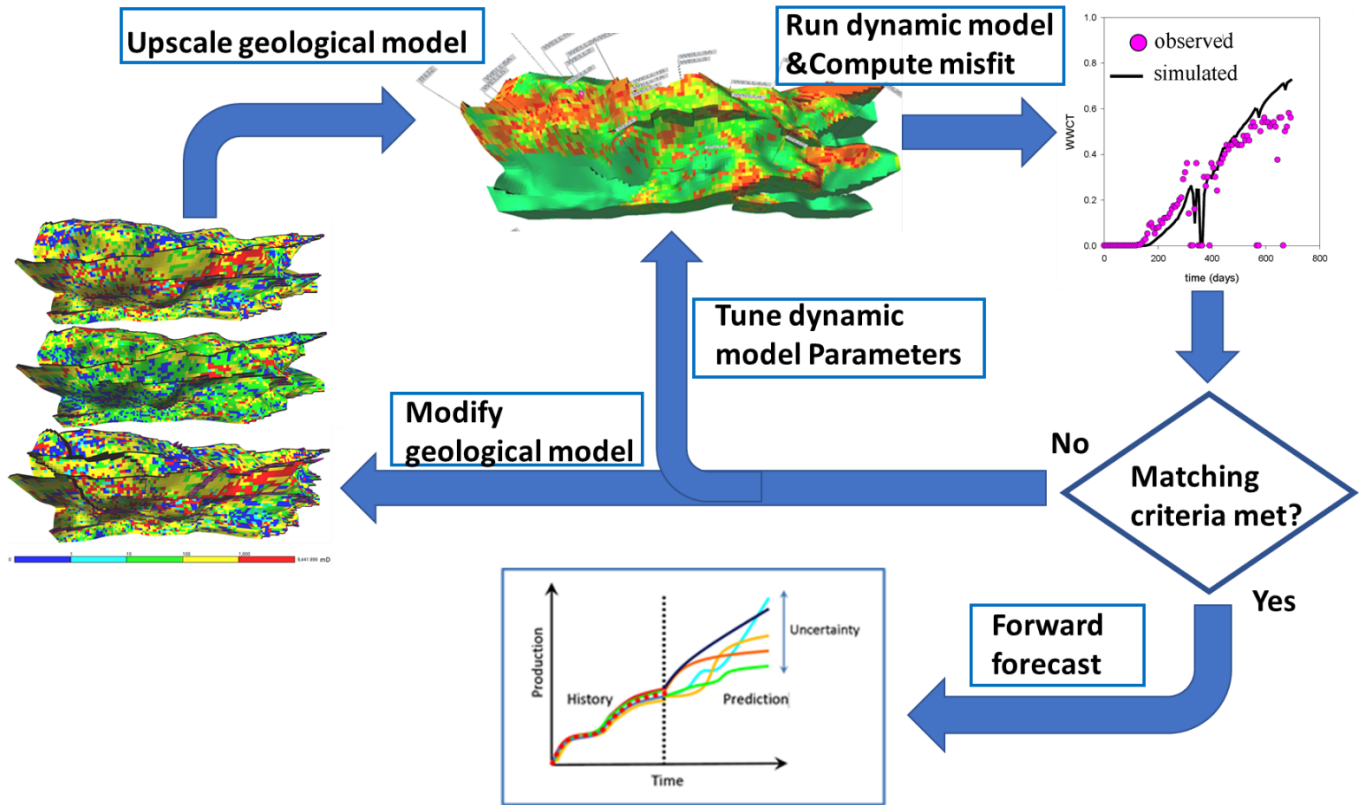


Figure 2-9. Basic workflow during history matching - Big loop versus small loop.

### 2.5.1. Manual History Matching

Manual history matching is typically achieved by a repetitive trial-and-error process which involves a series of simulations where model parameters are adjusted manually to reduce the mismatch between the simulated and the observed data. This method takes time and is based on the experience, knowledge, and expert judgement. For large fields it may take months to yield a single acceptable model. It often merely results in the best practical solution within decision time and may eventually provide a reservoir description that may be impracticable and inconsistent with the geological interpretation. The process of manual history matching is summarised in the Figure 2-10.

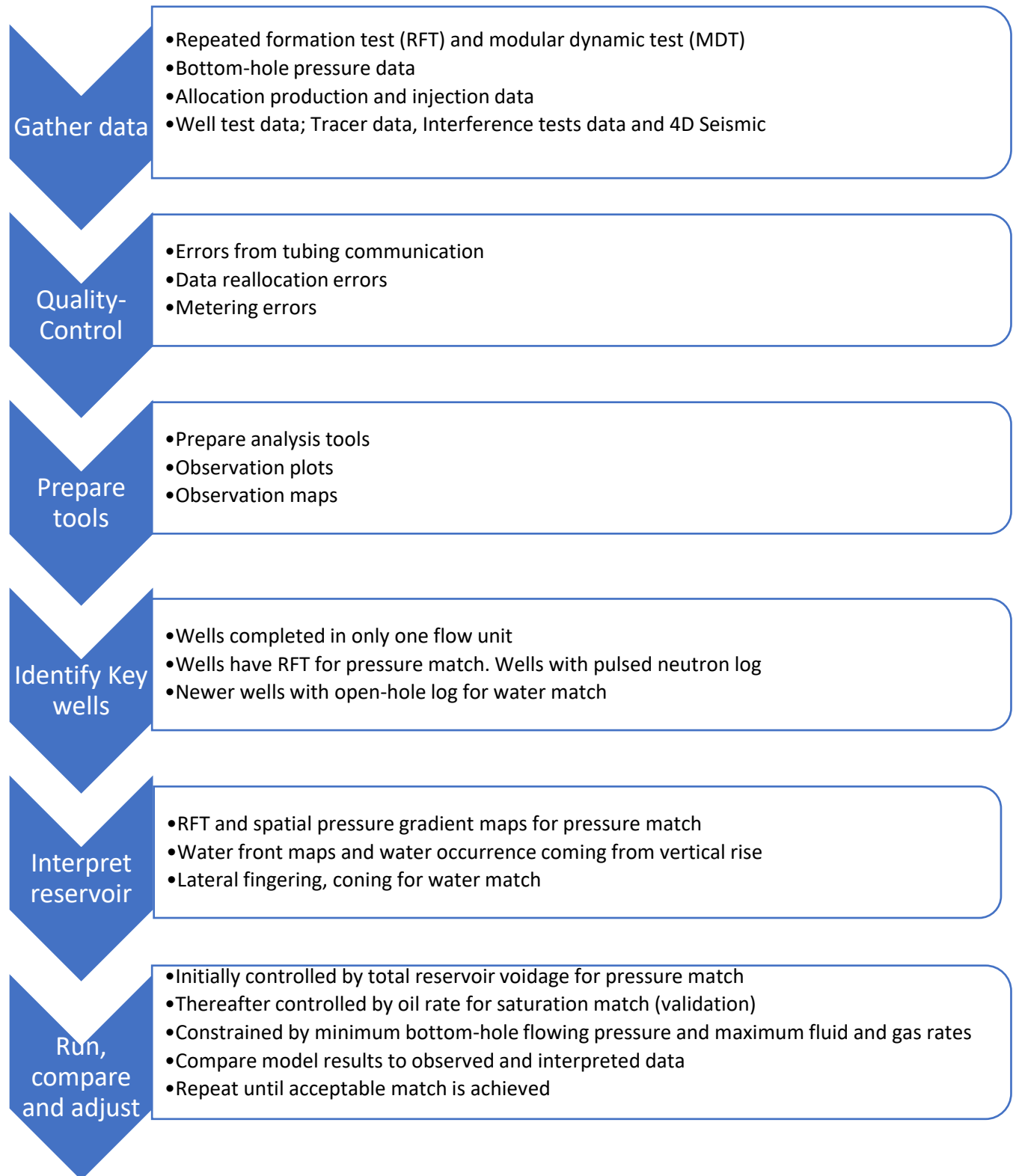


Figure 2-10. The manual history matching procedure (Kelkar and Perez 2002).

## 2.5.2. Assisted History Matching

Using modern computer hardware and software algorithms, history matching is increasingly automated (but not fully automated), which the exploration of a much larger parameter space (Oliver et al. 2008). Assisted history matching uses optimization techniques to minimise the objective function that is normally defined as a misfit (Eq. 2-24). However, given the large amount of data generated by assisted history matching, it is more difficult to ensure that the resulting models are geologically consistent or indeed to gain insights into the reservoir dynamics and underlying geology. Assisted history matching generally has the ability to generate many more history matched models and provide a better match than manual history matching (Gruenwalder et al. 2007).

In recent years, the field of optimisation and history matching has grown rapidly due to the recent developments in theory, algorithms, and the computational contributions of computer hardware to solve various problems in engineering and science (Kabir et al. 2003). In general, optimisation algorithms can be classified as local or global algorithms. Local algorithms seek to find a local minimum. However, most optimisation and history matching problems have more than one local optimum and minimum respectively and therefore finding a local minimum will not guarantee that the global minimum solution has been found as well (Mohamed et al.2010). Global optimisation algorithms on the other hand always achieve the global minimal of the objective function if the algorithms allow for a sufficiently large number of iterations. A good history matching practice is finding a trade-off between exploitation and exploration. Exploitation operations finds new solutions from existing ones by improving the parameter choices to minimize the misfit using information about the misfit surfaces. Exploration means finding new points in the search space that has not been explored without considering what have been learnt from previous sampling. Local optimisation algorithms are less explorative, but they are very strong in exploitation whereas the Global algorithms are very strong in exploring the parameter space, but less exploitative (Sambridge and Mosegaard 2002).



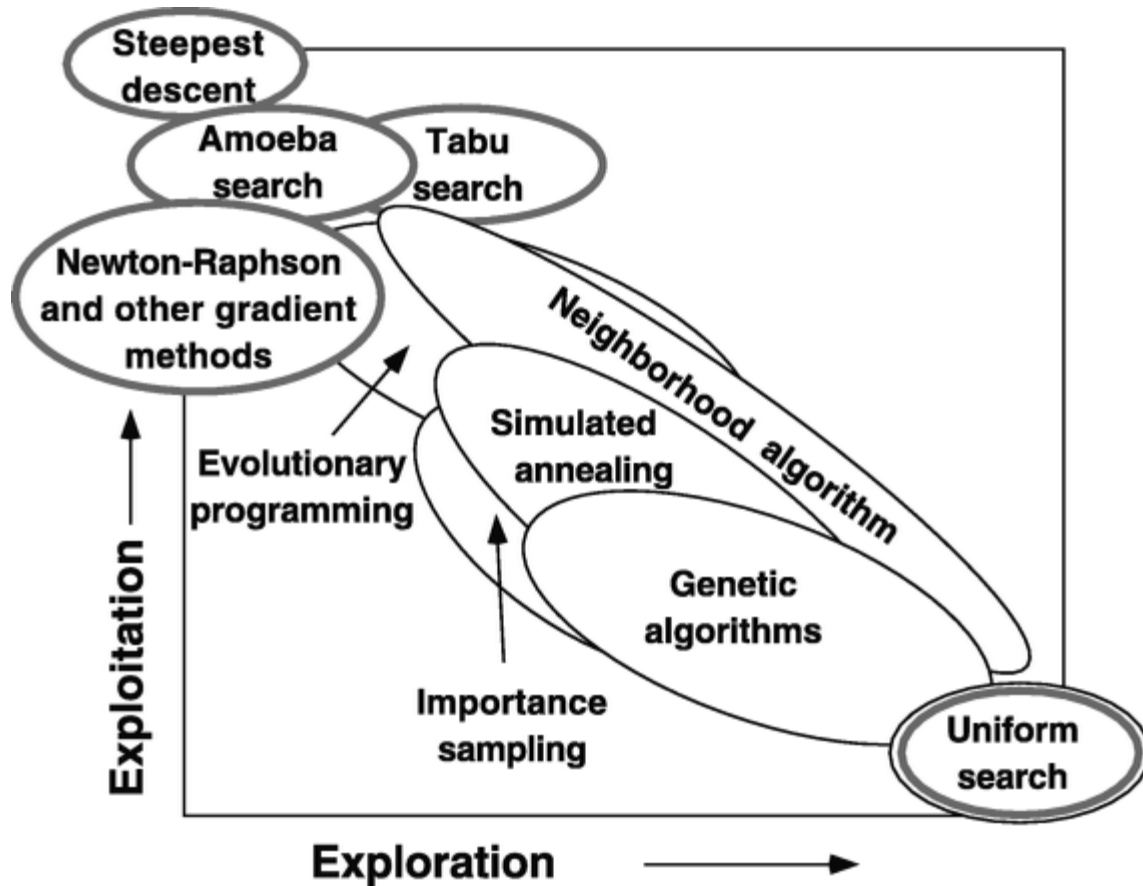


Figure 2-11. A schematic classification of optimisation algorithms according to their strength of exploitation and exploration (from Sambridge and Mosegaard 2002).

Generally, there are three classes of assisted history matching, deterministic methods, stochastic methods, and data assimilation.

### 2.5.2.1 Deterministic Methods

Deterministic methods take advantage of the analytical properties of the problem to solve the optimisation problem. They are also called local optimization methods since they always find a local minimal of the objective function. Deterministic methods are divided into two subgroups, gradient-based and sensitivity-based methods.

Gradient-based methods such as Gradient descent and Steepest descent method are one of the earliest methods of deterministic optimisation used in assisted history matching. They calculate the derivative of objective functions with respect to the model parameters that are being adjusted, so as to minimise the objective function (Jahns 1966; Coats et al. 1970; Thomas et al. 1972). Gradient-based methods can be quick and efficient but in certain cases these methods can either get stuck in local minima or may not converge in some other cases. Another drawback of gradient methods is that it derives only one good solution instead of a variety of good solutions.

Sensitivity-based methods such as Gauss-Newton methods, Sparse Equations or Least Squares methods calculate sensitivity coefficients of the objective function which are defined as the

partial derivatives that yield the change in model response as a function of the change in reservoir properties. The sensitivity coefficients can be computed using Adjoint technique (Oliver et al. 2008).

### 2.5.2.1.1 The Adjoint Technique

The adjoint technique is an efficient way to accurately calculate the gradient of a function with respect to the function's variables. It is particularly useful in a history matching study with many model parameters. The adjoint state variables are solutions to the linear equation system, although the forward equation system can be non-linear. The adjoint techniques calculates the gradient of objective functions (e.g. oil rate, water rate and flowing bottom hole pressure) with respect to the grid block properties. A single Adjoint model run is used to backpropagate the mismatch between the measured and modelled production data. The propagated error field is then converted into an estimate of the exact gradient of the objective function with respect to any of the grid block parameters, regardless of dimensionality of the problem. A Gradient-based method can then be used with the computed gradient to select the new search directions within the parameter space. The adjoint state variables are solutions of equations in which mass is injected at the location and time of an observation. This mass is then propagated backwards in time along pathways which only integrate the properties that contribute to the observation (Rao and Mishra 1996; Wu et al. 1998; Almuallim et al.2010) . The mismatch for a parameter (e.g. oil production rate) can be defined as the sum of the squared difference between historical and simulated data. Equation 2-25 mathematically represents the mismatch quantify, where  $d$  varies from 1 to the total number of history data points.

$$\text{Misfit, D} = \sum_d \left( \frac{\text{obs}_d - \text{mod}_d}{\sigma_d} \right)^2, \quad 2-25$$

For each well, there are four misfit quantities, which include the mismatch in gas production rate, oil production rate, water production rate and bottom-hole pressure. The objective function has a weight for every well, and a weight for each parameter.

All misfit parameters as expressed mathematically as follows:

Gas production misfit parameter  $D_{Gas}$  is defined as

$$D_{Gas} = \sum_d w_{gas} \left( \frac{\text{obs}_{gas_d} - \text{mod}_{gas_d}}{\sigma_d} \right)^2, \quad 2-26$$

Oil production misfit parameter  $D_{oil}$  is defined as

$$D_{oil} = \sum_d w_{oil} \left( \frac{\text{obs}_{oil_d} - \text{mod}_{oil_d}}{\sigma_d} \right)^2, \quad 2-27$$

Water production misfit  $D_{water}$  is defined as

$$D_{water} = \sum_d w_{water} \left( \frac{obs_{water_d} - mod_{water_d}}{\sigma_d} \right)^2, \quad 2-28$$

BHP misfit parameter  $D_{BHP}$  is defined as

$$D_{BHP} = \sum_d w_{BHP} \left( \frac{obs_{BHP_d} - mod_{BHP_d}}{\sigma_d} \right)^2. \quad 2-29$$

The total misfit  $E$  is obtained by the weighted sum of these individual misfit parameters

$$D = D_{gas} + D_{oil} + D_{water} + D_{BHP}, \quad 2-30$$

where  $w_{gas}$ ,  $w_{oil}$ ,  $w_{water}$ ,  $w_{BHP}$  represents the weighting factors for gas, oil, water and BHP respectively.

The overall objective function  $D$ , is obtained by a total weighted summation over every well  $j$  is expressed as :

$$D = \sum_j w_j D_j, \quad 2-31$$

where  $j$  varies from 1 to the total number of wells,  $w_j$  represents the weighting factor of the well  $j$  and  $D_j$  represents the total mismatch score for that well.

The objective is to minimize the above function using adjoint technique. Adjoint technique computes the partial derivative  $\frac{\partial D}{\partial x}$ , of the objective function with respect to each parameter  $x$ , such as permeability, porosity and kv/kh ratio at the grid block level.

### 2.5.2.2 Stochastic Methods

Stochastic methods are based on derivative-free algorithms. Their convergence rate is typically slower than that of gradient methods, but they are not trapped in local minima. These algorithms include a random component and obtain the global minimum by its ability to allow the search to occasionally move in the direction of a worse solutions.

Different variants of stochastic algorithms exist, with different levels of sophistication and complexity, such as random search, hill-climbing, and population-based evolution algorithms. Population-based stochastic algorithms are common in history matching. They provide a flexible framework in which the exploration of the search space is followed by local search in previously identified regions, leading to a more effective search, i.e. better exploitation. Specific variants of population-based stochastic algorithms that have been applied to history matching problems include simulated annealing (Sultan et al. 1994), genetic algorithms (Romero et al. 2000), evolutionary strategies (Schulze-Riegert et al. 2001), neighbourhood algorithms (Subbey et al. 2003), scatter search (April et al. 2003), tabu search (Yang et al. 2007), population-based Incremental learning (Petrovska and Petrovska 2009), particle Swarm optimization (Mohamed et

al. 2010), differential evolution (Hajizadeh et al. 2010), or ant-colony optimization (Hajizadeh 2010).

### **2.5.2.3 Data Assimilation Methods**

Data assimilation methods perform a sequential calibration of the model parameters to observation data in a time series. Data assimilation methods takes two different approach, which could be either ensemble smoother or Ensemble Kalman Filter (EnKF). Ensemble smoother approach performs the global updates in model parameters through recursive updates in the time-space domain, on the other hand, the EnKF performs the global update in time domain. Ensemble Kalman Filter (EnKF) is the most widely used data assimilation method for history matching (Evensen et al. 2007). Similar techniques such as Kalman Filter (KF) (Kalman 1960) are frequently applied to linear filtering and prediction problems. EnKF which was invented by Evensen (1994) as a technique of extending the classical KF to nonlinear problems by executing KF using Monte Carlo methods. Each time historic data becomes available, EnKF optimises and updates the parameters such as porosity, permeability and (Evensen et al. 2007). EnKF can be used to integrate production data by sequentially updating an ensemble of reservoir models during simulation. Therefore, each reservoir state vector consists of three types of parameters i.e. static (e.g. porosity and permeability, etc.), dynamic (e.g. cell pressure, water, oil, and gas saturation, etc.) and production data (such as gas-oil ratio, bottomhole pressures and water cut etc.). For a comprehensive review on the application of EnKF on reservoir engineering, refer to (Aanonsen et al. 2009), and a comparative analysis between ensemble smoother and EnKF is published in (Skjervheim and Evensen 2011).

The advantage of EnKF is its simple formulation that can easily be applied in history matching. Liu and Oliver (2005) showed that EnKF is very efficient and robust compared to gradient-based methods. The disadvantage of the EnKF is that it typically underestimates uncertainty due to the use of small ensemble sizes. Small ensemble sizes are important for computational efficiency, but introduce sampling errors and limit the degree of freedom to assimilate data. Consequently, it results in underestimation of ensemble variance after data assimilation with EnKF. The underestimation of posterior variances effectively indicates the underestimation of uncertainty in the reservoir model parameter after data assimilation. EnKF also requires additional parameterisation to adapt to a discrete variable and is not well suited for parameters with multi-modal distributions (Naevdal et al. 2005).

## **2.6. Parameterisation of Uncertain Properties**

Uncertainty in oil and gas reservoirs is due to geological heterogeneity, the sparsity of geological data, the localised measurements of production data at wells which results in a low information content, and the limited accuracy of any measurements. Key sources of the uncertainty are the structure of the reservoir, the spatial distribution of rock properties (e.g. porosity and permeability), and the reservoir fluid which is controlled by poorly understood reservoir properties.

The use of a set of discrete interpretable quantities that captures the key element of a system to describe a complex system is termed parameterisation. The procedure for carrying out the parameterization for uncertainty analysis is to identify the essential model components which have the greatest impact on the fluid flow and degree of uncertainty, and then define the prior range for each of these parameters. Parameterisation methods can be classified into two groups (Oliver and Chen 2011): spatial zonation and transform-domain methods. In spatial zonation, the reservoir model is divided into zones and a common property multiplier is applied to a property in all the grid cells within the zone (Gavalas et al. 1976; Shah et al. 1978; Jahns 1966). Spatial zonation method is important because geological and facies regions can be defined as zones. Spatial zonation method is suitable when the prior knowledge is reliable. The major challenges of this method are associated to the identification of the number, location and shape of the individual zones and artificial discontinuities that exist at the boundaries of identified regions (Khaninezhad and Jafarpour 2011). The Transform-domain methods are effective when the prior model is not properly known. Transform-domain method aim at lowering the redundancy in grid-based property descriptions by considering that geologic features exhibit strong correlations across different scales that commonly lend themselves to compact transform-domain representations. Many transform-domain parameterisation methods such as principle component analysis (PCA), discrete cosine transform (DCT) and discrete wavelet transform (DWT) have been used in subsurface flow systems (Bhark et al. 2011; Jafarpour et al. 2010).

Parametrisation aims to adjust the number of uncertain model parameters to a much lower dimension because of the low information content obtained in most production data (Oliver et al., 2008). The choice of a parameterisation method in field applications is not straightforward because the selection of model parameters to be estimated and the identification of the optimal number of model parameters can be difficult.

## 2.7. Probabilistic Uncertainty Quantification

Significant research efforts focus on how to quantify uncertainty in oil and gas reservoirs. Bayesian method has been the most widely applied technique. The Bayesian method is an inductive probability as it attempts to provide the probability of future event based on the amount of data present. The Bayesian method quantifies the uncertainty in the reservoir forecast if there is poor information of some reservoir properties (Bond et al. 2007). Another application of Bayesian method is the Bayesian inference, where the initial estimate of uncertainty is updated to a new posterior estimate using observed data. The Bayesian method is given by

$$p(m|O) = \frac{p(O|m)p(m)}{\int p(O|m)p(m) dm}, \quad 2-32$$

where the prior probabilities  $p(m)$  consists initial probabilities for the model parameters,  $p(O|m)$  is the likelihood function that measures the degree the observed and modelled data

differ and  $p(m|O)$  is the new posterior probability of the model parameters based on observations  $O$ . Bayes Theorem can be simplified as

$$\text{posterior} \propto \text{likelihood} \times \text{prior.} \quad 2-33$$

Prior information stands for the level of knowledge of the unknown model parameters prior to seeing the observed data. Prior information can be grouped into three based on how much information we have (Bond et al. 2007): 1). Non-informative prior distributions assign equal probability to all values in the parameter's ranges. Typically, non-informative prior is defined as a uniform distribution. 2). Highly informative prior distribution is used if there is a substantial knowledge available regarding the possible value of a model property. A normal distribution defined by the mean and standard deviation is a common representation of this type of distribution. 3). Moderately informative distribution refers to a case where there is limited knowledge about the model property.

The likelihood of a reservoir model is commonly computed by using the misfit based on the observed data and the simulation response of the reservoir. For instance, if we are matching on oil rate, then the likelihood,  $p(O|m)$ , is the probability that the measured observation  $q_{obs}$  is equal to the simulated response  $q_{sim}$  of the reservoir model  $m$ . Assuming that the measurements errors at any time are Gaussian, independent, identically distributed (all have the same variance) with zero mean error, and there are no simulation errors, the likelihood at timestep  $t$  can be defined as:

$$p(O_t | m) = \frac{1}{\sigma\sqrt{2\pi}} \exp \left\{ -\frac{1}{2} \frac{(q_{obs} - q_{sim})_t^2}{\sigma^2} \right\}, \quad 2-34$$

where  $v$  is the standard deviation of the measurement error,  $q_{obs}$  and  $q_{sim}$  are the observed and simulated data, respectively.

As the measurement errors are assumed to be independent between timesteps, the joint probability density is calculated by the product of probabilities of each measurement for  $p$  data points, as given by

$$p(O | m) = \left( \frac{1}{\sigma\sqrt{2\pi}} \right)^N \prod_{t=1}^N \exp \left\{ -\frac{1}{2} \frac{(q_{obs} - q_{sim})_t^2}{\sigma^2} \right\}. \quad 2-35$$

As  $\left( \frac{1}{\sigma\sqrt{2\pi}} \right)^N$  is a constant:

$$p(O | m) \propto \prod_{t=1}^N \exp \left\{ -\frac{1}{2} \frac{(q_{obs} - q_{sim})_t^2}{\sigma^2} \right\}. \quad 2-36$$

Hence, if we use misfit definition  $M$  in Equation (2.21), we can define the likelihood function as in Equation (2.x6) so that by minimising the misfit  $M$  we maximise the likelihood (Tarantola 2005).

$$p(O | m) \propto e^{-M}$$

2-37

The posterior probability distribution (PPD) is the most crucial aspect of uncertainty quantification. PPD can be described as the modification of probability distribution function (PDF) integrating the information provided by the production data. *Figure 2-12* shows the Bayesian framework for uncertainty quantification.

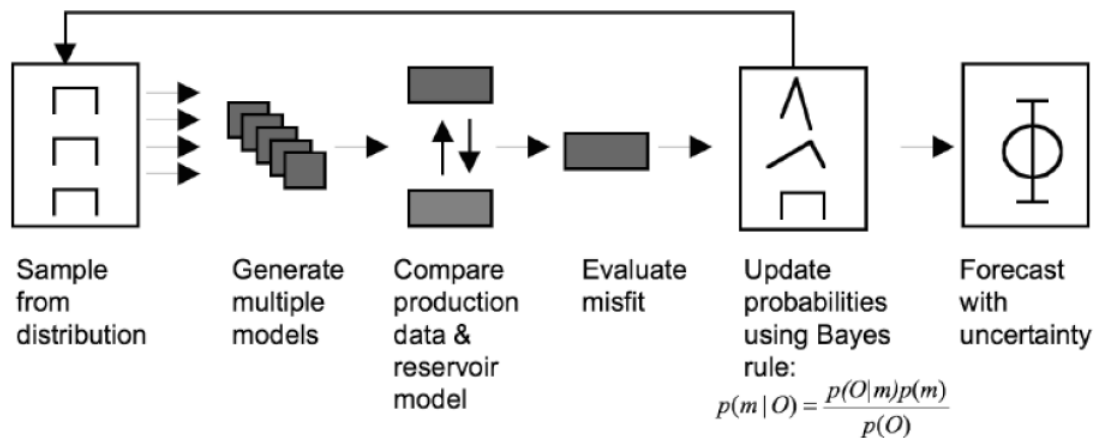


*Figure 2-12. Bayesian framework for uncertainty quantification (after Christie et al. 2013)*

Uncertainty quantification using the conventional history matching technique can be carried out using three methods:

- (1) Methods that categorise the PPD locally around the Maximum Likelihood (ML), or Maximum a posteriori (MAP) (when the prior is incorporated): The Linearization of the maximum posteriori (LMAP) is an example of this approach. The maximum a posteriori (MAP) estimate is first determined, then approximate conditional realizations, is generated using linearization about the MAP estimate (Davis 1987). LMAP has an advantage of a single base case history matching, however, the generated realization may provide a poor estimate of the uncertainties in data mismatch.
- (2) Methods that use a subset of the ensemble: Randomised maximum likelihood (RML) is an approach to generate conditional realization from a subset of an ensemble of history matched models (Kitanidis 1995). A study has been presented which show that the RML

method samples the posterior probability density function (PDF) correctly if data and the model are linearly correlated (Reynolds et al. 1999). Nevertheless, no rigorous theoretical foundation exists for the method when the correlation between data and model is nonlinear, which is the case when the data represent production data (Oliver 1996).

- (3) Methods that sample from the complete ensemble: Markov Chain Monte Carlo (MCMC) is an example of algorithms used to sample the full posterior probability density function (PDF) (Slotte et al. 2008). This process usually requires a massive number of steps to converge to the appropriate distribution even with small number of uncertain parameters and may be unrealistic to achieve using full physics simulation. In order to minimize the computational cost, a proxy model is built to represent the global objective functions and then MCMC is applied to the response surface.

## 2.8. Summary

This chapter started with a review of the various EOR methods available, where we discussed chemical methods, Gas injection, thermal methods, and microbial methods. This chapter further provided a discussion on the geological uncertainties and different ways to account for uncertainties in reservoir models such as best guess, multiple stochastic approach, and multiple deterministic approach. We pointed out the importance of having an adequate number of realizations of geological models to reduce risk and account for uncertainties in reservoir forecast especially when modelling a capital-intensive project like EOR. We further discussed the mechanism of polymer flooding in providing mobility control and hence improvement to the macroscopic sweep efficiency. We also discussed different types of polymers and described the characteristics of two most popular polymers used in polymer flooding which are Xanthan and HPAM. A mathematical model that captures all the key components of flow of polymer in porous media was presented and each flow phenomena were further discussed. This chapter also presented a review on history matching techniques and optimization algorithms such as deterministic and stochastic and data assimilation. We also discuss different ways to approach the parameterization of uncertain parameters during history matching. Finally, this chapter presented a workflow for probabilistic uncertainty quantification using Bayesian Theorem.

We presented two optimization methods i.e. nominal and robust optimization and we further established that robust optimization is usually not applied in EOR modelling such as polymer flooding due to computational efforts and therefore to reduce risk we applied robust optimization. Even though robust optimisation has been applied to water flooding, the geological realisations employed do not usually capture geological uncertainties that are not possible to parameterise during history matching such as top structure, shale-cut offs in determining the net-to-gross, fault models as well as uncertainties due to history matching technique. We apply robust optimization to robustly quantify the financial upside and downside of polymer flooding. Robust optimization helps us to integrate the uncertainties that are encountered during the entire reservoir modelling workflow (i.e., geological and interpretational uncertainties) as well as history matching uncertainties.



Polymer flooding is a promising but capital-intensive enhanced oil recovery (EOR) approach and therefore requires comprehensive and rigorous screening and risk evaluation (Sorbie 1991). Reservoir simulation is a valuable tool for carrying out this assessment, but usually does not capture all the uncertainties associated with the geological heterogeneity and complexity present in the reservoir, as well as the physical uncertainties associated with the polymer flood itself. It is necessary to use adequate reservoir models to reduce the risks associated with polymer flooding. In other words, we need to account for a realistic range of uncertainties relevant to geology and modelling decisions rather than modifying a single base case (Bentley and Ringrose 2017). According to "Flora's Rule" (Ringrose and Bentley 2015), if an EOR process such as polymer flooding changes the fluid-rock interactions and mobility ratios, it is not guaranteed that key geological uncertainties are properly captured in a reservoir model that was previously history matched for a different recovery mechanism. It is therefore possible that geological uncertainties are not adequately propagated into future predictions of reservoir performance, particularly when the history matched model is centred around a single base case.

History matching is a way of reducing uncertainties in the input variables of a reservoir model. History matching uses historical production data of a field to determine the reservoir properties that cannot be measured. History matching is achieved by tuning the reservoir properties to eliminate the mismatch between the simulated and observed production data. Once the simulated data matches the production history, the history matched reservoir model can be used for future production forecasts. History matching is an ill-posed problem and the relationship between input and response variables is highly non-linear, i.e. different combinations of the uncertain model properties can yield results that match the same production data. History matching can be broadly categorized by two approaches, deterministic and stochastic history matching. Deterministic methods obtain a single, or sometimes a small number of, history matched models, often through manual tuning of model parameters or by using a deterministic optimization algorithm (Oliver and Chen 2011). In contrast, stochastic history matching techniques aim to obtain an ensemble of models that covers the space of uncertain model parameters more broadly. Our study will examine how each approach impacts the projected economics of a polymer EOR scheme.

# Chapter 3. Methodology

## 3.1. The Watt Field

Several synthetic reservoir models such as Brugge field, CSPE10, PUNQ model, Olynus challenge etc., have been developed to carry out studies on enhanced oil recovery, upscaling, history matching and optimization (Peters et al. 2009; M. A. Christie and Blunt 2001; Dehghan Monfared et al. 2014). These model realizations miss out geological, interpretational, and modelling uncertainties encountered during reservoir characterization and modelling. These uncertainties are difficult to parameterize and include but are not limited to the presence and location of the faults, the depositional environment, the top structure of the reservoir, shale cut-offs, rock typing methods.

The Watt Field is a synthetic field based on real field data generated to address geological, interpretational and modelling uncertainties encountered during reservoir characterisation and modelling (Arnold et al. 2013). The interpretational and modelling uncertainties are around the following areas:

- I. Top structure model – seismic interpretation of the top structure defines the enclosure size and can be quite uncertain from the data and the depth conversion.
- II. Fault network modelling – fault location, dimensions and the connectivity of the network defines the partitioning of the reservoir.
- III. Grid resolution – The resolution of the grids that can capture adequately the geological features of a reservoir model.
- IV. Facies modelling methods – choice of algorithm to populate model with facies which is influenced by the depositional environment of the reservoir.
- V. Facies interpretations – how the facies are interpreted from well logs through shale cutoffs
- VI. Poro-perm transforms from the available well data – how to model permeability and porosity between the wells for the individual facies.
- VII. Relative permeability data.

The field was appraised using six wells, Wells A to F, and 16 horizontal production wells located at the central part of the reservoir, 5 horizontal and 2 vertical injectors were subsequently used to develop the field.

Top structure and wireline data is based on real field data, whereas, the fluid properties, the relative permeability, and capillary data are synthetic. Core data which contains the Porosity and permeability for Wells A and C were provided. Neutron Density porosity data is provided for all wells A to F. Six relative permeability data, three for the coarse sand facies (code 0) and three for the fine sand (code 1) were provided.

### 3.1.1. Overview of the Watt Field

The Watt Field (Arnold et al. 2013) is a semi-synthetic reservoir model based on real reservoir data and includes a broad range of geological uncertainties and modelling decisions. The reservoir has an area of 12.5 km by 2.5 km and is about 190 m thick. Most of the reservoir lies below the oil water contact. The initial pressure of the reservoir is 2500 psi as measured from Repeat Formation Testing (RFT) and well test data. The Watt Field was appraised using six wells and developed using 12 horizontal production wells located across the central part of the reservoir and 7 injectors around the edges. A synthetic field development plan was used in this study. In the original development plan, the horizontal multi-lateral wells aimed to maximize the distance from the oil water contact because of the low relief of the field and increase oil production from the top oil layer of the reservoir.

The depositional environment of the Watt Field is interpreted as a braided river system. Facies consist of coarse sand, fine sand, and shales. Key geological uncertainties are the top structure, shale cut-offs to define net to gross and the location and presence of faults (Arnold et al. 2013). Three possible fault models were developed, the first with only East-West trending faults, the second with additional North-South trending sub-seismic fault, and the final one with an additional number of sub-seismic faults. The Watt Field also considers uncertainties in the reservoir modelling itself in that both, pixel and object-based modelling, were used to predict the facies distribution while applying three different cut-off values of 0.5, 0.6, and 0.7. Permeability-porosity cross plots from the cored wells were used to model the permeability of each facies between wells. The reservoir is water-wet and two different two-phase relative permeability curves based on the Corey model are included in the model. The viscosities of oil and water are 10cp and 1cp, respectively. The PVT properties are uniform. Table 3.1 summarises the key reservoir properties. For further details on the Watt Field please refer to Arnold et al. (2013).

The geological and interpretational uncertainties considered in this thesis will be discussed in the subsequent sections.

Table 3-1. Table of uncertainties considered in the Watt Field model. The combination of top structure, fault model and facies cut-off uncertainty results in 81 different combinations/realizations.

Model property	Description	File name	Total of 81 different combinations of these properties
Top Structure	1	TS-1	
	2	TS-2	
	3	TS-3	
Fault Model	1	FM-1	
	2	FM-2	
	3	FM-3	
Facies Model (Cut-offs)	0.6	CO-1	
	0.7	CO-2	
	0.8	CO-3	
Grid	100 m by 100 m by 5 m	G-1	
	100 m by 100 m by 10 m	G-3	
	200 m by 200 m by 5 m	G-3	

### 3.1.2. Geological and Interpretational Uncertainties

#### 3.1.2.1 Top Structure

Uncertainties in the top structure are accounted for by developing a number of possible tops from the same depth converted horizon, conditioned to three different sets of well picks. Three different well picks were chosen by three different interpreters from the same wireline data with a variation in top structure height of between 2 and 20 meters depending on the well (Figure 3-1 Figure 3-2). The seismic horizon was tied to each well pick. Due to the inherent uncertainties in this process, three different possible depths of the top structure models were developed. Wells A and B showed a very good correlation and high precision in well picks and thus indicates a small uncertainty, whereas the well picks of Wells E and F had an uncertainty of approximately 10 meters.

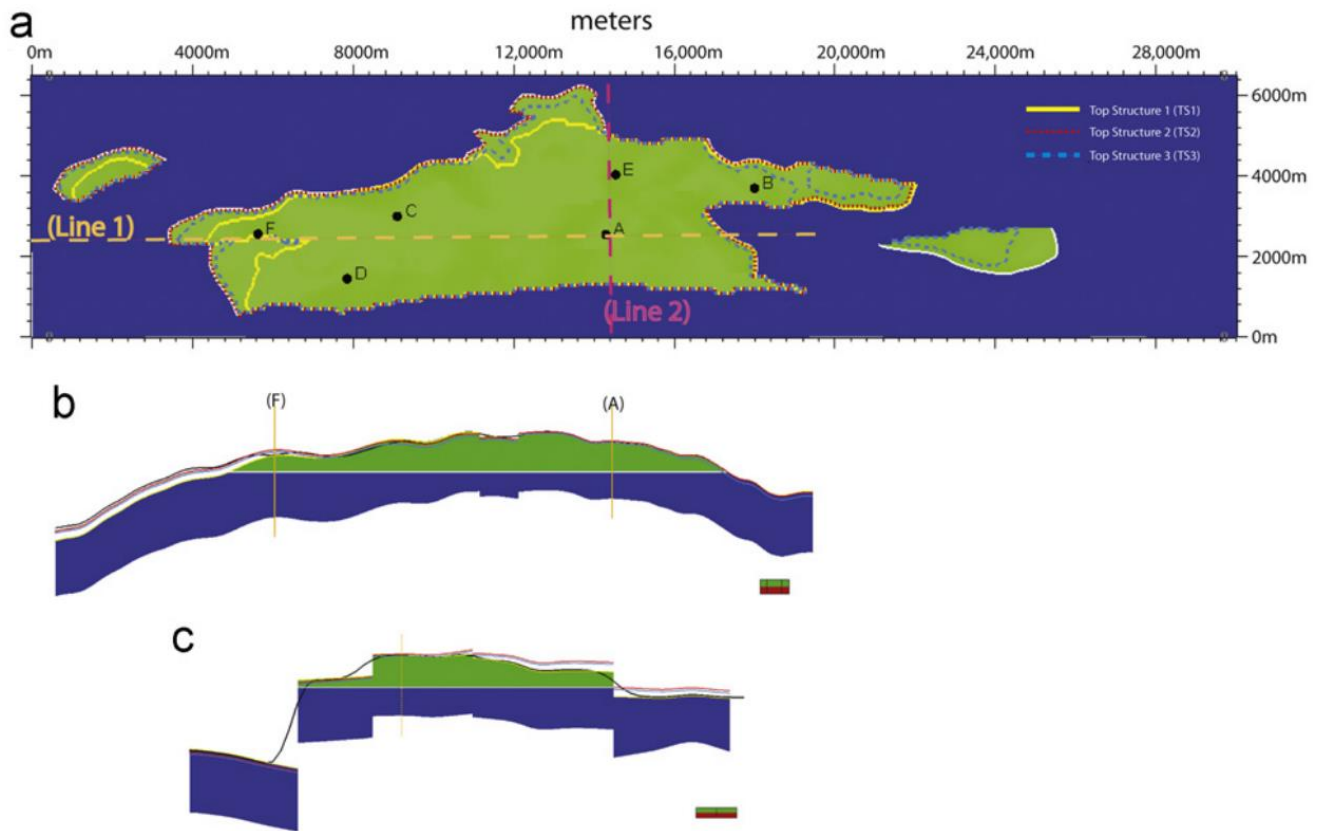


Figure 3-1. Seismic top structure and major identified faults modelling (a) is the plan view of the reservoir, (b) is a cross section (Line 1), (c) is a cross section (Line 2) (from Arnold et al. 2013).

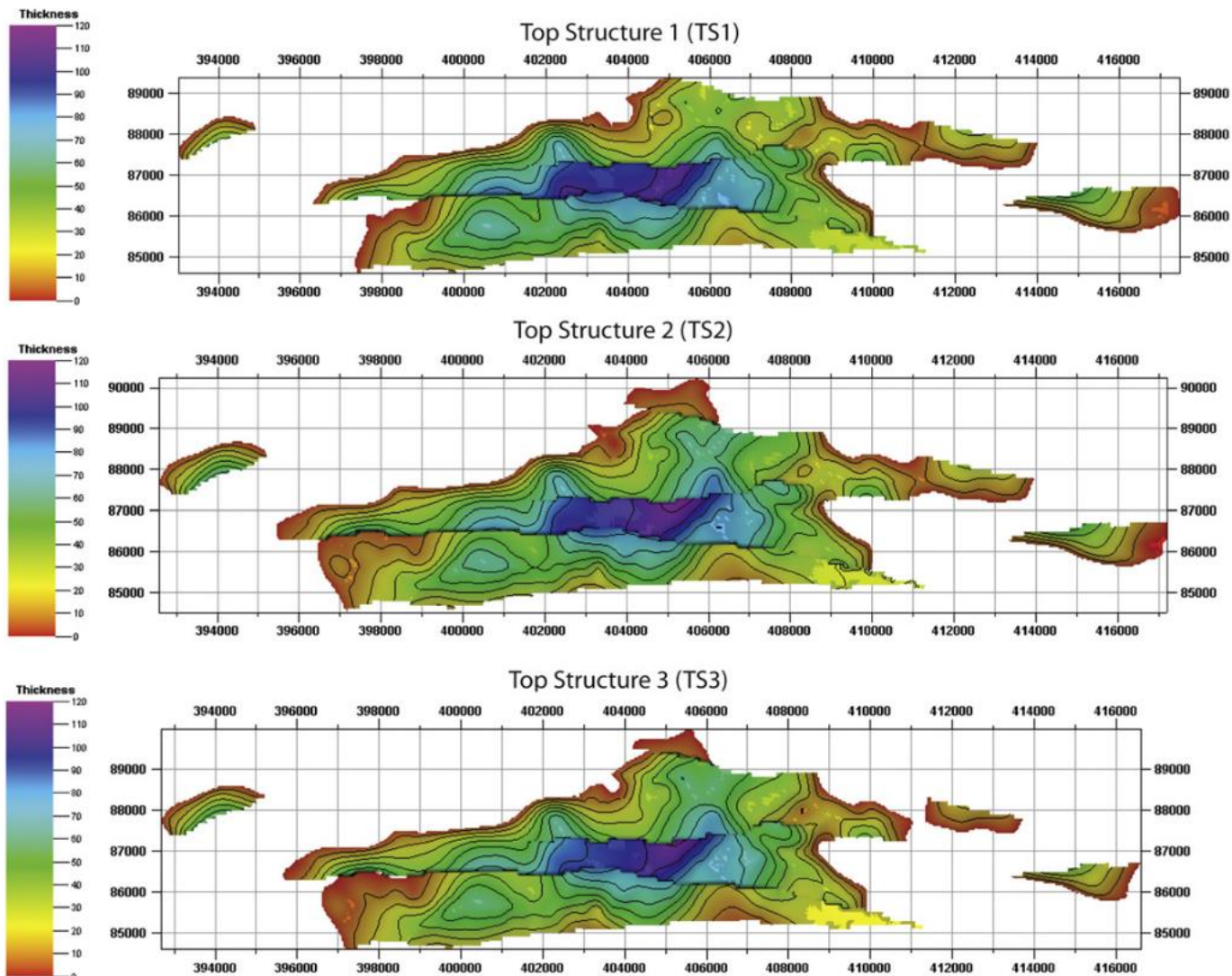


Figure 3-2. Example of three top structural models of the Watt Field (from Arnold et al. 2013).

From the interpretation of the seismic data several faults were identified and then depth converted together with the top structure. Faults displacements are calculated from the top structure curvature and therefore contain an implicit uncertainty in the throw along the faults. All the observed faults strike in a general East-West direction. There is no large-scale faulting apparent in the seismic data in other directions, but sub-seismic faulting may be possible. Hence the impact of sub-seismic faults striking in a North-South is investigated, because such faults would impact on connectivity between wells. No significant fault displacement is apparent in the appraisal and the development wells, and hence any displacement across the North-South striking faults is likely to be small.

To capture these uncertainties, three faults models in the reservoir were developed (Figure 3-3). The first model contains only East-West striking faults. The second model contains additional

North-South striking sub-seismic faults with displacements of less than 10m. The third contains additional sub-seismic North-South striking faults.

Another important uncertainty is the sealing potential of the faults, caused by juxtaposition of sedimentary units and the creation of a low-permeability damage zone in the fault core. For simplicity, the Watt Field only considers simple constant and uniform fault transmissibilities for each fault model.

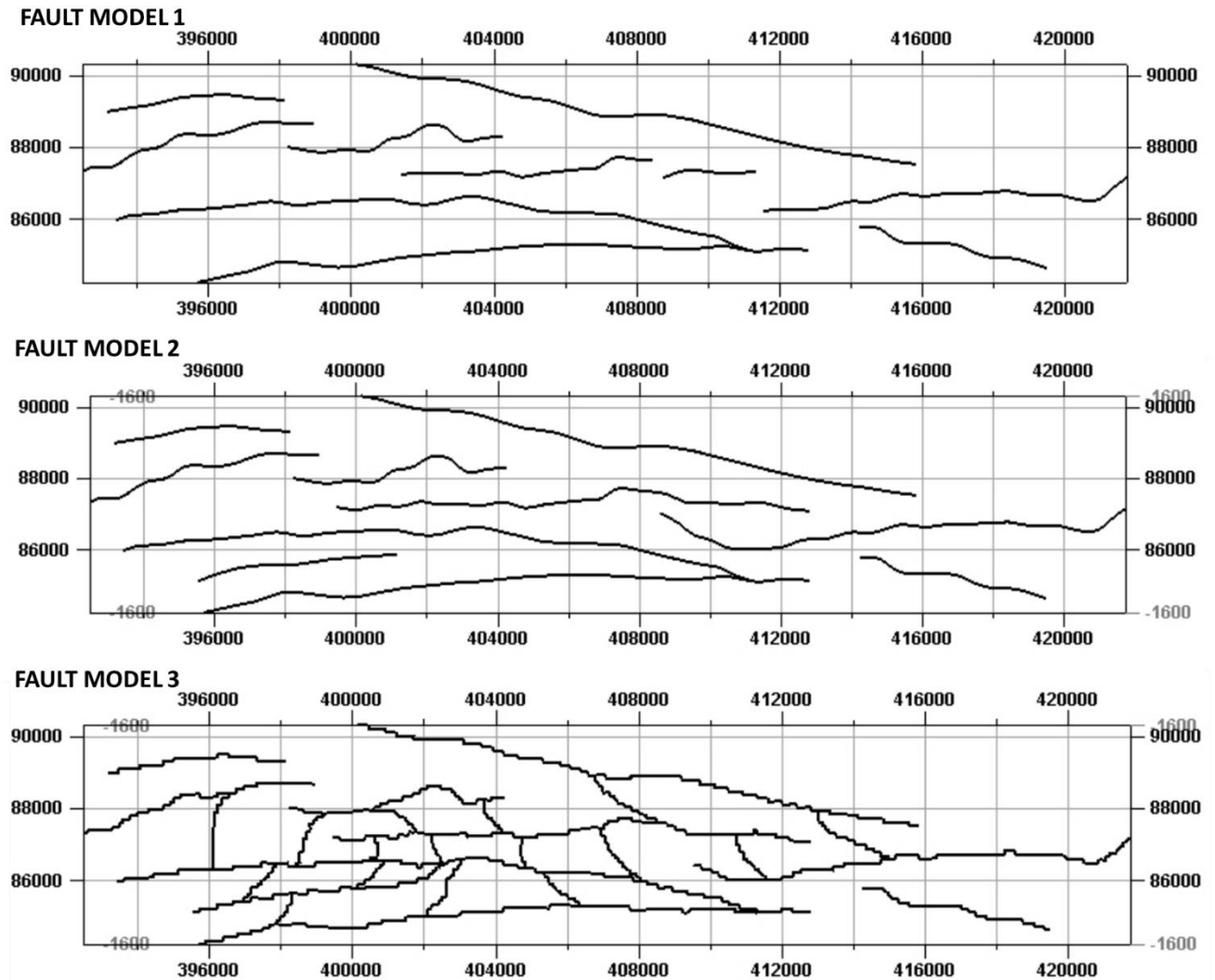


Figure 3-3. Uncertainty in fault network models of the Watt Field developed by three different interpreters (from Arnold et al. 2013).

### 3.1.2.2 Facies modelling

Facies can be detected in the wells in cored sections if provided. There is a large amount of noise in the gamma data provided for this reservoir which makes it less effective as a predictor for the facies. Alternatively, the facies were detected using relative porosity difference (RPD) with different shale cut-offs (0.6, 0.7 and 0.8) being used to classify the coarse sand facies. Three cut-off values were established, and the facies logs for all 6 appraisal wells were predicted. Facies logs were developed for each cut-off (Figure 3-4). Shale cut-off is used to distinguish between sand and shale and allows the identification of total sand intervals. This implies that for a shale cut-offs of 0.6, rocks with more than 60 percent are considered as non-reservoir rock, while rocks with equal to or less than 60 percent are considered as reservoirs. Average permeability increased from 557md to 623md as shale cut-off was increased from 0.6 to 0.8. Also the standard deviation of permeability was also seen to increase with shale cut-off (i.e., from 1440md to 1628md). This implies that heterogeneity of the reservoir increased, creating more high permeability channels which can impact sweep efficiency. Pixel modelling techniques and object modelling techniques were used to populate the properties of the static models resulting in different realisations of geological models. A comprehensive and well detailed modelling of the Watt Field reservoir model can be found in the appendix section of Arnold et. al. (2013).



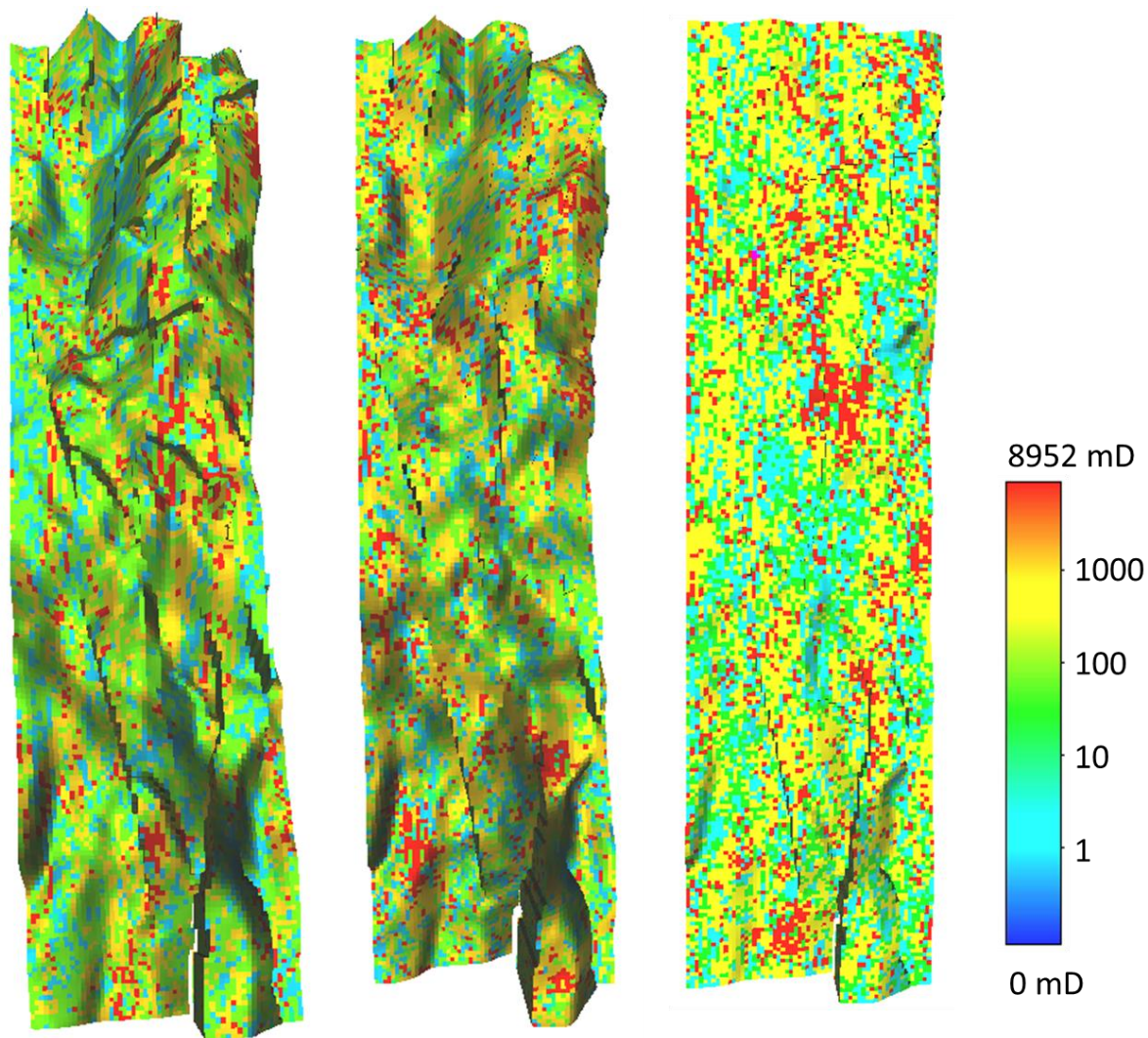


Figure 3-4. Permeability distribution of the Watt Field model for three different cut-offs.

### 3.1.2.3 Porosity-permeability modelling

As aforementioned, Permeability data is provided as core plug data in Wells A and C. Prediction of permeability in the other wells were done using a direct prediction from identified poro-perm correlations (Figure 3-5). This can be developed where no core plug data is available using log predictions like neutron density porosity. Figure 3-6 shows the correlation between neutron density and core plug porosity estimates and the probability histograms for both measurements of porosity. The good correlation and similar probability distributions suggests we can expect good porosity predictions from the neutron density logs in the other wells. Figure 3-7 is the 3D model that shows the porosity and permeability distribution of one realisation of the Watt Field model.

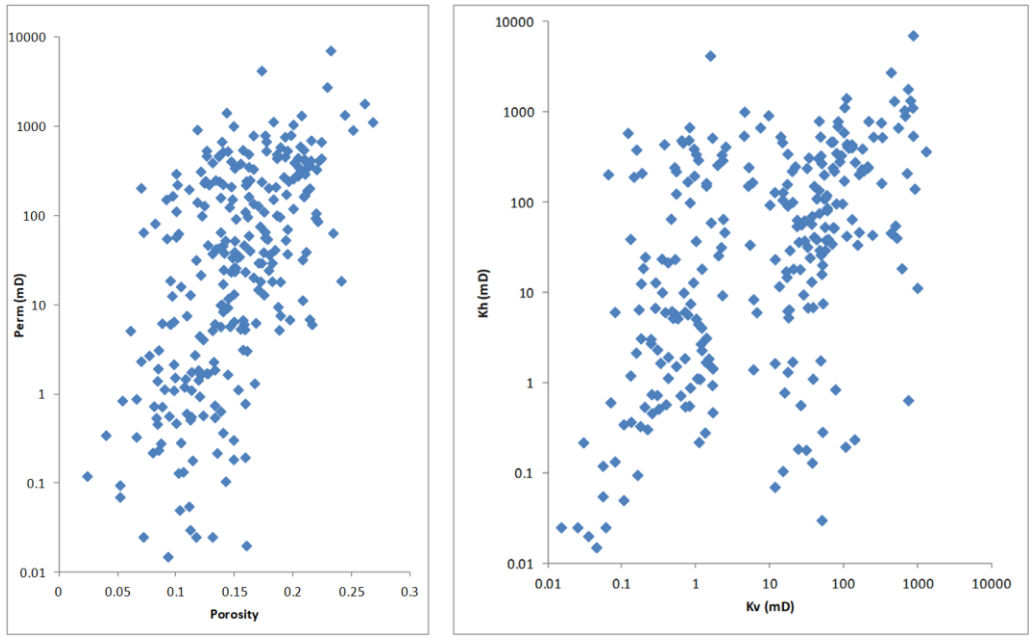


Figure 3-5. Porosity Permeability (left) and kv/kh (right) plot for Well C (from Arnold et al. 2013).

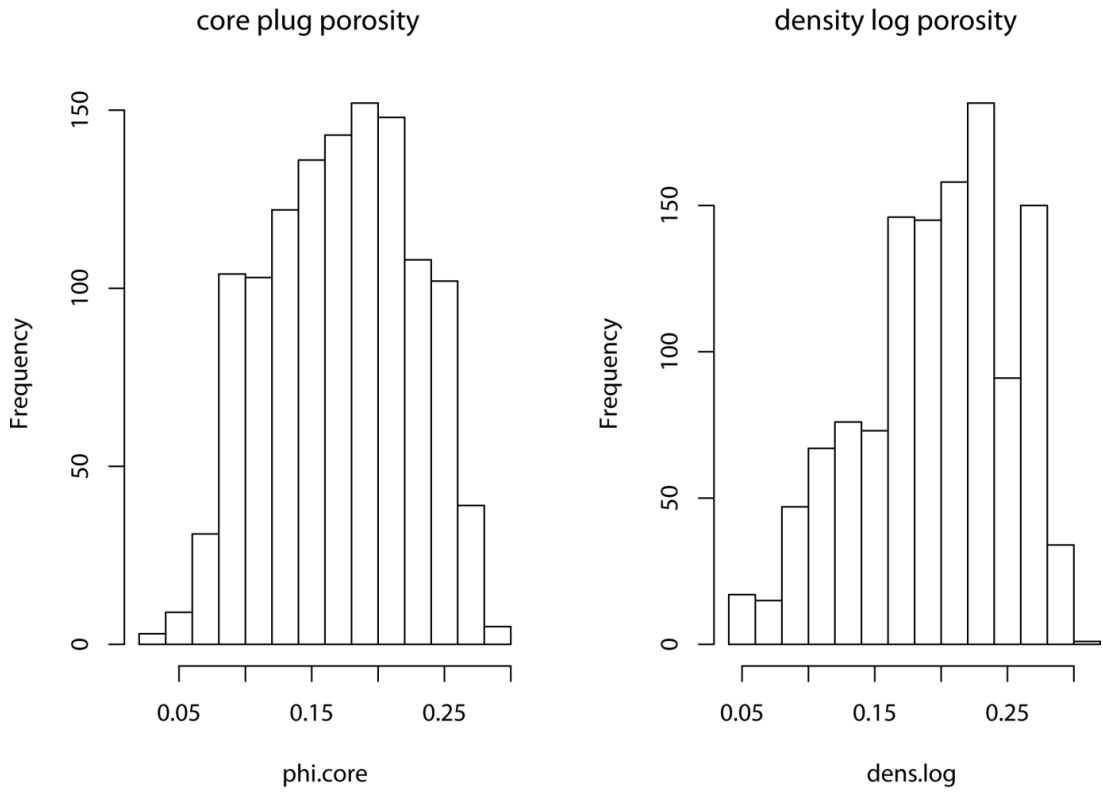
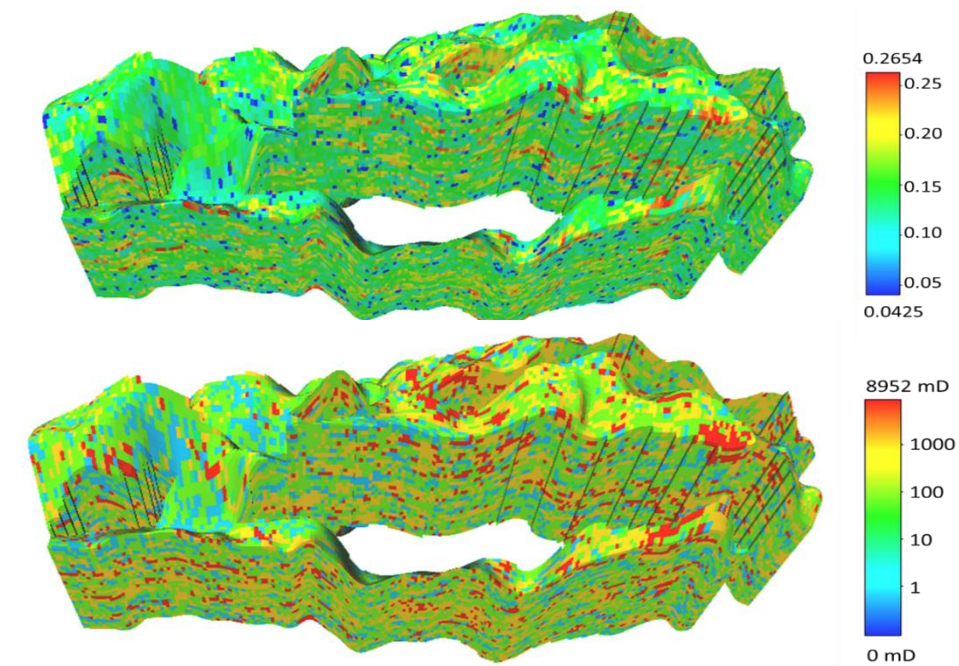


Figure 3-6. Porosity distributions for well core plug data and neutron density predictions. The two distributions are very similar (from Arnold et al. 2013).



*Figure 3-7. 3D model of the Watt Field showing porosity distribution (top) and permeability distribution (bottom) for one geological realisation.*

Six relative permeability curves were available, three each for the coarse and fine sand facies generated from cores taken from three different wells A, C and F (Figure 3-8) The  $S_{or}$  values for fine sand are 0.02, 0.23 and 0.0 for Wells A, C and F respectively. Whereas, the  $S_{or}$  values for coarse sands are 0.4, 0.0, and 0.1 for Wells A, C and F respectively. The available data shows that capillary pressure is negligibly small, so it is not considered in the models.

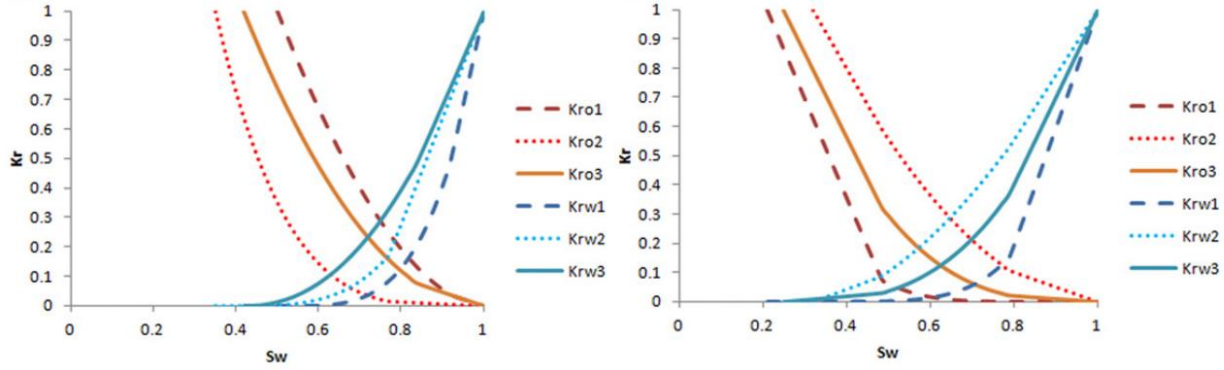


Figure 3-8. Relative permeability curves from Wells A, C and F for the fine sand (left) and coarse sand (right) facies.

The saturation of which  $k_r$  become 0 is the end point saturation of the relative permeability curve. Irreducible water saturation  $s_{wirr}$  or the connate water saturation  $s_{wc}$  is the end point saturation for water. Whereas, the end point saturation for oil is called the residual oil saturation  $s_{or}$ . The value of relative permeabilities at end point saturation can indicate wettability as follows:

For water-wet system,  $k_{rw}(s_{or}) \ll k_{ro}(s_{wirr})$  and for oil-wet system,  $k_{rw}(s_{or}) \approx k_{ro}(s_{wirr})$

### 3.1.3. Truth Model

One of the 81 realizations was selected as the truth case from which we generated the production data (oil, water and gas rates and BHP data) (Figure 3-9) for later history matching of the remaining 80 realisations. The production data was generated for 2933 days (8 years). The STOIP for the truth case is 1.6 Billion bbl and it will take about 40 years to recover about 60% of the STOIP using the current field development scenario. The truth case model (Figure 3-10) was operated at a maximum well production rates of 12,500 bbl/day and a minimum BHP of 1000 psi for the producer and a field injection rate of 70,000 bbl/day with a maximum BHP limit of 3500 psi. Rates were the primary control mode for both producer and injectors whereas BHP limits were the secondary control mode. However, during injection there was a period where the BHP limits were reached and the primary control switched to BHP leading to a decrease in injection rate. For producers, at certain period, the minimum BHP limit of 1000psi were reached in some wells and the production rates also decreased to avoid the pressure from dropping below bubble point resulting in a three phase flow. Figure 3-11 and show the third layer and cross section of the Watt Field after 40 years of production and Figure 3-12 shows the cumulative oil production for all the 26 realisations after 40 years.

A Gaussian noise of 15% of the value was introduced in the data to simulate the impact of measurement error in the data.

Table 3-2. Key Parameters of the Watt Field model.

Parameter	Value	Unit
Dimension	12500 x 2500 x 190	m
Resolution	226 x 59 x 40	-
Number of cells in the model	533,360	-
Rock compressibility	4e-6	1/psi
Mean Porosity	0.18	-
Mean Permeability	471	mD
Kv/Kh Ratio	0.1	-
Initial Reservoir Pressure	2500	psi

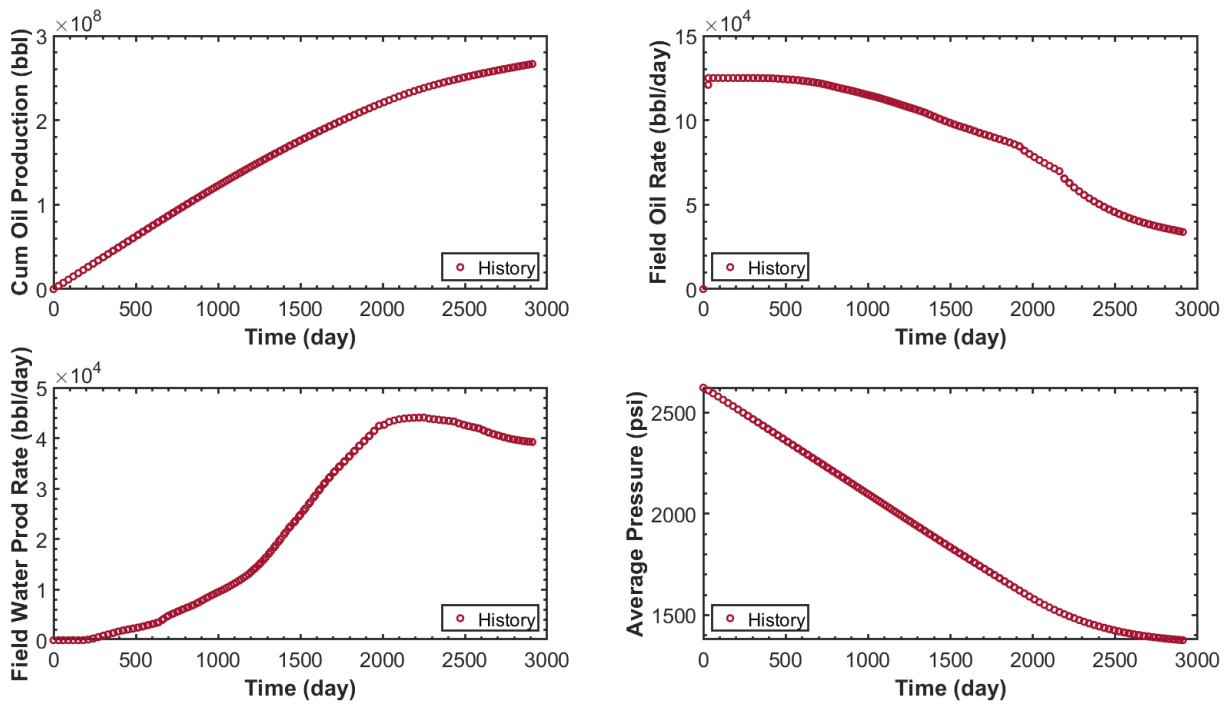


Figure 3-9. Historic production data (oil rate, water rate, cumulative oil production and average reservoir pressure) generated from the truth case model.

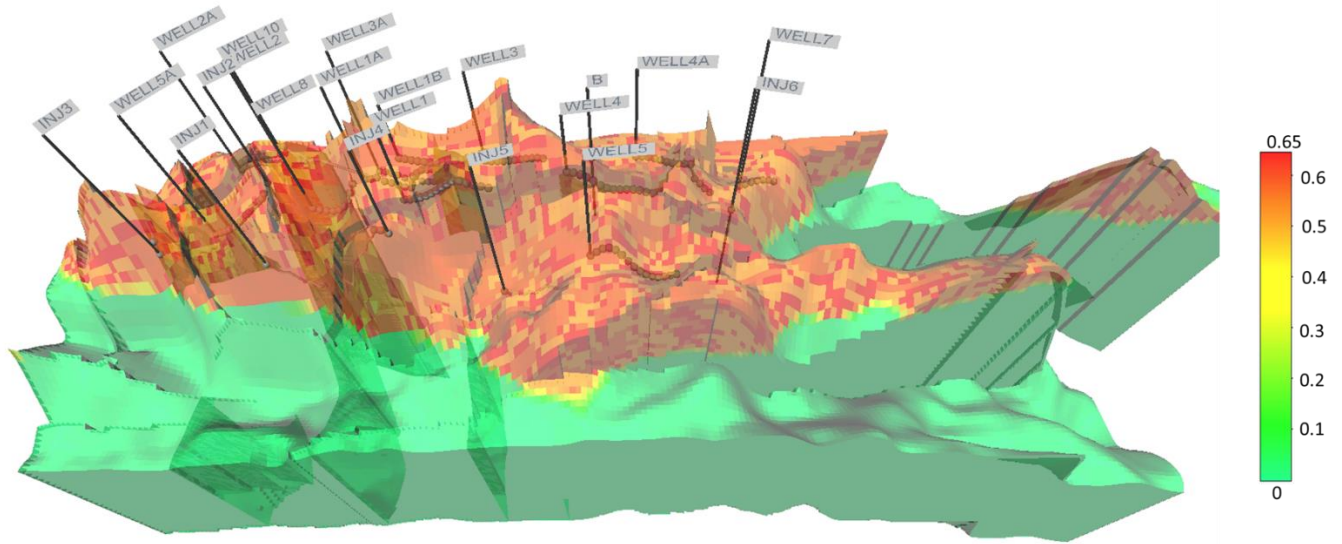


Figure 3-10. 3D view of the Watt Field model showing oil saturation as well as the location of injection and production wells.

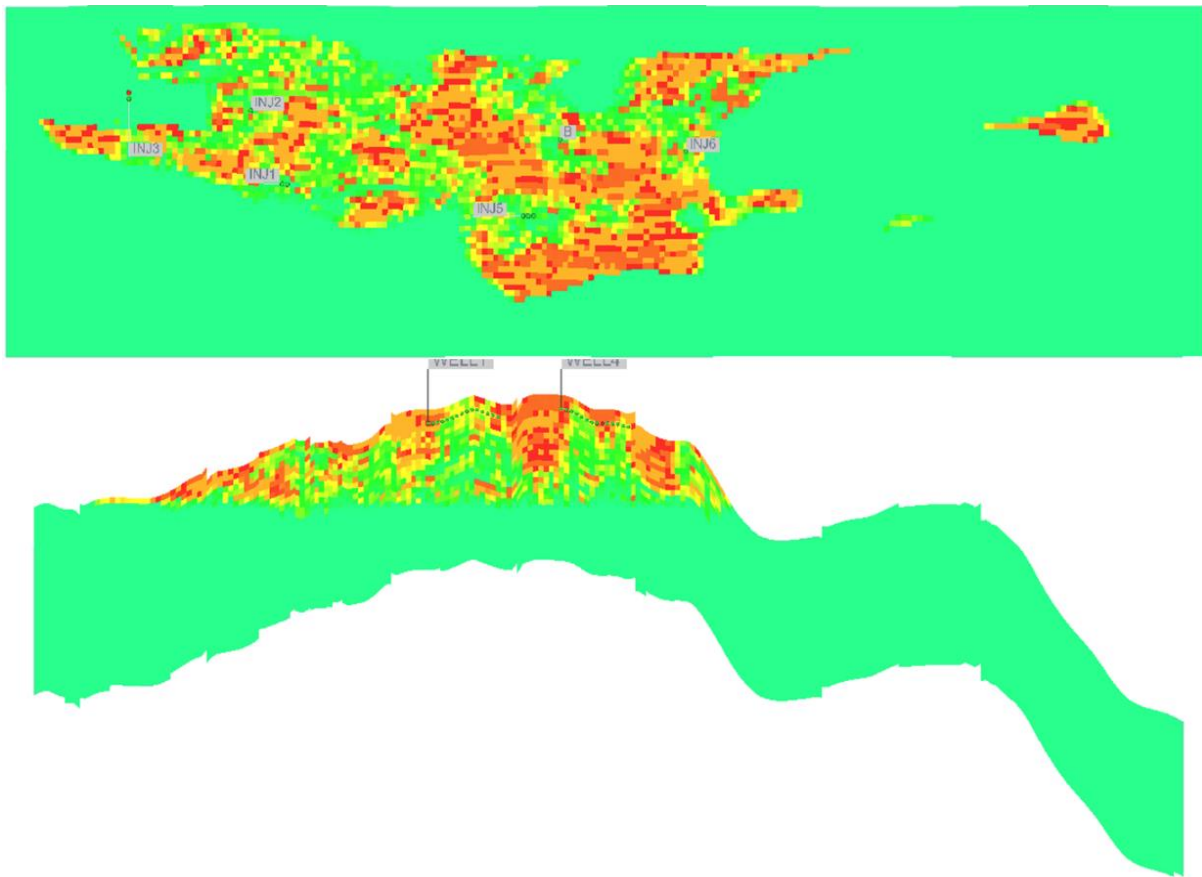


Figure 3-11. Third layer (top) and cross section (bottom) of the Watt Field model showing oil saturation as well as the location of injection and production wells after 40 years of production.

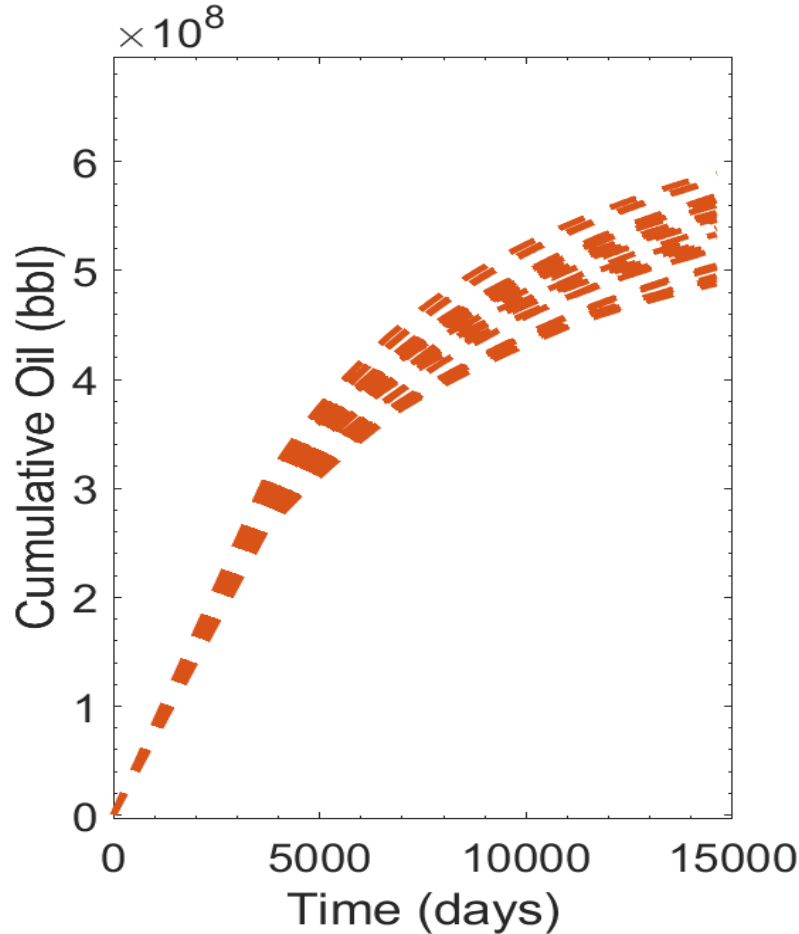


Figure 3-12. Forecast for cumulative oil production assuming a do-nothing scenario for all realisations after 40 years of production.

## 3.2. Particle Swarm Optimisation

PSO is a population-based stochastic optimization algorithm originally proposed by Kennedy and Eberhart (1995). It is inspired by the simulation of the social behaviour of a flock of birds (Mohamed et al. 2010) and was originally adopted to balance the weights in neural networks. PSO is comparatively straightforward and easy to implement, computationally efficient. In the oil and gas industry, PSO has been applied to history matching (Mohamed et al. 2010; Kato et al. 2014; Fernández Martínez et al. 2012), well placement optimisation (Onwunalu and Durlofsky 2010) and drilling (Irgens and Lavenue 2007; Self et al. 2016).

PSO starts with an initial population of random solutions and then looks for optimal solutions by updating subsequent generations of the initial solution. The individuals iteratively assess their candidate solutions and remember the location of their best success so far within the search space, making this data available to their neighbours. The particles are also able to see where their neighbours have had success. Movements through the search space are guided by these successes,

with the population usually converging towards good solutions. The balance between exploration (i.e. testing a broader parameter space) and exploitation (i.e. faster convergence to a solution) in search for multiple optima is maintained by iteratively updating the motion of the particle. The best solution the particle has seen, and the best solution across the whole population, are used to update the velocity of each particle, and consequently its position (Eberhart and Kennedy 1995). The particle's position  $x$  is updated by the velocity vector elements  $v$  as

$$x_q^{p+1} = x_q^p + v_q^{p+1}, \quad 3-1$$

where  $p$  and  $q$  are the iteration and parameter counters, respectively. The velocity  $v$ , which is transporting each particle, is updated through

$$v_q^{p+1} = \omega v_q^p + c_1 r_1 * (pbest_q^p - x_q^p) + c_2 r_2 * (gbest^p - x_q^p), \quad 3-2$$

where  $\omega$ ,  $c_1$  and  $c_2$  are coefficients which weigh previous velocity (inertia), best known position  $pbest_q^p$ , and position of neighbourhood particle  $gbest^p$ .  $r_1$  and  $r_2$  are random numbers generated between 0 and 1 that weigh  $best_q^p$  and  $gbest^p$ , respectively, for acceleration towards the best position.

In this thesis, we used PSO algorithm within CMOST for history matching and polymer flood optimisation.



Table 3.3. PSO Algorithm (Eberhart and Kennedy 1995)

<b>Step 1</b>	<b>Initialize the algorithm by generating an initial set of <math>n_{init}</math> models (or particles) at random locations (<math>x_q^{p=0}</math>) in a parameter space and with an random velocity (<math>v_q^{p=0}</math>) at each particle .</b>
<b>Step 2</b>	Calculate the misfit value for each model (or particle).
<b>Step 3</b>	For each particle $i$ , update the position and value of $pbest$ (. If current fitness value of one particle is better than its $pbest$ value, then its $pbest$ value and the corresponding position are replaced by the current fitness value and position, respectively.
<b>Step 4</b>	Find the $gbest$ (global best) fitness value and the corresponding best position of the entire population of $gbest$ , and update if required.
<b>Step 5</b>	<p>Update the velocity for each particle using Equation 3-1 The updated velocity is determined by the previous iteration velocity and the distance of the respective particle from the <math>pbest</math> and <math>gbest</math> location. Initially, the velocity is randomly generated with <math>v_q^{p=0} \in [-v_{max}, v_{max}]</math>. If a particle violates the velocity limit <math>v_{max}</math>, its velocity will be set back to the limit.</p> $v_q^{p+1} = wv_q^p + c_1r_1 \times (pbest_q^p - x_q^p) + c_2r_2 \times (gbest^p - x_q^p)$ <p>where</p> <ul style="list-style-type: none"> <li><math>v_q^p</math> is the velocity of particle <math>i</math> at iteration <math>p</math>;</li> <li><math>x_q^p</math> is the position of particle <math>i</math> at iteration <math>p</math>;</li> <li><math>c_1</math> is the weighting factor, termed as cognitive component that represents the acceleration constant that changes the velocity of the particle towards <math>pbest_q^p</math>;</li> <li><math>c_2</math> is the weighting factor, termed as the social component that represents the acceleration constant that changes the velocity of the particle towards <math>gbest^p</math>;</li> <li><math>r_1</math> and <math>r_2</math> are two random vectors with each component corresponding to a uniform random number between 0 and 1;</li> <li><math>pbest_q^p</math> is the <math>pbest</math> of particle <math>i</math> at iteration <math>p</math>;</li> <li><math>gbest</math> is the global best of the entire swarm at iteration <math>p</math>;</li> <li>and <math>w</math> is an inertia weight that determines the tendency of a particle to continue in the same direction it has been moving.</li> </ul>
<b>Step 6</b>	Update the position of each particle using as in Equation 3-2
	$x_q^{p+1} = x_q^p + v_q^{p+1}$
<b>Step 7</b>	Repeat steps 2 to 6 until maximum iteration is reached.

### 3.2.1. PSO History Matching

In total, 26 of the available 81 different geological realizations were used in this study to constrain the problem to a manageable size. These geological realizations were selected in such a way that the key interpretational uncertainties inherent to the Watt Field are adequately captured in our workflow. Geological uncertainties accounted for include three different faults models, the depositional model, the modelling algorithm (object- and pixel-based modelling), three different top structure, shale cut-offs (0.5, 0.6, 0.7) and permeability distributions.

For the stochastic approach using PSO, history matching start with a realization of the Watt Field Model. The original 40 layers were divided into 8 layers to reduce the number of parameters. The top layers consist of 4 cells thick with the lower 2 layer being 8 cells thick. The reservoir properties were modified with multipliers in each of the 8 layers to reduce the misfit. The individual misfit components (i.e. oil rates, water rates, gas rates, well bottom-hole pressure and average reservoir pressure) were assigned an equal weight of 1 and summed up to a single objective function using a weighted average. We could use this weighting because of the high level of confidence we have in our historical data, which was generated synthetically from a known “truth case”. Our weighting eliminated any bias and we therefore did not consider it necessary to assign a higher weight to a specific objective function. The history matching then modified the reservoir properties in such a way that this misfit is minimized. Table 3-3 illustrates the reservoir properties and their ranges that were modified to obtain an acceptable match between the simulated reservoir response and the production data generated from the truth case model. Note that we used individual multipliers for each property. The base case value for a multiplier is always 1. We maintained a constant multiplier for each uncertain reservoir properties across each layer of the reservoir to reduce the number of uncertain parameters as the PSO algorithm becomes inefficient in high dimensional problems.

*Table 3-3. Uncertain reservoir properties adjusted during history matching.*

<b>Reservoir Properties</b>	<b>Range of Multiplier</b>
Porosity (-)	0.05 – 1.3
Permeability (md)	0.05 – 10
Kv/Kh Ratio (-)	0.01 – 10
Fault Transmissibility Multiplier (-)	0 – 1

*Table 3-4. Input parameters used in PSO algorithm*

<b>Parameters</b>	<b>Values</b>
Number of particles	20
Inertia weight, $w$	0.729
Cognitive component, $c_1$	1.50
Social component, $c_2$	1.50

PSO algorithm then runs 500 iterations with different combinations of uncertain parameters to determine the best-so-far model for the 26 selected geological realizations. The ensemble of best-so-far models from PSO are used for uncertainty analysis and comparison with the best matched model from adjoint ensembles.

### 3.3. Adjoint Technique

Recall from Chapter 2, the total misfit  $D$  is obtained by the weighted sum of these individual misfit parameters (Equation 2-31).

The objective is to minimize the above function using adjoint technique. Adjoint technique computes the partial derivative  $\frac{\partial D}{\partial x}$ , of the objective function with respect to each parameter  $x$ , such as permeability, porosity and kv/kh ratio at the grid block level.

A gradient-based optimizer is coupled with the adjoint technique in SENEX to find a solution in an iteration of the following optimization steps (Ruijian et al., 2009)

1. The initial set of input parameters  $m$  is taken from a reference solution or an initial prediction. In our case the parameter set includes all porosity, horizontal permeability and  $kv/kh$  values at the grid blocks. The dimension of the input parameter is hence of order of  $10^6$ .
2. The objective function  $D(x)$  is calculated from the forward run of reservoir simulator and the corresponding sensitivity  $dD/dx$  is calculated using the adjoint system. In this thesis we focus on oil, gas, and water rates as well as pressure data on a well-by-well basis.
3. The optimization step uses sensitivities that were calculated analytically included in  $\delta x^{l+1}$  from the previous simulation run  $l$  in order to calculate an updated set of model parameters  $x^{l+1}$  as  $x^{l+1} = x^l + \delta x^{l+1}$ .
4. The number of regression steps is either continued until a maximum number of steps  $N_L$  is reached or convergence is obtained.

Similarly to PSO, the deterministic approach using Adjoint technique commences history matching with a realization and modification were made on the reservoir properties at each grid cell to reduce the misfit. We applied the adjoint type technique implemented in the commercial simulator SENEX (Senex 2013) to calculate analytical sensitivities for all well-based responses with respect to horizontal and vertical grid block permeabilities. The calculated sensitivities were then used in an iterative optimization to improve the misfit at the well level. Sensitivities and parameter updates were calculated for approximately 533,360 values (i.e. the total number of grid blocks) for each uncertain property (i.e. porosity, permeability, and Kv/Kh ratio) at the grid block level. We used the same properties as for the PSO-based history matching, i.e. oil rates, water rates, gas rates, well bottom-hole pressures, and average reservoir pressure to compute the misfit between simulated and observed production data. To avoid unphysical property updates in porosity and permeability, constraints were defined for porosity (-10% to +10%), horizontal permeability (-10% to +50%) and vertical permeability (-10% to +50%). The matching process commenced by a simulation run of the initial model where the sensitivity of the objective function with respect to each reservoir property at each grid cell was computed. A new set of reservoir parameters were then generated based on the calculated sensitivities. This new set of parameters formed the input for the next simulation run. The iteration continued while the mismatch was successively minimized and terminated when a satisfactory match was

achieved or when no further improvement was observed. Figure 3-13 shows the workflow employed by SENEX to reduce the misfit between the simulated and observed data.

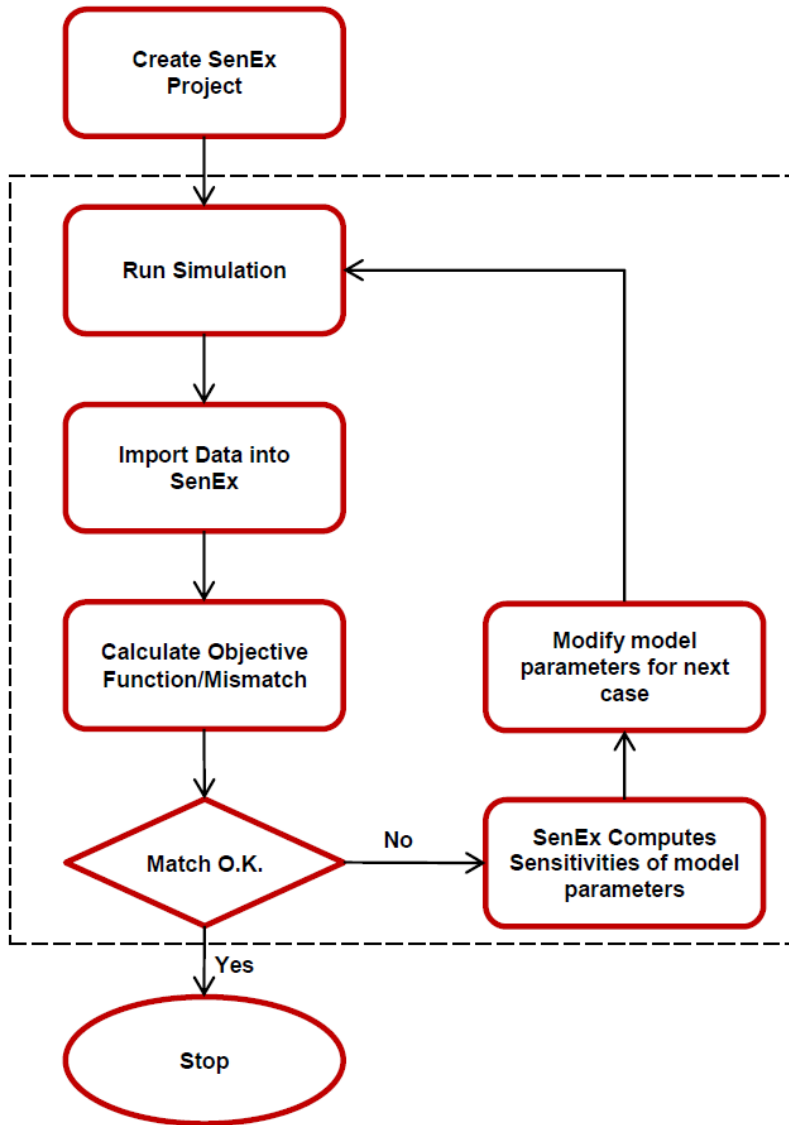


Figure 3-13. Workflow used by SENEX in adjoint based history matching process (from SENEX 2013).

Note: The parameter limits for both history matching techniques were set after sensitivity analysis. Since both techniques takes different approach in modifying the reservoir, the recommended parameter limits varied. Adjoint suggested lower range in parameter because it considered each property of a grid block as a parameter whereas in PSO, reservoir properties were modified using layering method.

### 3.4. Design of Experiment

Design of experiment (DoE) refers to the design of an experiment which has the purpose of analysing the variations of information under a certain condition that directly affects the variation (Elvind, 1992). An experimental design predicts the outcome by introducing changes in the combinations of the input reservoir parameters. The change in one or more input parameters is usually assumed to result in the change of the output variable (production response). Control variables (equation of the reservoir simulator) are also identified. The aim of DoE is not only to identify suitable variables (input, response, and control), but also to plan and deliver the experiment in a statistically optimal manner in the presence of limited computational resources. A major concern in DoE is often related to the reliability of the design. However, carefully selecting the input variables and making sure proper and detailed documentation is provided can mitigate these concerns (Fletcher 1970).

To make a choice of an experimental design, the aim is to select a design which produces highest insight of characteristics employing the lowest number of sampling (Astakhov 2012). Furthermore, the chosen experimental design technique should also provide confidence that the sampled points are a true representation of the design space (Ruby-Figueroa 2016). The choice of an experimental design is influenced by the nature of the problem being studied and the magnitude of resources available such as time, computational power, and the extent the problem has been defined (Cavazzuti 2013).

There are two key approaches to DoE, orthogonal design and random design. The orthogonal design assumes that the model parameters and input variables are statistically independent and uncorrelated and can be varied independently. Orthogonal design explores a larger search space and can represent model non-linearities (Seidenfeld 1992). The limitation of orthogonal design is that it is deterministic in nature and as such susceptible to collapse problems where one or more initial points appears to be irrelevant rendering the rest of the time-consuming computer experiment useless. Widely used orthogonal experimental designs are fractional and full-factorial design (Figure 3-14), central composite designs, and Box-Behnken designs. The random design involves the stochastic sampling of the model parameters in a random manner. Stochastic samplers are also known as space-filling designs because they are not constrained by sample sizes which are specific multiples of design parameters. The most used random design of experiment technique is the Latin Hypercube Sampling (LHS). LHS is not susceptible to collapse problem because if one or more input variable (reservoir parameter) appears to be unimportant, every point in the design will still provide some useful insight with respect to the influence of the other variables on the output (production response). Therefore, any experiment will be useful (Seidenfeld 1992). DoE is a key step for sensitivity analysis, history matching, and uncertainty analysis. DoE can also be used to train proxy models effectively (Elvind, 1992). Deterministic designs such as Box-Behnken, fractional factorial and central composite designs, are perfectly octagonal. These designs samples edges of the parameter space, and produce results that are biased towards extreme but are skewed against the contributions from samples in-between the extremes. However, LHS which is a more space filling and efficient technique were applied to

guarantee that each design variable has all parts of its ranges sufficiently represented in the sample.

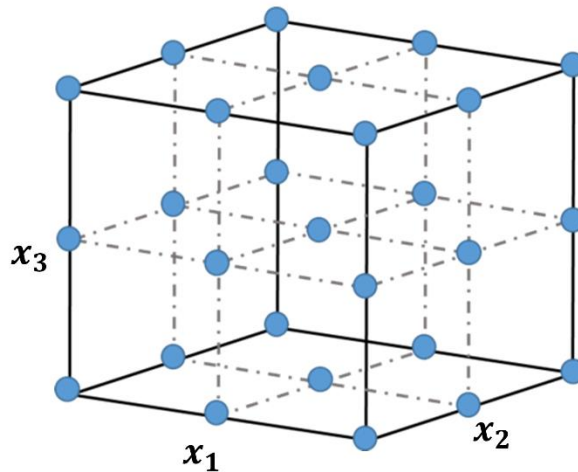


Figure 3-14. Full Factorial Design for a system with three parameters and three parameter settings (low, medium, high). Each dot connotes a parameter combination (after Astakhov 2012).

### 3.4.1. Latin Hypercube Sampling

LHS is a statistical technique for generating a near-random sample of plausible collections of parameter values from multidimensional distribution. As applied in statistical sampling, a Latin Square is a Square grid containing sample points provided each row and column contain only one sample. LHS is the extension of this assumption to a given number of dimensions, in which each axis aligned with a hyperplane contains one sample. In an experimental design with  $M$  variables, the range of each variable is divided into  $N$  equal levels and that there is only one point (or sample).  $N$  sample points are then placed to meet the requirements of a Latin hypercube. LHS then forces the total number of divisions to be the same for each variable. LHS does not require more samples for higher dimensional variables. As stated above a random procedure is employed to determine the sample points. The quality of the experimental design can be improved by randomization and optimization of point placement.

The popularity of LHS can be attributed to its flexibility to provide data for modelling techniques based on different statistical assumption and cover small to large design spaces. In addition, LHS can be optimized without considering the statistical assumptions of the model, more so, the choice of number of data points is quite flexible, and therefore can be determined based on the available resources. Another key strength of LHS is its non-collapsing capability i.e. if few input variables are considered non-influential to the response and are dropped out, the resulting design still remains a Latin hypercube design, although, it may be suboptimal. Therefore, if another set of properly designed data for the smaller domain is not affordable, the existing data will still be

useful. In addition, random samples can be taken one at a time, remembering which samples has initially be taken (Del Vecchio 1997).

We apply LHS (Figure 3-15) to generate training runs for the proxy model because of the efficiency of LHS in sampling the entire parameter space using a minimum number of sample points. The population of the properties of the static models were performed using a stochastic approach. Therefore, a stochastic sampling technique seems to be appropriate.

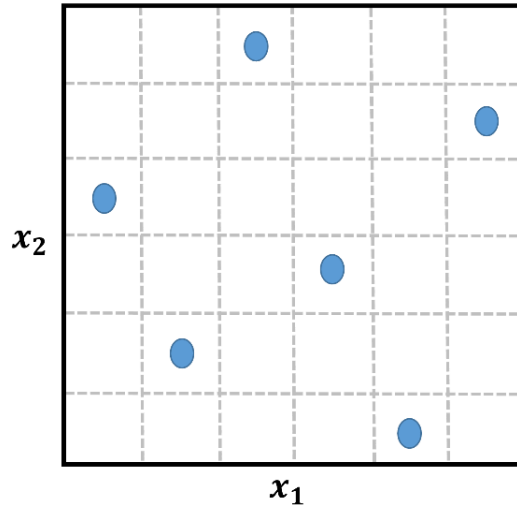


Figure 3-15: Latin Hypercube sampling for a system with two parameters and 6 parameter settings. Each dot represents a parameter combination (after Astakhov 2012).

### 3.5. Proxy Models

The non-linear behaviour of a full-physics reservoir model simulation can be approximated by a proxy model (also known as response surface), which provides a functional form that links the simulation output (e.g. well rates) to the input parameters of interest (e.g. well location or permeability variations). Proxy modelling has become an efficient way to study parameter sensitivities or decrease the computational cost for challenging reservoir simulation (e.g. Aissaoui and Moreno 2013; Babaei et al. 2015; Mohaghegh et al. 2015; Polizel et al. 2017). More so, proxy models have been successfully applied to augment the optimisation of water alternating gas injection in fractured carbonates reservoir (Agada et al. 2017; AlAmeri et al. 2020).

To generate a proxy model, an appropriate number of simulation runs, i.e. sampling points, is needed to train the proxy model for a range of input parameters. These sampling points can be chosen using experimental design in such a manner that the proxy model covers a broad range of input parameters and corresponding simulation outputs. The exact number of simulation runs to train the proxy model depends on the complexity of the problem and the DoE method that was selected.

Nevertheless, every proxy model is faced with these two main challenges. 1). Proxy model is limited in applications i.e. there only applicable to a particular objective function, and a

particular recovery mechanism. Also, they are limited to the specific parameter ranges used during the building of the proxy model. This implies that when a new objective function is introduced, or when the parameter ranges are modified, a new proxy model will need to be constructed. 2). The response surface of a proxy model changes as additional training runs are being introduced (Figure 3-16), therefore the position of the global optimal solution is also subject to change (Ahmadi et al 2018; Zubarev 2009; Jaberet al 2019).

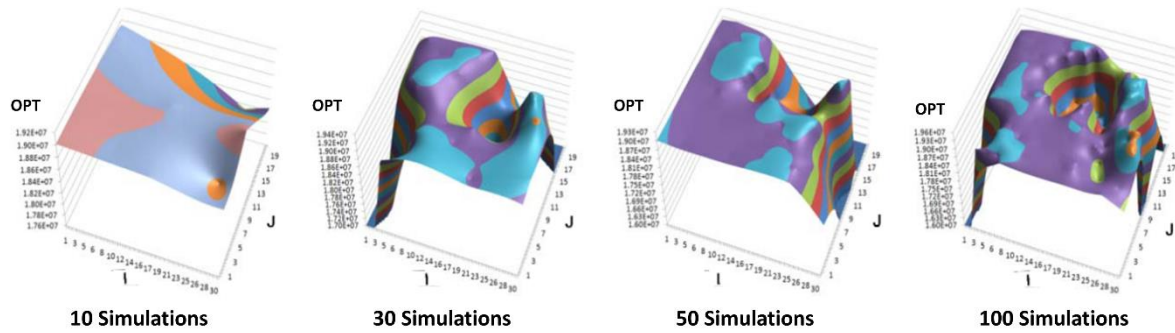


Figure 3-16. The evolution of the proxy model as the number of simulations for a single in fill well optimisation problem. (after Zubarev (2009)).

### 3.5.1. Polynomial Regression

For engineering application, the major challenge is usually the accurate identification of a suitable regression function which will adequately capture the essential features of the original problem. This challenge can be addressed by carrying out the optimization process iteratively and fitting new response surface approximations sequentially on a subsection of the entire design space. Typically, response surface approximations are implemented using first or second order polynomials. The general formulation for a quadratic polynomial regression is given by

$$y(x) = \beta_0 \sum_{i=1}^{n_d} \beta_i x_i, \tag{3-3}$$

and

$$y(x) = \beta_0 \sum_{i=1}^{n_d} \beta_i x_i + \sum_{i=1}^{n_d} \sum_{\substack{j=1 \\ j>i}}^{n_d} \beta_{ij} x_i x_j + \sum_{i=1}^{n_d} \beta_{ii} x_i^2, \tag{3-4}$$

where,  $x$  is a vector of input variables of length  $n_d$ ,  $x_i$  is a linear term,  $x_i^2$  is a quadratic term and  $\beta_0, \beta_i, \beta_{ii}$  represents unknown regression co-efficient constant for linear, cross and quadratic term respectively. To make sure that a suitable regression function  $\eta$  was chosen, the model adequacy should be assessed.



### 3.5.2. Proxy Model Validation

Cross-validation (Kohavi 1995) is usually performed to evaluate the proxy model through comparison with the full-physics simulation model. Cross validation is achieved by splitting the data into a training set and a validation set; the validation set does not contribute to the construction of the proxy model. Furthermore, a quantitative statistical measure can be used to assess model adequacy such as the co-efficient of determination  $R^2$  which can be expressed as

$$R^2 = 1 - \frac{SS_e}{SS_t}, \quad 3-5$$

where  $SS_e$  is the sum of squared residuals and  $SS_t$  is the total number of squares.  $R^2$  can be defined as the amount of variance in the sample response described by the fitted response surface.  $R^2$  ranges from 0 to 1, a value of  $R^2 = 1$  connotes a perfect fit and the absence of a residual. Precautions needs to be taken while handling this statistic. Increasing the regression function by adding new regressors will lead to an increase in the coefficient of determination not considering if it can improve the model predictive quality. In some cases, the response value at the sampling points are not approximated rather interpolated and therefore do not provide any information between the sampling points. To prevent this occurrence, the adjusted coefficient of determination  $R_{adj}^2$  can be employed.  $R_{adj}^2$  is expressed as

$$R_{adj}^2 = 1 - \frac{\mathbb{Y} - 1}{\mathbb{Y} - \mathfrak{p}} (1 - R^2), \quad 3-6$$

where  $\mathbb{Y}$ , is the number of independent variables,  $\mathfrak{p}$  is the size of the vector. The statistics of the adjusted  $R_{adj}^2$  does not necessarily increase as more data points are added rather it decreases as unnecessary data are added to the model.

Finally, prior to the deployment of the proxy model to approximate the full physics simulation, the accuracy of the model must be assessed. To examine the predictive ability of a proxy model, the set of sampling points is subdivided into two components. The first part is known as training data, it is used to generate the proxy model, while the second part is known as validation data which is used for validation.

## 3.6. Monte Carlo Markov Chain with Proxy-Based Rejection and Acceptance

Markov Chain Monte Carlo (MCMC) is a computer-based sampling technique (Rubinstein and Kroese 2016). MCMC enables the characterization of a distribution without having the full knowledge all of the distribution's mathematical properties by a random sampling of values out of the distribution. A key strength of MCMC is its ability to draw samples from distributions even when all that is known about the distribution is how to calculate the density for different samples (Ravenzwaaij et al. 2018). The name MCMC combines two features: *Monte-Carlo* and *Markov chain*. Monte-Carlo is the technique of predicting the properties of a distribution by assessing random samples from the distribution (Jim and David 2013). For instance, Monte-

Carlo computes the mean of a large sample of the distribution instead of computing the mean directly from the equation of the normal distribution. The merit of the Monte-Carlo technique is obvious: computing the mean of a large sample of data is much easier compared to computing the mean directly from the equation of the normal distribution especially in situations where random samples are easy to draw while the equations of the distributions are difficult to solve (Dunn and Shultis 2012). The Markov chain feature of MCMC is the concept that the random samples are created by a unique sequential process. Each random sample is used as a starting point to create the next random sample, consequently yielding a chain structure.

The Metropolis-Hastings MCMC method is one of the commonly used technique of MCMC (Rubinstein and Kroese 2016). The basic concept of Metropolis-Hasting MCMC is to conduct a random walk which is governed by a probabilistic criterion. The walk is being modified by the criterion accepting some moves while rejecting others so that the modified walk samples the target distribution. Table 3-6 explains the steps that are carried out by the Metropolis Hastings MCMC algorithm.

*Table 3-5. Metropolis-Hasting MCMC Algorithm (Liang et al.2010)*

<b>Step 1</b>	<b>Start with any initial model <math>\theta_0</math></b>
<b>Step 2</b>	Use the current point $\theta$ , sample a candidate point $\theta^*$ from an arbitrary proposal distribution $q(\theta_2/\theta_1)$ . The only restriction on the proposal distribution is that it is symmetric, i.e., $q(\theta_2 \theta_1) = q(\theta_1 \theta_2)$
<b>Step 3</b>	Given the candidate point $\theta^*$ , calculate the ratio of the density at the candidate ( $\theta^*$ ) and current points ( $\theta$ ),  $\alpha = \frac{p(\theta^* d)}{p(\theta d)}$ <span style="float: right;">3-7</span>
<b>Step 4</b>	If the candidate increases the density ( $\alpha > 1$ ), accept the candidate point (set $\theta = \theta^*$ ) and return to step 2. If the jump decreases the density ( $\alpha < 1$ ), then accept the candidate point with probability $\alpha$ , else reject it and return to step 2.

MCMC samples from the approximation of the posterior density function of history matched models. The technique by which the Adjoint and PSO methods converts misfit to likelihood is discussed in Chapter 2.

The computational cost of Metropolis-Hasting MCMC can be expensive when used to conduct a reservoir simulation studies. This is because the MCMC often needs thousands of simulation runs to converge to the required distribution. To compute the posterior, each iteration will need a full physics simulation which is usually time consuming for real field application. In addition, the acceptance rate of the MCMC is usually small as most candidates will be rejected and the computation effort required to run the full physics simulation is wasted.

To remedy this situation, where MCMC will require thousands of full physics numerical simulations, we apply the Proxy-based Acceptance-Rejection (PAR) sampling method. The

major benefit of the PAR method is the application of rapid proxy model application approximation of the posterior to infer if to accept or reject a candidate model. Full physics simulation is then conducted for only accepted candidates resulting in a massive save of computational effort.

MCMC with PAR framework in CMOST allowed us to carry out a robust uncertainty analysis in each ensemble of reservoir models (i.e. unconstrained, stochastic and adjoint ensemble) by incorporating all the geological realization in each ensemble. Quadratic polynomial regression (Equation 3-4) was chosen as the proxy model for this analysis because the study from the comparative analysis between Artificial Neural Network (ANN) and polynomial regression in modelling polymer flooding showed that polynomial regression is more reliable in prediction than ANN. More details are discussed in Chapter 5 of this thesis. To ensure good quality of the proxy model, we set an acceptable  $R^2$  and  $R^2$  adjusted value of 0.9 and 0.85 respectively for training and an acceptable  $R^2$  prediction value of 0.8 as stopping criteria. The implication of this is that the MCMC with PAR engine will keep generating new experiments until the stopping criteria is reached. When the stopping criteria is met, the results of the proxy model analysis such as summary of fit, analysis of variance and polynomial equation is produced. Furthermore, the result of Monte Carlo simulation i.e. P10, P50, P90 estimates are provided.

### 3.7. Polymer Data

As a result of high water cut, polymer flooding seemed to be an attractive EOR method to be applied to Watt Field. Therefore, the screening criteria of Saleh et al. (2014) was used to evaluate the feasibility of polymer and the result from the screening analysis suggested that the Watt Field was a good candidate for polymer flooding.

We used the data of Cannella et al. (1988) who performed experimental and theoretical studies of polymer flooding by injecting Xanthan into sandstone and carbonate cores. Polymer concentrations ranged between 0.1 to 2 lb/bbl, effective brine permeabilities from 40 to 8000 mD, and residual oil saturations from 25 to 80%. The resulting relationship between solution viscosity and polymer concentration and polymer adsorption profile was then used in the simulations (Figure 3-17). We used the Todd and Longstaff mixing parameter, which models the impact of viscous fingering during a first contact miscible gas flood but has also been used in polymer flood simulations to model the impact of viscous fingering on the polymer slug (Bondor et al. 1972). The Residual Resistance Factor (RRF) is used to represent the permeability reduction resulting from polymer adsorption and blocking of pore throats. It depends on permeability and polymer concentration. A maximum RRF of 4 and a minimum of 1 has been used in this study.

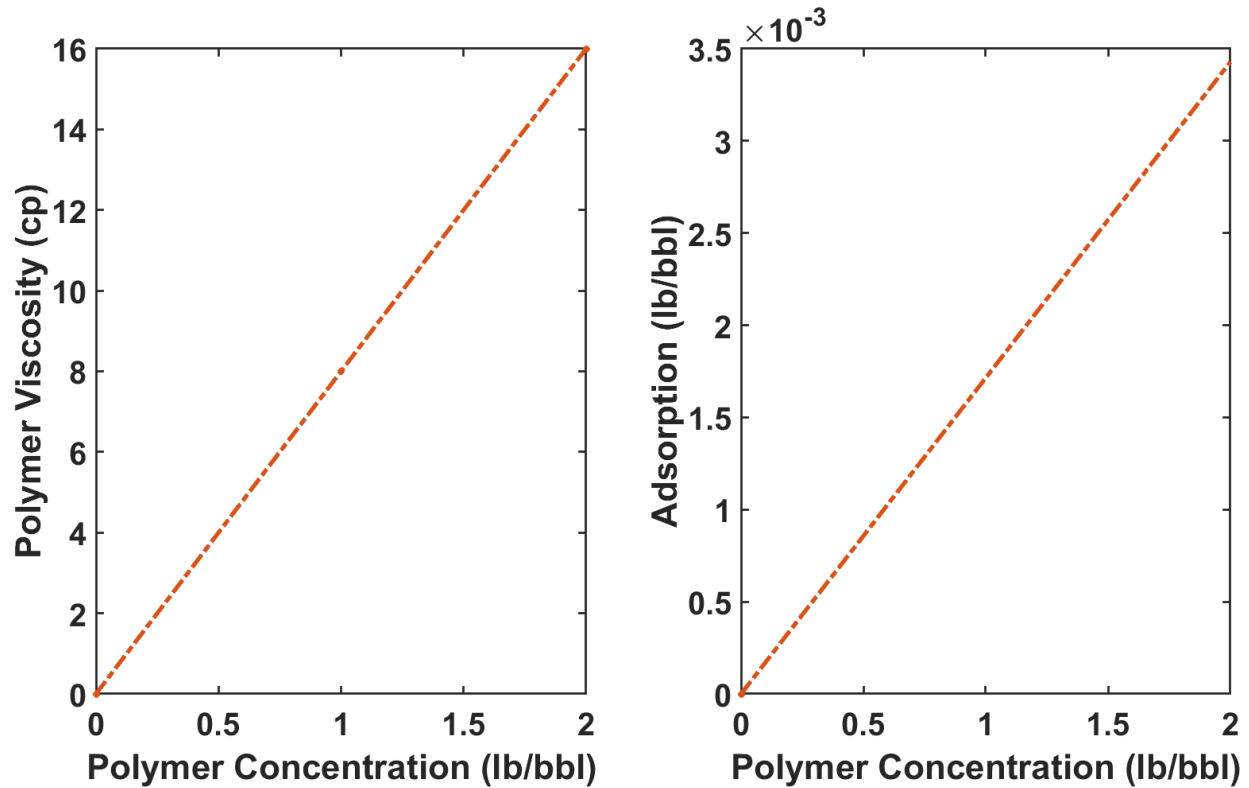


Figure 3-17. Polymer viscosity model (left) and polymer adsorption model (right) used in this study.

### 3.8. Summary

In this chapter, a case study that integrates both geological and interpretational uncertainties encountered in reservoir modelling which is often missed out has been presented. These uncertainties include, the top structure, fault network models, shale cut-offs in predicting net-to-gross, and modelling methods resulting in 81 different realisations of geological reservoir models. A truth case was defined from one of the available 81 realisations from where production data were generated from a prolonged water flood for history matching.

To enable us to study the impact of history matching techniques on the optimization of water flooding and polymer flooding, we presented the two history matching techniques applied in this thesis i.e. Adjoint and PSO techniques. This is necessary because the ensemble of reservoir models generated with different history matching technique will vary in size and diversity and may suggest different optimal strategies and associated risks. Experimental design was introduced focusing of space filling Latin Hypercube Sampling (LHS) which is a stochastic sampling technique used for this study and was chosen because of the stochastic population of reservoir properties in the Watt Field. LHS was used to generate training samples for the training of polynomial regression response surface. Monte Carlo Markov with Proxy-Based Rejection and Acceptance algorithm in CMOST which was used to generate P10, P50 and P90 estimates of the posterior probability distribution (PPD) for the history matched ensembles were described.

Finally, the polymer data from the experiment of Cannella et al. (1988) were used to generate a relationship between polymer viscosity and concentration, and polymer concentration and adsorption for modelling were presented.

# Chapter 4. Comparative Analysis of the Impact of History Matching Techniques on Reservoir Uncertainty Quantification

## 4.1. Introduction

In general, the production response obtained from the reservoir simulation of these geological realizations will not match the historic production data. Predictions from such reservoir models is unreliable unless the uncertain reservoir parameters are perturbed such that the response from the simulated model matches the observed production data. As discussed in Chapter 2, a single calibrated reservoir model is often not enough to account for uncertainties and associated risks in reservoir evaluation and management, it is therefore important to generate multiple history matched reservoir simulation models to adequately quantify the uncertainties in reservoir performance.

Recall from Chapter 2, assisted history matching is performed using optimisation algorithms, which are broadly classified as deterministic or stochastic based on their explorative and exploitative capabilities. Deterministic algorithms such as adjoint technique have the limitation that they only yield one, or at best a few, solutions and hence may not provide to reliable uncertainty estimates. (Oliver et al. 2008). However, deterministic algorithms have the advantage that they possess high convergence rates which saves time given that history matching process takes about 40% of the time used in reservoir simulation workflow (Gruenwalder et al. 2007). On the other hand, stochastic algorithms generate multiple history matched models and provide a more reliable uncertainty forecast but have lower convergence rates. However, if an ensemble of reservoir models that adequately capture the geological and interpretational uncertainties, is provided, it could be possible that the poor reliability in predicting the uncertainties by the deterministic algorithms such as the adjoint technique which is the major drawback is mitigated. Then, the fast convergence of adjoint technique could save significant CPU time during history matching. It will also be interesting to see how the two history matching techniques will affect our ability to forecast the performance prediction of a waterflood.

To investigate this hypothesis, we create an ensemble of history matched models using a deterministic method (adjoint technique) and a stochastic algorithm (PSO). Each technique includes the combination of parameterization and history matching algorithms and the parameter ranges that will be employed which is determined during the sensitivity analysis. We then perform a comparative analysis of the ensemble of reservoir models generated using these two history matching approaches. The comparative strategy will focus on the history match quality and rate of convergence, diversity of the ensemble and reliability of forecast.

## 4.2. Workflow

A trade-off between convergence and diversity is a good practice in history matching. Convergence refers to the rate of reduction of the mismatch in the objective function per iteration, whereas diversity refers to how diverse the matched models are distributed in the

objective space. History matching can be considered successful if a good trade-off is achieved within a reasonable time. In this study we will assess the performance of the two history matching techniques, adjoint and PSO using the following three criteria: Convergence speed and match quality, diversity, and reliability of forecasting. For the convergence speed and match quality, we observe the degree of reduction in history matching error per iteration of the history matching experiments and also compared final history match error of Adjoint and PSO techniques. The diversity of the matched models was assessed by visualising all the models in the objective space and we then plotted the average and range of each uncertain parameters for all the models matched using the two methods. Furthermore, the ensemble of history matched models is then sampled using MCMC with Proxy-based acceptance-rejection (PAR) algorithm in CMOST to robustly quantify the uncertainties in forecast. A qualitative analysis is performed on the reliability of the forecast based on the encapsulation of the truth case prediction within the probabilistic confidence range. To be specific, we examine the number of individual realisations in each ensemble that encapsulate the truth case model within its confidence interval. We use the Monte Carlo Probabilistic Distribution Functions (PDF) P10 and P90 lines as the confidence interval. Figure 1-1 shows a flow chart employed in this chapter.

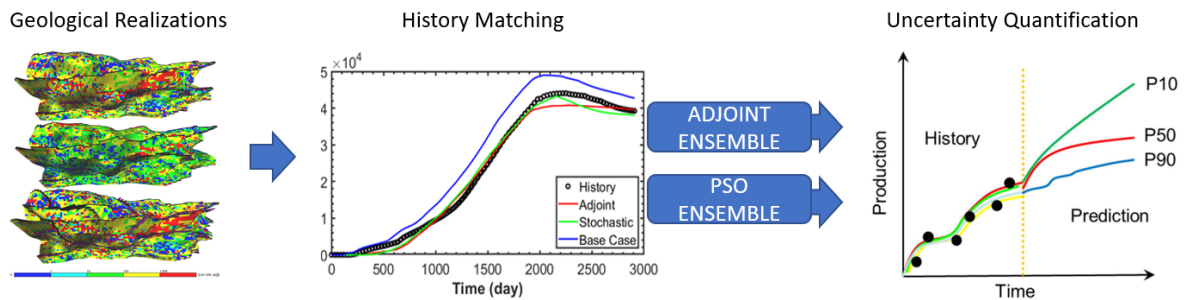
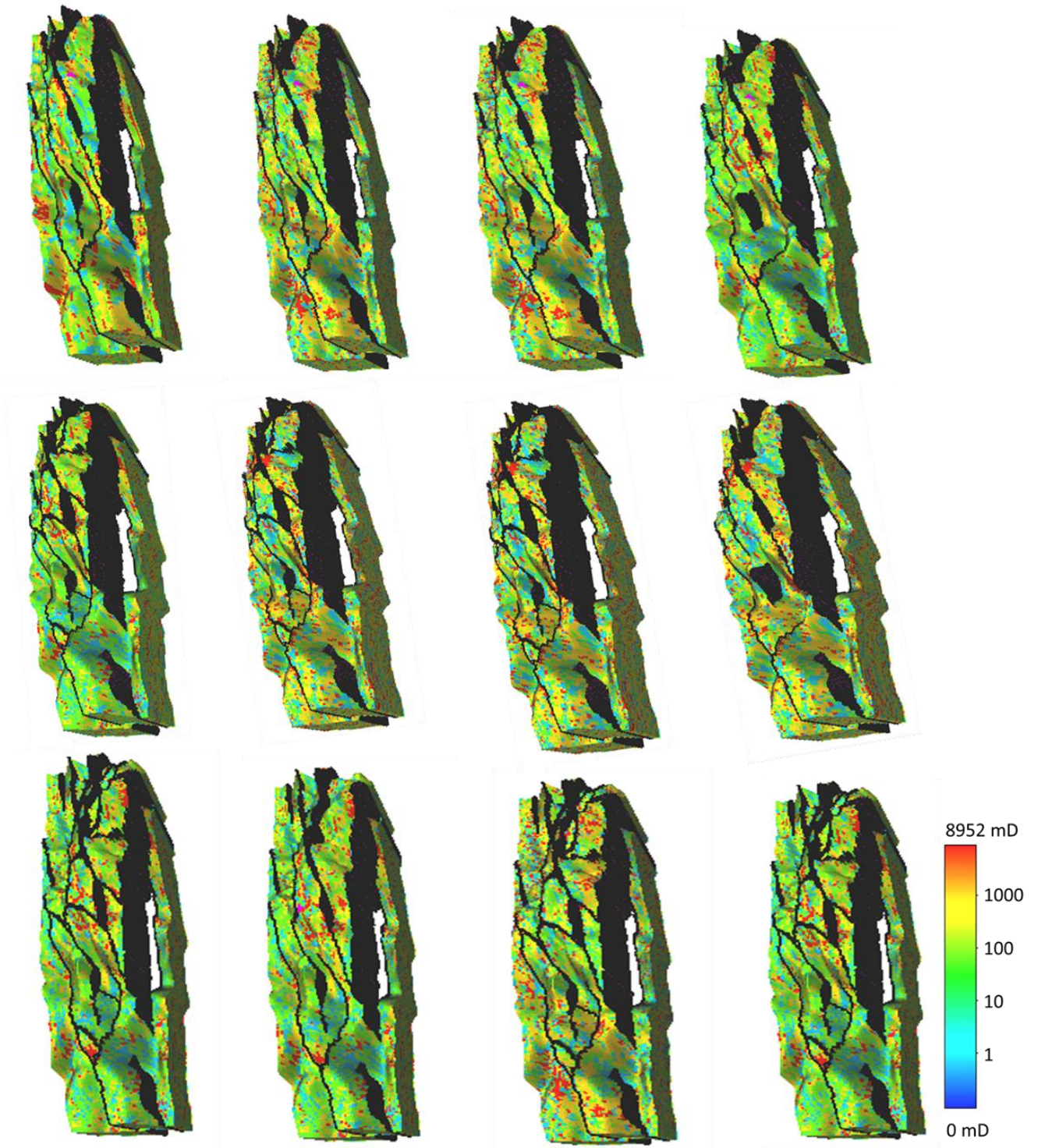


Figure 4-1. A flowchart describing the entire workflow used in this chapter

### 4.2.1. History Matching

As discussed from Chapter 3, we selected 26 out of the 81 geological realisations (*Figure 4-2*) to match the production data generated from 2933 days of prolonged water flooding of the truth case model. An ensemble of history matched models were created using PSO algorithm implemented in CMOST.



*Figure 4-2. Permeability distribution field of 12 of the 26 geological realisations of the Watt Field model used in this chapter*



### 4.2.1.1 Stochastic History Matching with PSO

History matching using this PSO, built on the previous work of Arnold et al. (2013), who performed history matching on this field using two parameterisation techniques i.e. layering and zonation methods. In the layering method, they divided the field into 8 different layers and assigned different reservoir properties and multipliers to each particular layer using PSO algorithm implemented in RAVEN. The result from the sensitivity study of algorithm configurations showed that flexi-PSO with the configuration shown in Chapter 3, produced a better overall match quality and hence it was used in this study. In the zonation method they divided the entire reservoir into 9 different sectors to allow tuning of individual wells differently and each sector was assigned different reservoir parameters and multipliers. We simplified the parameterisation because of the number of history reservoir models needed to be history matched. As stated in Chapter 3, a constant multiplier was assigned to each reservoir property across the entire reservoir to reduce the number of uncertain parameters as PSO can be trapped in local minima in high dimensional problems. The range of the reservoir property multipliers ranged from 0.05 to 1.3 for porosity, 0.05 to 10 for permeability, 0.01 to 10 for  $K_v/K_h$  ratio, and 0 to 1 for fault transmissibility. A similar result to that obtained by Arnold et al. (2013) was obtained using this parameterisation approach.

### 4.2.1.2 Adjoint Technique

The analytical sensitivity calculation using the adjoint technique employed in this work is deterministic by design. In order to generate alternative history matched cases, different start points (base case) are provided. The analytical sensitivity calculation is completely automatized and does not require further user interactions. Constraint definitions for rock property modification and the objective function definition are used to steer the history matching process. Constraints were defined for porosity (-10% to +10%), horizontal permeability (-10% to +50%) and vertical permeability (-10% to +50%). The misfit is evaluated for every iteration and the simulation is stopped when the misfit is no longer reducing. *Figure 4-3* illustrates the workflow for adjoint history matching in this chapter.

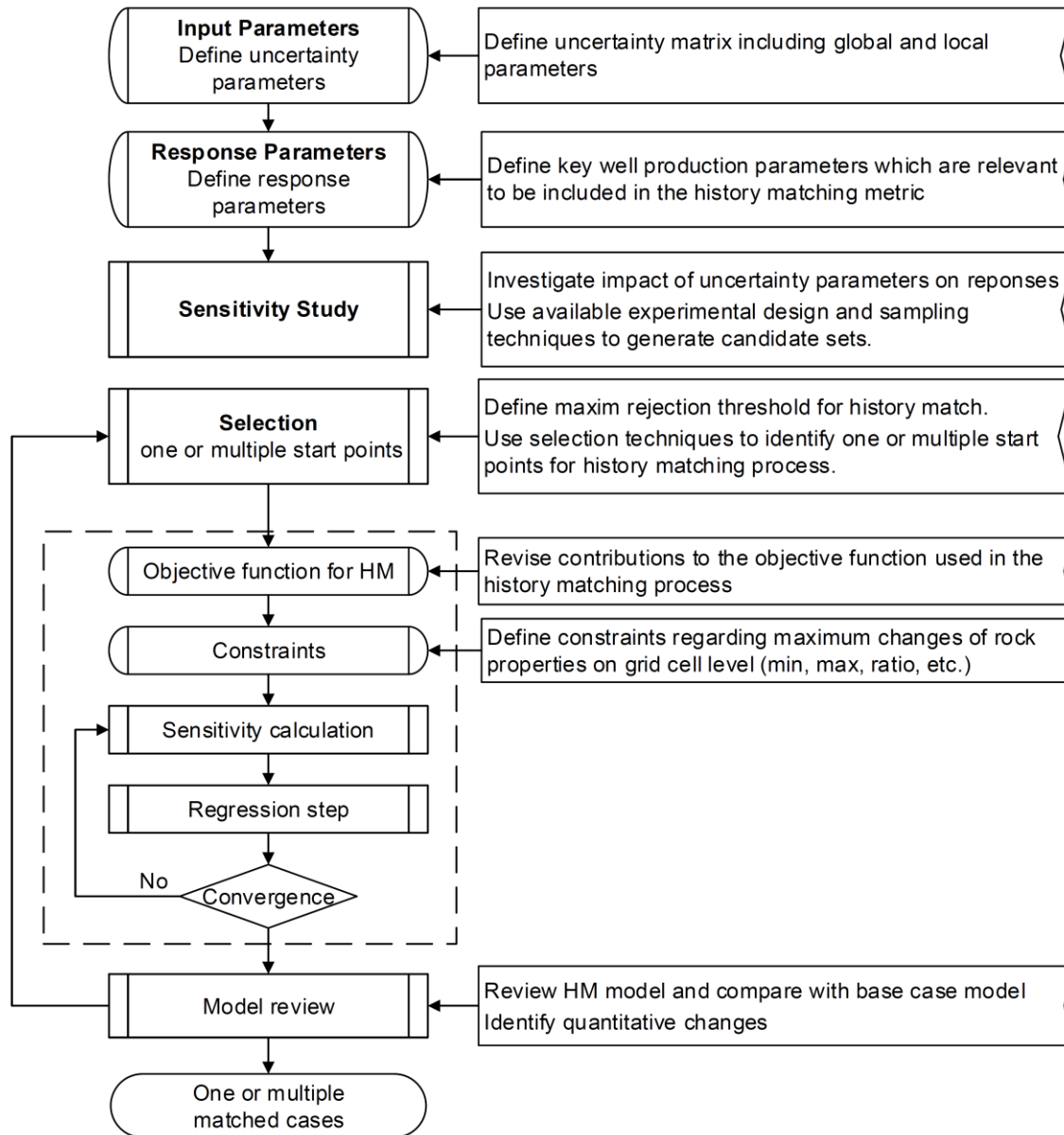


Figure 4-3. Workflow adjoint history matching employed to match the Watt Field model using SENEX (Senex 2013)

Note: We did not attempt to ensure geological consistency of the matched reservoir models with regularisation as it was beyond the scope of the thesis, rather the objective was to obtain ensemble of history matched models using different techniques.

The multiple models generated by different history matching techniques and the original model ensemble (base ensemble) were then integrated into the MCMC with PAR framework in CMOST. This is to robustly quantify the uncertainties in predicting the cumulative oil recovery for a period of 30 years. Polynomial regression was chosen as the proxy model option for this analysis. The stopping criteria were an acceptable  $R^2$  adjusted value of 0.9, and an acceptable  $R^2$  prediction value of 0.8. The number of simulation runs used for this uncertainty analysis were

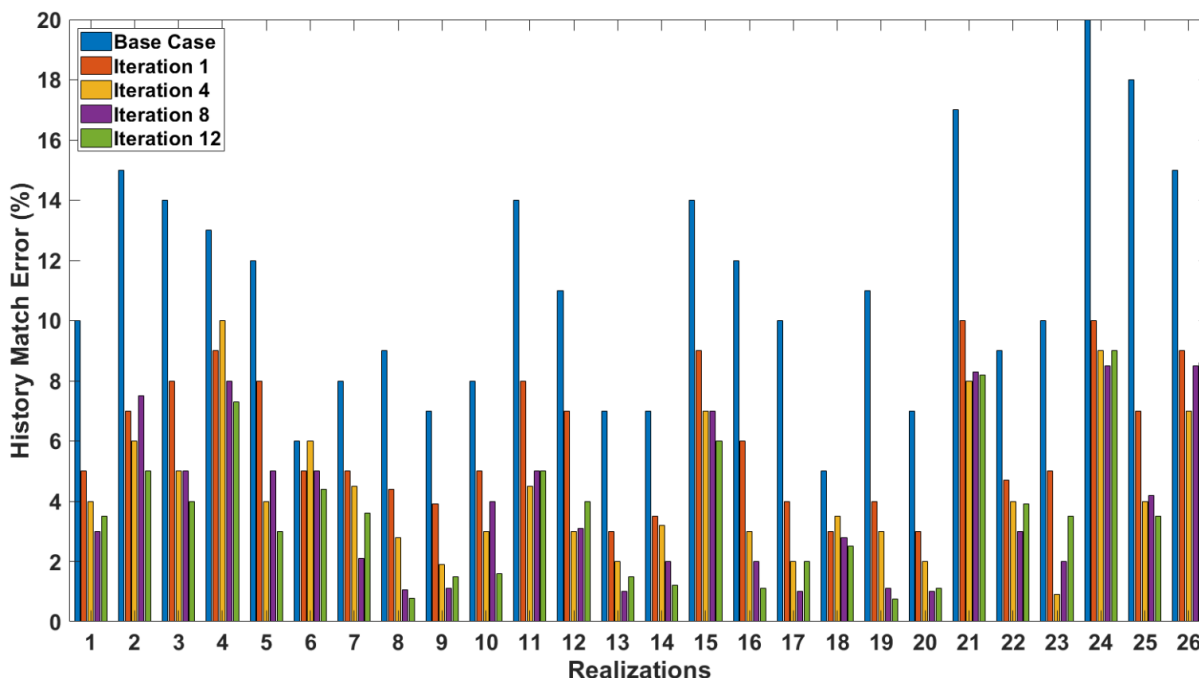
390 for each ensemble which is much lower compared to running an MCMC framework with about 208,000 of full physics simulation estimated by MCMC engine in CMOST.

## 4.3. Results

We analysed the result of history matching based on the aforementioned criteria: convergence speed and history match quality, diversity, and reliability of forecasting.

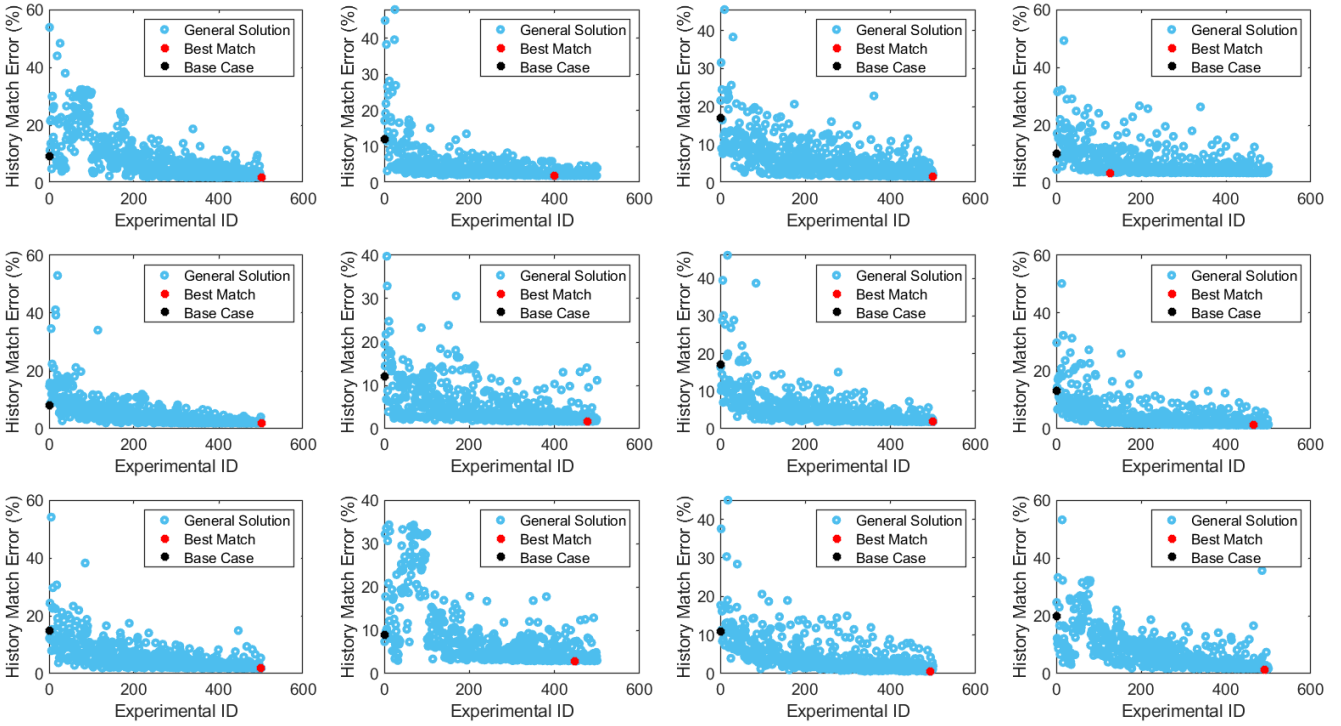
### 4.3.1. History match quality

Figure 4-4 and Figure 4-5 show the convergence of the history matching experiments observed for 26 geological realizations using the Adjoint technique and 12 representative realization using PSO, respectively. The Adjoint technique has a higher convergence speed than PSO. The Adjoint technique is able to reduce the misfit significantly within the first 12 iterations and the history matching experiments were stopped after 15 iteration as no further improvement in match quality was observed. The stochastic nature of PSO explores the parameter space more widely which reduces the convergence speed; it takes between 170 and 500 iterations until the best solution for is found for across the 26 realisations. Figure 4-6 shows the global history matching error for both, the Adjoint technique and PSO. The Adjoint technique yielded a better match across all the geological realizations except for two realizations where PSO outperformed the Adjoint technique. Figure 4-7 and Figure 4-8 compare the field-based and well-based recovery curves, respectively, for one of the history matched geological realizations. The Adjoint technique yields a high-quality match because it varies the permeability field in the vicinity of the wells but does not necessarily ensure geological consistency (Figure 4-9). Overall, these results show that the exploitative capability of the Adjoint technique to minimize the objective function contributes to faster convergence and smaller history matching error. In contrast, the explorative nature of PSO



algorithm to search the parameter space more broadly leads to slower convergence and a higher history match error.

*Figure 4-4. History match error minimization speed for 26 geological realisations using the Adjoint technique*



*Figure 4-5. History match error minimization speed for 12 geological realisation using PSO algorithm*

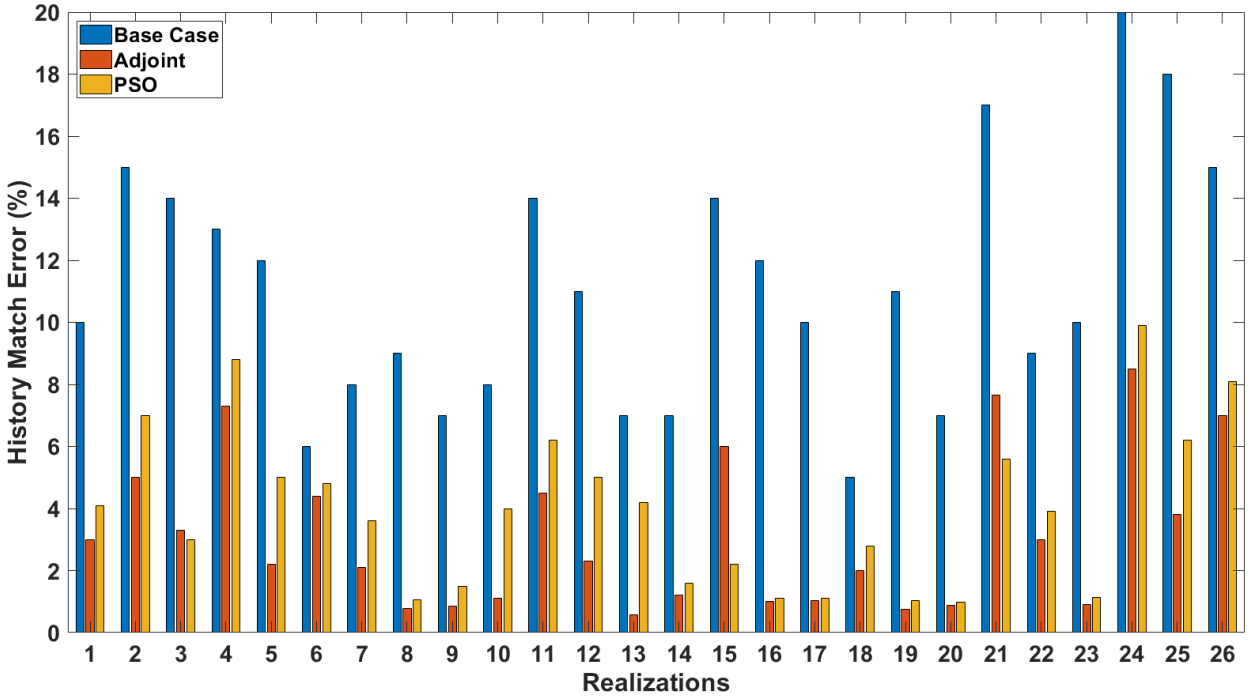


Figure 4-6. Global history match error for base (blue) and the best-so-far models for Adjoint technique (orange) and PSO algorithm (yellow)

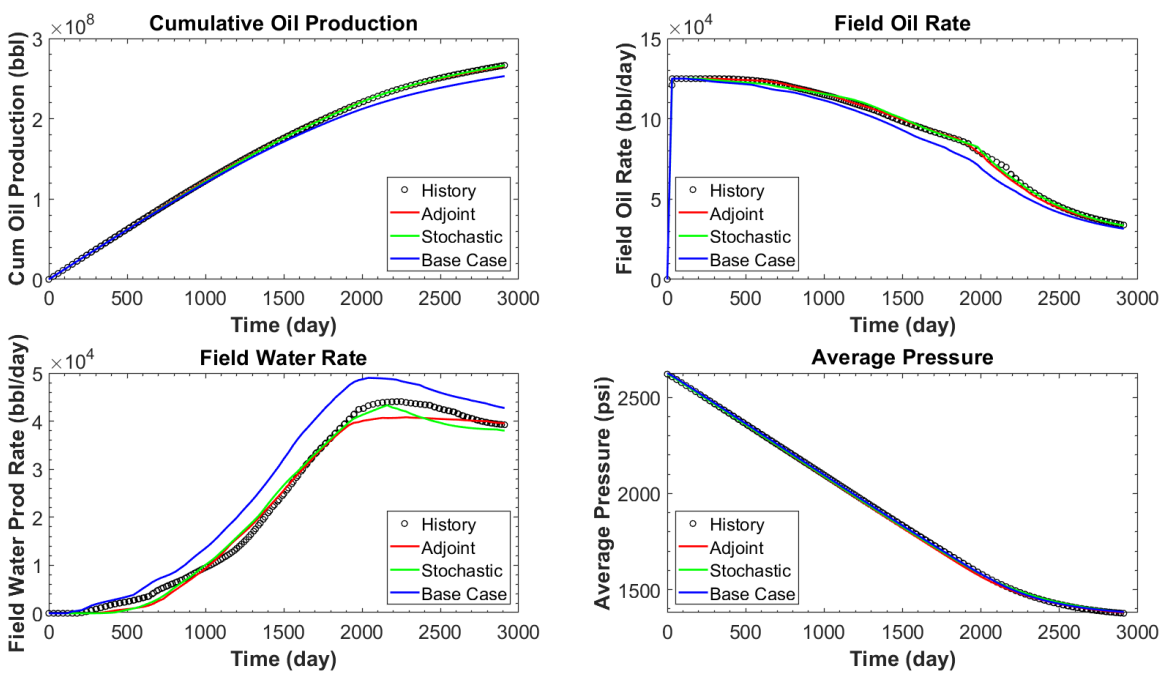


Figure 4-7. Example of field-based history matching results using the adjoint technique and the PSO method for one geological realization of the Watt Field.

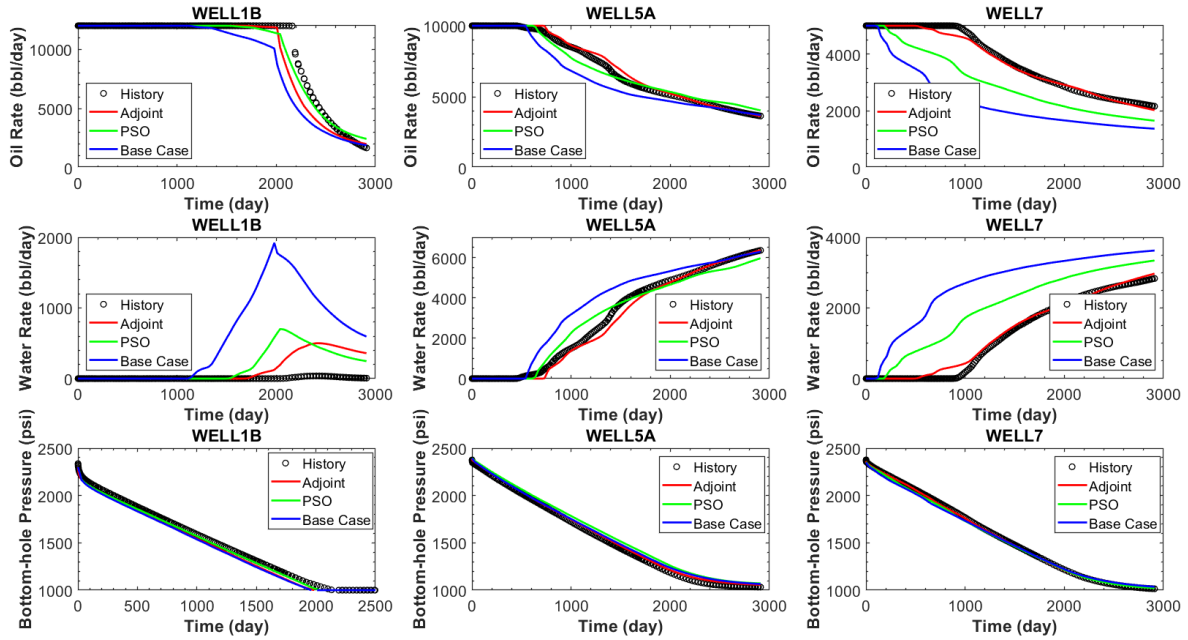


Figure 4-8. Example of well-based history matching results using the adjoint technique and the PSO method for one geological realization of the Watt Field.

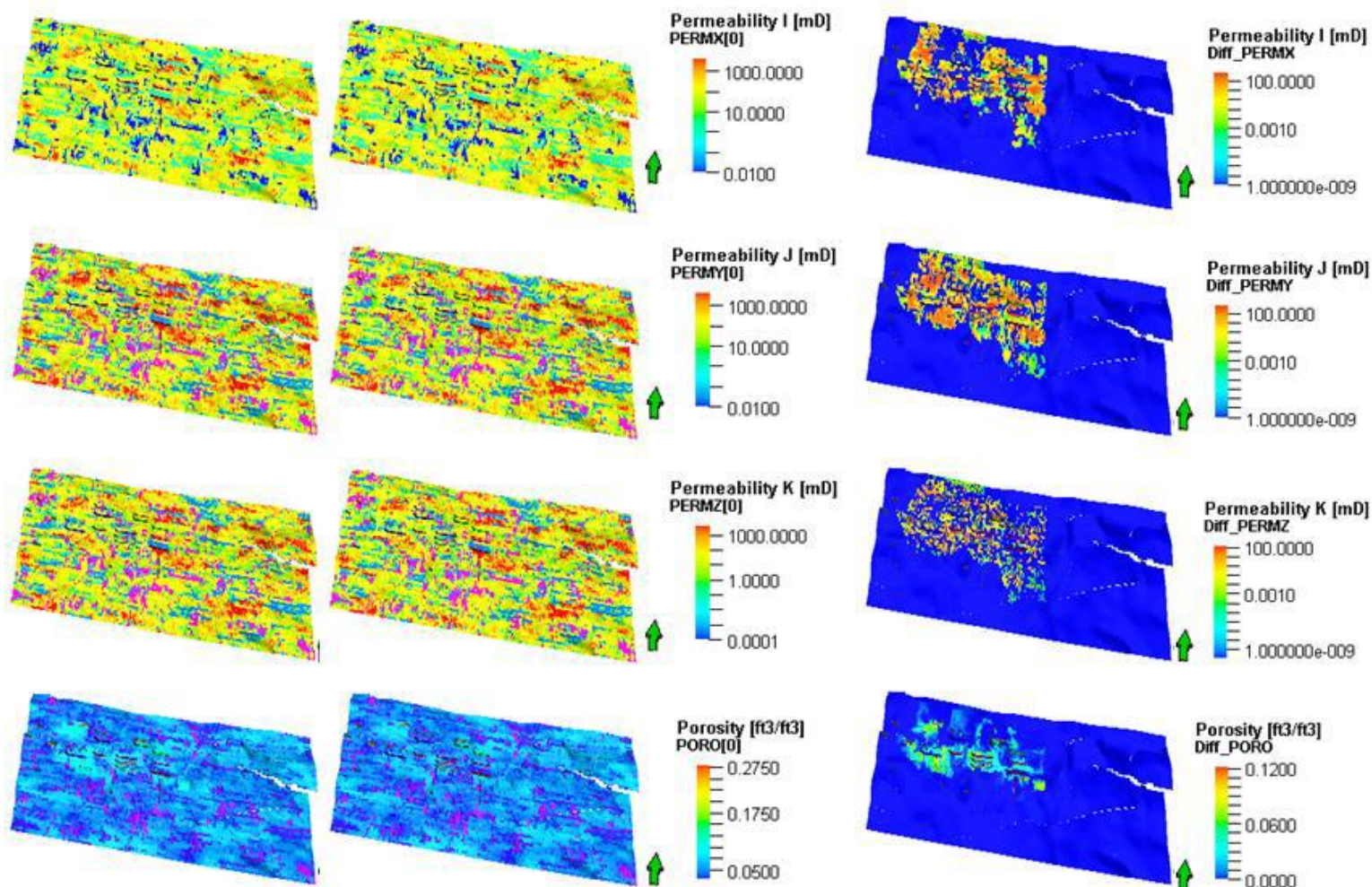


Figure 4-9. Porosity (bottom) and permeability (top) for the original reservoir model (left), the history matched model (middle) as well as the difference map (right) using an adjoint technique. Note how parameters are changed only in the location of the wells.

PSO changes the reservoir parameters more broadly, and across the entire reservoir, during the history matching process (Figure 4-10). Note that the stochastic history matching leads to an increase in the average permeability by a factor of two or more for most realizations, which implies that fluids flow more easily in the reservoir. However, the higher flow rates in the reservoir are often countered by a decrease in fault transmissibility along major fault using an adjoint technique. Note how parameters are changed only in the location of the wells. Figure 4-11 shows permeability distribution for 6 of the 26 realisations of the Watt Field model before and after history matching using Adjoint technique and PSO.

Stochastic history matching also had the tendency to increase the pore volume compared to the Adjoint technique (Figure 4-12).

More generally, the broader change in history-matched reservoir model parameters is because the stochastic algorithm is able to explore the parameter space more widely, which leads to a

more diverse range of history matched models for each geological realization (*Figure 4-13*). Hence a wider range of uncertainty in the production forecast compared to the adjoint technique can be expected. However, since we consider an ensemble of geological models, the drawback of narrower uncertainty ranges arising from the adjoint technique is somewhat mitigated.

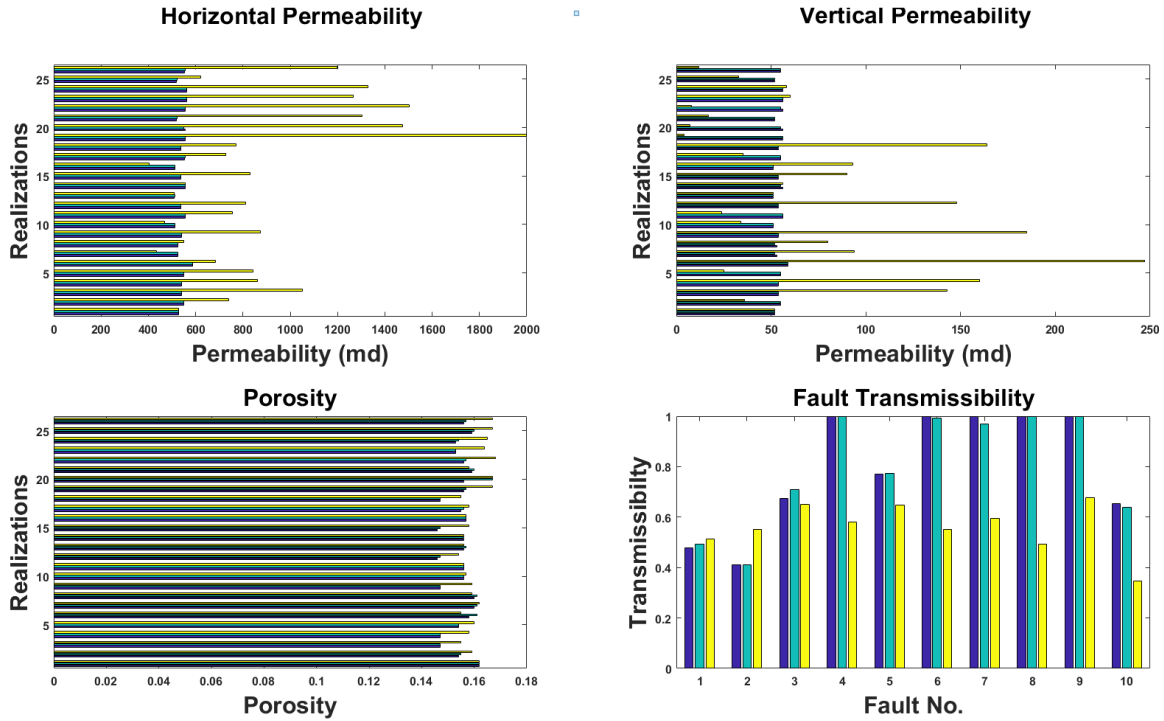


*Figure 4-10. Average horizontal and vertical permeability, porosity, and transmissibility for each of the 26 geological realizations before (blue) and after history matching using the adjoint technique (green) and stochastic history matching (yellow).*



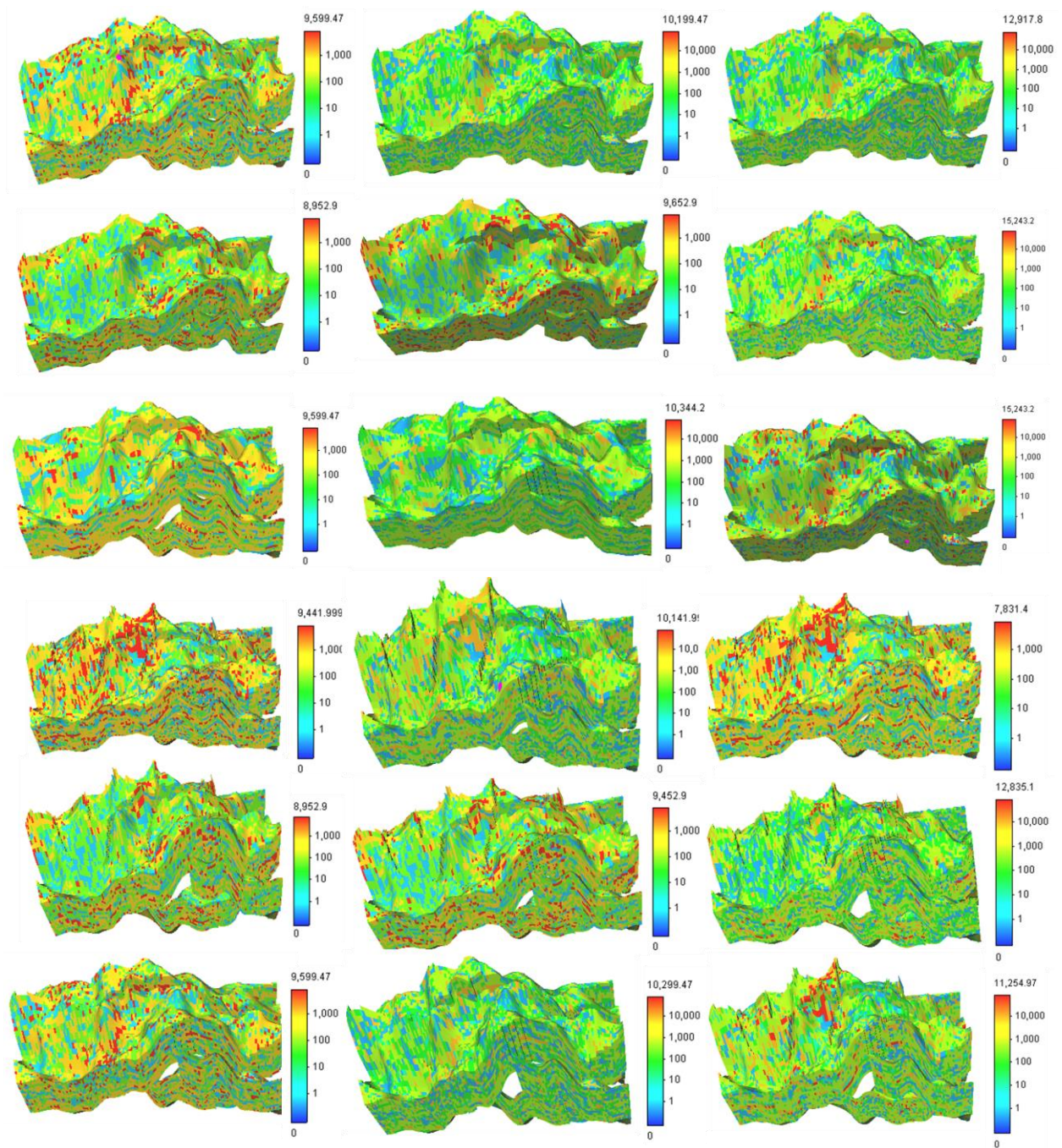


Figure 4-11. Permeability distribution for 6 of the 26 realisations of the Watt Field model before (left) and after history matching using Adjoint technique (middle) and PSO (right).

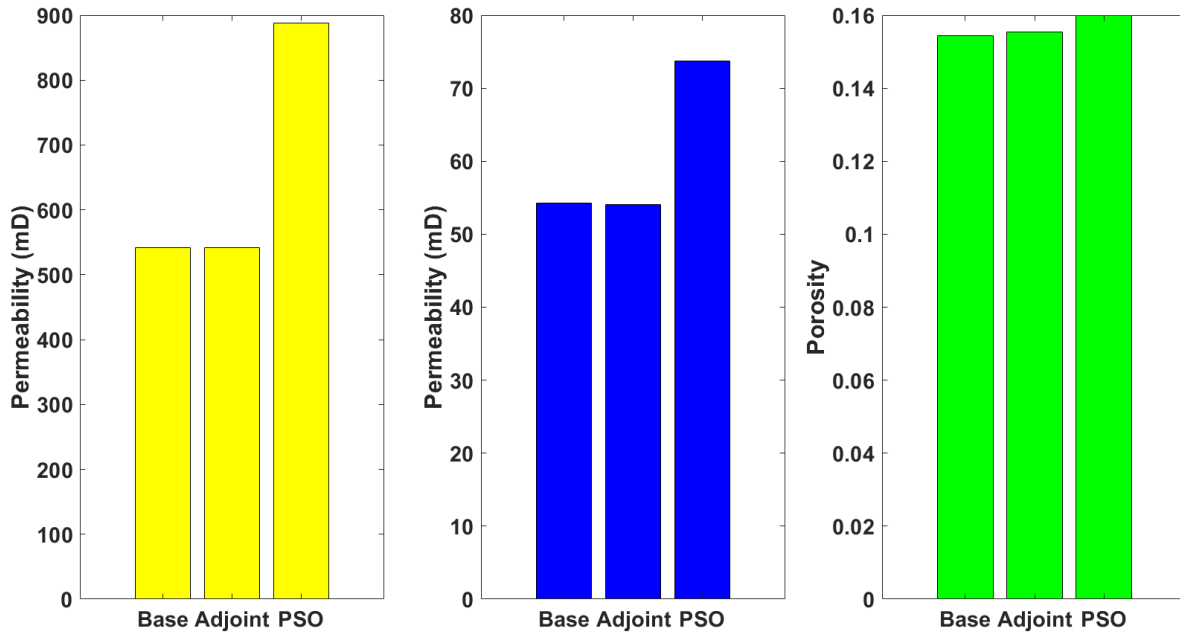


Figure 4-12. Averages of horizontal permeability (left), vertical permeability (center), and porosity (right) across the 26 geological realizations before (Base) and after history matching using the adjoint method (Adjoint) and stochastic history matching (PSO).

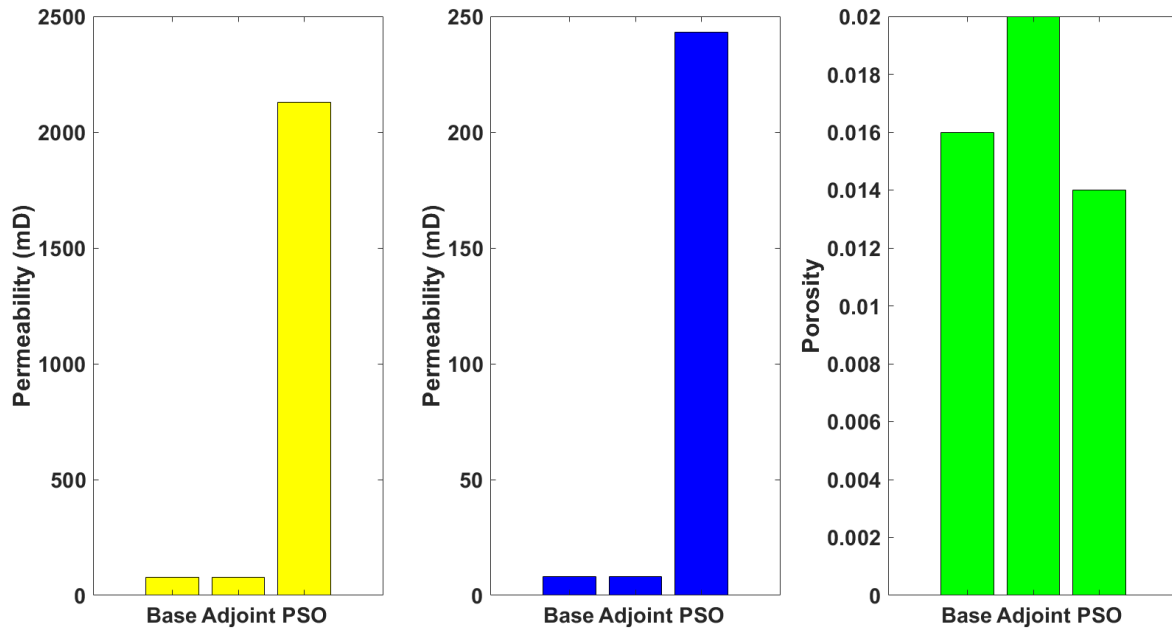


Figure 4-13. Variance in horizontal permeability (left), vertical permeability (center), and porosity (right) across the best matched cases of 26 geological realizations before (Base) and after history matching using the adjoint method (Adjoint) and stochastic history matching (PSO).

### 4.3.2. Reliability of the Forecast

After the generation of ensemble history matched models by the Adjoint and PSO techniques, we then compared the uncertainty estimates calculated based on both techniques. Following the history matching, we forecast production for 30 years assuming a do-nothing scenario, i.e. continuing in a do-nothing scenario, the results show that PSO-based history matched models yielded a more robust forecast and wider spread of uncertainties in cumulative oil production (Figure 4-14). Furthermore, we evaluated the uncertainty prediction in cumulative oil production presented as a posterior probability distribution (PPD) i.e. the P10, P50, and P90 credible intervals (Figure 4-15). The credible intervals, i.e. the difference between P90 and P10 at the end of the forecast period, is also provided for comparison. A boxplot is used to represent the average distribution of the cumulative oil production for each ensemble (i.e. Base case, Adjoint technique and PSO) (Figure 4-16) as well as for the cumulative oil production distribution for each individual realization (Figure 4-17). The reference model, i.e. the “truth case” for which the production data was generated, lies above the P10 line of the base case ensemble whereas the Adjoint and PSO ensembles encapsulate the truth. The results for the models that were history matched using PSO showed more robust and wider range of distribution in cumulative oil production (37 Mbbl), while the models that were history matched with the Adjoint technique predicted a narrower distribution of uncertainty in cumulative oil production (36 Mbbl) after 40 years of forecast. This is due to high diversity of models in the PSO ensemble as opposed to much similar matched models in Adjoint ensemble. It can also be noted that the forecast for the models that were history matched using PSO is more reliable compared to the models that were history matched using the Adjoint method because more forecasts for the models matched with PSO encapsulate the “real” production data from the truth, i.e. reference, model. *Figure 4-17* shows that 13 out of the 26 realization of the Adjoint ensemble encapsulate the truth, whereas 15 of the individual realization in the PSO ensemble encapsulate the truth (Figure 4-18).

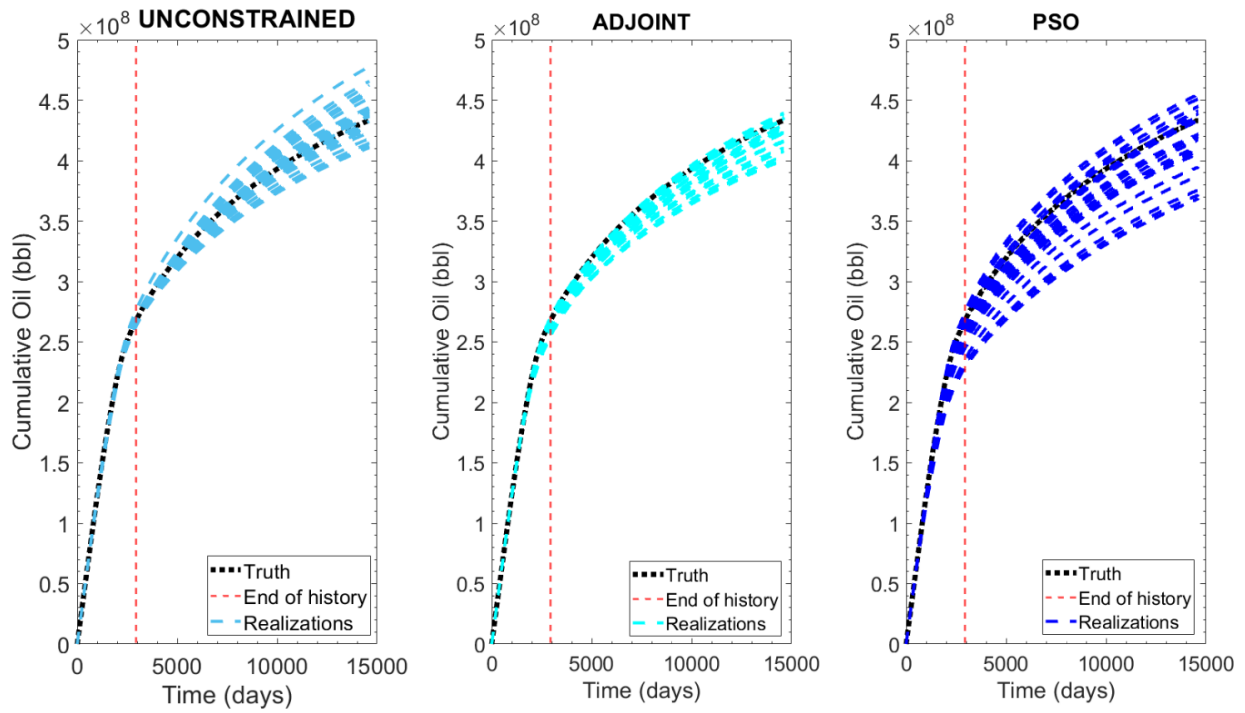


Figure 4-14. Forecast for cumulative oil production assuming a do-nothing scenario before – unconstrained (left) and after history matching using the Adjoint technique (centre) and PSO technique (right).

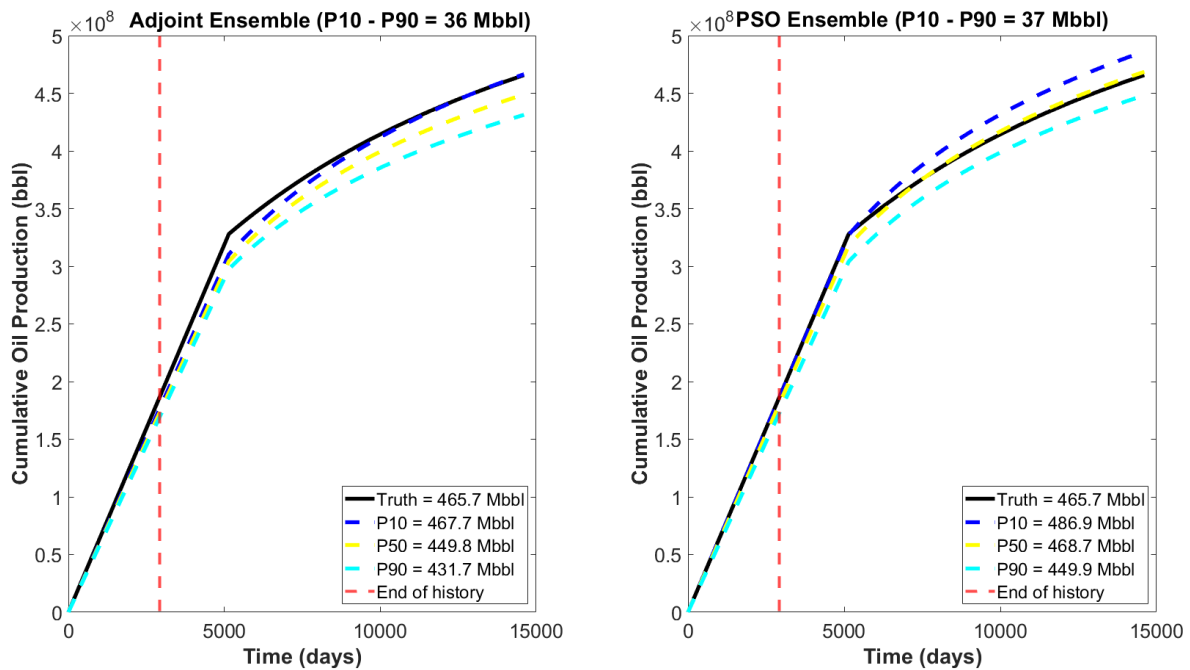


Figure 4-15. Recovery prediction uncertainties based on PSO ensemble (left) and PSO ensemble (right)

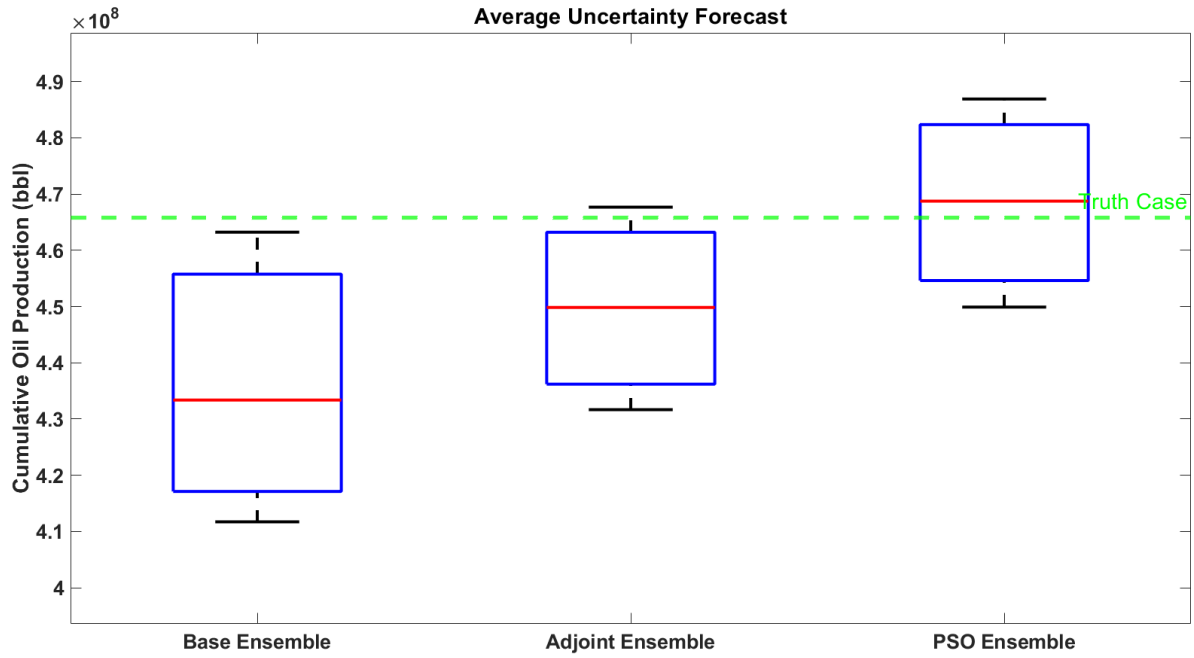


Figure 4-16. Boxplots of average uncertainties forecast obtained based on the base, Adjoint and PSO Ensemble.

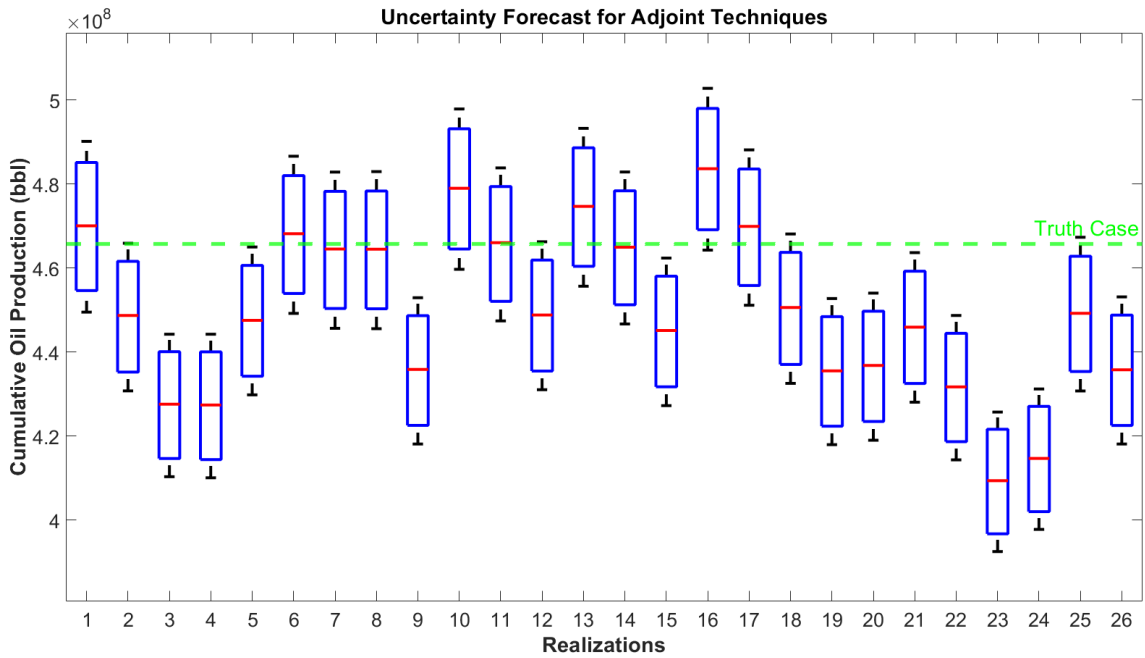


Figure 4-17. Boxplots of uncertainties forecast obtained based on the individual 26 realizations of the Adjoint Ensemble.

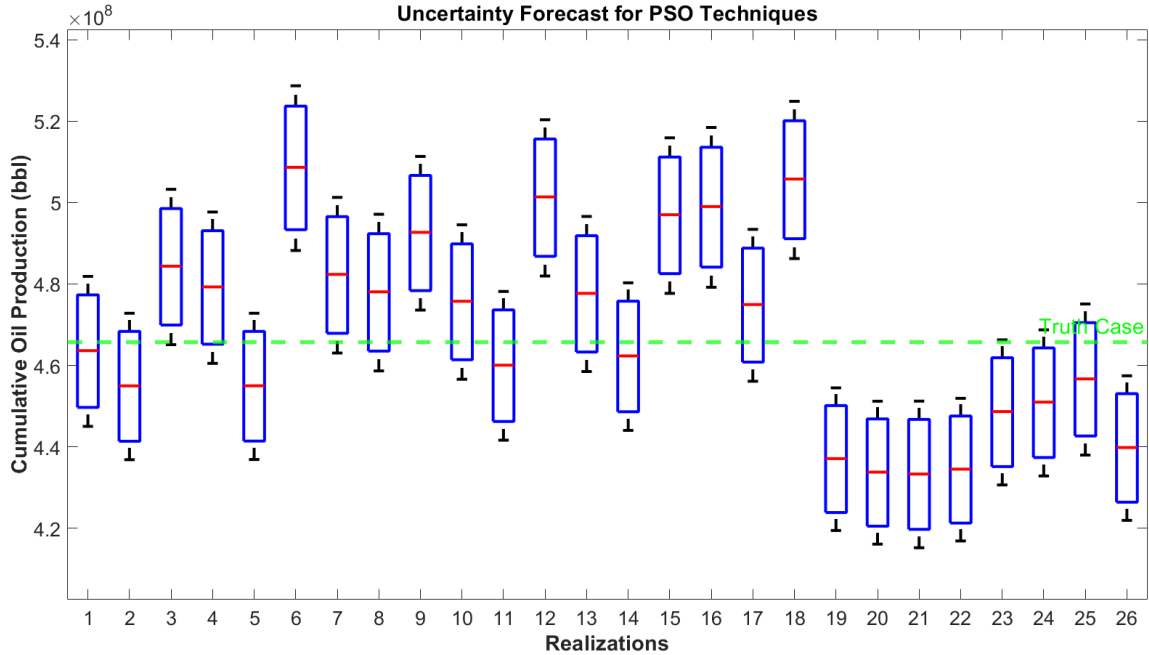


Figure 4-18. Boxplots of uncertainties forecast obtained based on the individual 26 realizations of the PSO Ensemble.

## 4.4. Discussion

To reduce risk, it is important that reservoir models capture key geological uncertainties especially those that cannot easily be parameterized during history matching, such as shale cut-offs to define net-to-gross, top structure models, fault network, and modelling methods. These kinds of geological heterogeneities are included in the semi-synthetic yet realistic Watt Field (Arnold et al. 2013). Simulation results from a geological model normally do not match the observed production results immediately, and hence the models need to be adapted until there is good agreement between simulated and observed production data through the process of history matching. Obtaining a good match does not guarantee a good production forecast. Therefore, history matched models need to be evaluated to ensure a reliable forecast. The MCMC with PAR framework enabled us to estimate the uncertainty in the forecast i.e. P10, P50, and P90 estimates for the history matched ensembles and the original ensemble and for the individual realisation member in each ensemble. The average cumulative oil prediction in the PSO ensemble was wider compared to the uncertainty prediction from the adjoint ensemble. This is common knowledge in the field of history matching as PSO is more explorative and therefore yields a more diverse set of models while the Adjoint technique is more exploitative and produces matched models that are quite similar. Furthermore, the reliability of forecast in the PSO ensemble was also higher than the Adjoint ensemble as more of the uncertainties predicted by individual ensemble encapsulated the truth case than in adjoint technique. Therefore, the diversity of a history matched ensemble varies from one history matching technique to another, and results in variation in the range of uncertainty estimation. Our findings agree with the work

of Erba and Christie (2007), who compared the uncertainty estimation of two stochastic methods i.e. the genetic algorithm and neighbourhood. Their study shows that neighbourhood algorithm with higher explorative capacity generated a more diverse ensemble of history matched models which led to a wider range in uncertainty estimation. However, the uncertainty prediction after 30 years by PSO and Adjoint ensemble were similar, with a difference of about 1 Mbbl in the range of uncertainty estimation. The similarity in uncertainty estimation establishes the fact that deterministic methods can be improved by using multiple realisations of reservoir model. In other words if a small number of geological models that adequately capture the key geological uncertainties can be designed, then a deterministic method such as the adjoint technique may be a good choice as it saves significant CPU time due to its fast convergence.

## 4.5. Summary

In this chapter, we investigated how different history matching technique can impact the uncertainty estimations of recovery forecasting in a heterogenous clastic reservoir using MCMC with PAR algorithm. 26 of the 81 geological realization of the Watt Field, a semi synthetic reservoir model was used to carry out this analysis. We generated two ensembles of different quality using Particle Swarm Optimisation (PSO) and Adjoint technique. We further assessed the quality in terms of convergence speed and match quality, the degree of exploration and diversity in the models, and lastly the reliability of forecasting.

From the results of the Watt Field case study we observed that stochastic history matching with PSO resulted in a more diverse sets of history matched ensemble than the Adjoint technique. This diversity can be attributed to the exploration capability of the PSO algorithm to search the parameter space more broadly. The exploitative capability of the Adjoint techniques leads to a higher convergence speed and lower history match error of the best models than the PSO-based approach.

The results from the comparison of the uncertainty forecast show that PSO yielded a wider range P10 – P90 ranges that encapsulate the truth case, whereas Adjoint technique produced a narrower range. This due to high diversity that exist in the set of history matched models in the PSO ensemble compared to localized clusters of models in the Adjoint ensemble. Although the Adjoint ensemble yields a higher quality of history matched models, it does not guarantee a better capability in forecasting the future, which is in alliance with the finding of Tavassoli et al. (2004). The high diversity of the PSO ensemble used in uncertainty prediction produced a better forecast reliability compared to the Adjoint ensemble as more individual realization prediction of uncertainties of the PSO encapsulated the truth than the Adjoint technique. In conclusion, the higher exploration in the history matching process will more likely lead to a wider range in uncertainty forecast.

Based on the results from our study, we can infer that the robustness of uncertainty quantification process can be enhanced by multi-objective history matching, where the history match error can be minimized and the divergence in forecast can be maximized simultaneously.

# Chapter 5. Optimisation of polymer flooding in a Heterogenous Reservoir Considering Geological and History Matching Uncertainties

## 5.1. Introduction

Capturing geological and engineering uncertainties requires running a wide range of full-physics simulations that explore the parameter space in order to provide a useful insight for sensitivity analysis that enables uncertainty quantification and optimization of recovery processes in geologically complex reservoirs during EOR. Modelling polymer EOR is computationally expensive due to the complex nature of the displacement process and the complex multi-scale heterogeneity inherent to many reservoirs. Proxy-based optimization can reduce the number of simulations runs by creating an empirical, data-driven proxy model (for example through polynomial regression) that mimics the full-physics simulation runs (Queipo et al. 2005). Usually, a proxy model is built using a set of full-physics training runs, blind-tested and validated through additional full-physics simulation, and iteratively refined using further full-physics simulations (Koziel and Yang 2011). The objective of this chapter is therefore to analyse the performance of a polymer flood while considering geological uncertainties inherent to a heterogeneous clastic reservoir where the uncertainties are related, for example, to the number and locations of faults, the depth of the top structure, or the depositional model but also the modelling decisions (e.g. choice of shale cut-off and pixel vs. object based modelling) (Arnold et al. 2013). Furthermore, we compare the prediction and performance of a full-physics polymer flood optimisation to the proxy-based optimisation of polymer flooding.

In Chapter 4 we investigated how different history matching techniques can impact the uncertainty in estimating the forecasts of hydrocarbon recovery in a heterogenous reservoir by creating ensembles of reservoir models using two different approaches (Adjoint technique and PSO). The Adjoint ensemble converged faster with lower history matching error due to its exploitative nature but yielded a narrower forecast of uncertainty. In contrast, the PSO ensemble was more diverse and predicted a wider range of cumulative oil recovery. In this chapter we investigate how different history matching approaches (adjoint vs. stochastic method) and different optimisation methods (constrained vs. unconstrained) impact the predicted reservoir performance and optimal design of the polymer flood. Constrained optimisation employs the history-matched reservoir models whereas unconstrained optimisation employs reservoir models that have not been history matched. The advantage of unconstrained optimisation is a reduction in CPU time because the additional history matching step is not needed, but the resulting uncertainty in the production forecast may be larger than in the constrained optimisation.

We hypothesise that according to “Flora’s rule” (Ringrose and Bentley 2015), models that have been history matched for a different displacement process may not capture the relevant geological structures needed to predict a polymer flood adequately, and hence the difference between



constrained and unconstrained history matching will be small. We therefore investigate if and how different commonly used history matching techniques impact the way optimisation algorithms improve the design of a polymer injection strategy while considering geological uncertainty. To compare and contrast these differences, we carried out a quantitative analysis between the optimisation results while considering the different history matching methods, focusing specifically on the incremental net present value (NPV) and the associated variability in NPV forecast. The novelty of this chapter is the detailed investigation of how different history matching approaches and optimization methods impact the predicted performance and optimal design of a polymer flood, which indicates that an optimized polymer flood is beneficial compared to an optimized water flood even if geological uncertainties are not represented adequately in the reservoir models. Although the specific experimental design techniques (i.e. Latin Hypercube Sampling) and optimization algorithm (i.e. Particle Swarm Optimisation) are not new, the application of the experimental design and proxy modelling workflow to analyse polymer flooding to ensembles containing complex heterogeneous reservoirs has not been widely reported.

## 5.2. Workflow

In this study we used the same 26 models from the 81 geological realisations of the Watt Field already used in Chapter 4. We used the same ensembles of history matched model created in Chapter 4. A sensitivity analysis allowed us to determine the first-order parameters influencing a subsequent polymer flood. We first optimize the NPV on three dissimilar reservoir models that represents different uncertainties in the original ensemble using both full physics and proxy-based optimisation to validate the accuracy of a proxy-based optimisation. The polymer flood was then optimized for each geological model with or without history matching (i.e. for constrained and unconstrained history matching). Water flood optimisation was also conducted using the same methodology to determine incremental NPV. Finally, uncertainty analysis was carried out to determine the impact of history matching on the economic risks of a polymer EOR project. The commercial black-oil simulator IMEX was used for all full-physics simulations. *Figure 5-1* shows the flowchart describing the entire workflow employed in this study.

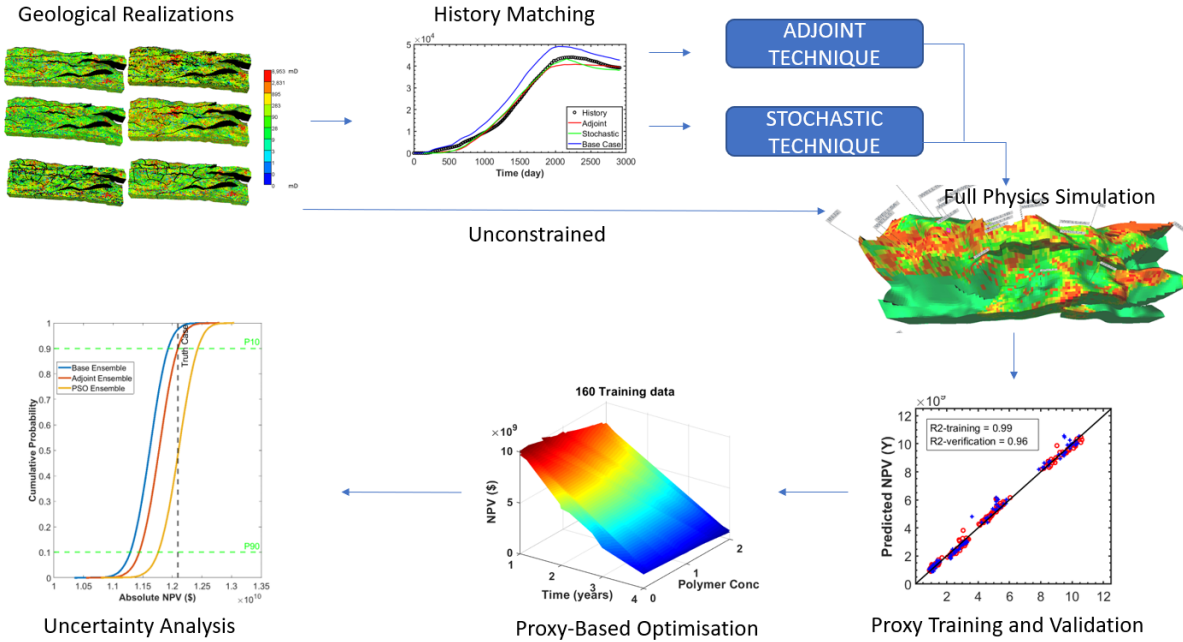


Figure 5-1. Flowchart showing the workflow used in this chapter.

## 5.2.1. Objective Function for Optimisation

We used NPV as the objective function to optimize the polymer flood because other quantities such as recovery factor may lead to incorrect results where the optimal solution may not necessarily be financially viable. A basic NPV calculation was used for the optimization process, assuming a constant price for oil (\$55/bbl), constant injection water handling costs (\$2/bbl), constant production water handling costs (\$3/bbl), constant polymer costs (\$2/lb), and a yearly discount rate of 10% (Janiga et al. 2017) given by

$$NPV = \sum_{t=0}^T \frac{C}{(1+r)^t}, \quad 5-1$$

where  $t$  is the time step,  $T$  is the total time,  $C$  is the model cash flow for each time step and  $r$  is the discount rate. The cash flow is given by

$$C = \left[ \left( OR * \frac{\$}{bbl} \right) - \left( PMR * \frac{\$}{lb} \right) - \left( IWR * \frac{\$}{bbl} \right) - \left( PWR * \frac{\$}{bbl} \right) \right], \quad 5-2$$

where  $OR$  is the oil rate,  $PMR$  the polymer mass rate,  $IWR$  the injected water rate, and  $PWR$  the produced water rate.

## 5.2.2. Parameter Screening

In order to evaluate the effect of the key design parameters such as polymer concentration, time to deploy polymer, the number and location of injection wells, or the injection rates on NPV, a sensitivity analysis was carried out before we commenced the optimisation. We first applied the one variable-at-a-time design to create tornado plots, and further used response surface-based sensitivity analysis to generate tornado charts which also account for the interactive effects between one parameter to another. Note that other experimental design methods such as the folded Plackett Burman design could be used to develop a Pareto chart to analyse the parameter interaction and uncertainties at even greater levels, but such an analysis was beyond the scope of this chapter as both of our sensitivity tests yielded the same qualitative results.

The base case is a polymer flooding with polymer concentration of 0.5, time of deployment of 3 years, and an injection rate of 12,000 stb/day. Reducing the polymer concentration decreased the NPV and increasing the polymer concentration slightly increased the NPV. Increasing the time of polymer deployment lowered the NPV, whereas, decreasing the time of polymer deployment increased the NPV. NPV was seen to increase as the injection rates increased in most injectors, whereas, some injectors are insensitive to injection rates. The sensitivity results presented in Figure 5-2 show that polymer concentration, time to deploy polymer, and injection rates are the most influential parameters when optimizing NPV in the Watt Field. These first order parameters were then used subsequently in the DoE process to generate training data for the proxy model.

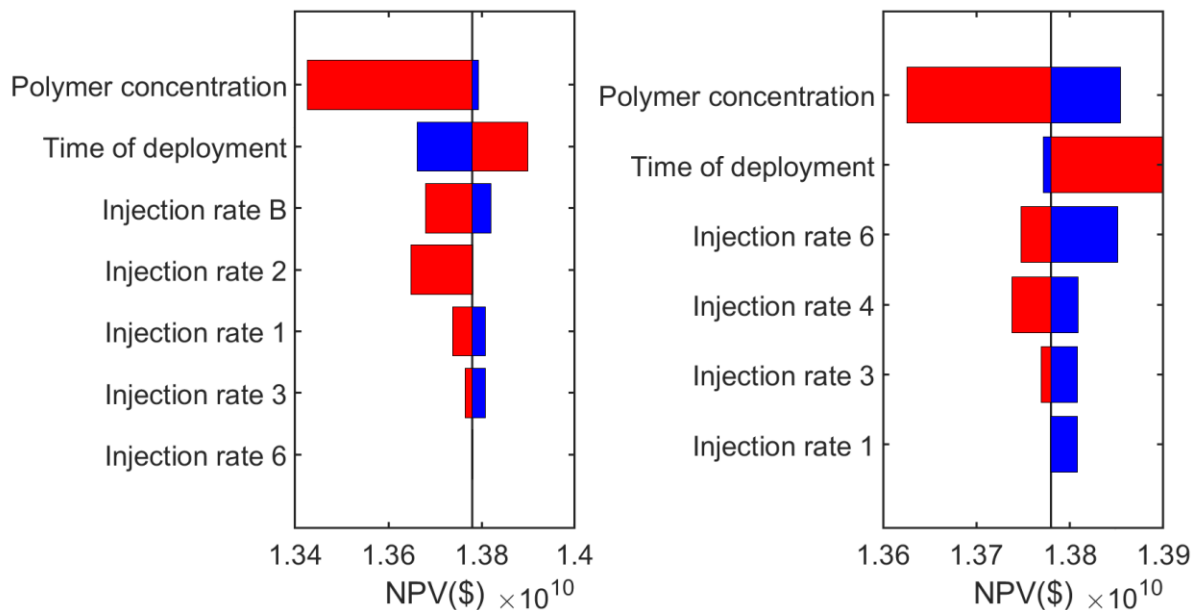


Figure 5-2. Results from sensitivity analysis using one-parameter-at-a-time approach (left) and response surface (right), showing the operational parameters that have the largest impact on NPV during polymer flooding in the Watt Field.

### 5.2.3. Optimisation and Design of Experiments

In the implementation of EOR in heterogenous reservoir, proxy models may be used to produce appropriate approximation of time-consuming computer simulation. The constructed proxy models can then be used to further understand the correlations and effect of the uncertain input parameter on the NPV, and also contribute to fast simulation optimisation and uncertainty analysis. The modelling parameters are categorised into two: The geological uncertainties and engineering uncertainties. The geological uncertainty is using the geological model mentioned in the previous section. In addition to that, we introduced faults transmissibility at the same range for all the faults across the three realizations. Nevertheless, transmissibility is not a separate entity, and will not change the concept of the geology described by the combination of the models mentioned above. Therefore, fault transmissibility is imposed on each geological realization as a variable parameter. Training data were generated with fault transmissibility between 0 and 1, which means from completely sealing to completely open. Similarly, a variable skin factor could have been introduced as an extra geological uncertainty to account for the loss of injectivity and productivity at wells, especially when injecting polymers at a very high concentration, but we decided to neglect this to enable us to focus on uncertainties at reservoir scale. The design control are those parameters we have control over and engineer or modify to achieve our objectives. As opposed to uncertain parameters which are not used in the optimization process, design parameters are employed to tune the reservoir behaviour to our desired need. Wells often contains numerous adjustable parameters such as the location and completion interval, and operational constraint e.g. Flow rate and BHP. In this study, the reservoir models were operated at a flow rate of 8000 bbl/day up to the point where minimum BHP limit of 1000 psi is reached, then the well control switches to BHP leading to decrease in production rates. The injectors were constrained with a surface injection rate of 11,000 bbl/day for a particular period until maximum BHP of 3500 psi which was set to avoid fracturing of the formation is reached. The injectors were then constrained by BHP resulting in the decrease of polymer injection rate and consequently impacted the displacement efficiency and oil recovery.

For proxy training, we used polymer concentration, time to deploy polymer and choice of the location for four injectors.

The LHS design in CMOST was used to vary the most influential uncertain parameters observed from sensitivity analysis for each of the three geological realizations. Fault transmissibility was varied from low transmissibility cases where the faults where completely sealing (FT=0) to high transmissibility cases where the faults are absolutely open (FT=1). Polymer concentration ranged from a waterflood scenario (polymer concentration of 0 lb/bbl) to a high polymer concentration of 2lb/bbl. Injection rate were maintained at a range of 10,000 stb to 18000 stb. Time to deploy polymer flooding varied from the first day to 10years after waterflooding. A normal prior probability distribution was assumed in the distribution of input parameters in the design space. Continuous uniform sampling within the data range were performed and treated discrete values as equally probable. Table 5.1 shows a summary of operational parameters used in the optimization of polymer flooding.

Table 5-1. Operational parameters for polymer flood (see Figure 5 3 for well locations).

Parameters	Range
Polymer concentration (lb/bbl)	0 to 2
Injection rate (stb/day)	10000 to 18000
Time to deploy polymer (days)	0 - 3650
Location of polymer injectors	INJ1, INJ2, INJ3, INJ4, INJ5, INJ6, and B

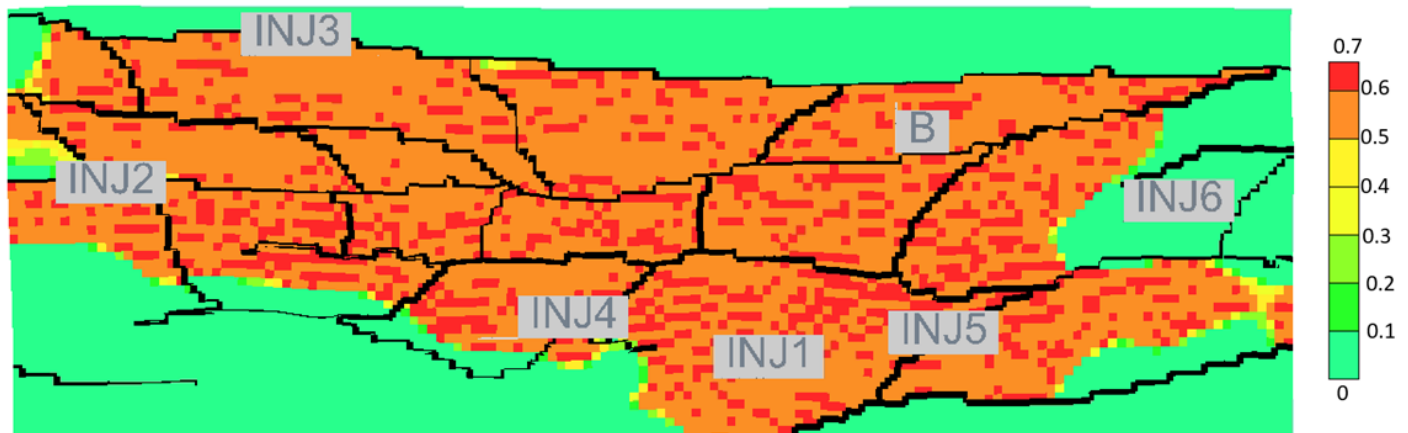


Figure 5-3. 2D plan view of a single geological realization of the Watt Field, showing the initial oil saturation, the location of the injector wells and the location of major faults.

## 5.2.4. Uncertainty Analysis

Recall that polymer flooding is a capital-intensive project and therefore requires rigorous screening and risk assessment. To quantify the economic risks of the polymer flood, we carried out a cross comparison where the optimal polymer design strategy for one geological realization was deployed to all 25 other realizations in the same ensemble. This approach allows us to estimate the financial downside if the optimal well controls that have been identified for one reservoir model are deployed to another reservoir model. In other words, we are testing how the NPV changes if sub-optimal well controls are used for reservoir models which make different assumptions about the reservoir geology. In this process we also calculate the incremental NPV achieved during the polymer flood in comparison to an optimized water flood.

Apart from geological uncertainties, there are sets of uncertainties related to fluid-rock interaction which should be considered, such as loss of viscosity due to degradation, polymer adsorption, residual resistance factor and inaccessible pore volume. To implement this analysis, the optimal polymer flooding and waterflood strategies for each individual realization in the three ensemble were integrated into the MCMC with PAR framework in CMOST to robustly quantify the uncertainties in the NPV prediction for each of the three different ensemble i.e. unconstrained (Base) ensemble, Adjoint and PSO ensemble. Table 5.2 shows the parameters and ranges used to carry out this risk assessment.

Table 5-2. Input Parameter and ranges for uncertainty quantification.

Parameter	Base	Range
Polymer Viscosity (cp)	67	50 - 67
Inaccessible Pore Volume Multiplier (-)	1	1 – 1.3
Polymer Adsorption Multiplier (-)	1	1 -1.3
Residual Resistance Factor (-)	1.2	1.1 – 1.3

## 5.3. Results

### 5.3.1. Proxy Modelling

Sensitivity analysis were carried out to test the optimal number of training data to create a highly accurate approximation that had great reliability in prediction. This is necessary as creating excess training data will increase the computational effort and may not significantly improve the accuracy of the prediction, while an inadequate number of data will lead to erroneous proxy prediction. Furthermore, the simulation input variables and its associated outputs were employed to train a polynomial regression and an Artificial Neural Network (ANN) algorithm to produce approximations for the simulation output. To determine the optimal number of training runs required to train the proxy model, a sensitivity analysis was carried out for the three geological realisations. A total of 100 full physics simulation and were performed using a black oil simulator IMEX (CMG, 2018) to train a proxy model using PR and ANN, then an additional 100 full physics simulations were run for validation. The co-efficient of determination  $R^2$  for both training experiments and validation experiments are shown in Table 5.3. The number of full physics simulation were gradually increased from 100 to 160, 300. A common observation is that ANN always shows a perfect  $R^2$  for training better that PR. However, PR provides a better  $R^2$  for prediction across all the models. A total number of 160 training data set proved to be sufficient fit for this approximation. A response surface for the NPV computed using polynomial regression and ANN for 16 training runs 100 training runs and 160 training runs are shown in Figure 5-4 and Figure 5-5. There was not much difference observed in the response surface despite the perfect  $R^2$  values of the ANN. Figure 5-6 provides a comparison of NPV predictions for the full-physics simulations and for the proxy models for three different geological realizations of the Watt Field. The error in the proxy model prediction can be the result of distinct changes in the heterogeneously distributed parameters such as permeability and porosity. Better predictive accuracy could be achieved through repeated and denser sampling of the parameter space in these specific regions, but this would significantly increase the CPU time.

The simulation output was used to generate the proxy model for polymer injection via polynomial regression. One proxy model was created for each of the 26 different geological realizations. Since there are three models for each geological realization – the original model prior to history matching and the two history matched models – a total of 78 proxy models were generated. Each proxy model accounts for the effect of polymer concentration, time to commence polymer flooding, and

the location of four injection wells on NPV. The quality of the proxy model was confirmed using additional validation runs. If needed, further training runs were added until the coefficient of multiple determination  $R^2$  indicated that the proxy model had sufficiently high quality. Polynomial regression was also used to generate a total of 78 proxy models for water flood optimization. The  $R^2$  values ranged from 0.91 to 0.99 across all 26 realizations. The quality of the Proxy models for waterflood was higher than polymer flood, this is because of less complex physics and fewer parameters in the experimental design as only the injection rates were considered as a variable parameter. The  $R^2$  values ranged from 0.99 to 1.0 across all 26 realizations.

Table 5-3. The  $R^2$  Training (Train) and Verification (Ver) values of Polynomial regression and ANN Neural Network for three geological realizations of the Watt Field.

No. of Data	TS1_FM1_CO1_PIX				TS2_FM3_CO3_PIX				TS3_FM2_CO3_OBJ			
	Polynomial Regression		ANN Neural Network		Polynomial Regression		ANN Neural Network		Polynomial Regression		ANN Neural Network	
	Train	Ver	Train	Ver	Train	Ver	Train	Ver	Train	Ver	Train	Ver
100	0.93	0.91	1	0.91	0.95	0.91	1	0.91	0.99	0.92	1	0.91
160	0.92	0.94	1	0.91	0.96	0.91	1	0.96	0.99	0.96	1	0.95
300	0.97	0.93	1	0.92	0.96	0.92	1	0.94	0.99	0.97	1	0.96

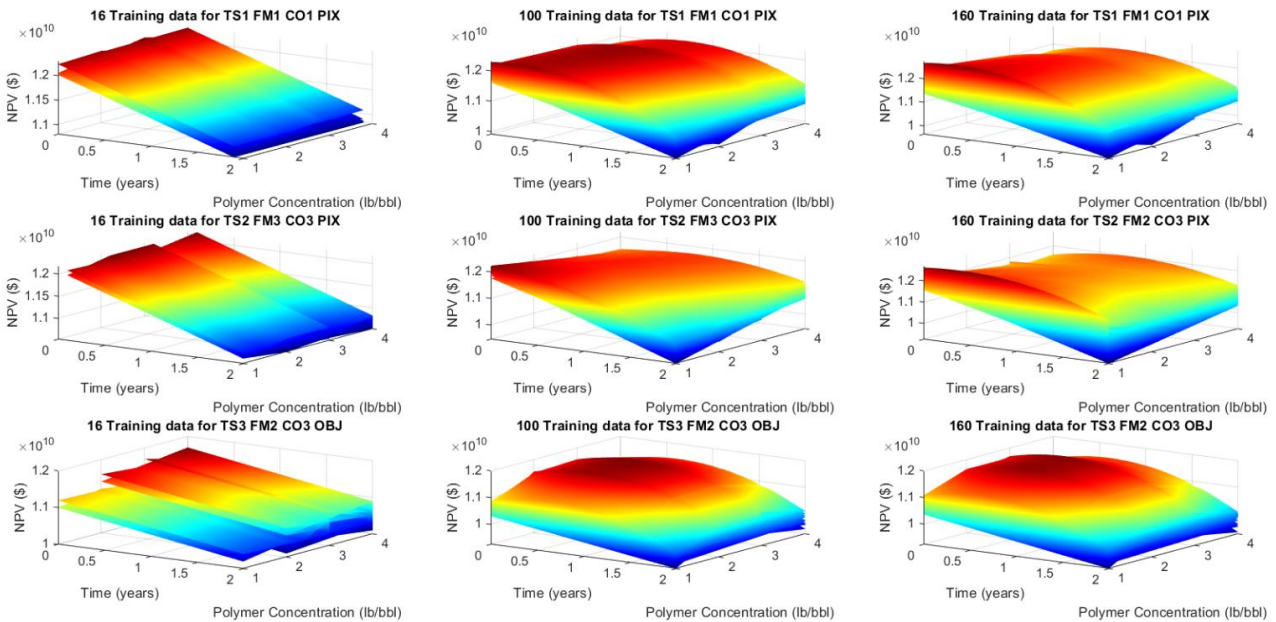


Figure 5-4. Response surfaces for the NPV computed using polynomial regression for 16 training runs (left), 100 training runs (centre), and 160 training runs (right).

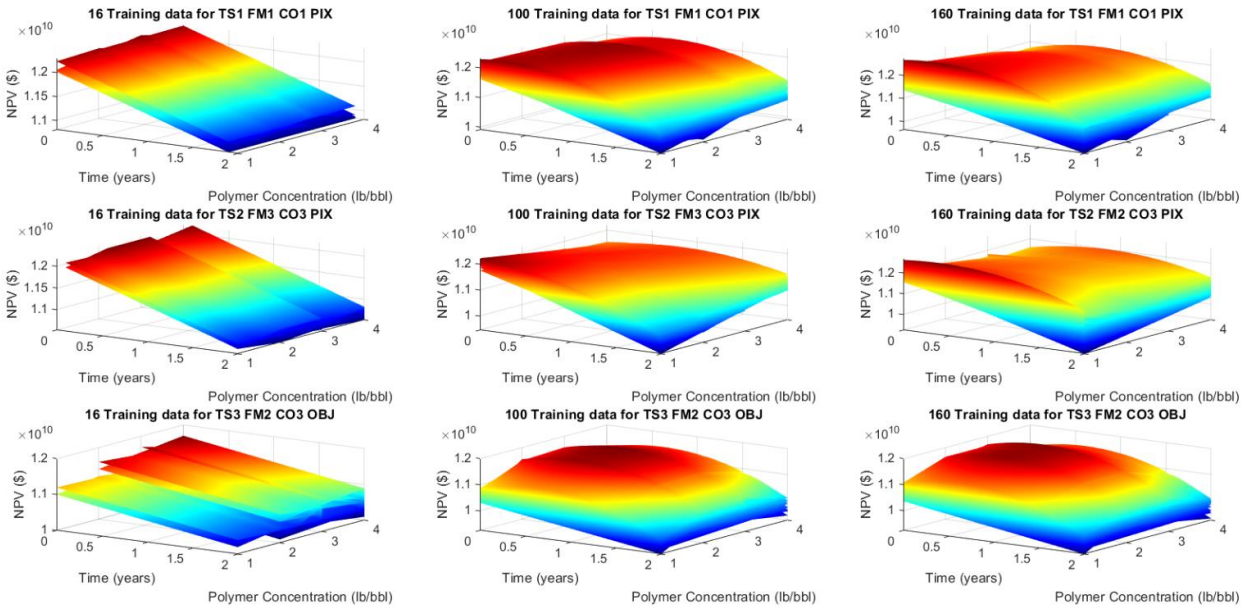


Figure 5-5. Response surfaces for the NPV computed using Artificial Neural Network for 16 training runs (left), 100 training runs (centre), and 160 training runs (right).

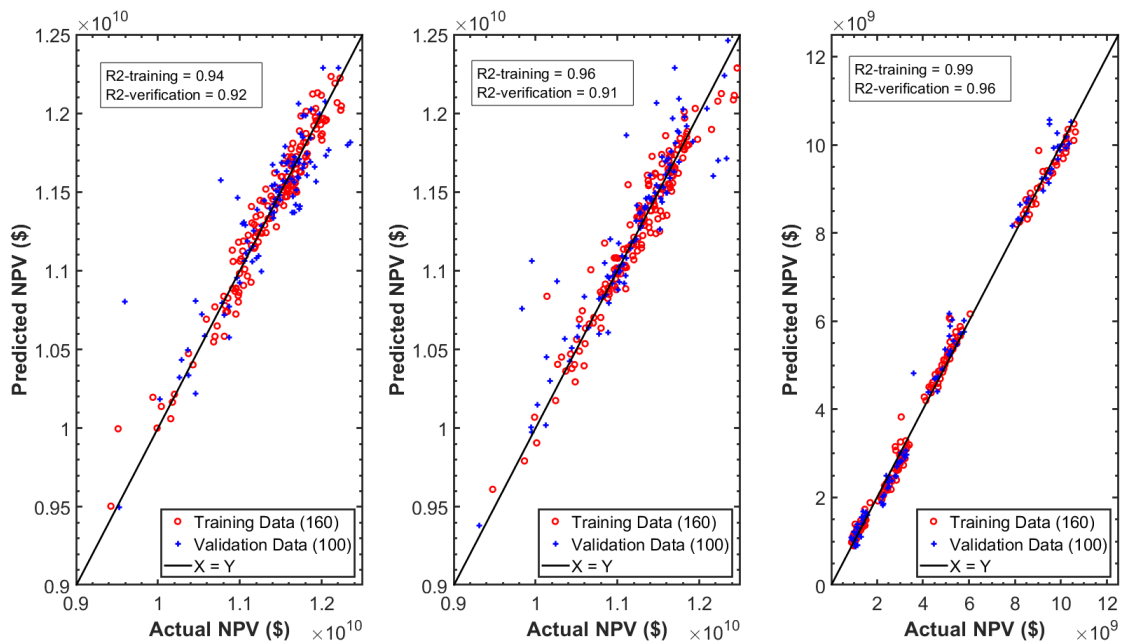


Figure 5-6. Comparison of NPV predictions for the full-physics simulations and for the proxy models for three different geological realizations of the Watt Field

PSO was then applied to each proxy model, i.e. the total of 78 proxy models, using the commercial simulator CMOST, to maximise the NPV by identifying the optimal injector location, the best time for polymer deployment, and the optimal polymer concentration. PSO was further coupled with the proxy models generated for the water flood using polynomial regression. This coupling had



the aim to optimize the NPV of a water flood for each realization by identifying the optimal water injection rates for each injection well.

To quantify the economic risks of the polymer flood, we carried out a cross comparison where the optimal polymer design strategy for one geological realization was deployed to all 25 other realizations in the same ensemble. This approach allows us to estimate the financial downside if the optimal well controls that have been identified for one reservoir model are deployed to another reservoir model. In other words, we are testing how the NPV changes if sub-optimal well controls are used for reservoir models which make different assumptions about the reservoir geology. In this process we also calculate the incremental NPV achieved during the polymer flood in comparison to an optimized water flood.

### **5.3.2. Adjoint vs PSO-Based History Matching**

The details of the methodology used in history matching is discussed in Chapter 4 of this thesis. The adjoint technique yields a high-quality match because it varies the permeability values in the vicinity of the wells but does not necessarily ensure geological consistency. However, during the forecast period of 30 years after history matching, assuming a do-nothing scenario, the PSO-based history matched models yield a more robust forecast and wider spread of uncertainties in cumulative oil production.

### **5.3.3. Proxy-Based vs Full Physics Optimisation**

PSO was employed to optimize NPV for the three realisations (TS1\_FM1\_CO1\_PIX, TS2\_FM3\_CO3\_OBJ and TS3\_FM2\_CO3\_OBJ) using full physics numerical simulation and proxy models generated from polynomial regression by identifying optimal injection locations for 4 polymer injectors as well as the time to deploy polymer and optimal polymer concentration. The idea is to compare and contrast the optimal strategy and absolute NPV of full physics optimisation and the optimisation on proxy models generated by polynomial regression. Also, PSO was used to maximize the NPV of the water flood in these models by identifying optimal injection rates for all the 7 injection wells. This is to enable us to compute the incremental NPV due to polymer flooding.

The result of full physics optimisation on TS1\_FM1\_CO1\_PIX geological realisation indicates that the sweep efficiency and field oil recovery factor improved significantly compared to waterflood. TS1\_FM1\_CO1\_PIX geological realisation predicted an absolute NPV of \$12.89 billion. The observed trend of low NPV at low and high polymer concentration is because very low polymer concentration is not sufficient to provide the adequate mobility control and sweep efficiency to recover more oil, while very high polymer concentration will lead to loss of injectivity and excess polymer are being wasted in the aquifer. The proxy-based optimisation predicted an absolute NPV of \$12.85 billion. Both optimisation methods identified the same optimal deployment strategy as they recommended to commence polymer flooding as early as possible, suggested 0.3 lb/bbl as optimal polymer concentration, and identified INJ6, INJ4, B and INJ1 as best polymer injectors. However, their choices of injection rates were seen to vary slightly as the proxy-based method underestimated the injection rates in some of the wells, hence

the difference in absolute NPV (see Table 5.4). The full physics optimization for this realization TS2\_FM2\_CO2\_PIX yielded an absolute NPV of \$12.99 billion, whereas the proxy-based optimisation predicted an absolute NPV of \$12.94 billion. They both identified similar optimal deployment strategy i.e optimal polymer concentration of 0.2 lb/bbl, optimal location for polymer injectors are INJ6, INJ4, B and INJ1, and recommended to start polymer injection as early as possible. A similar trend to the TS1\_FM1\_CO1\_PIX reservoir model where absolute NPV were seen to decline at very low and very high polymer concentration were identified in the NPV vs polymer concentration cross plot. The choices of optimal injection rates were also seen to vary slightly in this particular reservoir model. The full physics optimization on realization TS3\_FM2\_CO3\_OBJ yielded an absolute NPV of \$11.99 billion while the proxy-based optimization predicted an absolute NPV of \$11.96 billion. Both optimization approach also identified similar optimal deployment strategy of polymer concentration 0.3 lb/bbl, optimal location of polymer injectors (INJ1, B, INJ2 and INJ4) and recommended to commence polymer flooding as early as possible. There were also variations in the injection rates of some wells.

Generally, Proxy-based optimization slightly under-predicted absolute NPV compared to the Full-physics optimization with an error margin of 0.2 to 0.4% (see Table 5.5). Proxy-based optimization also identified similar optimal polymer deployment strategy except for the slight variation of the injection rates in a few wells, which results in the disparity observed in the absolute NPV (Figure 5-7). However, the cumulative injection rates for all the models were very close with only 1000 bbl/day difference between the Full-physics and Proxy-based optimisation. Injection rate is the least sensitive parameter from our sensitivity analysis, which is the reason why no significant error was introduced in the results of proxy-based optimisation using these three geological realizations.

The average CPU time was 15 hours to complete a polymer flood optimisation with 500 iterations for a single reservoir model when using a proxy model, compared to a CPU time of approximately 72 hours using full physics simulation and 8 CPUs simultaneously. Both optimizations were carried out using a standard desktop PC.

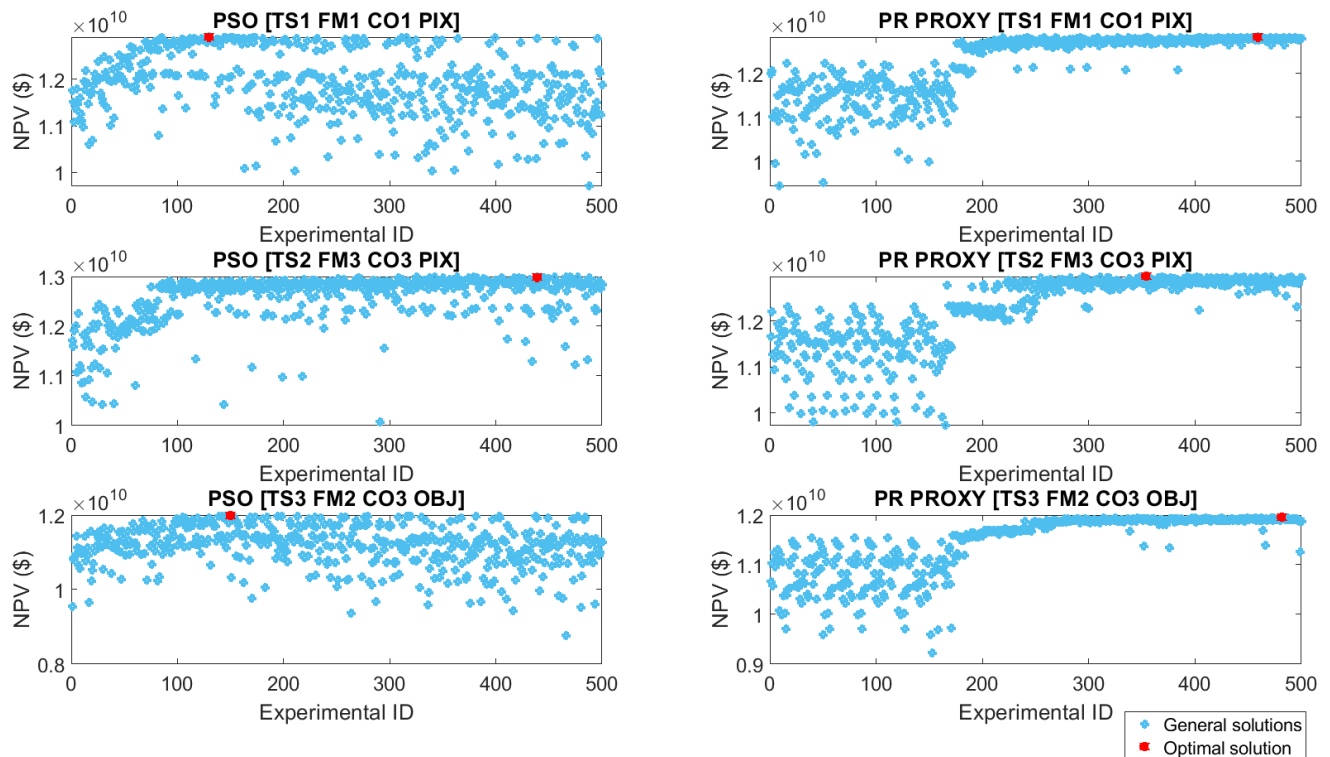


Figure 5-7. Optimization convergence of Full Physics (left) and Proxy-Based optimization(right) for three geological realization.

Table 5-4 Optimal injection rates for all the 7 polymer injectors in bbl/day.

	TS1_FM1_CO1_PIX		TS2_FM2_CO3_OBJ		TS3_FM2_CO3_OBJ	
Injectors	Full Physics Optimization	Proxy-Based Optimization	Full Physics Optimization	Proxy-Based Optimization	Full Physics Optimization	Proxy-Based Optimization
INJ1	18000	18000	18000	18000	18000	18000
INJ2	10000	16000	13000	11000	17000	18000
INJ3	18000	16000	13000	17000	16000	10000
INJ4	17000	15000	18000	18000	14000	18000
INJ5	18000	18000	18000	17000	18000	18000
INJ6	18000	17000	18000	16000	18000	18000
B	18000	18000	18000	18000	18000	18000
Total	117000	118000	116000	115000	119000	118000

Table 5-5. Absolute NPV for Full Physics and Proxy-Based Polymer Flood Optimization of the three realizations of the Watt Field.

Realizations	Full Physics NPV (\$Billion)	Proxy-Based NPV (\$Billion)	% Error
TS1_FM1_CO1_PIX	12.89	12.85	0.3
TS2_FM2_CO3_OBJ	12.99	12.94	0.4
TS3_FM2_CO3_OBJ	11.99	11.96	0.2

### 5.3.4. Constrained vs Unconstrained Optimisation

The result from the optimization of waterflood on the 26 selected geological realization showed a range of absolute NPV from \$10.1 billion to \$13 billion with an average of \$11.8 billion for unconstrained, ensemble while the absolute NPV of the Adjoint ensemble ranged from \$11.2 billion to \$12.6 billion with an average of \$11.9 billion and the PSO ensemble yielded an absolute NPV ranging from \$10.4 billion to \$13.1 billion with an average of \$12.3 billion (Figure 5-8). PSO ensemble predicted more NPV in most of the individual realization than the unconstrained and Adjoint ensemble because of the increase in oil in place during the matching process. The wide range in NPV can be attributed to the stochastic nature of PSO to search the parameter space more broadly which created high diversity of models in the ensemble.

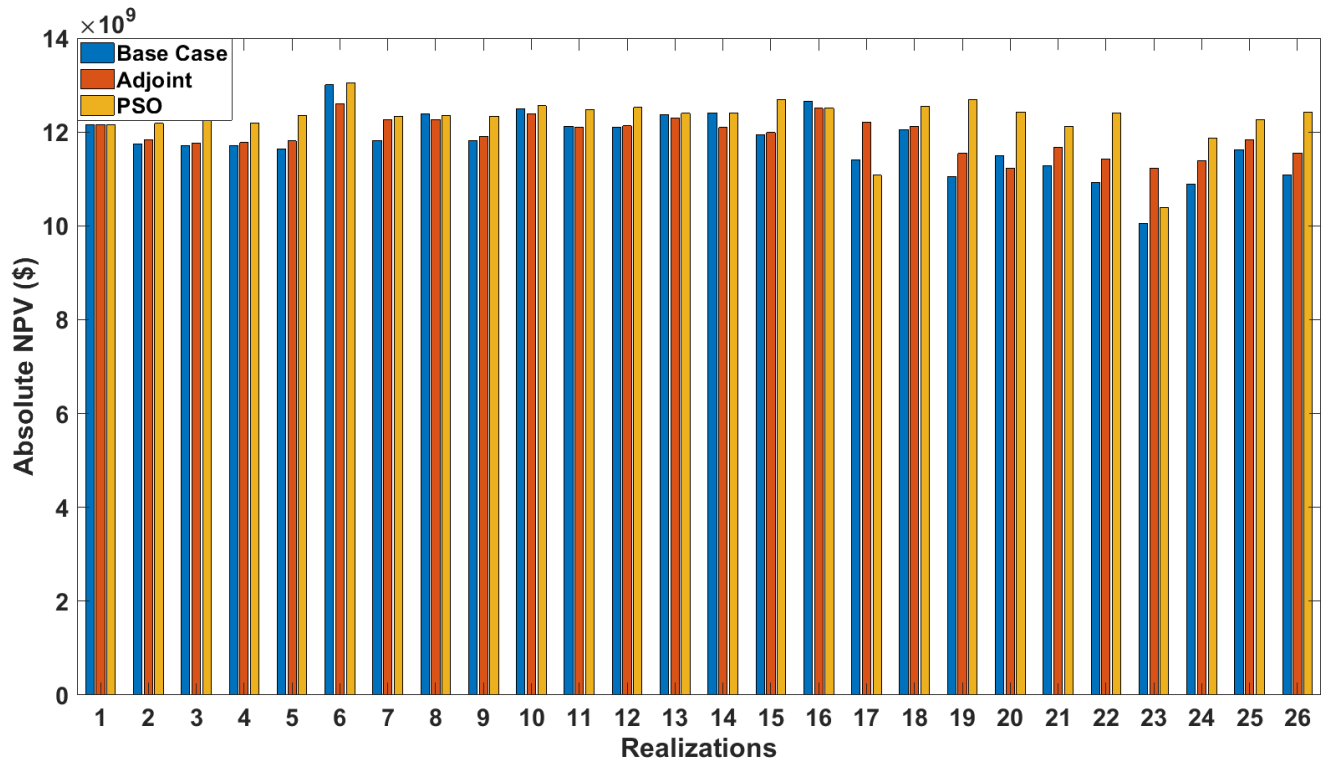
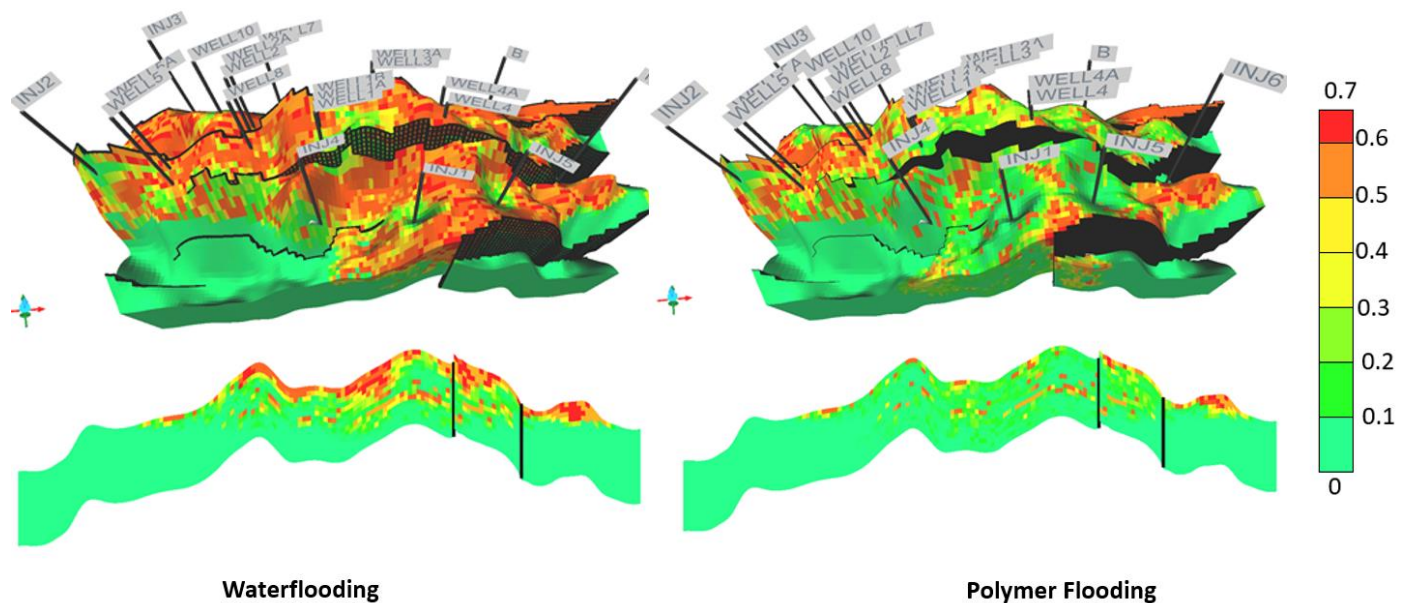


Figure 5-8. Absolute NPV for waterflood optimisation for Unconstrained, Adjoint and PSO ensemble

The results for the polymer injection simulations indicate that sweep efficiency and field oil recovery factor in the Watt Field could be improved significantly compared to waterflood (Figure

5-9). The optimal strategies for the constrained and unconstrained optimisation are presented in *Figure 5-10*. The unconstrained polymer flood optimisation yielded an incremental NPV for the 26 geological ranging from \$300M to \$1 Billion compared to an optimised water flood (*Figure 5-11*). There is considerable variability in the optimal injection strategy, with polymer concentration ranging from 0.2 to 0.3 lb/bbl and the best wells to inject polymers being identified as INJ2, INJ3, INJ6 and INJB. However, all simulation results suggested that it is reasonable to commence polymer flood as soon as possible after a water flood. To further understand how individual geological uncertainties and modelling decisions (i.e. top structure, fault model, cut-offs and modelling methods) impact polymer flooding, we compared the results of individual geological realisations. The optimal strategy suggested by each of the 26 realisations were analysed and then we counted the frequency of each optimal parameter across all the 26 realisations in each ensemble (*Figure 5-10*). This comparison showed that top structure, fault models and geological modelling approach changed neither the incremental NPV nor the optimal strategy for the polymer flooding significantly. These uncertainties can hence be regarded as low risk for this field. On the other hand, the uncertainties when interpreting petrophysical data to indicate shale cut-offs had a significant impact in the optimal strategy on polymer flooding, impacting the estimated incremental NPV by approximately \$340M.



*Figure 5-9. 3D view and cross section of the Watt Field model showing oil saturation as well as injection and production wells after 40 years of waterflood (left) and polymer flood (right).*

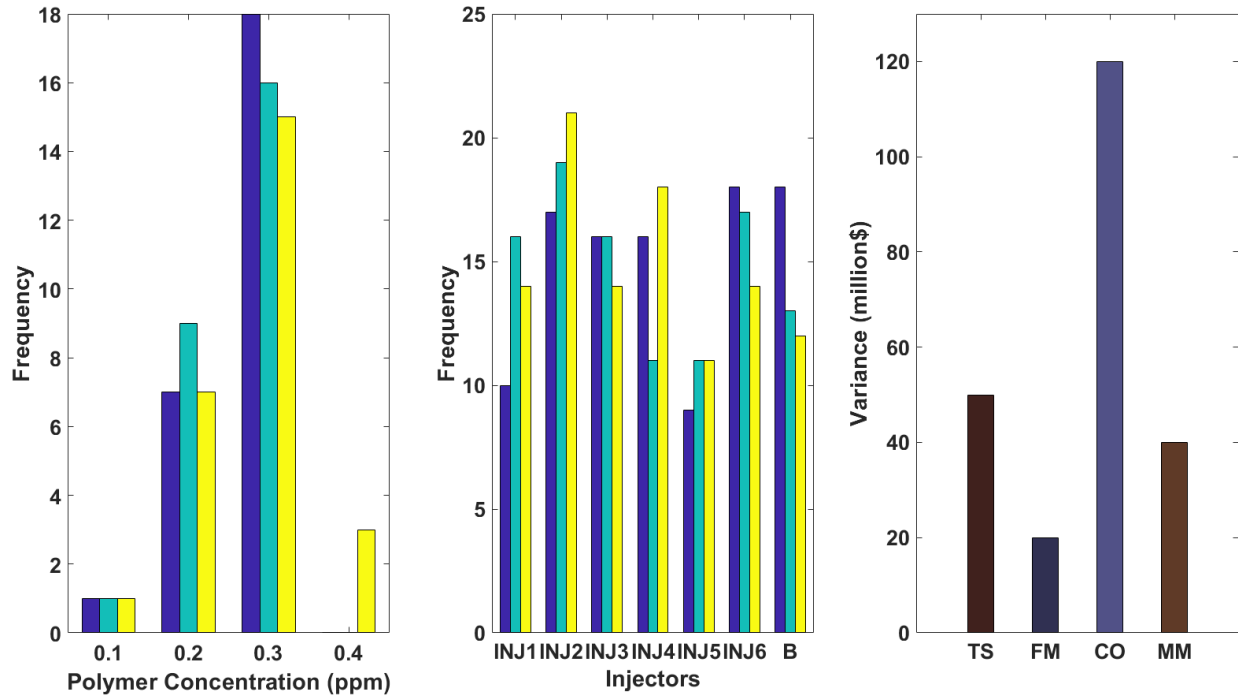


Figure 5-10. Optimal polymer concentrations (left) and location of injector wells (centre) for the unconstrained optimization (blue) and for optimization after history matching using the adjoint method (green) and stochastic history matching (yellow), and the range in NPV based on different geological uncertainties (right). TS refers to the Top Structure of the individual models, FM to the Fault Models, CO to the Cut Off value for the net-to-gross ratio, and MM to the Modelling Methods.

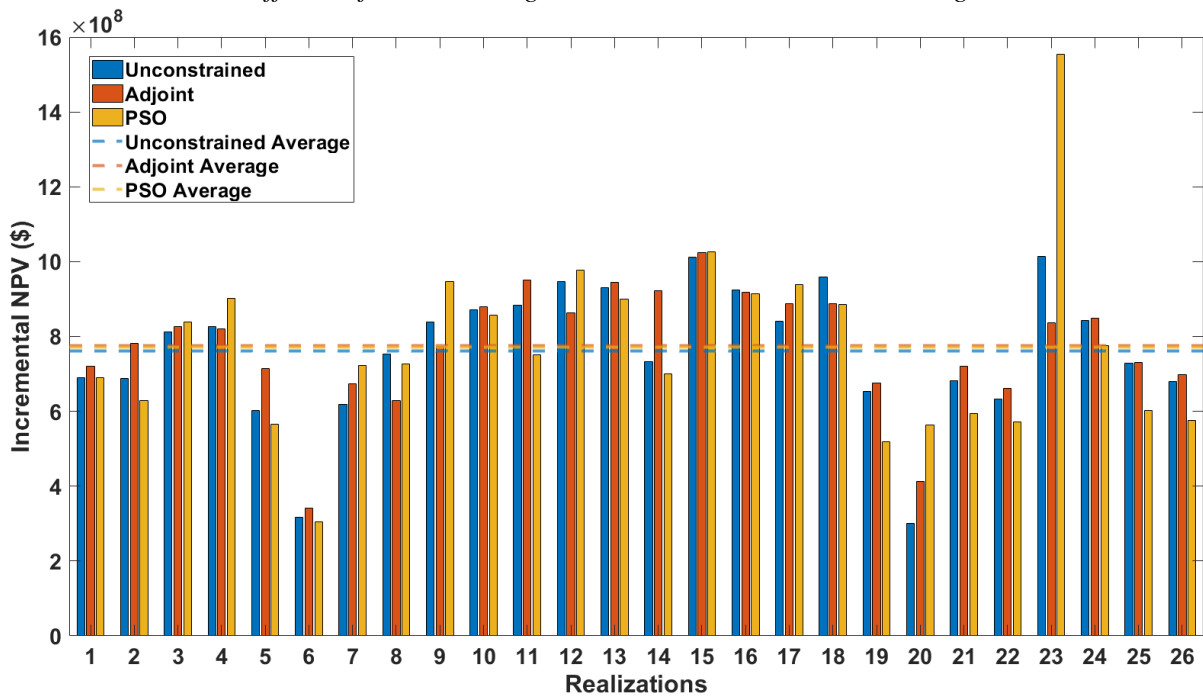


Figure 5-11. Incremental NPV for the the unconstrained optimization (Base Case) and for the optimization after history matching using the adjoint method and stochastic history matching.

To further analyse the impact of shale cut-offs, we grouped the 26 realisations according to the cut-off values (0.5, 0.6, 0.7). All geological realisations with the same shale cut-offs identified the same locations for the polymer injection wells. However, the incremental cumulative oil recovery was observed to drop on average as the shale cut-offs increased. This suggests that within the same shale cut-off value, the optimal polymer flooding strategy does not change much, and risk is reduced, while varying the shale cut-off changes the optimal polymer injection strategy significantly and thereby increases associated financial risk. It is worth to point out that the selection of shale-cut off is an uncertainty that is largely dependent on data interpretation and modelling decisions (Ringrose and Bentley 2015).

The polymer injection designs from the constrained (adjoint technique) optimization yielded an incremental NPV ranging from \$340M to \$1 Billion compared to the optimized water flood across all 26 realizations (Figure 5-11). These results also suggested to commence polymer flooding as early as possible. NPV showed the same trend for the optimal injection strategy and the same impact of geological uncertainties as in the unconstrained optimization. This similarity arose because the adjoint technique changed the reservoir properties only locally, if at all, during history matching. However, incremental NPV predictions were seen to narrow compared to the unconstrained optimization case (Figure 5-11) because the geological uncertainties associated with polymer flooding were not adequately propagated. The polymer injection designs from the constrained ensemble using a stochastic history matching technique are based on reservoir models that have significant variations in the reservoir properties. Hence major changes in the optimal polymer deployment strategy were observed compared to the other two optimization scenarios. The optimal polymer concentration ranged from 0.1 to 0.4 lb/bbl while injectors INJ1, INJ2, INJ3, and INJ4 were identified as the best wells to inject polymer. 25 geological realization suggested to commence polymer flood as early as possible whereas one realization recommended to commence polymer flood after 3 years. The incremental NPV ranges from \$305 Million to \$1.5 Billion. It was observed that the average cumulative NPV in stochastic ensemble was higher, but also had a higher risk, compared to the two other optimization scenarios (Figure 5-12). This difference is due to the ability of the stochastic algorithm to explore the parameter space more broadly, which created reservoir models where the initial oil in place increased.

The constrained optimization based on stochastic history matched models also showed a higher incremental NPV with a higher variance. As in the case for the higher overall NPV, this difference is due to the significant modification of the reservoir properties during the history matching process. For example, oil production increases more rapidly at early time but then water cut problems develop (Figure 5-12). These changes in reservoir properties after history matching amplify the apparent benefit of polymer flooding compared to the water flood. For example, the increase in vertical permeability during the history matching causes water to move more quickly from the aquifer which in turn increases the water cut and enhances the perceived benefit of the polymer flood. In contrast, a decrease in fault transmissibility during the history matching rendered the polymer flood less beneficial as much polymer is lost in the aquifer. Overall, the constrained optimization based on stochastically history matched models predicted the lowest average incremental cumulative oil production but yielded the highest incremental and cumulative NPV compared to the two other optimization scenarios (Figure 5-13).

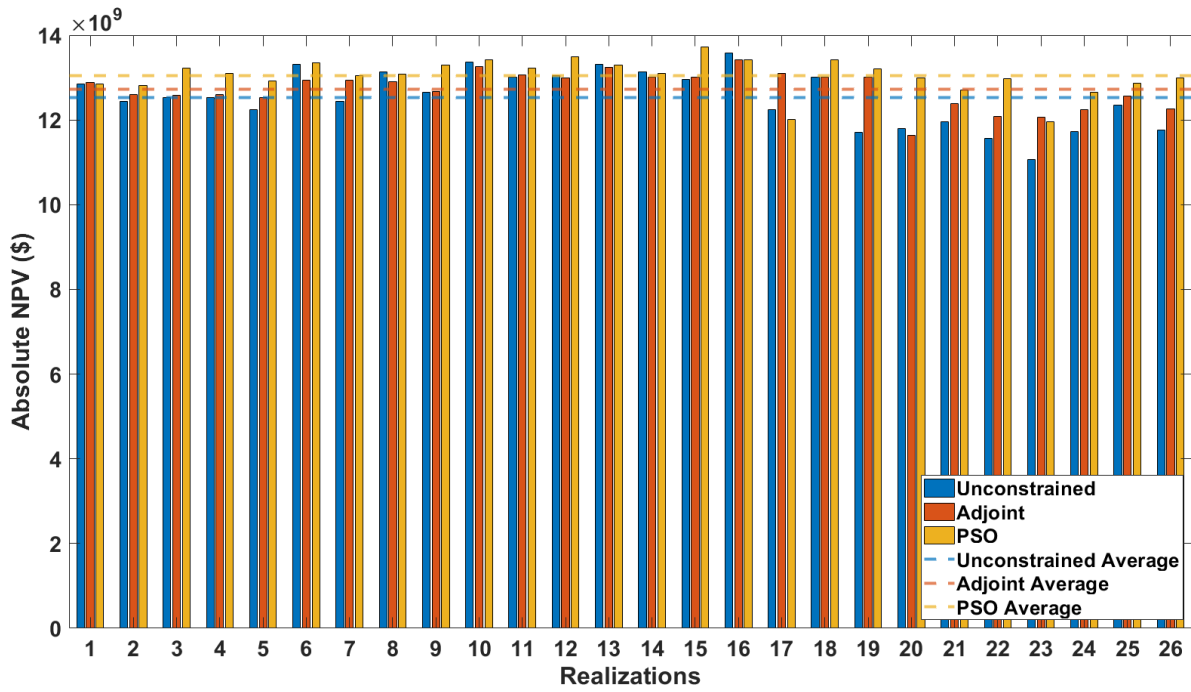


Figure 5-12. Absolute NPV for the the unconstrained optimization (Base Case) and for the optimization after history matching using the adjoint method and stochastic history matching.

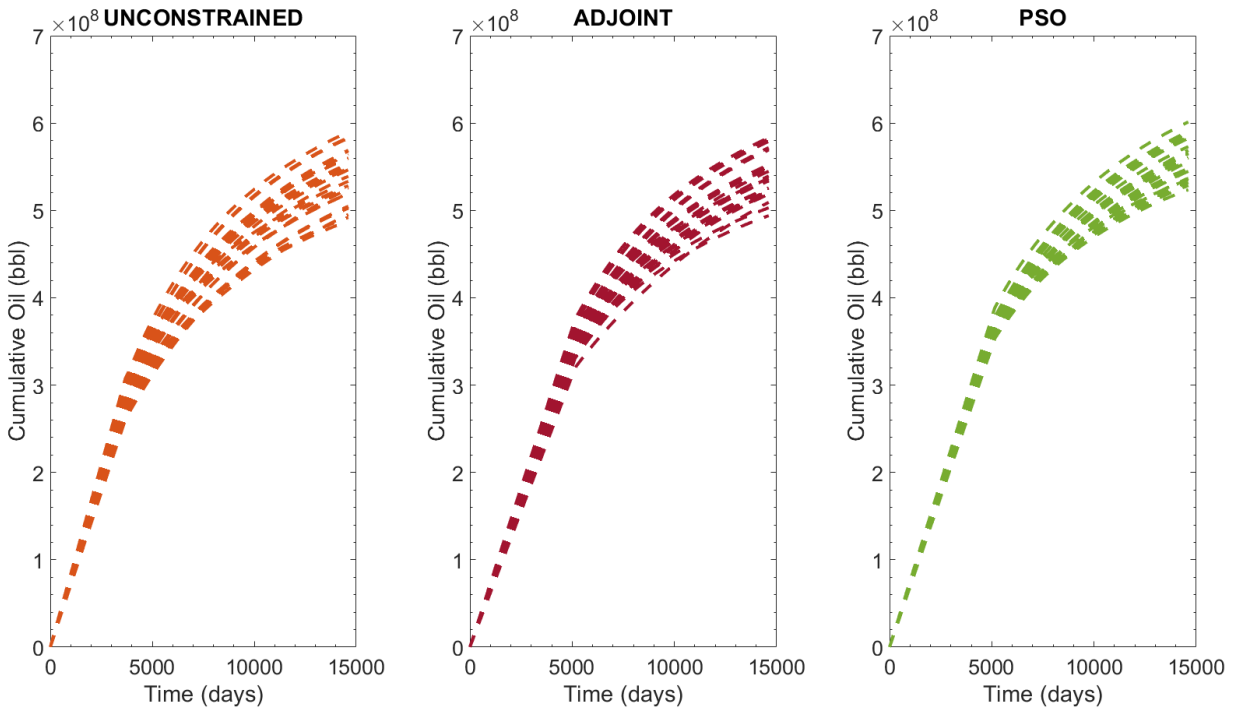


Figure 5-13. Cumulative oil production forecast for the unconstrained optimization (left) and for the optimization after history matching using the adjoint method (centre) and PSO-based history matching (right).



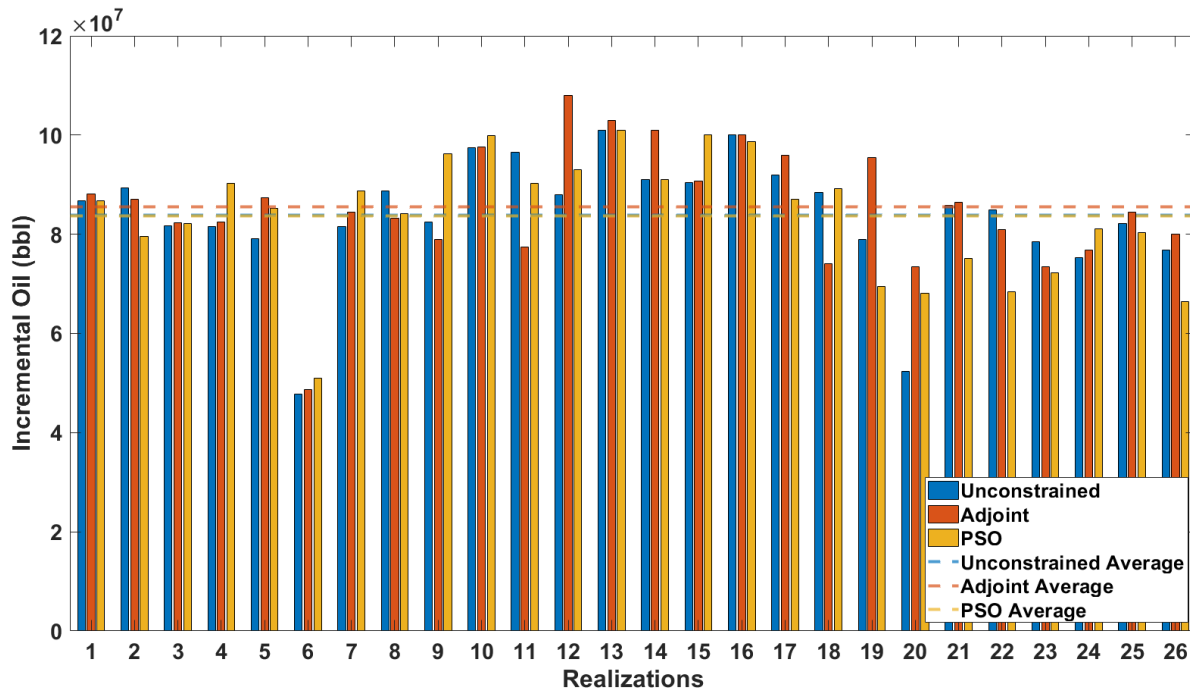


Figure 5-14. Incremental oil recovery for the unconstrained optimization (left) and for the optimization after history matching using the adjoint method (centre) and stochastic history matching (right). The different colours correspond to different top structures in the reservoir model.

## 5.3.5. Uncertainty Quantification

### 5.3.5.1 Cross Comparison

Figure 5-15 shows the result for three different realizations (REAL1, REAL13, and REAL26) from the three different reservoir model ensembles (Unconstrained, Adjoint, and PSO), i.e. for 9 different realizations. In the following, we refer to the “right” strategy as the optimal strategy that was identified for a particular reservoir model from a particular ensemble (e.g. the optimal polymer injection strategy for REAL1 from the Unconstrained ensemble). We refer to the “wrong” strategy if the optimal polymer injection strategy for a particular reservoir model from a particular ensemble is applied to all other 25 reservoir models from the same ensemble. In other words, we apply a cross-comparison to analyse how NPV changes if we apply an injection strategy that was optimised for a particular ensemble member is applied to all other ensemble members, each corresponding to its own geological interpretation and with its own optimal injection strategy. This comparison helps us to quantify the risks of applying a “sub-optimal” injection strategy to a reservoir because the corresponding reservoir model does not represent the real subsurface geology adequately.

Although the NPV decreases if the “wrong” polymer flood design is deployed, the NPV after the polymer flood is still higher than the NPV for the optimized waterflood. This observation implies that the polymer flood appears to be a low-risk choice and likely more beneficial than an optimized waterflood even if the well controls have been optimized using a reservoir model that makes incorrect assumption of the reservoir geology. For the unconstrained model, the variance of the decline in NPV ranged from \$100 million to 600 million. In contrast, for the constrained models, the variance of the decline in NPV ranged from \$145 million to \$496 million for the ensemble constrained using adjoint technique and ranged from \$100 million to \$600 million for the ensemble of geological model constrained using stochastic method.

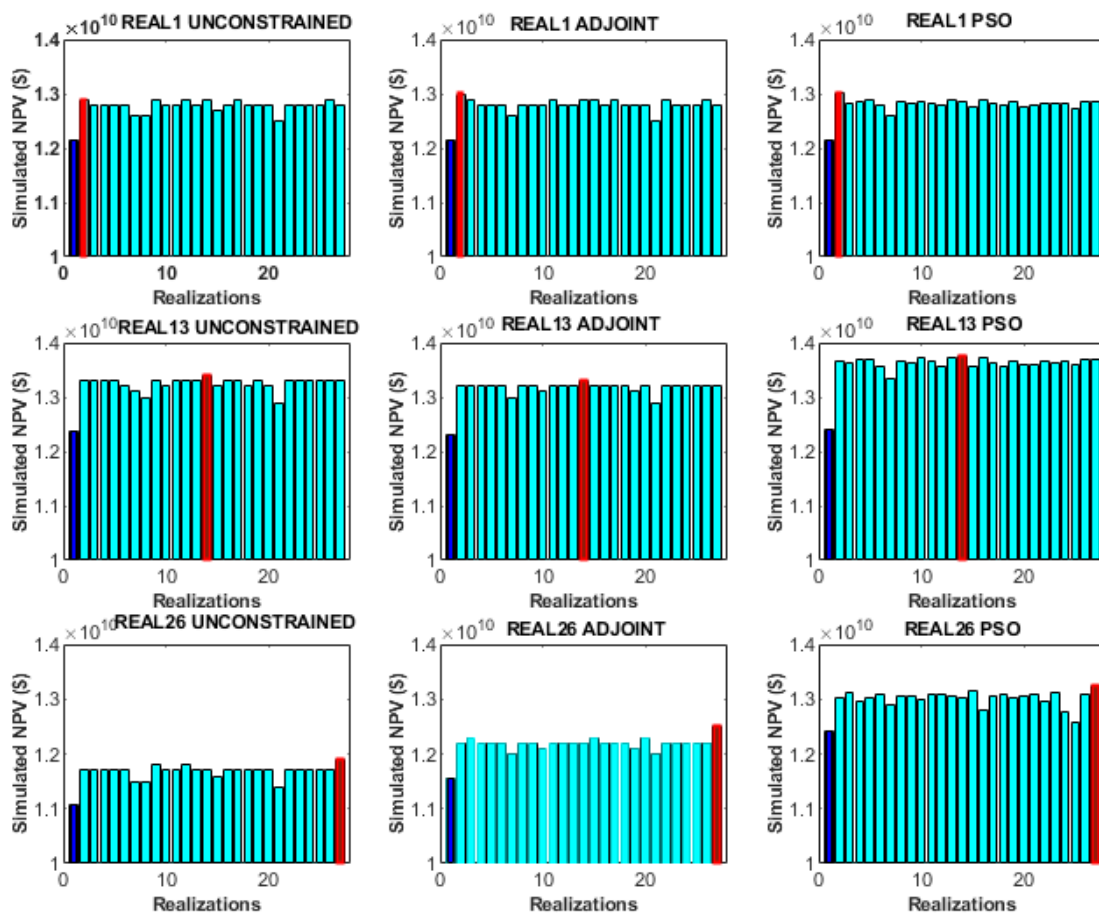


Figure 5-15. Cross-comparison of the optimal NPV for three different geological realizations (top to bottom) considering unconstrained and two constrained optimization techniques (left to right columns). During this cross-comparison, the optimal polymer flood design for one realization is deployed to all other 25 geological realizations to estimate the risk of using an incorrectly optimized polymer flood for a given reservoir geology by comparing the NPV for and optimized water flood (blue), NPV for the “right” optimal strategy (red) and NPV for the “wrong” optimal strategy for each realisations (light blue).

### 5.3.5.2 Uncertainty Forecasting

The result from the uncertainty analysis of the average distribution of the absolute NPV conducted for both waterflood and polymer flooding are presented in form of a posterior probability distribution (PPD) i.e. P10, P50, and P90 is represented with a boxplot shown in Figure 5-16. For the waterflood boxplot, the truth case was observed to be above the P10 – P50 credible interval for the Base (Unconstrained) ensemble, whereas the adjoint ensemble encapsulated the truth very slightly and the PSO ensemble confidently encapsulated the truth at P50 line. This is also in agreement with our discussion in the previous chapter about the ability of PSO to explore the parameter space more broadly and created a diverse set of models which samples the uncertainty space adequately. On the other hand, for the polymer flooding boxplot, the credible interval of the base and the adjoint ensemble could not encapsulate the truth case whereas the PSO ensemble encapsulated the truth case. Although PSO ensemble predicted the truth, the level of confidence was seen to drop from 50% probability in waterflood to a probability of 12% (Figure 5-16). A key take away from the results of this analysis is that the ensemble of history matched models that predicted the uncertainties in a waterflood correctly may not be able to correctly predict the uncertainties in the performance of an EOR such as polymer flooding especially if the history matching process is deterministic. This is in alliance with the aforementioned Flora's rule, which states that if an EOR process alters the fluid-rock interactions and mobility ratios, it is not guaranteed that key geological uncertainties are properly captured in a reservoir model that was previously history matched for a different recovery mechanism. To improve the predictability of an ensemble of reservoir models especially in EOR projects, diversity should be prioritised over match quality during history matching process, as we have shown that PSO ensemble with a lower match quality and high diversity delivered a more reliable uncertainty prediction for a polymer EOR.

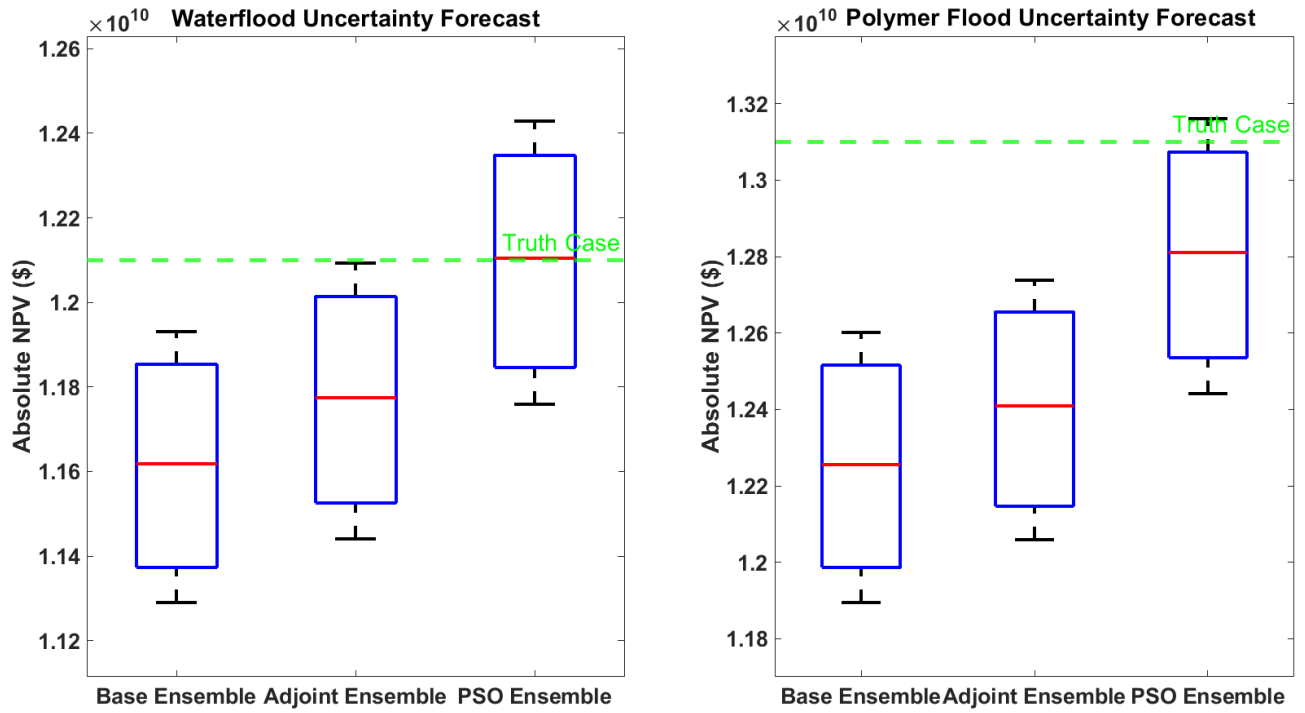


Figure 5-16. Boxplots of average absolute NPV uncertainties forecast for waterflood (left) and polymer flood (right).

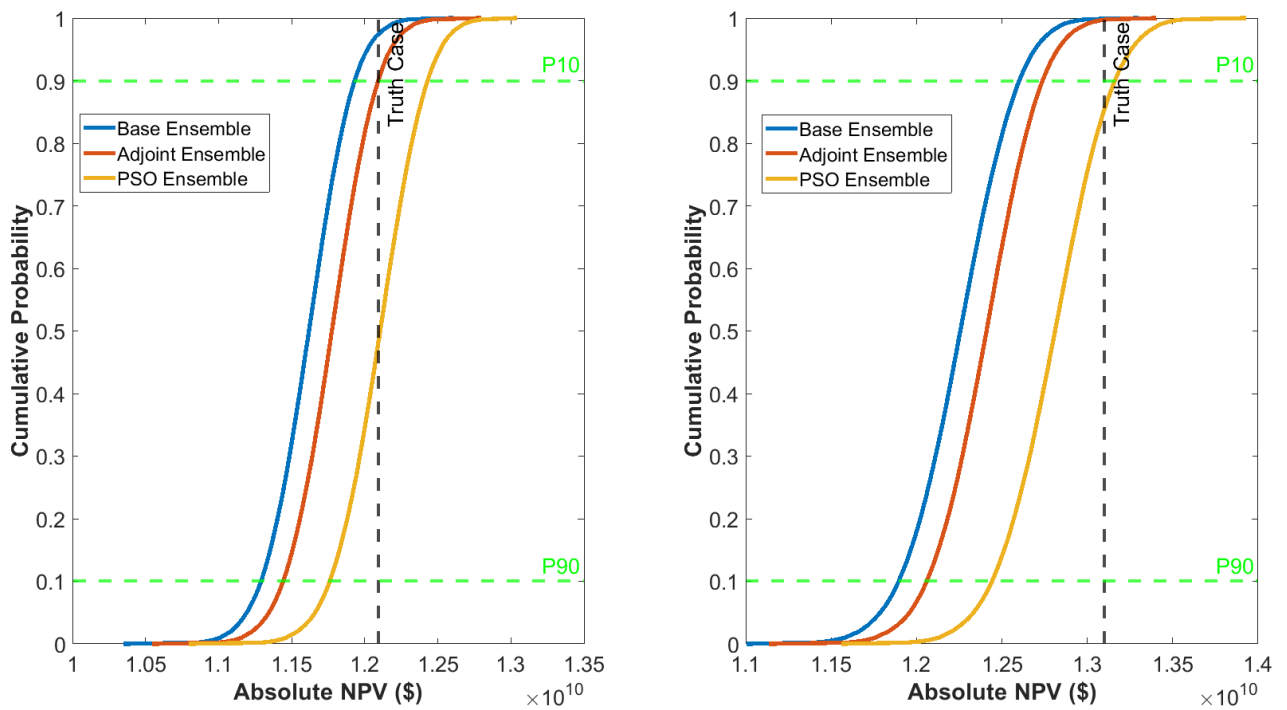


Figure 5-17. Cumulative Probability distribution of average absolute NPV uncertainties forecast for waterflood (left) and polymer flood (right).

## 5.4. Discussions

Although polymer flooding is a promising EOR technique, it is also capital-intensive and will therefore require adequate screening and risk assessment. Accounting for these geological uncertainties during reservoir modelling is important but making sure they are preserved during history matching and uncertainty quantification stages is even more important. It is well understood that geological uncertainties pertinent to the reservoir can be reduced during history matching where the uncertain parameters are adjusted to match the observed production data. However, different fluid fills in the reservoir interact differently with the same reservoir geology (Ringrose and Bentley 2015). It is therefore not guaranteed that key geological uncertainties are adequately propagated when forecasting future performance of a chosen EOR process if this EOR process changes the fluid rock-interaction and mobility ratios; hence EOR performance forecasts, such as the one discussed in this paper, may become unreliable. To test this hypothesis, we used the ensembles of history matched reservoir models created in chapter 4, i.e. the Adjoint technique and PSO. The type of history matching determined the size of the ensemble, the diversity across the ensemble members, the convergence speed, and the quality of the history match.

Reservoir simulation and optimization of polymer flooding in a heterogenous reservoir is complex and computationally expensive. By applying a proxy-based approach to approximate full physics numerical simulation with a lesser number of training and validation runs that cover the parameter space and account for key uncertainties, we can significantly lower the computational effort. These proxy models can assist in understanding, the relationships and interdependencies of uncertain input parameters and accelerate the simulation and optimization of polymer flooding under geological uncertainties. Even though proxy models are considerably quicker to run compared to full physics simulations, it is crucial that such an approximation should be used with care. The accuracy of the proxy model must be properly assessed in order to provide a high predictive capability, using the appropriate goodness-of-fit measures such as the coefficient of determination  $R^2$ . Although the accuracy of a proxy model increases with an increase in the training data, a point is often reached where adding more data will not yield any noticeable increase in the accuracy of the proxy model and only increases the computational cost. An initial sensitivity analysis to determine the first-order parameters needed to construct a reliable and efficient proxy model were carried out. For this particular application, the results from the sensitivity analysis suggested that 160 training datasets were sufficient to approximate the polymer flooding in the Watt Field with good accuracy, i.e. high  $R^2$  value. Small discrepancies between the proxy model and full physics simulations are likely due to the presence of complex geological structures (e.g. the faulted nature of the Watt Field) and distinct changes in the resulting parameter distribution.

This chapter therefore provides a complex, semi-synthetic, yet realistic case study that highlights the benefits of applying response surfaces, generated with polynomial regression, for the optimization of polymer floods, carried out with a PSO algorithm, in complex and heterogenous reservoirs under geological uncertainty. Using three different model ensembles for the Watt Field (i.e., unconstrained, Adjoint and PSO), this chapter showed that the NPV, sweep efficiency and oil recovery in this field were significantly improved by polymer flooding compared to waterflood due to improvement in mobility ratio leading to a more stable displacement. However, the optimal

injection strategy and range in NPV prediction were seen to vary from one ensemble to another. The result of cross comparison where optimal polymer injection strategy for one geological realization is applied to all other realizations in the same ensemble showed a slight decline in NPV but was still higher than the NPV for optimized waterflood for those realizations. The result from cross comparison indicates that the risk of polymer flooding may be low in this field and that polymer flooding may be more beneficial even though the reservoir model used to carry out the optimization makes an incorrect assumption of reservoir geology. Further uncertainty estimation using MCMC with PAR showed that the unconstrained ensemble did not encapsulate the NPV of the truth case both for polymer flooding and water flooding, hence the importance of history matching in reducing the risk. Adjoint ensemble encapsulated the NPV of the truth case for water flooding at P10 but did not capture the NPV of the truth case for the polymer flooding within its credible interval (i.e. between P10 – P90). Missing out the NPV of the truth case, implies that the use of multiple realization may mitigate the limitation of the Adjoint technique in terms of poor uncertainty estimation during water flooding as also seen in chapter 4, but may not adequately capture the uncertainties associated to change in fluid-rock interaction due to change in recovery mechanism such as polymer flooding. On the other hand, the PSO ensemble was seen to encapsulate the truth case for both recovery processes, although the confidence level dropped from 50% for water flooding to 12% for polymer flooding. PSO ensemble being able to encapsulate the truth case can be attributed to its high diversity. These observations are therefore in alliance with the aforementioned Flora's rule and become more obvious if the history matching process is deterministic. For a more reliable forecasting, we therefore recommend a stochastic approach such as the PSO method, possibly coupled to a multi-objective algorithm such that the history matching error can be minimized and the diversity across the matched models can be maximized simultaneously (Hutahaeen et al. 2015).

## 5.5. Summary

In this chapter we demonstrated how a wide range of geological uncertainties inherent to a heterogeneous clastic reservoir and different possible engineering controls could impact the efficiency of a polymer flood. We compared the unconstrained (i.e. without history matching) and constrained (i.e. with prior history matching) optimisation of a polymer flood in a heterogeneous reservoir using adjoint techniques and PSO-based stochastic algorithms to history match the reservoir models prior to optimization. The optimized polymer flood could yield an additional NPV ranging from \$300 million to \$1.5 billion compared to an optimized water flood. This variability in incremental NPV is due to the geological uncertainty of the reservoir. Importantly, shale cut-offs, which are an uncertainty related to data interpretation, are a key property that affects the optimization a polymer flood. Other geological uncertainties such as formation thickness or fault location have significantly less impact.

We observed that the optimal polymer deployment varied as a function of the different history matching techniques. Constrained optimization based on stochastic history matching yielded a higher NPV with a larger variance compared to unconstrained optimization or constrained optimization that employs an adjoint technique for history matching. This difference arises because the stochastic algorithm explores a much broader parameter space and creates scenarios where porosity in the oil-bearing regions of the reservoir is increased, which leads to an increase in the

oil in place. Results from cross comparison where optimal polymer strategy for one geological realisation was applied to all other realizations showed that the polymer flood is low risk and likely more beneficial than a water flood, even if the polymer deployment was optimized based on incorrect assumptions concerning the reservoir geology. The result from uncertainty analysis using MCMC with PAR validates our hypothesis (Flora's rule), as the confidence in predicting the uncertainty in NPV declined moving from water flooding to polymer flooding.

# Chapter 6. Summary, Conclusions and Future Work

## 6.1. Summary and Conclusion

It is a well-established fact that polymer flooding can improve the sweep efficiency of an oil reservoir thereby increasing the recovery factor. However, polymer flooding is not widespread due to economic reasons and therefore requires adequate screening and risk evaluation. There are significant uncertainties associated with reservoir characterization, reservoir modelling and history matching. Uncertainties also exist when modelling polymer in porous media such as polymer degradation, adsorption, and inaccessible pore volume. These uncertainties consequently reduce the predictability of reservoir simulation models to study field-scale polymer injection and therefore using reservoir simulation to design and optimize field-scale polymer flooding remains challenging.

This thesis has succeeded in testing, applying, and expanding a workflow that integrates geological and interpretational uncertainties and uncertainties associated with the choice of history matching algorithms to robustly estimate the financial upside and downside of polymer flooding. This thesis contributes to the research of methods for history matching, uncertainty quantification in reliable forecasting and polymer flooding optimization, and further provided validation of Flora's rule which is the central hypothesis.

The thesis was organized in the following manner: Chapter 1 reviewed the current world energy market interactions including the transition to clean energy, and how these new conditions influence investment decisions by oil companies for EOR projects, specifically polymer EOR. Chapter 2 outlined the current understanding and outstanding challenges related to polymer flooding with specific emphasis on how polymer flooding can be optimized in the presence of geological uncertainties. This chapter further presented a review of history matching, optimization, and uncertainty quantification techniques. Chapter 3 described a case study which integrated both geological and interpretational uncertainties that are difficult to parameterize during history matching i.e. the Watt Field, and further presented the methodology adopted for this study.

Chapter 4 investigated how two classical history matching techniques i.e. the Adjoint technique and PSO impact the estimation of uncertainties when predicting future recovery in a heterogenous clastic reservoir. The results of the comparison of these two history matching techniques show that an ensemble of reservoir models that were history matched using PSO is more robust and diverse compared to an ensemble of reservoir models that was history matched using the Adjoint technique. The reason for this difference is due to the explorative nature of PSO, whereas the Adjoint technique was more exploitative, leading to better convergence rates and improved match quality. Although the model ensemble generated with PSO yielded better forecasts in cumulative oil production because a larger number of reservoir models contain geological concepts that are close to that of the truth model, the forecasting accuracy of the ensemble generated with the Adjoint technique was improved because a larger number of



reservoir models that span a wider range of geological uncertainties was considered, rather than just a single base case with an upside and downside. Therefore, both history matching technique predicted that a range of approximately 1 MMbbl in cumulative oil production after 30 years of production. The Adjoint ensemble matched models were very similar to the truth case in terms of average horizontal and vertical permeability, average porosity and average transmissibilities. High variations is observed with the history matched ensemble matched with PSO. More so, average STOIP across the Adjoint ensemble was the same as the truth case, whereas the average ensemble for the PSO ensemble were seen to increase by 0.9 %. From Figure 4-11 which shows the prior and history matched models show that the facies models were preserved as such applying a second misfit that conditions on the geostatistics may not yield a different result.

Chapter 5 compared the performance of proxy-model based and full-physics optimization of the NPV for a polymer flood, using three different geological realizations of the Watt Field. Latin Hypercube Sampling was used to create 160 training runs to build a polynomial regression proxy model. The proxy models were iteratively validated and improved with extra training data until the quality of the proxy model was sufficiently high. The proxy models were then coupled with a PSO algorithm in CMOST to maximise the NPV, comparing the performance of an optimised polymer flood to the base-case of an optimised water flood. Full physics PSO optimization was also conducted using the same three geological realizations. Both optimization approach yielded similar NPV and optimal strategies for the three realizations with only slight differences in the optimal injection rates. Chapter 5 further examines how different history matching techniques impact the outcome of the optimization of the polymer flood. Proxy-model based optimisation was used to maximise NPV in the three ensembles of reservoir models (Unconstrained ensemble, PSO ensemble and Adjoint ensemble). The results from this analysis show that the optimal polymer deployment strategy varied as a function of different history matching techniques. The ensemble that was history matched using PSO yielded a higher NPV and a larger range of NPV values due to the PSO's ability to explore a much broader parameter space. Specifically, the ensemble generated using PSO contained scenarios where the porosity in the oil bearing region in the reservoir was increased, leading to an increase in oil in place. Results from cross comparison where the optimal strategy for one realization was applied to all other realizations showed that, in general, polymer flooding has a low risk and may be more beneficial than water flooding even if polymer flooding was not fully optimized for a given reservoir geology. Finally, uncertainty estimates for the NPV were calculated for the polymer flood and water flood using the MCMC with PAR framework in CMOST. It was found that the model that was history matched using PSO yielded a more reliable forecast that included the actual truth case while the ensemble generated with the Adjoint technique could only provide reliable forecasts for the water flood which included the truth case. This observation can be explained by Flora's rule because a change in recovery mechanism causes the fluids to interact differently with the same reservoir geology, which impacts the way how the uncertainty in NPV is estimated and forecasted.

In conclusion, based on our analysis, the best strategy for this field will be to commence polymer flooding as early as possible, with the optimal polymer strategy suggested by PSO ensemble due to its reliability of forecast. In general, polynomial proxy approximation has proven to be a good

choice in modelling polymer flooding in heterogenous and complex clastic reservoir as this study shows similar results between proxy optimisation and full physics optimisation. Therefore, there may not be any need for full physics optimisations. Finally, the result of the cross comparison where the optimal strategy for one realization was applied to all other realizations showed that, even if we do not have the complete understanding of the geology, as long as we optimize a polymer flood, it may still be more beneficial compared to a water flood.

## 6.2. Future Work

This thesis focuses on the analysis and optimization of polymer flooding to improve oil recovery in heterogenous clastic reservoir, specifically how the history matching of a water flood impacts the ability to forecast the range of NPV during a polymer flood where the reservoir fluids interact differently with the same reservoir geology compared to the original water flood. There are aspects related to this work presented in this thesis that could be improved, including but not limited to the following:

- The history matching process only considered two different techniques. It would be interesting to see how other history matching approaches such as EnKF or Bayesian methods change the result in this thesis, in terms of history matching quality, optimization, and uncertainty quantifications.
- The thesis only considered the optimization of a single objective. Often there are different competing objectives that influence that influence the optimization process, and it therefore would be interesting to apply multi-objective history matching and optimization to increase the diversity of the history matched models and analyse if a more robust estimation of uncertainty can be obtained.
- In this thesis, only 26 of the 81 geological realizations of the Watt Field model were used, and only one proxy model was built for each realization to keep calculations manageable. It would be interesting to analyse how the results will change if all 81 realizations are used and a single proxy model is built for all the realizations.
- Polynomial regression was applied to create the proxy models. It would be interesting to investigate how other approaches to create proxy models such as Polynomial Chaos Expansion, Radial Basis Functions, or machine learning techniques impact the optimization and uncertainty estimates, and also computational efficiency.
- In this thesis, the viscosity contrast between the oil and formation brine was relatively small. A larger viscosity and mobility contrast could accentuate the differences between the water flood and polymer flood even more and could be investigated.
- A compare-and-contrast study where other EOR techniques that impact fluid-structure interactions compared to a water flood, such as water-alternating-gas injection, are affected by constrained and unconstrained optimization.
- To complete the study within a reasonable time, we stopped the simulations after 40 years, while the absolute NPV was still increasing with time. It will be interesting to see how the result of this study will change if the simulations run time were extended to the period where the absolute NPV start decreasing with time.

- We constructed a total of 78 realisations i.e. 26 realisations per ensemble for a total of three ensembles. To simplify things even more, a study where only a total of three proxy models is constructed (one per ensemble) can be built and compared to the result of this study.
- The truth case model that we used to generate the production data from a prolonged waterflood was model based and it will be interesting to further investigate a scenario where the truth case model does not have similar input with other geological realisations.
- We did not attempt to ensure geological consistency during history matching. It will be interesting to see how our result may change if regularisation is applied to ensure geological consistency of the history matched reservoir models.

## Bibliography

- "2014 Worldwide EOR Survey - Oil & Gas Journal." n.d. Accessed September 7, 2017.  
<http://www.ogj.com/articles/print/volume-112/issue-4/special-report-eor-heavy-oil-survey/2014-worldwide-eor-survey.html>.
- Aanonsen, Sigurd I., Geir Nøvdal, Dean S. Oliver, Albert C. Reynolds, and Brice Vallès. 2009. "The Ensemble Kalman Filter in Reservoir Engineering-A Review." *SPE Journal*.  
<https://doi.org/10.2118/117274-PA>.
- Abu-shiekah, Issa M., Robbert A. Nieuwenhuijs, Ryan Wade Ross, Gary Howell Lanier, Abdulaziz Hikal Al-Belushi, Faisal Saadi, Sami Mubarak Al Nofli, Said Amor Al-harthy, and John N.M. Van Wunnik. 2012. "Developing a Layered Heterogeneous Precambrian Reservoir by Polymer Flooding." In *SPE EOR Conference at Oil and Gas West Asia*. Society of Petroleum Engineers.  
<https://doi.org/10.2118/154465-MS>.
- Agada, Simeon, Sebastian Geiger, Ahmed Elsheikh, and Sergey Oladyskin. 2017. "Data-Driven Surrogates for Rapid Simulation and Optimization of WAG Injection in Fractured Carbonate Reservoirs." *Petroleum Geoscience* 23 (2): 270–83. <https://doi.org/10.1144/petgeo2016-068>.
- Ahmadi, Mohammad Ali, Sohrab Zendejboudi, and Lesley A. James. 2018. "Developing a Robust Proxy Model of CO<sub>2</sub> Injection: Coupling Box–Behnken Design and a Connectionist Method." *Fuel* 215: 904–14. <https://doi.org/10.1016/j.fuel.2017.11.030>.
- Aissaoui, Karim, and Manuel Moreno. 2013. "A Comprehensive Approach for History Matching a Giant and Complex Oil Reservoir." In *SPE Reservoir Characterisation and Simulation Conference and Exhibition*. Abu Dhabi, U.A.E. <https://doi.org/10.2118/165990-ms>.
- AlAmeri, Saeeda, Mohamed AlBreiki, and Sebastian Geiger. 2019. "History Matching Under Geological Constraints Coupled with Multi-Objective Optimisation to Optimise MWAG Performance - A Case Study in a Giant Onshore Carbonate Reservoir in the Middle East." <https://doi.org/10.2118/196715-ms>.
- AlAmeri, Saeeda, Mohamed AlBreiki, and Sebastian Geiger. 2020. "History Matching Under Geological Constraints Coupled with Multiobjective Optimization To Optimize MWAG Performance: A Case Study in a Giant Onshore Carbonate Reservoir in the Middle East." *SPE Reservoir Evaluation & Engineering* 23 (02): 534–50. <https://doi.org/10.2118/196715-PA>.
- Alhuthali, Ahmed Humaid H., Akhil Datta-Gupta, Bevan Bun Wo Yuen, and Jerry Pasco Fontanilla. 2008. "Optimal Rate Control Under Geologic Uncertainty." In *SPE Symposium on Improved Oil Recovery*. Society of Petroleum Engineers. <https://doi.org/10.2118/113628-MS>.
- Almuallim, H., K. Edwards, and L. Ganzer. 2010. "History-Matching with Sensitivity-Based Parameter Modifications at Grid-Block Level." In *72nd European Association of Geoscientists and Engineers Conference and Exhibition 2010: A New Spring for Geoscience. Incorporating SPE EUROPEC 2010*, 2:1210–21. Society of Petroleum Engineers. <https://doi.org/10.2118/131627-ms>.
- April, J., F. Glover, J. Kelly, M. Laguna, M. Erdogan, B. Mudford, and D. Stegemeier. 2003. "Advanced Optimization Methodology in the Oil and Gas Industry: The Theory of Scatter Search Techniques with Simple Examples." In *SPE Hydrocarbon Economics and Evaluation Symposium*. Society of Petroleum Engineers. <https://doi.org/10.2118/82009-MS>.

- Arnold, D, V Demyanov, D Tatum, M Christie, T Rojas, S Geiger, and P Corbett. 2013. "Hierarchical Benchmark Case Study for History Matching, Uncertainty Quantification and Reservoir Characterisation." *Computers and Geosciences* 50: 4–15. <https://doi.org/10.1016/j.cageo.2012.09.011>.
- Astakhov, Viktor P. 2012. "Design of Experiment Methods in Manufacturing: Basics and Practical Applications." In *Statistical and Computational Techniques in Manufacturing*. Vol. 9783642258596. [https://doi.org/10.1007/978-3-642-25859-6\\_1](https://doi.org/10.1007/978-3-642-25859-6_1).
- Babaei, Masoud; Indranil; Pan, and Ali; Alkhatib. 2015. "Robust Optimization of Well Location to Enhance Hysteretical Trapping of CO<sub>2</sub>: Assessment of Various Uncertainty Quantification Methods and Utilization of Mixed Response Surface Surrogates." *Water Resources Research* 51 (12): 9402–24. <https://doi.org/10.1002/2015WR017418>.
- Bentley, Mark. 2015. "Modelling for Comfort?" *Petroleum Geoscience*, 2014–89. <https://doi.org/10.1144/petgeo2014-089>.
- Bentley, Mark, and Philip Ringrose. 2017. "Future Directions in Reservoir Modelling: New Tools and 'fit-for-Purpose' Workflows," 2–11. <https://doi.org/10.1144/PGC8.40>.
- Bera, Achinta, and Tayfun Babadagli. 2015. "Status of Electromagnetic Heating for Enhanced Heavy Oil/Bitumen Recovery and Future Prospects: A Review." *Applied Energy*. Elsevier Ltd. <https://doi.org/10.1016/j.apenergy.2015.04.031>.
- Bhark, Eric, Behnam Jafarpour, and Akhil Datta-Gupta. 2011. "An Adaptively Scaled Frequency-Domain Parameterization for History Matching." *Journal of Petroleum Science and Engineering* 75 (3–4). <https://doi.org/10.1016/j.petrol.2010.11.026>.
- Bond, Clare E., A. D. Gibbs, Z. K. Shipton, and S. Jones. 2007. "What Do You Think This Is? 'Conceptual Uncertainty' In Geoscience Interpretation." *GSA Today* 17 (11). <https://doi.org/10.1130/GSAT01711A.1>.
- Bondor, Paul L. n.d. "SPE Distinguished Lecturer Program The SPE Foundation through Member Donations and a Contribution from Offshore Europe." Accessed June 11, 2020. [www.spe.org/dl](http://www.spe.org/dl).
- BP. n.d. "BP Starts-up Clair Ridge Production | News and Insights | Home." Accessed October 1, 2020a. <https://www.bp.com/en/global/corporate/news-and-insights/press-releases/bp-starts-up-clair-ridge-production.html>.
- BP. n.d. "Overview | Energy Economics | Home." Accessed October 2, 2020b. <https://www.bp.com/en/global/corporate/energy-economics/energy-outlook/introduction/overview.html>.
- Broome, J.H., J.M. Bohannon, and W.C. Stewart. 1986. "The 1984 Natl. Petroleum Council Study on EOR: An Overview." *Journal of Petroleum Technology* 38 (08): 869–74. <https://doi.org/10.2118/13239-PA>.
- Bryant, Rebecca S., and Thomas E. Burchfield. 1989. "Review of Microbial Technology for Improving Oil Recovery." *SPE Reservoir Engineering (Society of Petroleum Engineers)* 4 (2): 151–54. <https://doi.org/10.2118/16646-pa>.
- Burnett, David B. 1975. "Laboratory Studies of Biopolymer Injectivity Behavior Effectiveness of Enzyme Clarification." In *Society of Petroleum Engineers - SPE California Regional Meeting, CRM 1975*.

- Society of Petroleum Engineers. <https://doi.org/10.2118/5372-ms>.
- Cannella, W.J., C. Huh, and R.S. Seright. 1988. "Prediction of Xanthan Rheology in Porous Media." In *SPE Annual Technical Conference and Exhibition, 2-5 October, Houston, Texas*, 353–68. Society of Petroleum Engineers. <https://doi.org/10.2523/18089-MS>.
- Cavazzuti, Marco. 2013. "Chapter 2: Design of Experiment." In *Optimization Methods: From Theory to Design Scientific and Technological Aspects in Mechanics*. <https://doi.org/10.1007/978-3-642-31187-1>.
- Chang, H.L. 1978. "Polymer Flooding Technology Yesterday, Today, and Tomorrow." *Journal of Petroleum Technology* 30 (08): 1113–28. <https://doi.org/10.2118/7043-PA>.
- Chen, S., H. Li, D. Yang, and P. Tontiwachwuthikul. 2010. "Optimal Parametric Design for Water-Alternating-Gas (WAG) Process in a CO<sub>2</sub>-Miscible Flooding Reservoir." *Journal of Canadian Petroleum Technology* 49 (10): 75–82. <https://doi.org/10.2118/141650-PA>.
- Chen, S., H. Li, D. Yang, and P. Tontiwachwuthikul. 2012a. "An Efficient Methodology for Performance Optimization and Uncertainty Analysis in a CO<sub>2</sub> EOR Process." *Petroleum Science and Technology* 30 (12): 1195–1209. <https://doi.org/10.1080/10916466.2010.501354>.
- Chen, S., H. Li, D. Yang, and P. Tontiwachwuthikul. 2012b. "An Efficient Methodology for Performance Optimization and Uncertainty Analysis in a CO<sub>2</sub> EOR Process." *Petroleum Science and Technology* 30 (12): 1195–1209. <https://doi.org/10.1080/10916466.2010.501354>.
- Chen, Yan, and Dean S. Oliver. 2010. "Ensemble-Based Closed-Loop Optimization Applied to Brugge Field." *SPE Reservoir Evaluation & Engineering* 13 (01): 56–71. <https://doi.org/10.2118/118926-PA>.
- Chierici, Gian Luigi. 1995. *Principles of Petroleum Reservoir Engineering*. Berlin, Heidelberg: Springer Berlin Heidelberg. <https://doi.org/10.1007/978-3-642-78243-5>.
- Christie, M.A., and M.J. Blunt. 2001. "Tenth SPE Comparative Solution Project: A Comparison of Upscaling Techniques." In *SPE Reservoir Simulation Symposium*. Society of Petroleum Engineers. <https://doi.org/10.2118/66599-MS>.
- Christie, Michaela, James Glimm, John W. Grove, David M. Higdon, David H. Sharp, and Merri M. Wood-schultz. 2005. "Error Analysis and Simulations of Complex Phenomena." *Los Alamos Science*.
- Christie, Mike, Dmitry Eydinov, Vasily Demyanov, Jack Talbot, Dan Arnold, and Vassilii Shelkov. 2013. "Use of Multi-Objective Algorithms in History Matching of a Real Field." *SPE Reservoir Simulation Symposium, Woodlands, Texas USA*, 18–20. <https://doi.org/10.2118/163580-ms>.
- Claridge, E.L. 1972. "Prediction of Recovery in Unstable Miscible Flooding." *Society of Petroleum Engineers Journal* 12 (02): 143–55. <https://doi.org/10.2118/2930-pa>.
- CNPC. 2016. "China National Petroleum Company." 2016.
- Coats, K.H., J.R. Dempsey, and J.H. Henderson. 1970. "A New Technique for Determining Reservoir Description from Field Performance Data." *Society of Petroleum Engineers Journal* 10 (01): 66–74. <https://doi.org/10.2118/2344-PA>.
- Cohen, Yoram, and F. R. Christ. 1986. "POLYMER RETENTION AND ADSORPTION IN THE FLOW OF POLYMER SOLUTIONS THROUGH POROUS MEDIA." *SPE Reservoir Engineering (Society of Petroleum Engineers)*. <https://doi.org/10.2118/12942-PA>.

- Dale, Spencer, and Bassam Fattouh. 2018. "Peak Oil Demand and Long-Run Prices." *Energy Insight*. Vol. 25.
- Davidson, Jeffrey E., and Bret L. Beckner. 2003. "Integrated Optimization for Rate Allocation in Reservoir Simulation." *SPE Reservoir Evaluation & Engineering* 6 (06): 426–32. <https://doi.org/10.2118/87309-PA>.
- Davis, Michael. 1987. "Production of Conditional Simulations via the LU Triangular Decomposition of the Covariance Matrix." *Mathematical Geology* 19 (2): 91–98. <https://doi.org/10.1007/BF00898189> DO.
- Dehghan Monfared, A., A. Helalizadeh, H. Parvizi, and K. Zobeidi. 2014. "A Global Optimization Technique Using Gradient Information for History Matching." *Energy Sources, Part A: Recovery, Utilization and Environmental Effects* 36 (13): 1414–28. <https://doi.org/10.1080/15567036.2011.551929>.
- Delamaide, Eric. 2014. "Polymer Flooding of Heavy Oil - From Screening to Full-Field Extension." In *Society of Petroleum Engineers - SPE Heavy and Extra Heavy Oil Conference - Latin America 2014, LAHO 2014*. <https://doi.org/10.2118/171105-ms>.
- Dominguez, J. G., and G. P. Willhite. 1977. "RETENTION AND FLOW CHARACTERISTICS OF POLYMER SOLUTIONS IN POROUS MEDIA." *Soc Pet Eng AIME J* 17 (2).
- Doren, Jorn Van, Sippe Douma, Bart Wassing, Hans Kraaijevanger, and Bert Rik De Zwart. 2011. "Adjoint-Based Optimization of Polymer Flooding." In *Society of Petroleum Engineers - SPE Enhanced Oil Recovery Conference 2011, EORC 2011*, 1:498–505. Society of Petroleum Engineers. <https://doi.org/10.2118/144024-ms>.
- Dunn, William L., and J. Kenneth Shultis. 2012. "Markov Chain Monte Carlo." In *Exploring Monte Carlo Methods*. <https://doi.org/10.1016/b978-0-444-51575-9.00006-3>.
- Eberhart, Russell, and James Kennedy. n.d. "A New Optimizer Using Particle Swarm Theory." In *MHS'95. Proceedings of the Sixth International Symposium on Micro Machine and Human Science*, 39–43. Accessed March 28, 2018. <https://doi.org/10.1109/MHS.1995.494215>.
- Energy, Rystad. 2020. "Rystad Energy - Rystad Energy Insights - July 2020." 2020. <https://www.rystadenergy.com/newsevents/news/newsletters/CompanyArchive/cn-july-2020/>.
- Erba, D., and M Christie. 2007. "How Does Sampling Strategy Affect Uncertainty Estimations?" *Oil & Gas Science and Technology-Rev. IFP* 62 (2): 155–67. <https://doi.org/10.2516/ogst:2007014>.
- Essen, Gijs van, Maarten Zandvliet, Paul Van den Hof, Okko Bosgra, and Jan-Dirk Jansen. 2009. "Robust Waterflooding Optimization of Multiple Geological Scenarios." *SPE Journal* 14 (01): 202–10. <https://doi.org/10.2118/102913-PA>.
- Evensen, G. 1994. "Sequential Data Assimilation with a Nonlinear Quasi-Geostrophic Model Using Monte Carlo Methods to Forecast Error Statistics." *Journal of Geophysical Research* 99 (C5). <https://doi.org/10.1029/94jc00572>.
- Evensen, Geir, Joakim Hove, Hilde Meisingset, Edel Reiso, Knut Sponheim Seim, and Ø. Espelid. 2007. "Using the EnKF for Assisted History Matching of a North Sea Reservoir Model." In *SPE Reservoir Simulation Symposium*. Society of Petroleum Engineers. <https://doi.org/10.2118/106184-MS>.

- ExxonMobil Corporation. 2019. "Outlook for Energy: A Perspective to 2040." *Technical Reprint*.  
<https://doi.org/10.1017/CBO9781107415324.004>.
- Fernández Martínez, Juan Luis, Tapan Mukerji, Esperanza García Gonzalo, and Amit Suman. 2012. "Reservoir Characterization and Inversion Uncertainty via a Family of Particle Swarm Optimizers." *Geophysics* 77 (1). <https://doi.org/10.1190/geo2011-0041.1>.
- Field, A North Sea. 1992. "Elvnd Damsleth," no. December.
- Fletcher, R. 1970. "A New Approach to Variable Metric Algorithms." *The Computer Journal* 13 (3): 317–22. <https://doi.org/10.1093/comjnl/13.3.317>.
- Gavalas, G. R., P. C. Shah, and J. H. Seinfeld. 1976. "RESERVOIR HISTORY MATCHING BY BAYESIAN ESTIMATION." *Soc Pet Eng AIME J*. <https://doi.org/10.2118/5740-PA>.
- Gibbs, James A. 2017. "Is the World Facing 'Peak Demand' Rather Than 'Peak Supply'?" 2017. <http://fivestates.com/is-the-world-facing-peak-demand-rather-than-peak-supply/>.
- Green, Don W., and G. Paul. Willhite. 1998. *Enhanced Oil Recovery*. Henry L. Doherty Memorial Fund of AIME, Society of Petroleum Engineers. <http://store.spe.org/Enhanced-Oil-Recovery--P21.aspx>.
- Gruenwalder, Markus, Stefan Poellitzer, Torsten Clemens, and Omv E&p. 2007. "SPE 106039 Assisted and Manual History Matching of a Reservoir With 120 Wells, 58 Years Production History and Multiple Well Completions."
- Hajizadeh, Yasin. 2010. "Ants Can Do History Matching." In *SPE Annual Technical Conference and Exhibition*, 19–22. Society of Petroleum Engineers. <https://doi.org/10.2118/141137-STU>.
- Hajizadeh, Yasin, Michael A. Christie, and Vasily Demyanov. 2010. "Comparative Study of Novel Population-Based Optimization Algorithms for History Matching and Uncertainty Quantification: PUNQ-S3 Revisited." In *Abu Dhabi International Petroleum Exhibition and Conference*. Society of Petroleum Engineers. <https://doi.org/10.2118/136861-MS>.
- Huh, C., E. A. Lange, and W. J. Cannella. 1990. "Polymer Retention in Porous Media." In . [https://doi.org/10.1007/978-94-011-3044-8\\_5](https://doi.org/10.1007/978-94-011-3044-8_5).
- Hutahaean, J. J., V. Demyanow, and M. A. Christie. 2015. "Impact of Model Parameterisation and Objective Choices on Assisted History Matching and Reservoir Forecasting." In *Society of Petroleum Engineers - SPE/IATMI Asia Pacific Oil and Gas Conference and Exhibition, APOGCE 2015*. <https://doi.org/10.2118/176389-ms>.
- IHS Markit. 2020. "The Future of Conventional Exploration | IHS Markit." 2020. <https://ihsmarkit.com/research-analysis/future-of-exploration.html>.
- Irgens, Morten, and William Lashar Lavenue. 2007. "Use of Advanced Optimization Techniques to Manage a Complex Drilling Schedule." In *Proceedings - SPE Annual Technical Conference and Exhibition*. Vol. 6. <https://doi.org/10.2118/110805-ms>.
- Jaber, Ahmed Khalil, Sameer Noori Al-Jawad, and Ali K. Alhuraishawy. 2019. "A Review of Proxy Modeling Applications in Numerical Reservoir Simulation." *Arabian Journal of Geosciences* 12 (22): 1–16. <https://doi.org/10.1007/s12517-019-4891-1>.
- Jafarpour, Behnam, Vivek K. Goyal, Dennis B. McLaughlin, and William T. Freeman. 2010. "Compressed History Matching: Exploiting Transform-Domain Sparsity for Regularization of Nonlinear Dynamic



- Data Integration Problems." *Mathematical Geosciences* 42 (1). <https://doi.org/10.1007/s11004-009-9247-z>.
- Jahns, Hans O. 1966. "A Rapid Method for Obtaining a Two-Dimensional Reservoir Description From Well Pressure Response Data." *Society of Petroleum Engineers Journal* 6 (04): 315–27. <https://doi.org/10.2118/1473-PA>.
- Janiga, Damian, Robert Czarnota, Jerzy Stopa, Paweł Wojnarowski, and Piotr Kosowski. 2017. "Performance of Nature Inspired Optimization Algorithms for Polymer Enhanced Oil Recovery Process." *Journal of Petroleum Science and Engineering* 154 (March): 354–66. <https://doi.org/10.1016/j.petrol.2017.04.010>.
- Jarrell, Perry M., and Society of Petroleum Engineers (U.S.). 2002. *Practical Aspects of CO<sub>2</sub> Flooding*. Society of Petroleum Engineers. <http://store.spe.org/Practical-Aspects-of-CO2-Flooding-P48.aspx>.
- JENNINGS RR, ROGERS JH, and WEST TJ. 1971. "FACTORS INFLUENCING MOBILITY CONTROL BY POLYMER SOLUTIONS." *JPT, Journal of Petroleum Technology*.
- Jim E, Griffin, and Stephens David A. 2013. "Advances in Markov Chain Monte Carlo." In *Bayesian Theory and Applications*. <https://doi.org/10.1093/acprof:oso/9780199695607.003.0007>.
- Kabir, C. S., M. C.H. Chien, and J. L. Landa. 2003. "Experiences with Automated History Matching." *JPT, Journal of Petroleum Technology* 55 (4). <https://doi.org/10.2118/0403-0073-jpt>.
- Kalman, R. E. 1960. "A New Approach to Linear Filtering and Prediction Problems." *Journal of Fluids Engineering, Transactions of the ASME* 82 (1). <https://doi.org/10.1115/1.3662552>.
- Kato, Yoshitake, Hirofumi Okano, and Satoru Takahashi. 2014. "Application of PSO and MOPSO to Gas Injection Analysis." In *Society of Petroleum Engineers - International Petroleum Technology Conference 2014, IPTC 2014 - Innovation and Collaboration: Keys to Affordable Energy*. Vol. 4. <https://doi.org/10.2523/18074-ms>.
- Kelkar, Mohan, and Godofredo Perez. 2002. *Applied Geostatistics for Reservoir Characterization*. Society of Petroleum Engineers.
- Khaninezhad, M. Reza M., and Behnam Jafarpour. 2011. "Hybrid Parameterization of Reservoir Properties for Robust History Matching under Geologic Uncertainty." In *Society of Petroleum Engineers - SPE Reservoir Characterisation and Simulation Conference and Exhibition 2011, RCSC 2011*, 192–205. Society of Petroleum Engineers. <https://doi.org/10.2118/146934-ms>.
- Kitanidis, P. K. 1995. "Quasi-Linear Geostatistical Theory for Inversing." *Water Resources* 31 (10): 2411–19.
- Kohavi, Ron. 1995. "A Study of Cross-Validation and Bootstrap for Accuracy Estimation and Model Selection." *International Joint Conference on Artificial Intelligence*, 1137–45. <https://doi.org/10.1067/mod.2000.109031>.
- Kokal, S, and A Al-Kaabi. 2010. "Enhanced Oil Recovery: Challenges and Opportunities." *Global Energy Solutions*.
- Koziel, Slawomir., and Xin-She. Yang. 2011. *Computational Optimization, Methods and Algorithms*. Springer.
- Lake, Larry W. (University of Texas at Austin). 1989. *Enhanced Oil Recovery*. Printed by Society of

- Petroleum Engineers. <http://store.spe.org/Enhanced-Oil-Recovery--P436.aspx>.
- Lake, Larry W, Russell Johns, Bill Rossen, and Gary Pope. 2014. *Fundamentals of Enhanced Oil Recovery*.
- Lake, Larry W, Raymond L Schmidt, and Paul B Venuto. 1992. "A Niche for Enhanced Oil Recovery in the 1990s." *Oilfield Review* 17 (January): 62–67.
- Liang, Faming, Chuanhai Liu, and Raymond J. Carroll. 2010. *Advanced Markov Chain Monte Carlo Methods: Learning from Past Samples*. *Advanced Markov Chain Monte Carlo Methods: Learning from Past Samples*. John Wiley and Sons. <https://doi.org/10.1002/9780470669723>.
- Liu, Ning, and Dean S. Oliver. 2005. "Critical Evaluation of the Ensemble Kalman Filter on History Matching of Geologic Facies." *SPE Reservoir Evaluation & Engineering* 8 (06): 470–77. <https://doi.org/10.2118/92867-PA>.
- Manrique, E, C Thomas, Ravi Ravikiran, M Izadi, Michael Lantz, J Romero, and Vladimir Alvarado. 2010. "EOR: Current Status and Opportunities." In *Proceedings of the 2010 SPE Improved Oil Recovery Symposium Held in Tulsa, Oklahoma, USA, 24–28 April 2010*. This. Society of Petroleum Engineers. <https://doi.org/10.2118/130113-MS>.
- Mantilla, Cesar A., and Sanjay Srinivasan. 2011. "Feedback Control of Polymer Flooding Process Considering Geologic Uncertainty." In *Society of Petroleum Engineers - SPE Reservoir Simulation Symposium 2011*, 2:1152–69. Society of Petroleum Engineers. <https://doi.org/10.2118/141962-ms>.
- McCormack, M. P., J. M. Thomas, and K. Mackie. 2014. "Maximising Enhanced Oil Recovery Opportunities in UKCS through Collaboration." In *Society of Petroleum Engineers - 30th Abu Dhabi International Petroleum Exhibition and Conference, ADIPEC 2014: Challenges and Opportunities for the Next 30 Years*. <https://doi.org/10.2118/172017-ms>.
- McGuire, P. L., A. P. Spence, F. I. Stalkup, and M. W. Cooley. 1995. "Core Acquisition and Analysis for Optimization of the Prudhoe Bay Miscible-Gas Project." *SPE Reservoir Engineering (Society of Petroleum Engineers)* 10 (2): 94–100. <https://doi.org/10.2118/27759-PA>.
- Meyer, Richard F., and Emil D. Attanasi. 2013. "USGS Fact Sheet 70-03: Heavy Oil and Natural Bitumen--Strategic Petroleum Resources." USGS. 2013. <https://pubs.usgs.gov/fs/fs070-03/fs070-03.html>.
- Mohaghegh, S. D., F. Abdulla, M. Abdou, R. Gaskari, and M. Maysami. 2015. "Smart Proxy: An Innovative Reservoir Management Tool; Case Study of a Giant Mature Oilfield in the UAE." In *Abu Dhabi International Petroleum Exhibition and Conference*. Abu Dhabi, U.A.E. <https://doi.org/10.2118/177829-ms>.
- Mohamed, Linah, Michael A. Christie, and Vasily Demyanov. 2010a. "Comparison of Stochastic Sampling Algorithms for Uncertainty Quantification." *SPE Journal* 15 (01): 31–38. <https://doi.org/10.2118/119139-PA>.
- Mohamed, Linah, Mike Christie, and Vasily Demyanov. 2010b. "Reservoir Model History Matching With Particle Swarms." In . <https://doi.org/10.2118/129152-ms>.
- Mokheimer, Esmail M. A., M. Hamdy, Zubairu Abubakar, Mohammad Raghieb Shakeel, Mohamed A. Habib, and Mohamed Mahmoud. 2019. "A Comprehensive Review of Thermal Enhanced Oil Recovery: Techniques Evaluation." *Journal of Energy Resources Technology* 141 (3). <https://doi.org/10.1115/1.4041096>.

- Morel, D., M. Vert, S. Jouenne, and E. Nahas. 2008. "Polymer Injection in Deep Offshore Field: The Dalia Angola Case." In *Proceedings - SPE Annual Technical Conference and Exhibition*. <https://doi.org/10.2118/116672-ms>.
- Mrokowska, Magdalena M., and Anna Krztoń-Maziopa. 2019. "Viscoelastic and Shear-Thinning Effects of Aqueous Exopolymer Solution on Disk and Sphere Settling." *Scientific Reports* 9 (1): 1–13. <https://doi.org/10.1038/s41598-019-44233-z>.
- Muggeridge, Ann, Andrew Cockin, Kevin Webb, Harry Frampton, Ian Collins, Tim Moulds, and Peter Salino. 2014a. "Recovery Rates, Enhanced Oil Recovery and Technological Limits." *Philosophical Transactions of the Royal Society A: Mathematical, Physical and Engineering Sciences* 372 (2006). <https://doi.org/10.1098/rsta.2012.0320>.
- Muggeridge, Ann, Andrew Cockin, Kevin Webb, Harry Frampton, Ian Collins, Tim Moulds, and Peter Salino. 2014b. "Recovery Rates, Enhanced Oil Recovery and Technological Limits." *Philosophical Transactions of the Royal Society A: Mathematical, Physical and Engineering Sciences*. Royal Society. <https://doi.org/10.1098/rsta.2012.0320>.
- Naevdal, Geir, Liv Merete Johnsen, Sigurd I. Aanonsen, and Erlend H. Vefring. 2005. "Reservoir Monitoring and Continuous Model Updating Using Ensemble Kalman Filter." *SPE Journal* 10 (01): 66–74. <https://doi.org/10.2118/84372-PA>.
- "Oil & Gas News (OGN)." 2015. Oman Review 2015: PDO Is Pioneering EOR Technologies. 2015. [https://www.oilandgasnewsworldwide.com/Article/39588/PDO\\_is\\_pioneering\\_EOR\\_technologies](https://www.oilandgasnewsworldwide.com/Article/39588/PDO_is_pioneering_EOR_technologies).
- Oliver, Dean S. 1996. "Multiple Realizations of the Permeability Field from Well Test Data." *SPE Journal* 1 (2): 145–53. <https://doi.org/10.2118/27970-PA>.
- Oliver, Dean S, Albert C Reynolds, and Ning Liu. 2008. *Inverse Theory for Petroleum Reservoir Characterization and History Matching*. Cambridge University Press. <https://doi.org/10.1017/CBO9780511535642>.
- Onwunalu, Jérôme E., and Louis J. Durlofsky. 2010. "Application of a Particle Swarm Optimization Algorithm for Determining Optimum Well Location and Type." *Computational Geosciences* 14 (1). <https://doi.org/10.1007/s10596-009-9142-1>.
- OPEC. 2017. "OPEC World Oil Outlook 2017." 2017.
- Peters, E., R. J. Arts, G. K. Brouwer, and C. R. Geel. 2009. "Results of the Brugge Benchmark Study for Flooding Optimization and History Matching." In *SPE Reservoir Simulation Symposium Proceedings*, 2:822–42. Society of Petroleum Engineers. <https://doi.org/10.2118/119094-ms>.
- Petrovska, Iryna, and Iryna Petrovska. 2009. "Estimation of Distribution Algorithms for Reservoir History-Matching Optimisation." <https://spiral.imperial.ac.uk/handle/10044/1/5720>.
- Polizel, Guilherme A., Guilherme D. Avansi, and Denis J. Schiozer. 2017. "Use of Proxy Models in Risk Analysis of Petroleum Fields." In *SPE Europec Featured at 79th EAGE Conference and Exhibition*, SPE-185835. Paris, France. <https://doi.org/10.2118/185835-MS>.
- Pye, David J. 1964. "Improved Secondary Recovery by Control of Water Mobility." *Journal of Petroleum Technology*. <https://doi.org/10.2118/845-pa>.
- Queipo, Nestor V, Raphael T Haftka, Wei Shyy, Tushar Goel, Rajkumar Vaidyanathan, and P. Kevin

- Tucker. 2005. *Surrogate-Based Analysis and Optimization. Progress in Aerospace Sciences*. Vol. 41. <https://doi.org/10.1016/j.paerosci.2005.02.001>.
- Rama Rao, Banda S., and Srikanta Mishra. 1996. "Adjoint Sensitivity Analysis for Mathematical Models of Coupled Nonlinear Physical Processes." *IAHS-AISH Publication* 237.
- Ravenzwaaij, Don van, Pete Cassey, and Scott D. Brown. 2018. "A Simple Introduction to Markov Chain Monte–Carlo Sampling." *Psychonomic Bulletin and Review* 25 (1). <https://doi.org/10.3758/s13423-016-1015-8>.
- Reynolds, Albert C, Nanqun He, and Dean S Oliver. 1999. "Reducing Uncertainty in Geostatistical Description with Well-Testing Pressure Data." Edited by Richard A Schatzinger and John F Jordan. *Reservoir Characterization—Recent Advances*. American Association of Petroleum Geologists. <https://doi.org/10.1306/M711C10>.
- Ringrose, Philip, and Mark Bentley. 2015. *Reservoir Model Design: A Practitioner's Guide. Reservoir Model Design*. 2015th ed.
- Romero, C.E., J.N. Carter, A.C. Gringarten, and R.W. Zimmerman. 2000. "A Modified Genetic Algorithm for Reservoir Characterisation." In *International Oil and Gas Conference and Exhibition in China*. Society of Petroleum Engineers. <https://doi.org/10.2118/64765-MS>.
- Rubinstein, Reuven Y., and Dirk P. Kroese. 2016. *Simulation and the Monte Carlo Method: Third Edition. Simulation and the Monte Carlo Method: Third Edition*. <https://doi.org/10.1002/9781118631980>.
- Ruby-Figueroa, René. 2016. "Response Surface Methodology (RSM)." In *Encyclopedia of Membranes*. [https://doi.org/10.1007/978-3-662-44324-8\\_1998](https://doi.org/10.1007/978-3-662-44324-8_1998).
- Ruijian, L. I., A C Reynolds, and D S Oliver. 2009. "History Matching of Three-Phase Flow Production Data." *SPE Reprint Series*, 328–40. <https://doi.org/10.2523/66351-ms>.
- Saleh, Laila Dao, Mingzhen Wei, and Baojun Bai. 2014. "Data Analysis and Novel Screening Criteria for Polymer Flooding Based on a Comprehensive Database." In *SPE - DOE Improved Oil Recovery Symposium Proceedings*, 2:888–905. <https://doi.org/10.2118/169093-ms>.
- Sambridge, Malcolm, and Klaus Mosegaard. 2002. "Monte Carlo Methods in Geophysical Inverse Problems." *Reviews of Geophysics* 40 (3). <https://doi.org/10.1029/2000RG000089>.
- Sandiford, B.B. 1964. "Laboratory and Field Studies of Water Floods Using Polymer Solutions to Increase Oil Recoveries." *Journal of Petroleum Technology*. <https://doi.org/10.2118/844-pa>.
- Sandrea, Ivan, and Rafael Andrea. 2007. "Global Oil Reserves – Recovery Factors Leave Vast Target for EOR Technologies ." *Oil & Gas Journal* 105 (45): 1–8. [http://ipc66.com/publications/Global\\_Oil\\_\\_EOR\\_Challenge.pdf](http://ipc66.com/publications/Global_Oil__EOR_Challenge.pdf).
- Schulze-Riegert, R.W., J.K. Axmann, O. Haase, D.T. Rian, and Y.-L. You. 2001. "Optimization Methods for History Matching of Complex Reservoirs." In *SPE Reservoir Simulation Symposium*. Society of Petroleum Engineers. <https://doi.org/10.2118/66393-MS>.
- Schurz, George F. 1964. "Mobility Control, A New Tool Engineering." In *Fall Meeting of the Society of Petroleum Engineers of AIME*. Society of Petroleum Engineers. <https://doi.org/10.2118/986-MS>.
- Seidenfeld, T. 1992. "R. A. Fisher on the Design of Experiments and Statistical Estimation." In , 23–36. [https://doi.org/10.1007/978-94-011-2856-8\\_2](https://doi.org/10.1007/978-94-011-2856-8_2).

- Self, R. V., A. Atashnezhad, and G. Hareland. 2016. "Use of a Swarm Algorithm to Reduce the Drilling Time through Measurable Improvement in Rate of Penetration." In *50th US Rock Mechanics / Geomechanics Symposium 2016*. Vol. 1.
- Seright, R. S. 1983. "EFFECTS OF MECHANICAL DEGRADATION AND VISCOELASTIC BEHAVIOR ON INJECTIVITY OF POLYACRYLAMIDE SOLUTIONS." *Society of Petroleum Engineers Journal* 23 (3): 475–85. <https://doi.org/10.2118/9297-PA>.
- Seright, R. S., Mac Seheult, and Todd Talashek. 2009. "Injectivity Characteristics of EOR Polymers." In *SPE Reservoir Evaluation and Engineering*, 12:783–92. Society of Petroleum Engineers. <https://doi.org/10.2118/115142-PA>.
- Seright, R S. 2010. "Potential for Polymer Flooding Reservoirs With Viscous Oils."
- Shah, P. C., G. R. Gavalas, and J. H. Seinfeld. 1978. "ERROR ANALYSIS IN HISTORY MATCHING: THE OPTIMUM LEVEL OF PARAMETRIZATION." *Soc Pet Eng AIME J*.
- Sheng, James. 2010. *Modern Chemical Enhanced Oil Recovery (Theory and Practice)*. Journal of Chemical Information and Modeling. Gulf Professional Pub. <https://doi.org/10.1017/CBO9781107415324.004>.
- Sheng, James J. 2011a. *Modern Chemical Enhanced Oil Recovery*. *Modern Chemical Enhanced Oil Recovery*. <https://doi.org/10.1016/C2009-0-20241-8>.
- Sheng, James J. 2011b. *Modern Chemical Enhanced Oil Recovery*. *Modern Chemical Enhanced Oil Recovery*. <https://doi.org/10.1016/C2009-0-20241-8>.
- Skjervheim, J. A., and G. Evensen. 2011. "An Ensemble Smoother for Assisted History Matching." In *Society of Petroleum Engineers - SPE Reservoir Simulation Symposium 2011*. Vol. 2. <https://doi.org/10.2118/141929-ms>.
- Slotte, P A, E Smørgrav, and Statoilhydro Asa. 2008. "SPE 113390 Response Surface Methodology Approach for History Matching and Uncertainty Assessment of Reservoir Simulation Models."
- Sorbie, K.S. 1991. *Polymer-Improved Oil Recovery*. Glasgow and London: Blackie and Son Ltd. Vol. 28. Dordrecht: Springer Netherlands. <https://doi.org/10.1007/978-94-011-3044-8>.
- South, Suffield, Malaysia (Angsi, and Baram Delta. 2018. "Chemical Enhanced Oil Recovery (EOR) Market 2019-2029: Spending (\$m) and Production (MMbbls/Yr) Forecasts by Chemical (ASP, Polymer, Surfactant, Biopolymer, ASP/Polymer and Polymer/ Surfactant) Plus Forecasts for Major Regions and Countries and Leading Companies in the Sector 5.4 Global Alkali Surfactant Polymer Flooding (ASP) Market Analysis." Vol. 74. [www.visiongain.com/energy](http://www.visiongain.com/energy).
- Standnes, Dag Chun, and Ingun Skjevraak. 2014. "Literature Review of Implemented Polymer Field Projects." *Journal of Petroleum Science and Engineering*. Elsevier. <https://doi.org/10.1016/j.petrol.2014.08.024>.
- Stephen, Karl D. 2013. "Seismic History Matching with Saturation Indicators Combined with Multiple Objective Function Optimization." In *75th European Association of Geoscientists and Engineers Conference and Exhibition 2013 Incorporating SPE EUROPEC 2013: Changing Frontiers*, 5823–33. <https://doi.org/10.3997/2214-4609.20130165>.
- Subbey, Sam, Christie Mike, and Malcolm Sambridge. 2003. "A Strategy for Rapid Quantification of

- Uncertainty in Reservoir Performance Prediction.” In *SPE Reservoir Simulation Symposium*. Society of Petroleum Engineers. <https://doi.org/10.2118/79678-MS>.
- Sudaryanto, Bagus, and Yannis C. Yortsos. 2001. “Optimization of Displacements in Porous Media Using Rate Control.” In *SPE Annual Technical Conference and Exhibition*. Society of Petroleum Engineers. <https://doi.org/10.2118/71509-MS>.
- Sultan, A.J., Ahmed Ouenes, and W.W. Weiss. 1994. “Automatic History Matching for an Integrated Reservoir Description and Improving Oil Recovery.” In *Permian Basin Oil and Gas Recovery Conference*. Society of Petroleum Engineers. <https://doi.org/10.2118/27712-MS>.
- Taheri, Amir, and Valiahmad Sajjadian. 2006. “WAG Performance in a Low Porosity and Low Permeability Reservoir, Sirri-A Field, Iran.” In *SPE Asia Pacific Oil & Gas Conference and Exhibition*. Society of Petroleum Engineers. <https://doi.org/10.2118/100212-MS>.
- Tarantola, Albert. 2005. *Inverse Problem Theory and Methods for Model Parameter Estimation*. *Inverse Problem Theory and Methods for Model Parameter Estimation*. <https://doi.org/10.1137/1.9780898717921>.
- Tavassoli, Zohreh, Jonathan N. Carter, and Peter R. King. 2004. “Errors in History Matching.” *SPE Journal* 9 (3): 352–61. <https://doi.org/10.2118/86883-PA>.
- Thomas, L. Kent, L.J. Hellums, and G.M. Reheis. 1972. “A Nonlinear Automatic History Matching Technique for Reservoir Simulation Models.” *Society of Petroleum Engineers Journal* 12 (06): 508–14. <https://doi.org/10.2118/3475-PA>.
- Todd, M.R., and W.J. Longstaff. 1972. “The Development, Testing, and Application Of a Numerical Simulator for Predicting Miscible Flood Performance.” *Journal of Petroleum Technology* 24 (07): 874–82. <https://doi.org/10.2118/3484-pa>.
- Trangenstein, John A., and John B. Bell. 1994. “Mathematical Structure of the Black-Oil Model for Petroleum Reservoir Simulation.” *Journal on Applied Mathematics* 49 (3): 749–83. <https://doi.org/10.1137/0149044>.
- Tunio, Saleem Qadir, Naveed Ahmed Ghirano, Ziad Mohamed, and El Adawy. 2011. “Comparison of Different Enhanced Oil Recovery Techniques for Better Oil Productivity.” *International Journal of Applied Science and Technology* 1 (5). [http://www.ijastnet.com/journals/Vol\\_1\\_No\\_5\\_September\\_2011/18.pdf](http://www.ijastnet.com/journals/Vol_1_No_5_September_2011/18.pdf).
- Vecchio, R. J. Del. 1997. *Understanding Design of Experiments : A Primer for Technologists*. Hanser Publishers.
- Version, Senex. 2013. “SenEx User ’ s Manual,” no. April.
- Wang, Yupu, and He Liu. 2006. “Commercial Success of Polymer Flooding in Daqing Oilfield - Lessons Learned.” In *Proceedings - SPE Asia Pacific Oil and Gas Conference and Exhibition 2006: Thriving on Volatility*.
- Wu, Zhan, A.C. Reynolds, and D.S. Oliver. 1998. “Conditioning Geostatistical Models to Two-Phase Production Data,” January. <https://doi.org/10.2118/49003-MS>.
- Yang, Chaodong, Colin Card, Long Nghiem, and Eugene Fedutenko. 2011. “Robust Optimization of SAGD Operations under Geological Uncertainties.” In *Society of Petroleum Engineers - SPE Reservoir*

- Simulation Symposium 2011*, 1:700–715. Society of Petroleum Engineers.  
<https://doi.org/10.2118/141676-ms>.
- Yang, Chaodong, Long X. Nghiem, Colin Card, and Martin Bremeier. 2007. “Reservoir Model Uncertainty Quantification Through Computer-Assisted History Matching.” In *SPE Annual Technical Conference and Exhibition*. Society of Petroleum Engineers. <https://doi.org/10.2118/109825-MS>.
- Zekri, Abdulrazag Y., K.K. Jerbi, and Mohamed El-Honi. 2000. “Economic Evaluation of Enhanced Oil Recovery.” In *International Oil and Gas Conference and Exhibition in China*. Society of Petroleum Engineers. <https://doi.org/10.2118/64727-MS>.
- Zerkalov, Gregory. 2015. “Polymer Flooding for Enhanced Oil Recovery.” 2015.  
<http://large.stanford.edu/courses/2015/ph240/zerkalov1/>.
- Zhang, Guoyin, and R. S. Seright. 2014. “Effect of Concentration on HPAM Retention in Porous Media.” In *SPE Journal*. <https://doi.org/10.2118/166265-PA>.
- Zubarev, D I. 2009. “Pros and Cons of Applying Proxy-Models as a Substitute for Full Reservoir Simulations.” In *SPE Annual Technical Conference and Exhibition*, SPE 124815. Louisiana, USA.  
<https://doi.org/10.2118/124815-MS>.